MODELLING AN *IN VITRO* HAEMATOPOIETIC STEM CELL NICHE USING POLY (ETHYL ACRYLATE) SURFACES

Paula Emily Sweeten

(BSc Hons)

Submitted in fulfilment of requirements for the degree of Doctor of Philosophy (PhD)

The Centre for the Cellular Microenvironment
Institute of Molecular, Cell and Systems Biology
School of Medical, Veterinary and Life Sciences
University of Glasgow
Glasgow
G12 8QQ

April 2019

Abstract

Haematopoietic stem cells (HSCs) are multipotent stem cells with the capacity to either self-renew or differentiate into oligolineage progenitor cells, and then mature blood cells. HSCs have a diverse range of medical applications, and HSC transplantation can be used to cure certain types of blood cancer including leukaemia and lymphoma. However, current cell culture techniques do not allow for the long-term culture of HSCs, and have restricted the extent to which HSCs numbers can be expanded in the laboratory. Thus, it is necessary to develop culturing techniques that allow for long-term culture and expansion of HSC numbers in the lab.

HSCs reside in the bone marrow alongside a second type of multipotent stem cell termed mesenchymal stem cells (MSCs). Both cell types exist in a unique microenvironment called 'the niche', which is responsible for regulating differentiation, proliferation and maintenance of these stem cells. It is understood that MSCs associate with HSCs in the niche, and support maintenance of the HSC phenotype by expressing HSC maintenance factor transcripts. Consequently, developing niche models featuring MSCs has been the focus of recent research aimed at achieving the long-term culture of HSCs.

Many recent studies have focused on incorporating the use of MSCs and soluble growth factors in the media of MSC/HSC co-cultures to promote the long-term culture of HSCs. However, the high concentrations of media growth factors required to elicit responses in HSC long-term repopulating abilities are costly and have been shown to cause off-target effects. Use of substrate-bound growth factors can induce sustained signalling, meaning reduced quantities of growth factors can elicit similar responses in a more-effective way.

This study has focused on the development of a 3D *in vitro* bone marrow niche system, utilising a range of novel biomaterials including: a substrate composed of poly (ethyl acrylate) (PEA) substrate and fibronectin; a combination of substrate-bound growth factors; a monolayer of MSCs; a type I collagen gel capable of mimicking the elastic properties of the niche and a media capable of supporting an MSC/HSC co-culture. Results show the potential of this system to maintain a greater number of HSCs in their stem cell state, relative to controls.

Table of Contents

Abstract 2
List of Tables 7
List of Figures 8
Acknowledgement 10
Author's Declaration 11
Definitions/Abbreviations 12
CHAPTER 1 14
Chapter 1 General Introduction 15
1.1 Stem Cells 15
1.2 Haematopoietic Stem Cells 16
1.2.1 The Haematopoietic Cell Hierarchy 17
1.2.2 The Identification of HSC Markers 18
1.2.3 Haematopoiesis 20
1.2.4 The Clinical Demand for HSCs 21
1.3 Mesenchymal Stem Cells 23
1.3.1 MSC classification 23
1.3.2 Osteogenic Differentiation of MSCs 24
1.3.3 Cytokine Secretion of MSCs 26
1.4 The Haematopoietic Stem Cell Niche 27
1.4.1 Cellular Localisation within the HSC Niche 29
1.4.2 The Role of Cytokines as HSC Maintenance Factors in the niche 31
1.4.3 Cell Surface Proteins as HSC maintenance Factors 34
1.5 Biomaterials 35
1.5.1 Biomaterial Systems for HSC Niche Models 36
1.5.2 Biomaterials for the modulation of MSC phenotype 37
1.6 Biomaterial applications of poly (ethyl acrylate) 38
1.6.1 The Use of PEA Surfaces in Growth Factor Tethering 40
1.6.2 Integrins and Cell Adhesion at the Material Interface 40
1.6.3 Integrin/Growth Factor Crosstalk 41
1.7 The Use of Growth Factors and ECM Matrices in Bioengineering Applications 42
1.7.1 Evidence of the Success of Direct Growth Factor Presentation in Bioengineering Applications 43
1.7.2 Justification for the Use of Directly Presented GFs in HSC Niche Models 45
1.7.3 The Use of ECM Matrices and their Potential in HSC Niche Models .. 45
1.8 Aims and Objectives 48
CHAPTER 2 51
Chapter 2 Materials and Methods 52
2.1 Materials and Reagents 52
2.1.1 Cell Culture Reagents 52
2.1.2 PEA/PMA Proteins 52
2.1.3 In Cell Western (ICW) Reagents 53
2.1.4 Immunostaining Reagents 53
2.1.5 Primary Antibodies for Immunostaining and ICW 53
2.1.6 Scanning Electron Microscopy (SEM) Reagents 54
2.1.7 Primary Antibodies for FLOW Cytometry 54
2.2 Preparation of Cell Culture Solutions 55
2.3 General Cell Culture Methods 58

2.3.1 STRO-1$^+$ MSC Culture 58
2.3.2 Bone Marrow Extraction 58
2.3.3 STRO-1 positive selection using Magnetic-Activated Cell Sorting (MACS) 59
2.3.4 Monolayer STRO-1$^+$ Culture on Surfaces 59
2.3.5 Fixation of STRO-1$^+$ MSCs 59
2.3.6 CD34$^+$ HSC Culture 60
2.4 General Material Preparation Methods 61
2.4.1 PEA and PMA Sample Preparation 61
2.4.2 FN Coating of PMA and PEA Samples 61
2.4.3 BMP-2/NGF/PDGF/VEGF Coating of PEA Samples 61
2.4.4 Collagen Gel Preparation 62
2.5 Statistical Analyses 62
CHAPTER 3 64
Chapter 3 Material Characterisation 65
3.1 Introduction 65
3.1.1 The Importance of MSCs and OBs in HSC Niche Models 65
3.1.2 PEA as a Potential HSC Niche Model Biomaterial 66
3.1.3 The Role of Collagen Gels in HSC Niche Models 67
3.2 Aims and Objectives 67
3.3 Materials and Methods 68
3.3.1 Atomic Force Microscopy (AFM) 68
3.3.2 Quantification of BMP-2 and NGF adsorption of PEA surfaces 68
3.3.3 Collagen Gel Stiffness Testing Using Rheology 69
3.4 Results 70
3.4.1 FN Conformation on PEA Surfaces 70
3.4.2 BMP-2 Adsorption of PEA Surfaces 71
3.4.3 NGF Adsorption of PEA Surfaces 72
3.4.4 Elastic Modulus of Collagen Gels 73
3.4.5 Young's Modulus of Collagen Gels 74
3.5 Discussion 75
CHAPTER 4 78
Chapter 4 Stromal Layer Characterisation 79
4.1 Introduction 79
4.1.1 The role of a stromal layer in a PEA + FN HSC niche model 79
4.1.2 MSCs in HSC niche models 79
4.1.3 OBs in HSC niche models 80
4.1.4 Expression of HSC maintenance factors in HSC niche models 81
4.2 Aims and Objectives 82
4.3 Materials and Methods 84
4.3.1 Collagen gel function 84
4.3.2 In Cell Western^{TM} (ICW) Assay 84
4.3.3 Immunostaining 85
4.3.4 Fluorescence Microscopy 85
4.3.5 Scanning Electron Microscopy (SEM) 85
4.3.6 MTT Assay 86
4.3.7 Flow Cytometry Staining 86
4.3.8 T Cell Suppression Assay 87
4.4 Results 89
4.4.1 STRO-1$^+$ MSC morphology is unaffected by substrates 89
4.4.2 STRO-1 protein expression results in 10% FBS media 90
4.4.3 Niche protein expression results in 2% FBS media 93

4.4.4 Niche protein expression results in 2% human serum media for 14 days and 5GF media for 7 days 98
4.4.5 Niche protein expression results in 2% human serum media for 14 days and 3GF media for 7 days 102
4.4.6 Flow cytometry analysis of additional MSC marker expression in 2% HS and 3GF media 106
4.4.7 Assessing MSC function using T cell suppression assay 107
4.4.8 CXCL-12 secretion from STRO-1$^+$ cells cultured on niche model candidate substrates in varying media compositions 109
4.4.9 THPO secretion from STRO-1$^+$ cells cultured on niche model candidate substrates in varying media compositions 112
4.4.10 Cell number analyses 115
4.5 Discussion 116
4.5.1 Discussion of MSC phenotype 117
4.5.2 Discussion of osteogenic phenotype 118
4.5.3 Discussion of HSC maintenance factor expression results 120
4.5.4 Chapter conclusions 121
CHAPTER 5 123
Chapter 5 Metabolomic Analysis of MSCs 124
5.1 Introduction 124
5.1.1 Metabolomics 124
5.1.2 Metabolomic Pathways of Relevance 124
5.1.3 Metabolomics and MSCs in bioengineering 126
5.2 Aims and Objectives 127
5.3 Materials and Methods 128
5.3.1 Sample Preparation 128
5.3.2 Liquid Chromatography Mass Spectrometry (LCMS) 129
5.3.3 Data Analysis 129
5.4 Results 130
5.4.1 The effect of niche models on amino acid metabolism 130
The effect of niche models on carbohydrate metabolism 132
5.4.2 The effect of niche models on lipid metabolism 134
5.5 Discussion 137
CHAPTER 6 140
Chapter 6 HSC Characterisation 141
6.1 Introduction 141
6.1.1 Characterisation of the classic HSC phenotype 141
6.1.2 The relevance of CD34$^+$CD38$^+$ and CD34$^-$CD38$^+$ progenitors 141
6.1.3 Commitment of progenitors to differentiation lineages 142
6.2 Aims and Objectives 142
6.3 Materials and Methods 144
6.3.1 HSC culture 144
6.3.2 Flow cytometry 144
6.4 Results 151
6.4.1 CD34$^+$CD38$^-$ cells in candidate models 151
6.4.2 CD34$^+$CD38$^+$ cells in candidate models 160
6.4.3 CD34$^-$CD38$^+$ cells in candidate models 168
6.5 Discussion 176
6.5.1 CD34$^+$CD38$^-$ phenotype retention & lineage commitment 176
6.5.2 CD34$^+$CD38$^+$ phenotype development & lineage commitment 177
6.5.3 CD34$^-$CD38$^+$ phenotype development & lineage commitment 179
6.5.4 Chapter conclusions 179

CHAPTER 7 183
Chapter 7 Discussion 184
7.1 General Discussion 184
7.1.1 Utilising PEA substrates and collagen gels in HSC niche models 185
7.1.2 Characterising MSC phenotype in models comprising PEA substrates and growth factors 185
7.1.3 Metabolomic changes in MSCs cultured in HSC niche models 187
7.1.4 Responses of HSCs to HSC niche models 189
7.2 Thesis Conclusion 191
7.3 Overview relating this thesis to related studies 193
7.4 Recommendations for Future Model Development 194
7.5 Future Potential of HSC Niche Models & Clinical Relevance 196
List of References 198

List of Tables

Table 1-1 Cell surface marker expression associated with HSC hierarchy 19
Table 1-2 The biological functions of mature blood cells 21
Table 1-3 Proteins associated with MSC immunophenotype 24
Table 1-4 Cell types that regulate HSCs..... 28
Table 1-5 Cytokines associated with the HSC niche 33
Table 1-6 Examples of the use of directly presented growth factors..... 44
(Table 1-7 ECM Matrices in HSC Niche Models..... 47
Table 6-1 Flow cytometry antibody mixes 145
Table 6-2 FLOW cytometry antibody list 146
Table 6-3 Methods for improving future HSC work 181

List of Figures

Figure 1-1 Stem cell self-renewal and differentiation 16
Figure 1-2 The hierarchy of haematopoietic stem cells 17
Figure 1-3 The HSC differentiation tree..... 20
Figure 1-4 BMP-2 signalling in osteogenic differentiation 26
Figure 1-5 The HSC niche 29
Figure 1-6 The structural organisation of a fibronectin molecule..... 39
Figure 1-7 Schematic of in vitro HSC niche model during different stages of cell culture 48
Figure 3-1 FN fibrillogenesis occurs on PEA surfaces..... 70
Figure 3-2 The surface density of BMP-2 on PEA + FN surfaces..... 71
Figure 3-3 The surface density of NGF on PEA + FN surfaces. 72
Figure 3-4 Storage modulus of collagen gels 73
Figure 3-5 The Young's modulus of collagen gels..... 74
Figure 4-1 Cell culture media timeline..... 83
Figure 4-2 Suppression assay CFSE gating strategy 88
Figure 4-3 SEM Images of STRO-1+ Cells on Substrates 89
Figure 4-4 ICW results for MSC marker expression after 21 days..... 91
Figure 4-5 ICW results indicative of osteogenesis after 21 days..... 92
Figure 4-6 ICW results for SCF and VCAM-1 expression after 21 days..... 93
Figure 4-7 ICW results for MSC marker expression in 2% FBS media 95
Figure 4-8 ICW results indicative of osteogenesis in 2% FBS media 96
Figure 4-9 ICW results for SCF and VCAM-1 expression in 2% FBS media 97
Figure 4-10 STRO-1 cell viability in media with different serum type and concentration 99
Figure 4-11 ICW results for MSC marker expression in 2% HS and 5GF media ... 100
Figure 4-12 ICW results for SCF and VCAM-1 expression in 2% HS and 5GF media 101
Figure 4-13 ICW results for MSC marker expression in 2% HS and 3GF media ... 103
Figure 4-14 ICW results indicative of osteogenesis in 2% HS and 3GF media 104
Figure 4-15 ICW results for SCF and VCAM-1 expression in 2% HS and 3GF media 105
Figure 4-16 Flow cytometry results for MSC marker expression in 2% HS and 3GF media..... 107
Figure 4-17 Proliferation index of T cells cultured with MSCs from HSC niche models 108
Figure 4-18 CXCL-12 ELISA data from culture in DMEM supplemented with 10% FBS..... 110
Figure 4-19 CXCL-12 ELISA data from culture in DMEM supplemented with 2% HS 111
Figure 4-20 THPO ELISA data from culture in DMEM supplemented with 10% FBS 113
Figure 4-21 THPO ELISA data from culture in DMEM supplemented with 2% HS. 114
Figure 4-22 Cell number analysis after 21 days of culture on niche model candidate substrates..... 116
Figure 5-1 Amino acid metabolite profile of MSCs on HSC niche model substrates 131
Figure 5-2 PCA plot of amino acid metabolites detected in MSCs cultured in HSC niche models containing glass + FN, PMA + FN, PEA + FN and PEA + FN + BMP-2&NGF substrates 132

Figure 5-3 Carbohydrate metabolite profile of MSCs on HSC niche model substrates.....133
Figure 5-4 PCA plot of carbohydrate metabolites detected in MSCs cultured in HSC niche models containing glass + FN, PMA + FN, PEA + FN and PEA + FN + BMP-2&NGF substrates 134
Figure 5-5 Lipid metabolite profile of MSCs on HSC niche model substrates....136
Figure 5-6 PCA plot of lipid metabolites detected in MSCs cultured in HSC niche models containing glass + FN, PMA + FN, PEA + FN and PEA + FN + BMP-2&NGF substrates 137
Figure 6-1 Substrates and media formulations used in HSC culture experiments 143
Figure 6-2 Flow cytometry gating strategy for progenitor identification 147
Figure 6-3 Flow cytometry gating strategy for progenitor populations associated with differentiation analyses 148
Figure 6-4 Gating strategy for CD7+ populations 149
Figure 6-5 Gating strategy for CD36+ populations 149
Figure 6-6 Gating strategy for CD41a+ populations.....150
Figure 6-7 CD34+CD38- populations in niche models using different substrates & media types. 153
Figure 6-8 CD34+CD38-CD7+ populations in niche models using different substrate and media types 155
Figure 6-9 CD34+CD38-CD36+ populations in niche model candidate systems using different substrate and media types. 157
Figure 6-10 CD34+CD38- populations in niche models using different substrates and media types 159
Figure 6-11 CD34+CD38+ populations in niche models using different substrates and media types 161
Figure 6-12 CD34+CD38+CD7+ populations in niche models using different substrate and media types 163
Figure 6-13 CD34+CD38+CD36+ populations in niche models using different substrates and media types.....165
Figure 6-14 CD34+CD38+CD41a+ populations in niche models using different substrates and media types.....167
Figure 6-15 CD34-CD38+ populations in niche models using different substrates and media types 169
Figure 6-16 CD34-CD38+CD7+ populations in niche models using different substrates and media types.....171
Figure 6-17 CD34-CD38+CD36+ populations in niche models using different substrates and media types.....173
Figure 6-18 CD34-CD38+CD41a+ populations in niche models using different substrates and media types.....175

Acknowledgement

I would like to offer thanks to my supervisors, Matthew Dalby, Manuel Salmerón-Sánchez and Joanne Mountford. I am extremely grateful to Matt for all of the encouragement, support and motivation he has provided me throughout the course of this PhD. He has presented me with a wealth of opportunities and chances to maximise my potential, for which I will be eternally grateful. I would also like to express my gratitude to Manuel for always providing direction, and to Joanne for helping me to navigate my way through the tribulations of HSC culture.

Secondly, I would like to offer thanks to colleagues at the Centre for Cell Engineering and Microenvironments for Medicine groups. Particularly, I would like to thank Ewan Ross. Without him, I would never have been able to conquer the second half of this PhD. I would like to further extend my thanks to Carol-Anne Smith, Monica Tsimbouri, Virginia Llopis-Hernandez, Annie Cheng, Marco Cantini and Hannah Donnelly for providing me with four years of technical and practical help. Other staff at the University of Glasgow beyond these laboratories have also been extremely helpful to me, for which I am thankful. Particular thanks is offered to Elaine Hunter for her motivation and reassurance.

Finally, I would like to express my utmost gratitude to my family and friends for being continually supportive and encouraging. Particularly, I would like to thank my parents, William and Lynn Sweeten, for giving me the confidence and drive to get this far. I would also like to thank my partner, Ross Ballantyne, for tolerating the ups and downs of this PhD, and for patiently supporting me through every part of it. In addition, I would like to thank my gran, Helen Mains, who wrote ‘Paula PhD’ on my honours degree graduation card, and is due credit for making me believe this would be possible, as well as for always reminding me of how lucky I have been to have this opportunity.

Author's Declaration

I hereby declare that the research reported within this thesis is my own work, unless otherwise stated, and that at the time of submission is not being considered for any other academic qualification.

Paula Sweeten

The 18th of April 2019.

Definitions/Abbreviations

Abbreviation	Full Name
AFM	Atomic force microscopy
ALCAM	Activated leukocyte-cell adhesion molecule
ALP	Alkaline phosphatase
BIT	BSA, insulin, transferrin
BM	Bone marrow
BMP-2	Bone Morphogenic protein-2
BSA	Bovine serum albumin
cKIT	(also referred to as CD117)
CAR	CXCL-12 abundant reticular
CD	Cluster of differentiation
CLP	Common lymphoid progenitor
CMP	Common myeloid progenitor
CXCL-12	C-x-c motif chemokine 12 (also referred to as SDF-1)
DAPI	4',6-diamidino-2-phenylindole
DMEM	Dulbecco's modified eagles medium
EC	Endothelial cell
ECM	Extracellular matrix
EDTA	Ethylenediaminetetraacetic acid
ELISA	Enzyme-linked immunosorbent assay
FACS	Fluorescence activated cell sorting
FAK	Focal adhesion kinase
FBS	Foetal bovine serum
FITC	Fluorescein isothiocyanate
FN	Fibronectin
G-CSF	Granulocyte colony stimulating factor
GF	Growth factor
GMP	Granulocyte monocyte progenitor
HA	Hyaluronic acid
HEPES	4-(2-hydroxyethyl)-1-piperazineethanesulfonic acid
HS	Heparan sulphate
HSC	Haematopoietic stem cell
HSPC	Haematopoietic stem and progenitor cell
Ig	Immunoglobulin
IGF-1	Insulin-like growth factor-1
IMDM	Iscove's modified eagles medium
ISCT	International Society for Cellular Therapy
Jag-1	Jagged-1
JAK	Janus kinase
Lin	Lineage
LT-HSC	Long term haematopoietic stem cell
MLCK	Myosin light chain kinase
MSC	Mesenchymal stem cell
MTT	4,5-dimethylthiazol-2-yl)-2,5-diphenyltetrazolium bromide
NGF	Nerve growth factor
OB	Osteoblast
OCN	Osteocalcin

OPN	Osteopontin
OSX	Osterix
PBS	Phosphate buffered saline
PCR	Polymerase chain reaction
PDGF	Platelet derived growth factor
PEA	Poly (ethyl acrylate)
PEG	Poly (ethylene glycol)
PMA	Poly (methyl acrylate)
PTH	Parathyroid hormone
ROCK	Rho-associated protein kinase
RUNX	Runt-related transcription factor
SCF	Stem cell factor
SDF-1	Stromal derived factor-1 (also referred to as CXCL-12)
SEM	Scanning electron microscopy
SFM	Serum free medium
SNS	Sympathetic nervous system
ST-HSC	Short term haematopoietic stem cell
STAT	Signal transducer and activator of transcription
TGF-β	Transforming growth factor beta
THPO	Thrombopoietin
VCAM-1	Vascular cell adhesion molecule-1
VEGF	Vascular endothelial growth factor

CHAPTER 1

Chapter 1 General Introduction

1.1 Stem Cells

At the end of the 19th century, the concept of stem cells began to develop based on the observation that some human tissues, such as skin, could self-renew throughout life. However, it was not until the 1908 meeting of the Congress of the Haematologic Society that the term stem cell was proposed for scientific use by Russian histologist, Alexander Maksimov (Bansal and Jain, 2015). Despite this early postulation of the existence of stem cells, their full potential did not begin to be understood until the 1960s, when Till and McCulloch published findings showing they had identified the first stem cells (Till and McCulloch, 1961). This conclusion was deduced from evidence showing that mice treated with supralethal radiation, could survive when bone marrow cells were intravenously injected. These cells were found to collect in the spleen in colonies, where the cells maintained their proliferative function. Later, it was found that these cells could replace the cells killed by radiation and could self-renew in the same way, and that bone marrow transplants could cure diseases and ultimately save lives (Wu et al., 1967, Thomas et al., 1975).

Although initial findings highlighted that stem cells possessed a key characteristic of being able to self-renew, these cells have a second important characteristic, which is their ability to differentiate (Thomson et al., 1998). Self-renewal allows stem cells to produce daughter cells that remain in the undifferentiated state (see Figure 1-1)(Watt and Hogan, 2000). Conversely, differentiation results in stem cells producing daughter cells with different patterns of gene expression. These daughter cells, known as progenitor cells, are more specialised (Jaenisch and Young, 2008). Progenitor cells are able to differentiate into more than one specialised cell type, but have a less capacity for self-renewal when compared to stem cells (Krause et al., 2001).

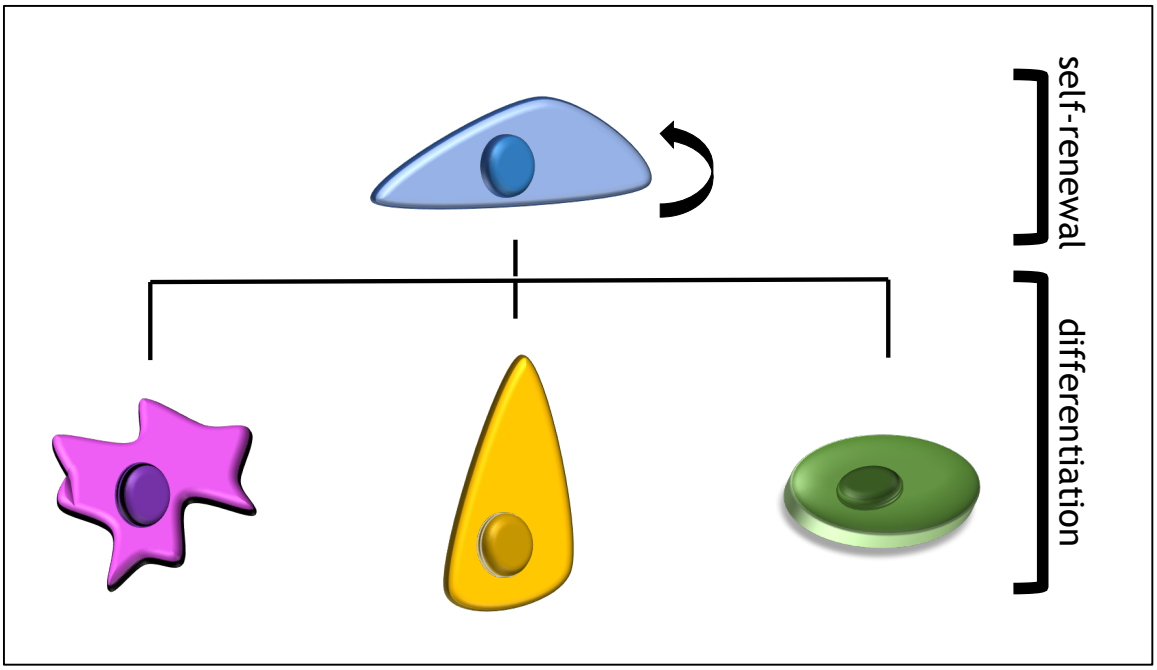

Figure 1-1 Stem cell self-renewal and differentiation
Stem cells have the capacity to undergo self-renewal, forming an identical copy of themselves, and also differentiation, whereby specialised and distinct cell types are formed.

It is common practice to classify stem cells according to their developmental potential, which is termed "potency" (Jaenisch and Young, 2008). At the top of the potency hierarchy is the totipotent stem cell. Totipotent stem cells form in the zygote, directly following fertilisation, and have the capacity to produce embryonic and extra-embryonic cell types (Williams et al., 1988). Pluripotent stem cells are later found to exist in the inner cell mass of the blastocyst, and have the ability to differentiate into all cell types of the embryo proper (Wagers and Weissman, 2004). Other stem cell potency classifications include multipotent stem cells, which can differentiate into a subset of cell lineages, and oligopotent stem cells, which are further restricted in the cell lineages they can develop into.

1.2 Haematopoietic Stem Cells

Haematopoietic stem cells (HSCs) are multipotent stem cells that give rise to mature blood cells via the process of haematopoiesis (Sieburg et al., 2006). In early development, HSCs are found in the foetal liver, and later the spleen (Wang and Wagers, 2011). In adults, HSCs reside in a third set of locations within the femur, pelvis and sternum, in an area termed "the niche" (Schofield, 1978). HSCs are scarce cells, representing <0.005% of the total cell population in these

niches (Kiel et al., 2005). Such niches are microenvironments that provide a diverse range of signals that influence and regulate HSC behaviour.

1.2.1 The Haematopoietic Cell Hierarchy

HSCs represent a heterogeneous population of cells, in terms of their capacity to self-renew, differentiate and length of life. During a series of experiments carried out and published in 2008 by the lab of Irving Weissman, a hypothesis was proposed that suggested HSCs are heterogeneous and can exist at different points within a hierarchy model (Chao et al., 2008, Morrison and Weissman, 1994). Cell surface marker expression assays and functional readout assays from this group and others were used to define a developmental hierarchy of HSCs. It was proposed that HSCs with lifelong self-renewal properties sat at the top of the hierarchy, and underwent mitosis to form multipoent progenitors (MPPs). Further downstream, it was proposed that the MPPs gave rise to oligopotent progenitors, known as common lymphoid progenitors and common myeloid progenitors (Figure 1-2) (Kondo et al., 1997, Akashi et al., 2000).

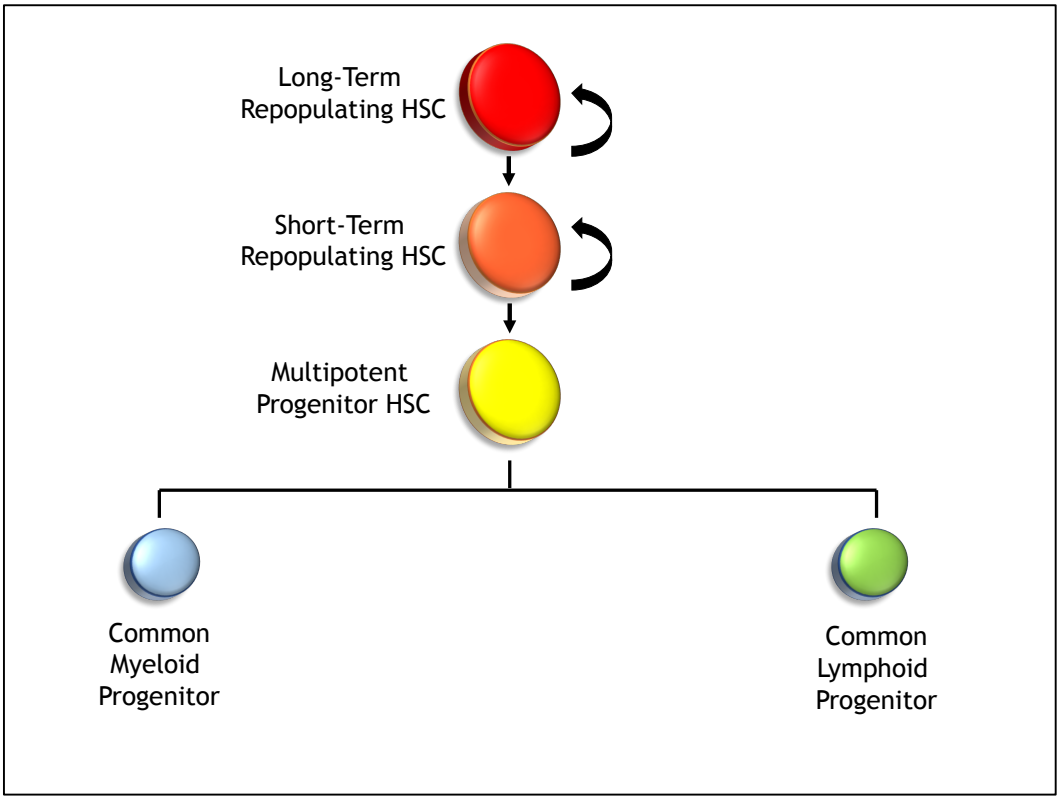

Figure 1-2 The hierarchy of haematopoietic stem cells
HSCs can exist as three different mulitpotent subtypes, referred to as long-term, short-term and multipotent progenitor HSCs. Differentiation of multipotent progenitor HSCs leads to the formation of common myeloid and lymphoid progenitors.

At present, it is most common to refer to HSCs in terms of their self-renewal capacity; HSCs can be sub-divided into two distinct populations known as short-term repopulating HSCs (ST-HSCs) and long-term repopulating HSCs (LT-HSCs) (Figure 1-2) (Cheshier et al., 1999). LT-HSCs are greater in their capacity to repopulate, and can reconstitute an animal for its entire lifespan (Weissman, 2000). Such HSCs are rich in clinical value and applicability and have been used in the treatment of a diverse range of pathologies including leukaemia and AIDS (Aversa et al., 2005, DiGiusto et al., 2010). Thus, these cells are of prime interest to the medical and scientific communities, striving to develop in-lab methods for the expansion of HSC populations for medical applications (Ivanova et al., 2002, Acar et al., 2015)

1.2.2 The Identification of HSC Markers

Despite the isolation of murine HSCs being a well-established process, the isolation of human HSCs has proven to be more challenging. It is understood that all mature haematopoietic cells express a mixture of mature lineage markers, and these cells are referred to as Lin positive (Lin^+). Conversely, haematopoietic stem and progenitor cells do not express these lineage markers, and so are said to be Lin negative (Lin^-) (Zhang et al., 2003). The CD34 antigen was identified in 1984 as a marker that could enrich for human haematpoietic stem and progenitor cells (HSPCs) (Civin et al., 1984, Visser et al., 1984). CD34 is the most commonly used antigen for the identification of HSCs in humans. However, due to the heterogeneous nature of these cells, exclusion of CD38 and CD45RA is normally also used in HSC isolation, as these markers are associated with more differentiated haematopoietic cell types (Terstappen et al., 1991, Lansdorp et al., 1990). Further to the expression of these cell surface antigens, CD90 expression can also be used to determine how primitive a HSC is. In 1992, Baum and colleagues demonstrated that $Lin^-CD34^+CD90^+$ could generate both lymphoid and myeloid progeny *in vitro* and *in vivo*, while cells that lacked CD90 ($Lin^-CD34^+CD90^-$) could not. It was proposed that these $CD90^+$ cells are at the top of the haematopoietic hierarchy, while $Lin^-CD34^+CD90^-$ cells may be more indicative of multipotent progenitors. Human trials involving the transplantation of autologous peripheral blood have also demonstrated that only $CD90^+$ cells give long-term engraftment (Michallet et al., 2000, Vose et al., 2001).

Although the different phenotypes of LT-HSCs and ST-HSCs of HSC have been characterised in mice and can be distinguished by their cell surface marker expression, such variation has not yet been characterised in humans. Currently, it is accepted that human short and long term repopulating HSCs, as well as MPPs, are phenotypically Lin^- $CD34^+$ $CD38^-$ $CD90^-$ $CD45RA^-$ (Table 1-1)(Majeti et al., 2007). However, it should be noted that ambiguity exists in the literature, and it has been proposed that $CD34^-$ cells also have multipotent potential (Osawa et al., 1996, Zanjani et al., 1998).

Table 1-1 Cell surface marker expression associated with HSC hierarchy (Adapted from (Chao et al., 2008, Baldridge et al., 2010, Osawa et al., 1996))

Haematopoietic Cell Name	Classification	Human Phenotype	Murine Phenotype
Haematopoietic Stem Cell (HSC)	multipotent	Lin^- $CD34^+$ $CD38^-$ $CD90^+$ $CD45RA^-$	Lin^- $Ckit^+$ $Sca1^+$ $Flk2^-$ $CD34^-$ $Slamf1^+$
Long-term repopulating HSC	multipotent	Lin^- $CD34^+$ $CD38^-$ $CD90^-$ $CD45RA^-$	Lin^- $Ckit^+$ $Sca1^+$ $Flk2^-$ $CD34^+$ $Slamf1^+$ KSL, $CD34^-$, $Flk2^-$ or KSL, $CD150^+$ $mCD34^{lo/-}$, $c\text{-}Kit^+$, $Sca\text{-}1^+$,
Short-term repopulating HSC	multipotent	Lin^- $CD34^+$ $CD38^-$ $CD90^-$ $CD45RA^-$	Lin^- $Ckit^+$ $Sca1^+$ $Flk2^-$ $CD34^-$ $Slamf1^-$
Multipotent progenitor (MPP) HSC	multipotent	Lin^- $CD34^+$ $CD38^-$ $CD90^-$ $CD45RA^-$	Lin^- $Ckit^+$ $Sca1^+$ $Flk2^+$ $CD34^-$ $Slamf1^-$
Common Lymphoid Progenitor (CLP)	oligopotent	Lin^- $CD34^+$ $CD38^+$ $CD10^+$	Lin^- $Flk2^+$ $IL7Ra^+$ $CD27^+$
Common Myeloid Progenitor (CMP)	oligopotent	Lin^- $CD34^+$ $CD38^+$ $IL3Ra^{low}$ $CD45RA^-$	Lin^- $Ckit^+$ $Sca1^{-/low}$ $CD34^+$ $FcgR^{low}$

1.2.3 Haematopoiesis

Haematopoiesis is a continuous and dynamic process that results in the formation of blood cells. It is estimated that one trillion new blood cells are required daily to sustain adult life, and with the exception of certain lymphocytes, most blood cells have a very short life span and must be replenished regularly to maintain homeostasis (Ogawa, 1993). The continuous production of these blood cells is dependent on the differentiation of HSCs, found primarily in the adult bone marrow (Rodriguez-Fraticelli et al., 2018). Following differentiation to form common myeloid and common lymphoid progenitors, haematopoiesis then continues to produce a range of mature blood cells with specialised functions (Figure 1-3).

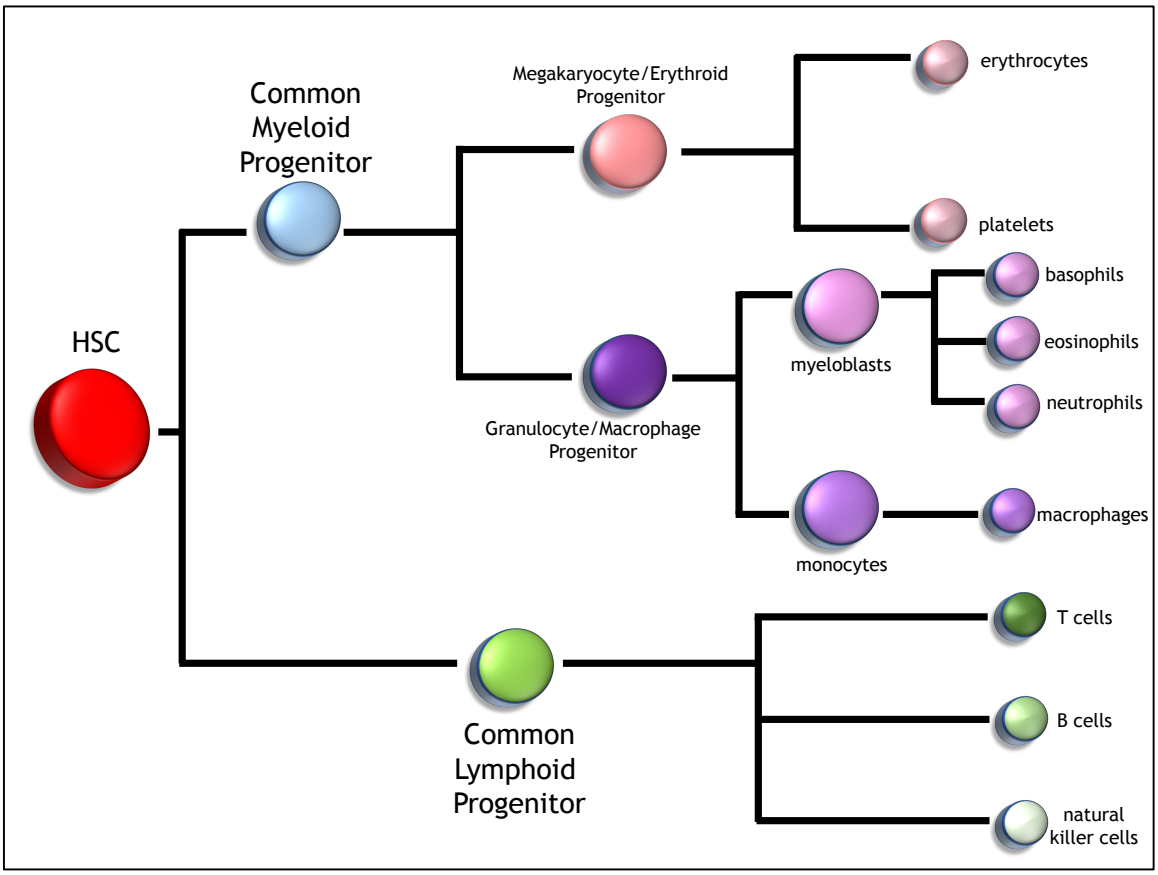

Figure 1-3 The HSC differentiation tree
Haematopoiesis is the process by which HSCs differentiate to form specialised haematopoietic cells. This process is dependent on HSCs first forming haematopoietic progenitors associated with differentiation lineages. These progenitors then give rise to specialised cell types with distinct functions . (Adapted from (Orkin and Zon, 2008))

The mature blood cells produced from haematopoiesis have a diverse range of functions, from regulating blood clotting to carrying out immunological functions, as described in Table 1-2 (Orkin and Zon, 2008).

Table 1-2 The biological functions of mature blood cells

Mature Blood Cell Type	Biological Function	Reference
erythrocyte	the transportation of oxygen and carbon dioxide	(Jensen, 2004)
platelet	blood clotting	(Webb et al., 1998)
basophil	modulation of histamine release during inflammation	(Hirai et al., 1988)
eosinophil	antiparisitic and bactericidal	(Carreras et al., 2003)
neutrophil	defense against microbe infection	(Jorgensen and Miao, 2015)
macrophage	phagocytosis of pathogens	(Savill et al., 1989)
T cell	death of infected cells	(Hori et al., 2003)
B cell	antibody production	(Köhler and Milstein, 1975)
natural killer cell	cytotoxicity against infections and cancer	(Trinchieri, 1989)

Although many haematopoietic cells are required daily in normal circumstances, minor maladies resulting in acute blood loss or infection, demand that haematopoiesis takes place at an even greater rate to produce a sufficient number of platelets for blood clotting or a sufficient number of white blood cells to combat the infection (Ogawa, 1993). Thus, haematopoiesis is not only a continuous process, but it is also a dynamic process that is vital to sustaining life.

1.2.4 The Clinical Demand for HSCs

Haematopoietic stem cell transplants (HSCTs) are often performed for patients with cancers of the blood or bone marrow, and is recognised as a potentially curative treatment for over 70 haematologic cancers (Bensinger et al., 2001).

Since the first successful series of HSCTs were carried out in the 1950s, the incidences of early transplant mortality have been shown to decline, correlating with the increased numbers of HSCT survivors (Thomas et al., 1959, Bhatia et al., 2007, Clark et al., 2016). Further, the European Society of Blood and Marrow Transplantation reported in 2013 that the number of allogeneic HSCTs in Europe doubled over a ten year period between the 1990s and 2000s (Passweg et al., 2015). Although autologous transplants were initially a popular means of HSCT, this report also indicated that growth in the numbers of allogeneic transplants have exceeded that of autologous transplants (Gratwohl et al., 2015, Passweg et al., 2015).

Clinical trials involving HSCTs are becoming increasingly popular as the interest in these cells heightens. Although numerous clinical trials are currently underway involving these cells, pioneering results have been obtained in the MIST trail, based on findings published in 2013 showing the improved health of T cells from HSCT patients relative to controls (Burman et al., 2013). In the MIST study, 110 people with highly active, drug resistant multiple sclerosis (MS) had autologous HSCTs re-infused into their blood following chemotherapy (Burt et al., 2018). Patients were followed up after a year and it was noted that only one out of 55 HSCT patients suffered a relapse, while 39 out of 55 in the drug control group did (Burt et al., 2018).

As the potential of HSCTs is becoming acknowledged and used in clinical trials, it is important to appreciate the considerable efforts also being made to maximise HSC engraftment following such treatment. Additional clinical trials are running with the aim of achieving maximal HSC engraftment, and have shown that transplanting HSCs with megakaryocyte cells can improve HSC engraftment (Trebeden-Negre et al., 2017). The success and progress noted in such clinical trials have contributed to pilot schemes such as the £4 million IMPACT clinical trial programme being established. Here, up to 12 clinical trails will be funded, with the aim of reducing the time taken for patients to gain access to treatments going through the clinical trials pipeline.

Taking these points into consideration, it is apparent that HSCTs are becoming a more widely accepted therapy than ever before, and so there is an increased demand for a means of keeping HSCs alive for longer *ex vivo*, as this would

increase patient reach (Schuster et al., 2012). Further, it is recognised that determining methods for the *ex vivo* expansion of HSCs could reduce the demand for high numbers of donors, and could provide a promising means of making HSCT a more economical process (Dahlberg et al., 2011).

1.3 Mesenchymal Stem Cells

Mesenchymal Stem Cells (MSCs) are multipotent stromal cells that were first isolated in 1974, and were later given their name in 1991 when it was acknowledged that MSCs could differentiate into cells of mesoderm origin (Friedenstein et al., 1974, Caplan, 1991). Such mesoderm cell types include osteocytes (bone cells), chondrocytes (cartilage cells) and adipocytes (fat cells). The most primitive MSCs can be obtained from the umbilical cord blood and the Wharton's Jelly of the umbilical cord tissue (Wang et al., 2004b). MSCs can also be sourced from the amniotic fluid during foetal development, the adipose tissue of adults, or most commonly from the adult bone marrow (Tsai et al., 2004, Kern et al., 2006). The adult bone marrow is widely accepted as one of the main MSC niches and is a unique microenvironment that provides instructional cues that maintain and regulate the fate of MSCs (Shi and Gronthos, 2003). Despite bone marrow extraction being the most common method for MSC extraction, MSCs only comprise 0.001 – 0.01 % of the total bone marrow cell number (Caplan, 1994). However, problems associated with the low extraction number are easily overcome due to the adherent nature of these cells to standard tissue culture plastic, which allows for their expansion *ex vivo* (Dominici et al., 2006). Although MSC expansion is easily achievable in the lab, it is important to note that ageing of MSCs is associated with decreased lifespan and differentiation potential (Stenderup et al., 2003, Ragni et al., 2013).

1.3.1 MSC classification

Three main criteria have been put into place by the International Society for Cellular Therapy (ISCT) for the characterisation of MSCs: MSCs must be able to adhere to plastic when cultured in standard conditions; MSCs must express CD73, CD90 and CD105; MSCs must be able to differentiate *in vitro* into osteoblasts, adipocytes and chrondrocytes (Dominici et al., 2006). Despite CD73, CD90 and CD105 expression being essential, the scientific community also accepts that

MSCs normally express additional surface markers such as STRO-1, as outlined in Table 1-3 (Psaltis et al., 2010).

Table 1-3 Proteins associated with MSC immunophenotype

Immunophenotype	Protein Type	Protein Role
$CD29^+$	integrin	cell adhesion
$CD44^+$	cell surface glycoprotein	cell adhesion, migration and cell-cell interactions
$CD73^+$	enzyme	conversion of AMP to adenosine
$CD90^+$	glycosylated membrane protein	cell-cell and cell-matrix interactions
$CD105^+$ (endoglin)	type I membrane glycoprotein	angiogenesis role
$CD106^+$ (VCAM-1)	cell adhesion protein	cell adhesion
$CD166^+$ (ALCAM)	type I transmembrane glycoprotein	cell adhesion
$CD271^+$	low affinity nerve growth factor (NGF) receptor	stimulates survival and differentiation of neuronal cells
STRO-1^+	cell surface antigen	unknown
$Nestin^+$	type VI intermediate filament protein	used to assess cell proliferation and migration

1.3.2 Osteogenic Differentiation of MSCs

Differentiation to form bone cells occurs when MSCs commit to the osteogenic lineage and differentiate to form osteoprogenitor cells and preosteoblasts, and then further to form osteoblasts (OBs) and osteocytes. This differentiation is dependent on a number of cytokines, including bone morphogenic protein 2 (BMP-2), transforming growth factor beta (TGF-β), parathyroid hormone (PTH) and insulin-like growth factor-1 (IGF-1) (Ryoo et al., 2006, Liu et al., 2013, Katagiri et al., 1990, Xian et al., 2012). In order for osteogenic differentiation to

occur, there must be expression of the key transcription factor Runt-related transcription factor 2 (Runx2). In 1997, Komori and colleagues published results showing that Runx2 knockout mice have an entire absence of bone as a result of arrested OB maturation. This group also proposed that Runx2 is the master transcription factor that directs MSCs to form OBs, because other transcription factors involved in osteogenesis, such as osterix (Osx) and Dlx5 are not expressed in the skeletal primordium of Runx2-/- mice, while Runx2 is expressed in the primordium of Osx-/- mice. Further, the Runx2 null phenotype cannot be rescued by the overexpression of other osteogenic factors (Hesse et al., 2010).

As mentioned, BMP-2 is a key cytokine that acts to facilitate osteogenic differentiation. Seminal work in 1965 identified BMP-2's family of bone-inducing agents in demineralised bone, and these were later termed bone morphogenic proteins (BMPs) (Urist, 1965, Urist and Strates, 1971). Once these recombinant BMPs were purified, it was observed that injection of BMP-2 into muscles was sufficient to induce ectopic bone formation (Wang et al., 1990). The mechanism of BMP-2 signalling has since been elucidated, and it is known that BMP-2 is dependent on SMADs, a group of signal transducers for receptors of the TGF-ß protein superfamily (Figure 1-4)(Nohe et al., 2002). Firstly, the BMP-2 molecule binds to a receptor type I and II, and the signal then transduces to their SMADs (Figure 1-4). These activated SMADs go on to regulate expression of transcriptional factors and co-activators including Dlx5, Osx and Runx2. Runx2 promotes the differentiation of MSCs into preosteoblasts, while Dlx5 is thought to facilitate osterix transcription, and in turn, osterix then promotes differentiation of preosteoblasts into osteoblasts (Lee et al., 2003).

It is important to note the potential of MSCs, in that they are a valuable cell type on their own, and are also equally as valuable when they have undergone osteogenic differentiation to form OBs. As will be discussed in sections 1.7-1.9, it is possible to use biomaterials as a means of presenting BMP-2 to MSCs. This can be used to generate cell cultures that feature OBs, while in some cases also maintaining a population of MSCs.

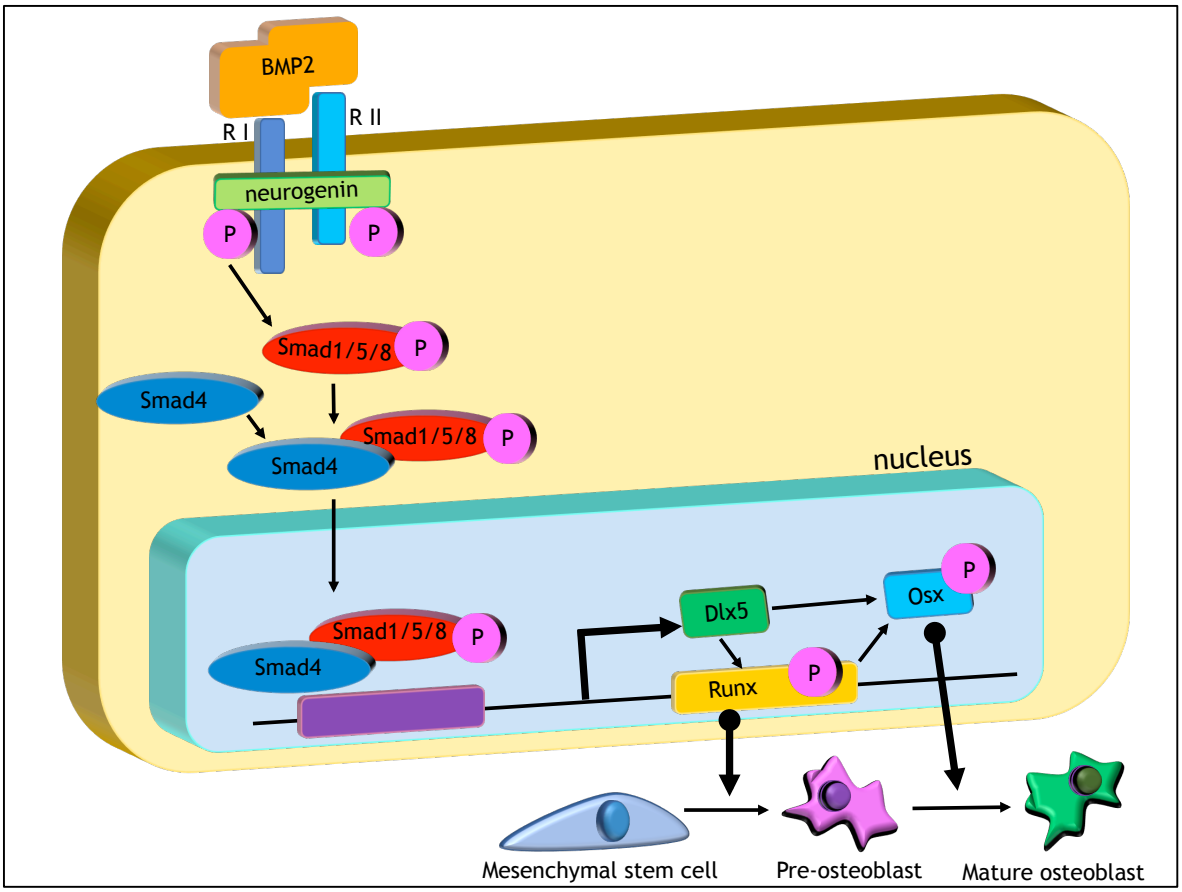

Figure 1-4 BMP-2 signalling in osteogenic differentiation
BMP-2 signalling is associated with the osteogenic differentiation of MSCs to form osteoblasts. This process occurs as the BMP-2 cytokine binds to receptors on the MSC surface, initiating a signalling cascade involving Smads. Transcription factors Runx2 and osterix become activated, leading to MSCs forming preosteoblasts and preosteoblasts forming mature osteoblasts, respectively.

1.3.3 Cytokine Secretion of MSCs

MSCs have a diverse range of roles including acting as cell sources for connective tissues, regulation of the immune response and also regulation of haematopoiesis (Aggarwal and Pittenger, 2005, Ball et al., 2007). This multifunctionality of MSCs has been attributed to the large number of cytokines and growth factors MSCs have been shown to secrete (Park et al., 2009). Despite MSCs commonly being sourced from donors of different ages, genders and ethnicities, it has been shown that the cytokine secretion profile of MSCs from distinct donors largely express common hybridisation patterns on cytokine antibody arrays (Park et al., 2009).Over 100 cytokines are known to be secreted from MSCs in normal conditions, and have been detected at a range of intensities (Park et al., 2009).

1.4 The Haematopoietic Stem Cell Niche

The concept of the HSC niche was introduced in 1978 by Schofield, and it has since been the focus of many researchers to create *in vitro* models that mimic the natural components of the niche (Schofield, 1978). The first attempt at creating such an *in vitro* niche was reported by Dexter, where a two dimensional monolayer of stromal cells extracted from the bone marrow were observed to sustain haematopoiesis *in vitro* (Dexter, 1982). However, a crucial problem existed with this model, in that the differentiation arising was restricted to certain lineages and maintenance of the stem cell population was relatively low. Later, evidence from studies in the *drosophila melanogaster* ovary showed that heterologous cell types could be found in close proximity to stem cells (Xie and Spradling, 1998). These heterologous cell types are referred to as niche cells, and it is now understood that a diverse range of HSC niche cell types exist, as outlined in Table 1-4 (Méndez-Ferrer et al., 2010, Calvi et al., 2003). To combat issues associated with the Dexter culture where the stem cell numbers in culture were low, more recent work has leaned towards using different stromal cell lines as factories to produce cytokines that regulate the maintenance and/or differentiation of HSCs.

Since the early work of Dexter, characterisation of the key components of the bone marrow niche has largely arisen from the use of conditional deletions of regulatory factors in candidate cell types in mouse models (Ding et al., 2012, Greenbaum et al., 2013). Further, imaging advances that have allowed for the visualisation of cellular localisations have also allowed for the identification of key cells with roles in HSC maintenance (Celso et al., 2009, Acar et al., 2015). A summary of the key cell types identified in such work is depicted in Table 1-4.

Cell Type	Evidence for Role in HSC Regulation	Reference
Mesenchymal Stem Cells (MSCs)	• Spatial localisation with HSCs in the BM. • High expression of HSC maintenance genes CXCL-12, KitL, Angpt1, Il7 & VCAM-1. • Conditional deletion reduces HSC number in the niche.	(Méndez-Ferrer et al., 2010)
CXCL-12 Abundant Reticular (CAR) cells	• Spatial localisation with nestin^{+} MSCs. • High expression of HSC maintenance genes SCF and CXCL-12.	(Pinho et al., 2013) (Kunisaki et al., 2013b) (Ding and Morrison, 2013)
Osteoblasts (OBs)	• Increasing the number of OBs using parathyroid hormone stimulation and Bone Morphogenic Protein 2 (BMP-2) led to an increased number of haematopoietic cells *in vivo* and *in vitro*. • Expression of HSC maintenance factor proteins IL-6, SCF, and CXCL-12 were higher in osteoblasts compared to controls. • HSCs are visualised to be attached to osteoblast cells via N-cadherin and ß-catenin junctions • Increased levels of BMP-2 signalling associated with osteoblasts through the receptor BMPR1A controls HSC number in the BM.	(Calvi et al., 2003) (Zhang et al., 2003)
Sympathetic Nerve Cells	• Mouse models with aberrant nerve conduction showed no egress of haematopoietic progenitors from the BM after GCSF stimulation • Ablation of neurotransmission indicated that norepinephrine induces OB suppression in response to GCSF, which allows for HSC release; sympathetic nerve cells regulate attraction of HSCs to the niche • Nestin^{+} MSCs that co-localise with HSCs express high levels of HSC maintenance factors	(Katayama et al., 2006) (Méndez-Ferrer et al., 2010)

Table 1-4 Cell types that regulate HSCs

1.4.1 Cellular Localisation within the HSC Niche

It is now understood that adult HSCs reside in specific BM locations, and it is more generally accepted that there are distinct niches within the BM, which was previously considered to exist as a single niche. These niches within the BM are now defined as endosteal niches, and vascular niches. Further to this, the vascular niches can be divided into arteriolar and sinusoidal niches (Zhang et al., 2003, Calvi et al., 2003, Kiel et al., 2005). The arteriolar niches are associated with supporting HSC quiescence, while the sinusoidal niches are associated with promoting HSC proliferation (Kunisaki et al., 2013a). Despite being spatially distinct and comprising different active cell types, each of the endosteal, arteriolar and sinusoidal niche types are regulators of HSC self-renewal, as shown in Figure 1-5.

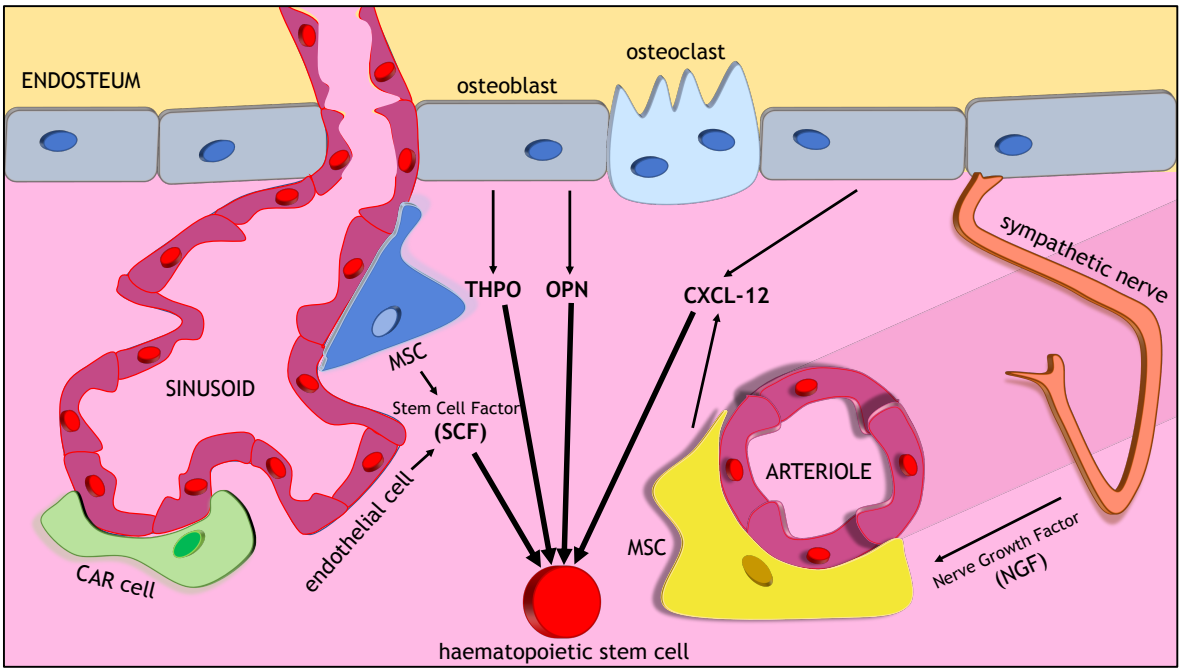

Figure 1-5 The HSC niche
The HSC niche is a dynamic microenvironment comprised of the vascular (sinusoid and arteriole) niches and the endosteal niche. Within each niche, a number of supportive cell types secrete cytokines that are responsible for regulating HSC behaviour and function. (Adapted from (Mendelson and Frenette, 2014))

The first evidence to support the existence of the endosteal niche was provided by Lord et al. in 1975, where primitive cells were shown to exist in close proximity to the endosteum of the mouse femur (Lord et al., 1975). Numerous *in vivo* studies followed this seminal work, and it was found that the osteoblasts associated with the endosteum secrete a range of cytokines associated with the expansion of haematopoietic progenitors (Taichman et al., 1996). Later work

also showed that co-transplantation of haematopoietic progenitors with osteoblasts supported engraftment and reconstitution of the haematopoietic system in lethally irradiated mice (Calvi et al., 2003). In order to understand the mechanisms by which osteoblastic cells regulate HSC self-renewal and differentiation, Calvi and colleagues have also shown that OBs express the notch ligand, Jagged-1, which is upregulated upon parathyroid hormone-induced OB activation. Activation of the parathyroid hormone 1 receptor induced notch signalling in HSCs, and this was shown to increase HSC number. Additional studies have also shown a role for Wnt signalling as a means of the OB-associated regulation of HSCs (Reya et al., 2003). When ectopic expression Wnt signalling proteins such as axin or the frizzled ligand-binding domain was induced, it was observed that reconstitution of the HSC compartment was reduced *in vivo*, and HSC growth was reduced *in vitro*. The group carrying out this work also observed that increased Wnt signalling correlated with increased expression of Notch in HSCs (Reya et al., 2003).

The first indication that another type of HSC niche may exist, in addition to the endosteal niche, was taken from the observation that HSCs are capable of self-renewal and differentiation during foetal development, before the existence of bone marrow cavities. In early human developmental biology, both endothelial cells and haematopoietic cells arise from a common embryonic precursor known as the hemangioblast, and these cell types have a close interaction throughout development (Kennedy et al., 1997). It has been shown that primary endothelial cells isolated from the yolk sac and para-aortic splanchnopleura support the maintenance and expansion of HSCs *in vitro* (Li et al., 2003). In addition, it is known that haematopoiesis occurs in the extramedullary tissues of adult humans, which lack an endosteum, for a large portion of their lives (Taniguchi et al., 1996). These observations allowed for the postulation of sinusoidal and arteriolar vascular niches, and further evidence supporting their existence has since been collected on the basis that cell types within these niches, such as endothelial cells and stromal cells, act as cytokine-producing factories for HSC regulation (Zhang et al., 2003, Kunisaki et al., 2013b).

1.4.2 The Role of Cytokines as HSC Maintenance Factors in the niche

Cytokines are a family of cell signalling molecules that may exist as peptides, proteins or glycoproteins, and regulate immunity, inflammation and haematopoiesis (Luster, 1998, Fossiez et al., 1996). The affinity of cytokines for their receptors is high, and a cytokine may exhibit autocrine, paracrine or endocrine action (Rose-John and Heinrich, 1994, Petraglia et al., 1996).

Haematopoietic cytokines are the principal regulator of haematopoiesis, and although the HSC signalling associated with these cytokines remains poorly understood, some evidence exists to suggest that these signalling molecules usually work by binding to their receptors and then activating Janus kinases (JAKs) (Leonard, 2001, Ihle et al., 1995). Depending on the receptor and cytokine combination, one of four possible Janus Kinases (JAKs) (JAK1, JAK2, JAK3 or Tyk2) becomes activated, in turn giving rise to phosphorylation other JAKs and the receptor subunit. This allows for the docking of SH2 proteins, a group of proteins that bind to phosphorylated tyrosine residues (Endo et al., 1997). Following SH2 protein docking, pathways such as the Ras pathway become activated, leading to the phosphorylation and activation of STATs (Calvisi et al., 2006). These STAT proteins are then translocated to the nucleus where they act as transcription factors, regulating the expression of genes associated with self-renewal and differentiation (Ward et al., 2000).

The cytokines associated with supporting HSCs have been largely identified by screening for stromal cells such as MSCs and OBs capable of supporting HSCs, and then using these stromal cell lines to isolate secreted proteins (Moore et al., 1997, Weisel et al., 2006). Many of these cytokines were originally selected using studies of genetically modified mice, and were then identified as HSC regulators based on their ability to support *in vitro* formation of HSC colonies.

For some time now, MSCs have been accepted as the main factories for the production of HSC supporting cytokines, but it is now understood that other cell types, such as endothelial cells, are also capable of secreting cytokines associated with HSC maintenance and proliferation. Each cell type can produce a

range of cytokines, and these cytokines can have varying effects on HSC behaviour (Table 1-5).

Table 1-5 Cytokines associated with the HSC niche

Cytokine Name	Effect on HSCs	Associated Cell Name	Reference
Stem Cell Factor (SCF)	Increases self-renewal	MSCs Osteoblasts Endothelial cells	(Ding et al., 2012) (Calvi et al., 2003) (Ding et al., 2012)
Vascular Cell Adhesion Molecule-1 (VCAM-1)	Regulates homing and adhesion	MSCs Endothelial cells	(De Ugarte et al., 2003) (Avraham et al., 1993)
Thrombopoietin (THPO)	Increases self-renewal	Osteoblasts	(Yoshihara et al., 2007) (Qian et al., 2007)
CXCL-12/SDF-1α	Increases self-renewal and retention in the BM	MSCs Osteoblasts Endothelial cells	(Greenbaum et al., 2013) (Omatsu et al., 2010)
Osteopontin (OPN)	Maintains population size Prevents apoptosis	Osteoblasts	(Stier et al., 2005)

1.4.3 Cell Surface Proteins as HSC maintenance Factors

Although many of the factors responsible for regulating the phenotype of HSCs in the niche are cytokines, cell surface proteins have also been shown to regulate HSC behaviour. For example, vascular cell adhesion molecule-1 (VCAM-1) is a cell adhesion protein, which is known to mediate interactions with a range of haematopoietic cell types (Peister et al., 2004, Frenette et al., 1998). VCAM-1 has been shown to be expressed in several cell types associated with the HSC niche, including MSCs, OBs and endothelial cells, and similarly to certain aforementioned cytokines, is considered an HSC maintenance factor by the field (Sugiyama et al., 2006).

Research in the late 1990s from Frenette and colleagues was pivotal in the identification of VCAM-1 as a HSC maintenance factor, as their experiments showed that mice treated with anti-VCAM-1 antibodies had far greater numbers of haematopoietic progenitor cells 14 hours after transplantation when compared to controls (Frenette et al., 1998). This preliminary study suggested an important role for VCAM-1 in haematopoietic cell homing to the BM, and then further evidence to support this role was also found by the same group, when it was noted that optimal recruitment of these cells to the BM following radiation was dependent on a combined action of VCAM-1 with endothelial selectins (Frenette et al., 1998).

In addition to VCAM-1, cadherin molecules have also been proposed to be involved in regulating HSC maintenance in the niche (Zhang et al., 2003). This concept was originally introduced by Zhang and colleagues when they showed that OBs and HSCs both express N-cadherin. N-cadherin is a transmembrane protein that mediates cell-cell adhesion, and is a vital component of adherens junctions (Takeichi, 1991). Following on from the seminal work of Zhang and colleagues, many other research groups have gone on to suggest that N-cadherin is required for retaining the long-term self-renewal of HSCs. For example, Haug and colleagues investigated how N-cadherin expression in HSCs correlates with their function, and found that haematopoietic cells with high N-cadherin levels were more differentiated than cells with lower levels of N-cadherin expression (Haug et al., 2008). It was observed that N-cadherin^{lo} cells were able to fully reconstitute the haematopoietic system, while N-cadherin^{hi} ones could not.

Thus, it was concluded that low expression levels of N-cadherin supports long-term self-renewal of HSCs. Since then, Hosokawa and colleagues have also identified a role for N-cadherin in HSC maintenance (Hosokawa et al., 2010). However, this group found that over-expression of N-cadherin in mouse models was sufficient to produce greater populations of slow cycling HSCs with long-term repopulating abilities (Hosokawa et al., 2010). Although both studies identify a role for N-cadherin in HSC maintenance, it is important to note that they suggest opposing effects of high levels of N-cadherin and other groups have disputed potential roles of N-cadherin (Bromberg et al., 2012, Kiel et al., 2009).

1.5 Biomaterials

Biomaterials can be defined as substances that have been engineered to interact with cells for a therapeutic or diagnostic purpose (Langer and Tirrell, 2004). Such engineering may include the production of physical cues such as topography and/or chemical cues such as growth factors (Dalby et al., 2014, Discher et al., 2009). Historically, biomaterials have been used for a diverse range of medical applications, for example as contact lenses, heart valves and hip prostheses (Ratner et al., 2004). However, the demand for medical devices and methods of cellular engineering are increasing, and so biomaterials are increasingly being used as methods of investigating or enhancing cell biology in the lab.

Some of the most commonly produced biomaterials are those that are able to mimic the natural extra-cellular matrix (ECM). These biomaterials are designed to closely recapitulate the native ECM, and thus allow for the successful culture of cells in an environment that is close to what they experience in nature (Engel et al., 2008, Anselme, 2000). The successful use of biomaterials capable of mimicking the ECM in 2D cultures has led to such biomaterials now being incorporated into 3D cultures, where the biomaterial may take the form of a 3D structure, or may be used as a base upon which cells are seeded and then surrounded with a different material (Habibovic et al., 2005, Lutolf et al., 2009).

1.5.1 Biomaterial Systems for HSC Niche Models

The clinical and financial value of HSCs is large, and consequently money and effort have been invested in developing reliable models of the HSC niche that recapitulate the fundamental interactions of the niche components (Fisk et al., 2005, Di Maggio et al., 2011). The most commonly designed model features a monolayer of stromal cells cultured in a plate, with HSCs in suspension in the media (Dexter, 1982, Ellis and Tanentzapf, 2010, Jing et al., 2010). However, more recently, researchers have been exploring the use of biomaterial-based 2D and 3D niche models in an attempt to gain tighter control and more closely mimic the BM niche *in vitro*.

It is well understood that components of the ECM can influence stem cell state (Connelly et al., 2010, Nilsson et al., 2005). In particular, the role of the ECM in HSC regulation is well-documented, and it has been shown that when HSCs are seeded on microwells, they produce their own ECM that regulates their quiescent or active states depending on the size of the well in which they sit (Connelly et al., 2010). Further, it has been shown that single ECM-associated proteins such as osteopontin (OPN) can influence HSC function (Rangaswami et al., 2006, Nilsson et al., 2005). For example, lack of OPN gives rise to a stroma-dependent increase in the numbers of LT-HSCs, as well as increased expression of JAG1 and ANGPT-1 (Nilsson et al., 2001). These results stress not only the importance of how ECM proteins can influence HSC behaviour alone, but also how they can indirectly influence HSCs by modulating the behaviour of MSCs in co-culture systems.

One of the most common features to appear in 3D models of the niche is a collagen type I gel. This gel has found commonplace use in 3D niche models as it has it has been shown to enhance the osteogenic potential of MSCs and facilitate bone-like matrix remodelling associated with the endosteal niche (Schneider et al., 2010). When constituted appropriately, the elasticity of collagen type I gels can mimic the elastic properties of the BM (Gattazzo et al., 2014). Similarly, collagen gels have been shown to have a Young's modulus of approximately 100 Pa, which is close to that of the HSC-occupied region of the bone marrow (Sobotková et al., 1988, Metzger et al., 2014). Such collagen type I gels have been effectively used to generate 3D models incorporating STRO-1^{+} MSCs

selected from the BM (Leisten et al., 2012). In a model comprising a monolayer of MSCs with a collagen gel on top and media above the collagen gel, HSCs were added into the media and allowed to either remain in suspension or migrate down through the gel. Results revealed that this model was capable of giving rise to two distinct populations of HSCs; those in suspension in the media and those within the collagen gel, in close proximity to the MSCs. Despite being simple in nature, this model elegantly illustrated the beneficial effects of a collagen gel-containing model, as it was observed that HSCs in the collagen gel had a more primitive phenotype. Further, this model demonstrated the importance of HSCs being in close contact with MSCs when maintenance of the stem cell phenotype of HSCs is desirable. Additional research has taken advantage of the ability of collagen type I to act as an ECM for *in vitro* HSC regulation models, and has shown that HSC culture within a collagen gel can give rise to increased numbers of colony-forming units and greater expression of negative cell cycle regulators (Oswald et al., 2006).

Further to the use of collagen gels in HSC niche models, biomaterials with additional stiffness, chemical and topographical characteristics are also being used to generate *in vitro* HSC niche models. For example, fibronectin-coated PET nanofibre meshes have been shown enhance the expansion and maintenance of HSCs (Feng et al., 2006). In addition, aminated nanofibre scaffolds with spacers composed of ethylene and butylene have been shown to give rise to fold increases of approximately 200 in HSC numbers (Chua et al., 2007). Thus, can be deduced that it is important to consider all physical properties when designing an *in vitro* HSC niche model.

1.5.2 Biomaterials for the modulation of MSC phenotype

The importance of including MSCs in HSC niche models is widely appreciated by the field, as it has been shown that co-culture models are better for HSC expansion and survival (Leisten et al., 2012, Jing et al., 2010). It is important to acknowledge the potential of biomaterials to modulate MSC phenotypes, as changes in MSC phenotype and protein expression levels will affect HSC phenotype and the reliability of HSC niche models (Yoshihara et al., 2007, Omatsu et al., 2010). In addition, it has been shown that OBs are important cells to feature in HSC niche models, and so investigating the potential of MSCs to

produce OBs via biomaterial application routes should be carefully considered (Nilsson et al., 2005).

Osteogenic differentiation of MSCs involves MSCs differentiating to form OBs, and is commonly induced *in vitro* by the presence of dexamethasone, ascorbic acid and ß-glycerol phosphate (Birmingham et al., 2012). Another commonly used method of inducing osteogenesis of MSCs to form OBs involves the use of Bone Morphogenic Protein 2 (BMP-2) (Ryoo et al., 2006). However, recent advances have led to an understanding that synergistic signalling leading to osteogenesis can be achieved when BMP-2 is supplied to MSCs in close proximity to adhesion-promoting RGD motifs or integrin binding sites (He et al., 2008, Llopis-Hernández et al., 2016). Inducing osteogenesis via synergistic signalling results in an increased production of OBs compared to BMP-2 signalling alone, and thus it is becoming a popular goal for new biomaterials approaches. However, the potential of synergistic signalling for HSC niche models should have particular attention paid to it, as it may provide a cost-effective means of providing a population of osteoblasts with the potential to support HSCs by secreting SCF, THPO, CXCL-12 and OPN (Nakamura et al., 2010a).

1.6 Biomaterial applications of poly (ethyl acrylate)

Poly (ethyl acrylate) (PEA) is a polymer with a hydrophobic character sufficient to induce fibronectin (FN) fibrillogenesis, a process whereby FN molecules bind together to form a network structure (Rico et al., 2009, Salmeron-Sanchez et al., 2011). This leads to the exposure of both the integrin binding domain and the growth factor binding domain of FN, allowing PEA with an adsorbed layer of FN to act as a valuable foundation for systems with cells responding to tethered growth factors (Llopis-Hernández et al., 2016).

FN is a glycoprotein that forms homodimers of two subunits of approximately 220 kDa (Erickson and Carrell, 1983). A single, carboxyl terminus disulfide bond links these subunits. Each of the subunits are made up of three types of repeating module (named Type I, Type II and Type III), and these modules mediate interactions with other molecules of FN, ECM constituents and cell surface receptors, as shown in Figure 1-6.

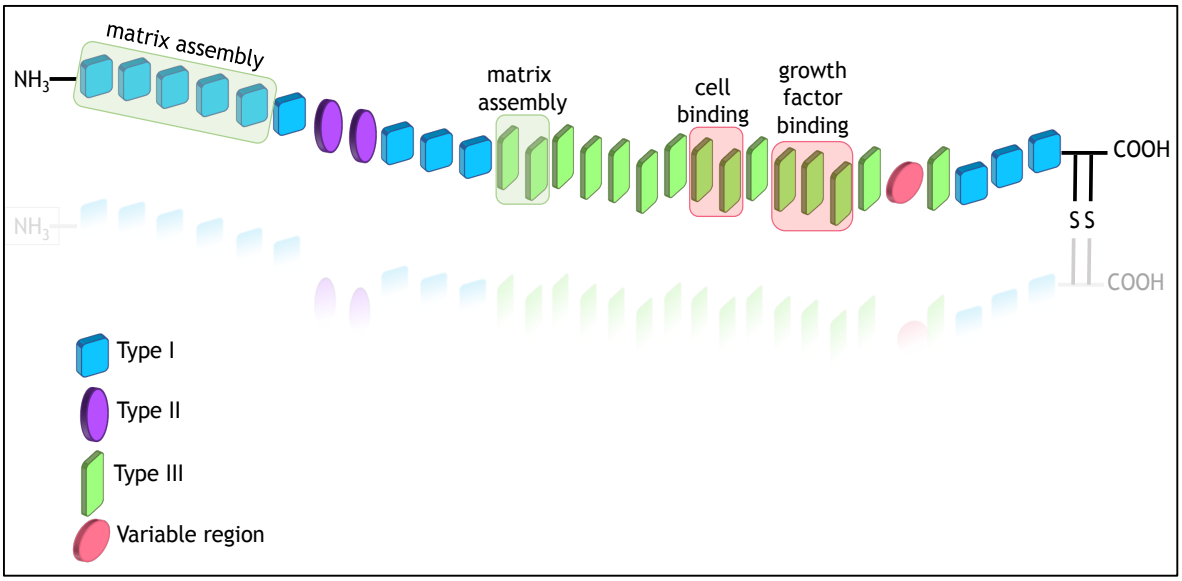

Figure 1-6 The structural organisation of a fibronectin molecule
Fibronectin is an ECM protein made up of type I, II and III repeats and functional regions. Key functional regions in fibronectin molecules include the cell binding and growth factor binding regions, located adjacent to one another. (Adapted from (Llopis-Hernández et al., 2016))

Early work showed that FN adsorption onto PEA resulted in a fibrillar FN organisation via interactions in the amino terminal 70 kDa fragment (Salmeron-Sanchez et al., 2011). Although not fully understood, it has been proposed that the interaction of PEA and FN induces conformational changes in the FN, which leads to unfolding and exposure of the FN arms. This unfolded conformation of FN has been shown to increase the surface area of FN on PEA, and has been suggested to favour protein-protein interactions between FNI_{1-5} and $FNIII_{1-2}$ domains located near the N terminus of FN (Pankov and Yamada, 2002, Dalby et al., 2018). These protein-protein interactions result in the formation of a FN network, which has the $FNIII_{9-10}$ and $FNIII_{12-14}$ domains accessible for cell interactions.

It has been shown that the open conformation of FN molecules, and resulting arrangement of FN on PEA, is sufficient to modulate cell behaviour (Ballester-Beltrán et al., 2012, Rico et al., 2016a). Published results show that myogenic differentiation of C2C12 muscle cells was enhanced on PEA + FN surfaces relative to controls (Ballester-Beltrán et al., 2012). In addition, later work has also shown that PEA + FN surfaces can also regulate MSC behaviour, and could maximise the self-renewal potential of MSCs (Rico et al., 2016b).

1.6.1 The Use of PEA Surfaces in Growth Factor Tethering

Despite these initial findings suggesting the potential of PEA surfaces for bioengineering applications, more recent findings have confirmed their value, as it has been shown that PEA + FN surfaces can also have growth factors tethered to them (Llopis-Hernández et al., 2016, Moulisová et al., 2017). Results have shown that growth factors, such as BMP-2 and VEGF can be tethered to FN, when FN is in the network conformation. This promotes synergistic presentation of the adjacent growth factor and integrin binding sites, and has been shown to elicit a valuable range of effects in different cell types. For example, it has been shown that BMP-2 bound to PEA + FN is sufficient to promote osteogenic differentiation in MSCs *in vitro*, as well as full regeneration of a non-healing none defect *in vivo* (Llopis-Hernández et al., 2016).

Such substrate bound growth factors are of great interest to the medical and scientific communities, as soluble growth factors are normally used in medical applications at supraphysiological concentrations, which is both dangerous and costly (Helfand, 2013). BMP-2 is one of the most frequently used growth factors in regenerative medicine, and despite it having FDA approval and being considered as “near-perfect” due to its lack of harmful effects reported in industry supported trials, it is now known to be life-threatening when supplied in high doses (Carragee et al., 2011). Thus, the use of solid substrate bound growth factors is highly appealing, as it has been shown that substrate bound growth factors result in sustained growth factor signalling, meaning that up to a 300 fold lower dose of substrate bound growth factor can elicit the same response as those in the soluble form (Fan et al., 2007, Zhu and Clark, 2014a, Llopis-Hernández et al., 2016).

1.6.2 Integrins and Cell Adhesion at the Material Interface

Cell adhesion to the interface of biomaterials such as PEA is mediated by their adhesion to intermediate proteins, known as ECM proteins. Using transmembrane receptors called integrins, cells can adhere to these intermediate ECM proteins, a common example of which is FN (Salmeron-Sanchez et al., 2011). Integrins are able to bind to peptide motifs on ECM proteins, and an example of such a motif is the Arg-Gly-Asp (RGD) cell attachment site (Ruoslahti, 1996). The binding of

cells to these RGD motifs induces G protein activation and phosphorylation cascades within cells (Luttrell et al., 1999). The phosphorylation cascades involve the phosphorylation of Rho-associated protein kinase (ROCK) and myosin light chain kinase (MLCK), which leads to actin/myosin contraction and the cytoskeleton of the cell exerting forces on the integrins (Seo et al., 2011). These forces cause the cytoskeleton to draw groups of integrins together, in a process known as clustering, which results in the formation of cell adhesions (Cavalcanti-Adam et al., 2008). Once these cell adhesions have formed, protein kinases collect at these sites, including focal adhesion kinase (FAK) (Sieg et al., 2000). These kinases cause further intracellular signalling cascades to take place, exerting control over cell fate. For example, it has been shown that MSCs require large adhesions in order to differentiate into OBs (Dalby et al., 2007). The large adhesions associated with OB differentiation induce an intracellular tension in the cytoskeleton that has been shown to activate ROCK, which in turn activates genes associated with OB differentiation (Dalby et al., 2007, McBeath et al., 2004).

1.6.3 Integrin/Growth Factor Crosstalk

Growth factors (GFs) are soluble, secreted polypeptides that can elicit a diverse range of responses in cells that may be associated with migration, proliferation, differentiation and survival. These molecules normally work in a local, paracrine fashion due to their short half-lives (Kontermann, 2011). Although the presentation of GFs is a valuable application for biomaterials, the efficiency of such GFs can be enhanced when there is the simultaneous activation of integrins and GF signalling networks (Phelps et al., 2010, Shekaran et al., 2014). This allows for lower concentrations of GFs to be used, avoiding the dangerous and harmful side effects of high doses (Helfand, 2013). A key example of how this co-presentation of integrins and GFs can positively influence bioengineering applications is how vascularisation associated with the presentation of VEGF in hydrogels with protease-degradable crosslinks can be enhanced when these gels are functionalised with RGD cues (Phelps et al., 2010). These RGD cues are detected by integrins and are used as attachment points, and so the results of Phelps and colleagues stresses the potential benefit to expressing cell attachment points in bioengineering applications alongside GFs (Chua et al., 2008). In addition, Shekaran and colleagues recently published results showing

that protease-degradable poly (ethylene glycol) (PEG) synthetic hydrogels, functionalised with integrin specific peptides, could promote bone regeneration more efficiently than when the integrin specific protein was absent (Shekaran et al., 2014). Although the precise molecular mechanisms concerning this apparent crosstalk between integrins and growth factors remain to be understood, Schwartz and Ginsberg have recently described integrins as functioning as nodes within webs of adhesion and GF signalling networks (Schwartz and Ginsberg, 2002). It is important that efforts are made to elucidate the functional mechanisms in these networks, as it is apparent that integrin/GF crosstalk holds the key to developing new biomaterial applications wherein low doses of GFs can be used to elicit valuable responses in cells.

1.7 The Use of Growth Factors and ECM Matrices in Bioengineering Applications

Many growth factors have ECM binding domains, and can bind to ECM components such as heparan sulphate and FN (Ashikari-Hada et al., 2004, Martino and Hubbell, 2010). As a result, growth factors have great potential in bioengineering applications, and are often used with biomaterials to mimic and/or recapitulate the natural ECM (Zhu and Clark, 2014b, Llopis-Hernández et al., 2016).

In the ECM, the varying distribution of ECM components with GF binding often means that growth factors are presented in spatio-temporal gradients, providing different levels of cell signalling at different locations (Discher et al., 2009). Thus, achieving an understanding of quantitative spatiotemporal information regarding GFs is a focus of many bioengineering researchers. For example, therapeutic neovascularisation is a division of regenerative medicine that seeks to rebuild networks of blood vessels (Li et al., 2006). However, it is acknowledged that the concentration and spatiotemporal localisation of growth factors in neovascularisation is critical to the successful development of 2D and 3D models of this process, and so many groups are focused on the development of mathematical models that can pinpoint where growth factors should be concentrated (Cao and Mooney, 2007). One of the main reasons that spatiotemporal presentation of GFs is important, is that presentation of such GFs in excess, or with a lack of precision, can often have catastrophic effects. As

mentioned in the previous section, high doses of BMP-2 can be life threatening (Tannoury and An, 2014). Similarly, excessive presentation of vascular endothelial growth factor (VEGF) can result in the VEGF moving away from the target site and inducing the formation of dormant tumours in non-target sites (Holmgren et al., 1995). It is therefore imperative that the concentration and spatiotemporal localisation of GFs are carefully considered whenever they are used in bioengineering applications.

1.7.1 Evidence of the Success of Direct Growth Factor Presentation in Bioengineering Applications

Although GFs can be incorporated into bioengineering applications in a number of ways, direct presentation of GFs is popular as it minimises model complexity. Typically, this direct presentation of GFs either involves physical adsorption of GFs on to biomaterials or the direct covalent immobilisation of GFs to biomaterials (Woo et al., 2001, Chen et al., 2013). These methods of direct GF presentation have become increasingly popular because they frequently involve tethering GFs to ECM proteins with integrin binding domains. This means that the bioengineered platform is not only a means of GF presentation, but also acts as a favourable platform for cell adhesion (Hutchings et al., 2003). Further, direct presentation of GFs has also been associated with extending their half-life, making them an economically valuable means of GF presentation (Bramono et al., 2012). The successful presentation of GFs coupled with the promotion of cell adhesions has resulted in a number of successful studies illustrating the potential of direct GF presentation, as summarised in Table 1-6.

Table 1-6 Examples of the use of directly presented growth factors

Growth Factor	Details of Success when Directly Presented in Bioengineering Applications	Reference
VEGF	VEGF was shown to enhance cell adhesion and survival of endothelial cells when bound to the ECM VEGF was shown to promote vascularisation and enhance tissue formation *in vivo* when bound to FN adsorbed on PEA surfaces	(Hutchings et al., 2003) (Moulisová et al., 2017)
BMP-2	BMP-2 was shown to enhance the osteogenic differentiation of MSCs, and to promote the healing of a wound defect *in vivo* when bound to FN absorbed on PEA surfaces BMP-2 was shown to have an elongated half life and to induce the osteogenesis of C2C12 myoblasts when bound to heparan sulphate ECM bound BMP-2 was shown to induce β3 integrin–dependent C2C12 cell spreading in C2C12 myoblasts, overriding the soft signal of the biomaterial	(Llopis-Hernández et al., 2016) (Bramono et al., 2012) (Fourel et al., 2016)
NGF	NGF bound to laminin and fibronectin was shown to approximately double the growth of human foetal sensory neurons over a ten day period NGF bound to fibronectin or laminin adsorbed on poly-L-lysine resulted in a 2-fold enhanced growth of neurites from PC12 cells, leading to accelerated axon generation	(Evercooren et al., 1982) (Orlowska et al., 2017)
PDGF	PDGF bound to fibronectin was shown to enhance the survival of mouse fibroblasts PDGF bound to fibronectin was shown to stimulate growth and migration of smooth muscle cells, and PDGF co-adsorbed with BMP-2 on fibronectin was sufficient to induce healing in a critical size cavalarial defect in rats. PDGF also enhanced MSC recruitment to the defect	(Lin et al., 2014) (Martino and Hubbell, 2010, Martino et al., 2011)

1.7.2 Justification for the Use of Directly Presented GFs in HSC Niche Models

As outlined in Table 1-6, evidence exists that demonstrates how directly presented GFs can elicit profound cellular responses when used in bioengineering applications. As discussed in sections 1.3.2 and 1.5.2, directly presented BMP-2 is a strong candidate for use in HSC niche models containing an MSC/HSC co-culture, as BMP-2 stimulates osteogenic differentiation of MSCs and may thus help to mimic the endosteal niche (Llopis-Hernández et al., 2016, Lévesque et al., 2010). However, it is important to acknowledge the potential significance of PDGF and VEGF in this context, as these GFs are vascular, and thus are strongly postulated to have a role in regulating HSC function within the vascular niche (Pinho et al., 2013, Hooper et al., 2009). Finally, it should also be acknowledged that NGF is likely to be released by the sympathetic nerves of the vascular niche, and has been identified as being linked to the circadian control of the HSC niche (Hanoun et al., 2015, Lucas et al., 2013). In summary, novel research investigating the potential of BMP-2, PDGF, VEGF and NGF within HSC niche models is justified.

1.7.3 The Use of ECM Matrices and their Potential in HSC Niche Models

As described, numerous bioengineering applications have been successful using GFs and ECM matrices. However, little research has been carried out using both GFs and ECM matrices within HSC niche models, and so future work in the bioengineering field may strive to fill this void, testing if using GFs in conjunction with ECM matrices may produce more functional and biomimetic HSC niche models.

Very few examples of the use of GFs and ECM matrices in the engineering of *in vitro* HSC niche models exist. The one published paper that does touch this subject was published in 2014 (Torisawa et al., 2014). In this model, a biomimetic bone marrow-on-a-chip model was created, using PDMS and a collagen type I gel that was infused with bone powder and bone morphogenic proteins, BMP-2 and BMP-4. The results show that a biomimetic niche model with similar architecture and physiology to that of the natural BM niche could be

created. In addition, it was shown that the model could produce similar proportions of HSCs to those found *in vivo*.

Although work considering the addition of GFs into HSC niche model bioengineering has not been extensively carried out, it is important to acknowledge the results obtained from ECM matrix-based models, and to consider the profound effects that these matrix-based models alone can have (Table 1-7).

(Table 1-7 ECM Matrices in HSC Niche Models

Niche Model Composition	ECM Matrix Used	Results	Reference
MSCs either below, or embedded in, collagen gels. HSCs added to the top of the gel and allowed to migrate in or through the gel	Collagen type I or collagen type III gel	Bone marrow MSCs can support the $CD34^+$ phenotype of HSCs in culture, while umbilical cord MSCs cannot. FN and collagen can enhance HSC migration and may contribute to phenotype maintenance.	(Leisten et al., 2012)
3D deceullularised bone scaffolds, with collagen + FN gels	Collagen type I & FN	Bone marrow MSCs and human umbilical cord vascular endothelial cells cultured in the presence of collagen type I + FN maintained the multipotent differentiation capacity of HSCs	(Huang et al., 2016)
Bone marrow MSCs cultured with HSCs in 3D bioceramic scaffolds	Collagen type I & fibrin	Both scaffolds supported expansion of $CD34^+$ cells, which was enhanced when MSCs were added to the cell culture. HSCs cultured in these 3D scaffolds with MSCs showed optimal engraftment and multilineage differentiation properties.	(Ferreira et al., 2012)
Microcavity arrays used for high-density cell culture of MSCs and HSCs in a 3D model	Collagen type I	CD34 expression was maintained for 14 days and HSC multilineage differentiation capacities remained functional after 14 days of culture.	(Wuchter et al., 2016)

1.8 Aims and Objectives

The aim of this thesis is to create a biomimetic HSC niche model capable of inducing an HSC supportive phenotype in MSCs, using PEA surfaces, FN, GFs, a collagen gel and a specialised media formulation. The model design is primarily based on the use of PEA + FN + GF substrates, upon which a monolayer of STRO-1^+ MSCs will be cultured. STRO-1^+ MSCs were chosen because they are: easily attainable from collaborators; cost-effective; known to have an HSC-supportive phenotype (Bensidhoum et al., 2004, Gonçalves et al., 2006) A type I collagen gel will then be loaded on top of the MSCs to create a 3D environment, mimetic of the stiffness of the BM niche. After a 2-week period of culture, HSCs will be added to the model, and left for approximately one week before being phenotyped to assess their proliferation and differentiation profiles.

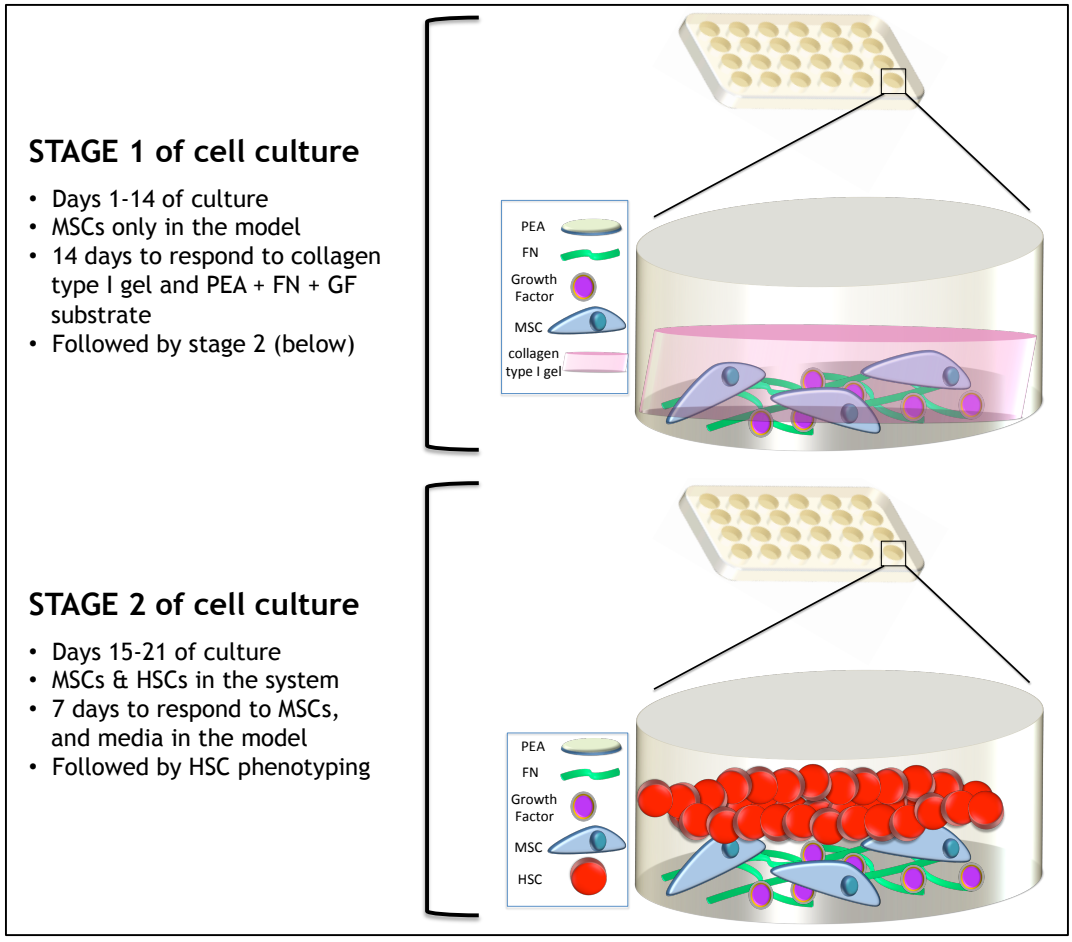

Figure 1-7 Schematic of in vitro HSC niche model during different stages of cell culture
The *in vitro* HSC niche model developed in this thesis comprises two distinct stages; from days 1-14 of the culture, MSCs only are present, to allow ample time for response to the PEA + FN + GF substrate, as well as the collagen gel. The HSCs are added to the model in stage 2, following removal of the collagen gel to reduce the analytical complexity of the model (as described in Chapter 4).

In order to meet the aim of this thesis, the following objectives are required to be met:

1. Characterisation of PEA surfaces

    - Verification of the formation of FN networks on PEA using atomic force microscopy (AFM).

    - Quantification of the surface density of growth factors when adsorbed on PEA + FN surfaces, using enzyme linked immunosorbent assays (ELISAs).

    - Verification of the elastic properties of the collagen type I gel using rheology.

2. Characterisation of the phenotype of MSCs cultured on PEA + FN + GF surfaces

    - Verification that MSCs maintain their stem cell phenotype, to some extent, when cultured on PEA + FN + GF surfaces.

    - Verification that MSCs undergo osteogenic differentiation, to some extent, when cultured on PEA + FN + GF surfaces.

    - Determine if MSCs express cell surface markers associated with HSC maintenance when cultured on PEA + FN + GF surfaces.

    - Determine if MSCs express secreted proteins associated with HSC maintenance when cultured on PEA + FN + GF surfaces.

    - Assess the effect of changing media type on MSC phenotype, in terms of maintaining stem cell phenotype, inducing osteogenesis and inducing expression of HSC maintenance markers.

- Determine the effect of culture on PEA + FN + GF on the abundance of metabolites present within MSCs, to investigate phenotypic differences in these cells relative to controls.

3. Characterisation of the phenotype of HSCs cultured in models featuring PEA + FN + GF surfaces

    - Determine the capacity of models featuring PEA + FN + GF surfaces to support maintenance of the $CD34^{+}CD38^{-}$ phenotype of HSCs.

    - Assess the capacity of PEA + FN + GF surfaces to induce the expression of the multipotent progenitor $CD34^{+}CD38^{+}$ phenotype when HSCs are cultured in models.

    - Assess the capacity of PEA + FN + GF surfaces to induce the expression of the progenitor $CD34^{-}CD38^{+}$ phenotype when HSCs are cultured in models.

    - Determine if PEA + FN + GF surfaces are sufficient to influence HSC differentiation down lymphoid, myeloid and erythroid lineages.

CHAPTER 2

Chapter 2 Materials and Methods

2.1 Materials and Reagents

2.1.1 Cell Culture Reagents

Reagent	Supplier
Dulbecco's Modified Eagle's Medium (DMEM)	Sigma-Aldrich, UK
Foetal Bovine Serum (FBS)	Sigma-Aldrich, UK
Human AB Serum (HS)	Sigma-Aldrich, UK
Minimum Essential Medium Non-Essential Amino Acids (MEM-NEAA)	Sigma-Aldrich, UK
L-Glutamine (200 mM) (100x stock)	Invitrogen, UK
Fungizone® Amphotericin B (250µg/ml)	Gibco by Life Technologies, UK
Sodium Pyruvate (100 mM)	Sigma-Aldrich, UK
Penicillin-Streptomycin (10 mg/ml stock)	Sigma-Aldrich, UK
Trypsin (10x solution)	Sigma-Aldrich, UK
Versene*	produced in house
Trypsin/Versene solution*	produced in house
4-(2-hydroxyethyl)-1-piperazine-ethanesulphonic acid (HEPES)	Fisher Scientific, UK
Phosphate-Buffered Saline (PBS)	Sigma-Aldrich, UK
HEPES saline*	produced in house
Ethylenediaminetetraacetic acid (EDTA)	Sigma-Aldrich, UK
Sodium Chloride	VWR Chemicals
Potassium Chloride	VWR Chemicals
Rat Tail Collagen Type I, > 2 mg/mL	First Link Ltd., UK
10x Modified Eagle's Medium	First Link Ltd., UK
Sodium Hydroxide (0.1 M)	Sigma-Aldrich, UK
Stem Cell Factor	Peprotech, UK
Flt3 Ligand	Peprotech, UK
Thrombopoietin	Peprotech, UK
Interleukin 3	Peprotech, UK
Interleukin 6	Peprotech, UK
Bovine Insulin Transferrin (BIT)	Stem Cell Technologies, UK
Iscove's Modified Dulbecco's Media (IMDM)	Thermo Fisher Scientific, UK

2.1.2 PEA/PMA Proteins

Reagent	Supplier
Fibronectin	Sigma-Aldrich, UK
Bone Morphogenic Protein-2 (BMP-2)	Sigma-Aldrich, UK
Nerve Growth Factor (NGF)	Sigma-Aldrich, UK
Platelet Derived Growth Factor (PDGF)	Sigma-Aldrich, UK
Vascular Endothelial Growth Factor (VEGF)	Sigma-Aldrich, UK

2.1.3 In Cell Western (ICW) Reagents

Reagent	Supplier
Odyssey Blocking Buffer	LI-COR, UK
IRDye Conjugated goat anti-mouse secondary antibody	LI-COR, UK
IRDye Conjugated goat anti-rabbit secondary antibody	LI-COR, UK
CellTag 700 Stain	LI-COR, UK
Tween 20	Sigma-Aldrich, UK
Phosphate Buffered Saline (PBS)	Sigma-Aldrich, UK

2.1.4 Immunostaining Reagents

Reagent	Supplier
Formaldehyde (38%)	Fisher Scientific, UK
Sucrose	Fisher Scientific, UK
4-(2-hydroxyethyl)-1-piperazine- ethanesulphonic acid (HEPES)	Fisher Scientific, UK
Magnesium Chloride Hexahydrate	Sigma-Aldrich, UK
Sodium Chloride	VWR Chemicals
Phosphate Buffered Saline	Sigma-Aldrich, UK
Bovine Serum Albumin (BSA)	Sigma-Aldrich, UK
Tween 20	Sigma-Aldrich, UK
Rhodamine Phalloidin	Molecular Probes, Life Technologies
Horse Biotinylated anti-rabbit IgG	Vector Laboratories, UK
Horse Biotinylated anti-mouse IgG	Vector Laboratories, UK
Fluorescein Streptavidin	Vector Laboratories, UK
Vectashield Mounting Medium (with DAPI)	Vector Laboratories, UK

2.1.5 Primary Antibodies for Immunostaining and ICW

Reagent	Supplier
Anti-STRO-1 antibody	Santa-Cruz, USA
Anti-ALCAM antibody	Abcam, UK
Anti-nestin antibody	Abcam, UK
Anti-osteocalcin antibody	Santa-Cruz, USA
Anti-osteopontin antibody	Santa-Cruz, USA
Anti-stem cell factor antibody	Abcam, UK
Anti-VCAM-1 antibody	Abcam, UK

2.1.6 Scanning Electron Microscopy (SEM) Reagents

Reagent	Supplier
Glutaraldehyde	Sigma-Aldrich, UK
Sodium cacodylate	Agar Scientific, UK
Osmium tetroxide	OxKem, UK
Uranyl acetate	Sigma-Aldrich, UK
Hexamethyldisilazane	Fluka Analytical, UK

2.1.7 Primary Antibodies for FLOW Cytometry

Reagent	Supplier
Anti-lineage (Lin) Cocktail (FITC fluorophore)	Invitrongen, UK
Anti-CD34 (PE fluorophore)	eBioscience, UK
Anti-CD38 (Cy7 fluorophore)	Invitrongen, UK
Anti-CD45 (A7 fluorophore)	Invitrongen, UK
Anti-CD7 (BV421 fluorophore)	BD Biosciences, UK
Anti-CD36 (APC fluorophore)	BD Biosciences, UK
Anti-CD41a (FITC fluorophore)	BD Biosciences, UK

2.2 Preparation of Cell Culture Solutions

Typsin/Versene Solution

Typsin/Versene solution was used to detach STRO-1$^+$ MSCs from substrates. The solution comprised a 1:20 Trypsin:Versene volume ratio. The versene solution was made in house using the following reagents:

- 150 mM NaCl
- 5 mM KCl
- 5 mM glucose
- 10 mM HEPES
- 0.5 % (v/v) phenol red solution

The pH was adjusted to 7.5 and the solution was autoclaved prior to use for sterility purposes.

HEPES saline solution

HEPES saline solution was used to wash cells prior to detachment with the trypsin/versene solution. It was made in house, as follows:

- 150 mM NaCl
- 5 mM KCl
- 5 mM glucose
- 10 mM HEPES
- 1 mM EDTA
- 0.5 % (v/v) phenol red solution

The pH was adjusted to 7.5 and the solution was autoclaved prior to use for sterility purposes.

Modified DMEM (standard media)

Modified DMEM was used as a standard cell culture media, and was made as follows:

- 500 mL DMEM
- 50 mL FBS or 10 mL FBS (depending on experiment)
- 10 mL Penicillin-streptomycin
- 5 mL Modified Eagle's Medium non-essential amino acids
- 5 mL sodium pyruvate

Human Serum (HS) Media

HS media was used as an alternative to the standard cell culture media, and was made as follows:

- 500 mL DMEM
- 10 mL HS
- 10 mL Penicillin-streptomycin
- 5 mL Modified Eagle's Medium non-essential amino acids
- 5 mL sodium pyruvate

Serum Free Media (SFM) Base

The SFM media base was used for the cell culture in experiments where HSCs were present. Following preparation of this base, either 3 or 5 GFs were added to make the 3GF or 5GF media types, respectively. The SFM base was made as follows:

- 98.75 mL of IMDM
- 25 mL of BIT
- 1.25 mL of L- glutamine

5GF Media

To make the 5GF Media, the appropriate volume of SFM base was taken, and the following 5 growth factors were added;

- SCF [50 ng/mL]
- Flt3 Ligand [50 ng/mL]
- TPO [25 ng/mL]
- IL-3 [50 ng/mL]
- IL-6 [50 ng/mL]

3GF Media

To make the 3GF Media, the appropriate volume of SFM base was taken, and the following 3 growth factors were added:

- SCF [100 ng/mL]
- Flt3 Ligand [100 ng/mL]
- TPO [50 ng/mL]

Cell Fixation Solution

- 90 ml of PBS solution
- 10 ml of Formaldehyde (38%)
- 2 g of Sucrose

Cell Permeabilisation Buffer

- 100 ml of PBS solution
- 10.3 g of Sucrose
- 0.292 g of Sodium Chloride
- 0.06 g of Magnesium Chloride Hexahydrate
- 0.476 g of HEPES
  (adjust the solution made above to pH 7.2)
- 0.5 mL of Triton X

FACS Buffer

- 5% FBS
- 1% BSA
- in PBS

2.3 General Cell Culture Methods

2.3.1 STRO-1$^+$ MSC Culture

STRO-1$^+$ MSCs were cultured in a T75 flask with standard lab media (modified DMEM) at 37 ^oC with 5% CO_2. When the cells reached confluency, the media was removed and cells were rinsed once with 5 mL of HEPES saline solution at 37 ^oC. Cells were then detached from the surface using 5 mL of trypsin/versene solution at 37 ^oC for 5 minutes. 5 mL of fresh, sterile modified DMEM was added to the trypsin/versene to neutralise the active trypsin, and the cell suspension was transferred to a universal tube and centrifuged for 4 minutes at 1400 rpm. The supernatant was removed following centrifugation, and the cell pellet was re-suspended in fresh, sterile modified DMEM of an appropriate volume. Once cells had reached confluence, they were passaged and split into 3 flasks.

2.3.2 Bone Marrow Extraction

Bone marrow samples were split into two equal volumes, bone chips were discarded and the remaining samples were centrifuged for 10 minutes at 1400 rpm. The supernatants were discarded and the pellets were re-suspended in 10 mL of fresh, sterile modified DMEM. The cell suspensions were then centrifuged for 10 minutes at 1400 rpm. The supernatants were discarded, and the cell pellets were re-suspended in 10 mL of fresh, sterile modified DMEM. The cell suspensions were then slowly overlaid onto a 7.5 mL Ficoll-Paque^{TM}, and centrifuged for 45 minutes at 1513 rpm. The central layers were extracted and placed into a universal with 10 mL of fresh, sterile modified DMEM. These universals were centrifuged for 10 minutes at 1400 rpm, and then the supernatant was removed and discarded, and the pellets were re-suspended in 10 mL of fresh, sterile DMEM before the centrifugation step was repeated. The supernatants were discarded and each pellet was re-suspended in 10 mL of fresh, sterile modified DMEM before being transferred into a vented flask, cultured at 37 ^oC at 5% CO_2.

2.3.3 STRO-1 positive selection using Magnetic-Activated Cell Sorting (MACS)

Selection of STRO-1^+ MSCs was carried out at the University of Southampton, by Ms Julia Wells, in the laboratory of Professor Richard Oreffo. The cells were derived from bone marrow tissue that would normally be discarded following routine total hip replacement surgery. Aspirate extracted from the trabecular bone marrow was centrifuged at 250 g for 4 minutes at 4 ^oC. The supernatant was discarded, and cells were re-suspended in modified alpha-MEM, before being passed through a 70 μm pore mesh. Red blood cells were removed using lymphoprep gradient solution with centrifugation. Cells in the buffy coat fraction were re-suspended in 10 mL of HEPES saline solution, and then incubated with a STRO-1 antibody in hybridoma supernatant. Human anti-IgM magnetic microbeads (Miltenyi Biotech, UK) were incubated with the cells of the buffy coat fraction, and cells positively labelled for STRO-1 were retained by the magnetic column used with the MACS kit. These STRO-1^+ MSCs were eluted from the column and transferred to T75 cell culture flasks for expansion, before being transported to the laboratory in Glasgow after reaching 80% confluency. Cells were maintained in the Glasgow laboratory as outlined in section 2.3.1.

2.3.4 Monolayer STRO-1^+ Culture on Surfaces

STRO-1^+ MSCs were seeded at $1x10^4$ cells per 12 mm diameter coverslip, for a period of 21 or 19 days, depending on the experiment. After 3 days of culture on the surfaces, a collagen gel was added to each well with a coverslip and cells in it. The collagen gel was allowed to form, and 0.5 mL of media was added on the same day. Media was changed on days 3, 6, 9, 12, 15 and 18 of cell culture. For experiments requiring further study of the STRO-1^+ cells, cell culture would be terminated on day 19 or day 21 depending on the experiment, by removing the media, rinsing once with sterile PBS and fixing the cells using cell fixation solution.

2.3.5 Fixation of STRO-1^+ MSCs

STRO-1^+ MSCs were fixed on the final day of their culture. The cell culture media was removed, cells were rinsed once with sterile PBS and cell fixation solution was added at 200 μL per well of a 24-well plate. The plate was incubated for 15

minutes at room temperature, before the fixation solution was removed and 200 µL of sterile PBS was added to prevent samples from drying.

2.3.6 $CD34^+$ HSC Culture

$CD34^+$ cells were obtained commercially from CalTag MedSystems, UK. They were stored at -80 ^oC in liquid nitrogen until required. When the cells were required, the vial of cells was transported from the -80 ^oC freezer, and immediately transferred to a 37 ^oC water bath, where it was left for 3 minutes to ensure defrosting. Cells were transferred to a 15 mL falcon tube, and 10 mL of SFM base media was added to the tube. The cell suspension was centrifuged for 10 minutes at 400 g, and the cell pellet was re-suspended in 2mL of 3GF or 5 GF media, depending on the media type being used for the rest of the experiment. Cells were counted using a haemocytometer and trypan blue, and then the remaining cell suspension was transferred to a central well of a 6 well plate and left overnight in an incubator at 37 ^oC and 5% CO_2.

Cells were seeded the day after being brought up from frozen. The cells were counted on this day, and the cell suspension was transferred from the central well of a 6-well plate to a 15 ml falcon tube. 20 µl of cells were taken from the well and transferred to an eppendorf tube for phenotyping via FLOW cytometry. The appropriate volume of 3GF or 5GF media was added to the remaining volume of cell suspension, to allow for the cells to be seeded at 5 x 10^4 cells per well of a 24-well plate. As these cells are non-adherent, it was not possible to change the media once the HSCs were added to the wells containing the polymer-coated coverslip, MSCs and HSCs. Thus, once the HSCs were added to the wells, they remained in the plate for 5 days.

2.4 General Material Preparation Methods

2.4.1 PEA and PMA Sample Preparation

PEA and PMA bulk polymers were synthesised using radical polymerisation of ethyl acrylate and methyl acrylate, respectively, initiated by benzoin as the photoinitiator at 1 wt %. Polymer solutions were prepared by dissolving PMA bulk polymers at 6 % w/v and PEA bulk polymers at 4 % w/v.

Glass coverslips of 12 mm diameter were sonicated in ethanol for 30 minutes and were rinsed with fresh ethanol before being dried in an oven at 60 ^{o}C for 30 minutes. Coverslips were left to cool to room temperature before 100 µl of PMA or PEA solutions were deposited onto the glass coverslips. Coverslips were spincoated with the PMA/PEA at a velocity of 3000 rpm for 30 seconds. Following spincoating, samples were dried *in vacuo* at 60 ^{o}C for 2 hours. Samples were sterilised for 30 minutes in UV light.

2.4.2 FN Coating of PMA and PEA Samples

Human plasma FN solution was prepared by diluting FN stock solutions to 20 µg/mL in Dulbecco's phosphate buffered saline (DPBS). PMA- or PEA-coated glass coverslips were coated with FN solution for 1 hour. Following FN adsorption, samples were washed once with DPBS before being transferred to wells of a 24-well plate and covered with 0.5 mL of DPBS for up to 4 hours before cell seeding.

2.4.3 BMP-2/NGF/PDGF/VEGF Coating of PEA Samples

PEA + FN + GFs samples were prepared by coating PEA samples with FN as outlined above. After the wash step, solutions of BMP-2, NGF, PDGF or VEGF at concentration 25 ng/mL were produced, and 100 mL of the appropriate growth factor was added to PEA + FN surfaces and incubated at room temperature for 2 hours. For combined GF surfaces, where more than one GF was adsorbed at once, 25 ng/mL solutions of the appropriate GFs were made and mixed in a 1:1 volume ratio.

2.4.4 Collagen Gel Preparation

All reagents used to make the gels were kept at 4 ^{o}C before preparing the gels. Gels were made in batches of 5-6ml, as producing a larger volume of gel would result in the gel setting before it was possible to distribute it in the relevant number of wells. To make one batch of gels, the following reagents were used;

- 2.5 ml of Rat tail collagen solution
- 1.0 ml of 0.1 M NaOH
- 0.5 ml of 10x DMEM
- 0.5 ml of FBS or HS (depending on the experiment)
- 0.5 ml of media (either DMEM with 10% FBS, 2% FBS or 2% HS depending on the experiment)

The FBS/HS, 10x DMEM and the media were all added to universal tube and stored on ice. In another universal tube, the NaOH and collagen were inverted together several times to mix. Following mixing, the NaOH/collagen solution was added to the serum/10xDMEM/media mixture, resulting in the formation of a yellow colour. To neutralise the collagen, more NaOH was added dropwise until a constant pink colour was observed, indicative of the neutralisation. The pH of the final solution was further checked using a pH probe, to ensure a pH range between 7.0 and 7.5. The final collagen solution was distributed between 5-6 wells of a 24-well plate, with 1 ml of collagen solution added per well. Plates were then incubated at 37 ^{o}C and 5% CO_2 for at least 30 minutes until the gels had formed. Following formation of the gel, 0.5 ml of the appropriate media for cell culture was added.

2.5 Statistical Analyses

Appropriate statistical tests were performed using Graphpad Prism 6 software. D'Agostino-Pearson tests were carried out to check for normality in data sets. If normal distribution of data points existed, one-way ANOVA, with multiple comparisons for data sets with three groups or more, was used followed by a Tukey post-hoc test. Failure to satisfy the requirements of a normality test resulted in the use of non-parametric, Kruskal-Wallis multiple comparisons tests. The statistical significance of results was determined by calculating the probability of the null hypothesis being true, using a pre-specified threshold (p-

value) of 0.05. If the confidence level was lower than 5%, the null hypothesis was rejected and the result was classified as being statistically significant.

CHAPTER 3

Chapter 3 Material Characterisation

3.1 Introduction

3.1.1 The Importance of MSCs and OBs in HSC Niche Models

The HSC niche in the bone marrow is home to both MSCs and HSCs, and it is understood that the MSCs dynamically regulate HSC behaviour in two main ways; by expression on cell surface markers, such as VCAM-1; by the expression of soluble cytokines known as HSC maintenance factors, such as SCF, CXCL-12 and THPO (Calvi et al., 2003, Ding and Morrison, 2013). The expression of these proteins regulates HSC quiescence, proliferation and differentiation, and is thus essential for homeostasis and life.

The importance of MSCs in keeping HSCs alive and functional is well understood, and thus many HSC niche models are designed to incorporate MSCs (Leisten et al., 2012, Ferreira et al., 2012). Some models feature the use of MSCs as an unmodified stromal layer, whereas more complex models are now investigating the potential of MSCs in conjunction with biomaterials that can enhance their role (Leisten et al., 2012). For example, it is known that certain biomaterials have the capacity to enhance MSC survival for long periods of time, and so such biomaterials and MSCs may be a valuable feature of long-term HSC niche models (Rico et al., 2016b). In addition, biomaterials can also modulate the phenotype of MSCs and can be used as a means of stimulating their expression of certain proteins, such as HSC maintenance factors (Calvi et al., 2003). While MSCs express their own HSC maintenance factors, osteogenic differentiation of MSCs leads to the formation of OBs, which secrete a different profile of HSC maintenance factors (Zhang et al., 2003). Consequently, the development of an HSC niche model that features a stromal layer of both MSCs and OBs with the combined effect of their unique cytokine profiles, would be potentially superior to current models that typically use only one cell type. Biomaterials can provide a means of stimulating osteogenic differentiation of MSCs to an extent, while also retaining some MSCs in their stem cell state, and such biomaterials may pave the way to the generation of more diverse HSC niche models that are more mimetic of the *in vivo* niche.

3.1.2 PEA as a Potential HSC Niche Model Biomaterial

PEA is a synthetic polymer upon which FN can be adsorbed, resulting in fibrillogenesis on the FN molecules and exposure of cell adhesion and growth factor binding regions (Llopis-Hernández et al., 2016). Consequently, PEA has the potential to function well in an HSC niche model, and can have its characteristics used in the following ways;

- The layer of FN adsorbed on PEA can provide a means of MSC attachment
- The FN can act to maximise the self-renewal potential of MSCs and thus may support a long-term HSC model
- GF signalling molecules can be bound to the FN, allowing for further control over MSC fate and control over the expression of HSC maintenance factors in MSCs.
- BMP-2 can be bound to the FN to stimulate osteogenic differentiation of some MSCs
- Substrate-tethered GFs allow for a lower dose of GF to be used compared to soluble GFs; PEA models safer and more economical than soluble GF models. Presentation of these GFs next to the cell binding domain of FN will further reduce the quantity of GF required to elicit the desired response

Previous studies using PEA and MSCs have suggested it is possible to both maintain MSC phenotype, while inducing some osteogenic differentiation of MSCs when BMP-2 is bound to FN adsorbed on PEA (See Section 1.6) (Rico et al., 2016b, Llopis-Hernández et al., 2016). However, it has yet to be determined if more than one GF can be adsorbed at one time. Adsorption of a combination of growth factors could provide a means of enhancing HSC maintenance factor expression in MSCs, while also promoting a degree of osteogenic differentiation. As a result, it seems that PEA could be used as a means of effectively co-culturing MSCs and OBs for a number of weeks in an HSC niche model. This would be very valuable, as it would allow for a mixed profile of MSC and OB HSC maintenance factors to be present in a novel model.

3.1.3 The Role of Collagen Gels in HSC Niche Models

Collagen gel is a commonly used component of HSC niche models for two main reasons; it can enhance the osteogenic differentiation of MSCs giving rise to the expression of valuable HSC maintenance factors; it can mimic the elastic properties of the bone marrow niche (Schneider et al., 2010, Metzger et al., 2014). Although promising data exists from the use of collagen gels in HSC niche models with MSCs cultured in a monolayer on glass substrates with a collagen gel loaded on top, there is a void that must be filled in terms of investigating the potential of collagen gels to enhance to effects of biomaterials on MSCs in such models (Leisten et al., 2012).

3.2 Aims and Objectives

This chapter aims to characterise PEA surfaces, as a means of assessing their suitability to function in an HSC niche model. In order to assess the suitability of PEA surfaces for incorporation into HSC niche models, it is necessary to ensure that the network conformation of FN, associated with exposure of GF and cell binding domains, is apparent when adsorbed on PEA. In addition, it is important to ensure that growth factors can be bound to FN, and to prove that when a combination of two GFs is adsorbed, one GF does not entirely out-compete the other.

To confirm the presence of FN networks on PEA, AFM will be used, and the structure of FN on PEA will be compared to that of FN adsorbed on a control polymer, poly (methyl acrylate) (PMA). PMA is similar to PEA in terms of wettability and surface chemistry, but has one less carbon present in the side chain. In order to assess the ability of the adsorbed FN layer on PEA to bind more than one GF, Enzyme-linked immunosorbent assays (ELISAs) will be used. The surface density of commonly used GFs, BMP-2 and NGF, will be determined and a conclusion will be drawn regarding the ability of both GFs to bind to one PEA + FN surface.

Further, this chapter aims to characterise the stiffness of the collagen gel that is used to make the HSC niche model with PEA + FN + GF surfaces 3D. To determine the stiffness of the collagen gel, rheology will be carried out.

3.3 Materials and Methods

3.3.1 Atomic Force Microscopy (AFM)

PEA and PMA samples were coated with FN at 20 µg/mL for 10 minutes and were then washed twice with DPBS, once with milliQ water and then dried with nitrogen gas flow. 4 areas of each sample were scanned to check for consistency in the FN conformation. A Nanowizard 3 from JPK atomic force microscope was used in tapping mode using cantilevers with a force constant of 3 N/m, a resonance frequency of 75 kHz and a pyramidal tip with an 8 nm radius. To quantitatively assess FN distribution, images were exported to Image J, where the skeletonize plugin was applied.

3.3.2 Quantification of BMP-2 and NGF adsorption of PEA surfaces

A BMP-2 DuoSet ELISA kit (DY355-05, R&D) and an NGF Duoset ELISA kit (DY256-05, R&D) were used to indirectly quantify the surface density of BMP-2 and NGF on PEA + FN + BMP-2, PEA + FN + NGF and PEA + FN + BMP-2&NGF surfaces. 200 µl of GF supernatant was retrieved from each PEA + FN sample, and this volume was split into 2, and an average of the two determined concentrations was used in the analysis. All methods were carried out as per the instructions in the user manual.

For each ELISA type, a 96 well plate was incubated overnight with a capture antibody for BMP-2 or NGF. The following day, the capture antibody was removed and each well was washed three times with a wash buffer (0.05% Tween-20/PBS). A blocking buffer (1% BSA in PBS) was then used to block the plates for one hour. The supernatant from the GF adsorption was removed from PEA + FN + BMP-2 or PEA + FN + NGF samples, and was diluted 10x in PBS to ensure the concentration of the samples fell within the working range of the ELISA kits.100 µl of diluted GF supernatant solution or 100 µl of standard was added to each well following the blocking step, and left to incubate at room temperature for 2 hours. (Standards were prepared in PBS starting at 3,000 pg/mL). Wells were washed three times using wash buffer, and 100 µl of detection antibody was added to each well and left to incubate at room temperature for 2 hours. The wash step was repeated, and 100 µl of

streptavidin-HRP was added to each well and incubated for 20 minutes at room temperature, with the plate wrapped in tinfoil to block out light. 100 µl of substrate solution was added to each well and the plate was incubated for 20 minutes at room temperature, wrapped in tinfoil. Finally, 50 µl of stop solution was added to each well.

For analysis, the 540 nm readings were subtracted from the 450 nm readings to correct for optical imperfections. Then, the BMP-2 or NGF concentration of each standard and the corresponding absorbance was logged and a standard curve was generated. The BMP-2 or NGF concentration was plotted against the absorbance values. Regression analysis was used to generate the best-fit curve and was used to determine the concentration of each unknown sample, representing the amount of BMP-2 or NGF in the supernatant. To determine the amount of BMP-2 or NGF adsorbed on the surfaces, the amount of BMP-2 determined to be in the supernatant was subtracted from the amount of BMP-2 in the solution used for the coating.

Results were analysed using a T-test on GraphPad Prism 6.

3.3.3 Collagen Gel Stiffness Testing Using Rheology

To determine the stiffness of the collagen gel, dynamic frequency sweep experiments were performed with the use of a strain-controlled Kinexus rheometer (Malvern, UK). A parallel plate geometry (20 mm) and 0.8 mm gap were used. The stage was maintained at 25 ^{o}C using an integrated temperature controller. To ensure that measurements were made in the linear viscoelastic regime, an amplitude sweep was carried out. The dynamic modulus of the hydrogel was measured as a frequency function, and frequency sweeps were carried out between 1 and 100 Hz, to measure the material's shear moduli. Measurements were repeated 3 times for reproducibility. Elastic modulus (G') values were extracted from the accompanying Kinexus software, and were plotted against the angular frequency values using GraphPad Prism 6. Young's modulus values were determined by taking the elastic modulus values and multiplying them by 3, assuming a Poisson's ratio of 0.5, in accordance with Hooke's law (Fung, 2013, Greenleaf et al., 2003).

3.4 Results

3.4.1 FN Conformation on PEA Surfaces

AFM images were obtained in tapping mode to confirm previous findings that PEA induces FN to adopt a network conformation, as a result of fibrillogenesis. AFM was also carried out to ensure that the control polymer, PMA, induces FN to adopt a globular conformation and does not support fibrillogenesis. The results are shown in Figure 3-1.

Both the height and phase demonstrated a well-connected network of FN fibrils on PEA surfaces, indicative of fibrillogenesis. However, the same could not be observed on PMA surfaces. This confirmed previously published findings and supported the hypothesis that PEA surfaces may have GFs tethered to them, and may act as a suitable foundation for a HSC niche model.

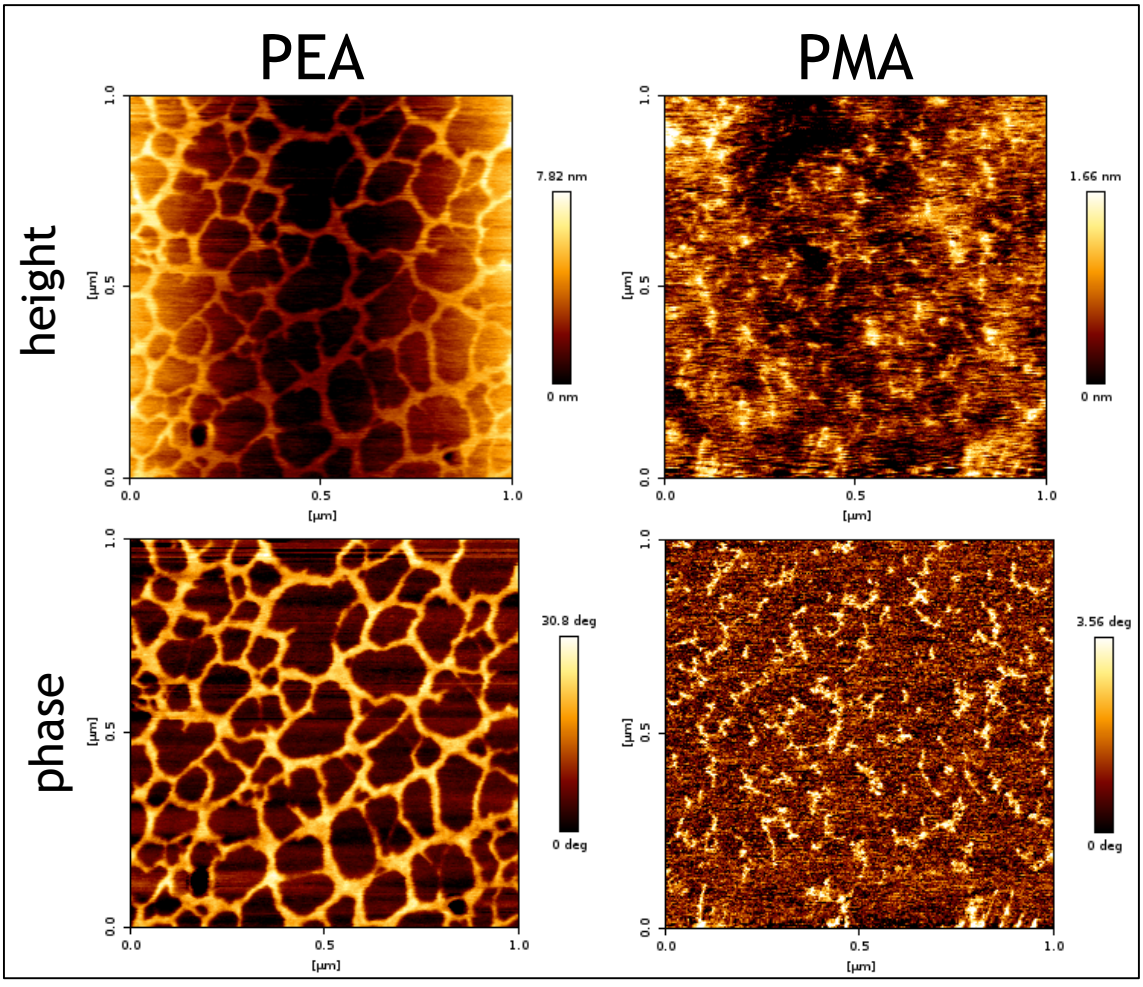

Figure 3-1 FN fibrillogenesis occurs on PEA surfaces.
Samples were coated with FN at 20 µg/mL for 10 minutes and height and phase images were obtained for both PEA and the control polymer PMA. Data indicates FN fibrillogenesis occurs on PEA but not on PMA surfaces.

3.4.2 BMP-2 Adsorption of PEA Surfaces

Figure 3-2 show results from a sandwich ELISA, carried out to quantitatively determine the ability of BMP-2 to bind to PEA + FN surfaces when it was supplied alone, and in a 1:1 concentration ratio with NGF. BMP-2 was adsorbed on its own at 25 ng/mL and a BMP-2/NGF mix solution was prepared using an equal volume of each GF, when the GFs were each at a concentration of 25 ng/mL.

As expected, the results showed that BMP-2 adsorbs onto PEA + FN surfaces when supplied on its own, or in a mix with NGF. Further, as expected, there was a greater surface density of BMP-2 on BMP-2 only surfaces, compared to surfaces where BMP-2 and NGF were co-adsorbed.

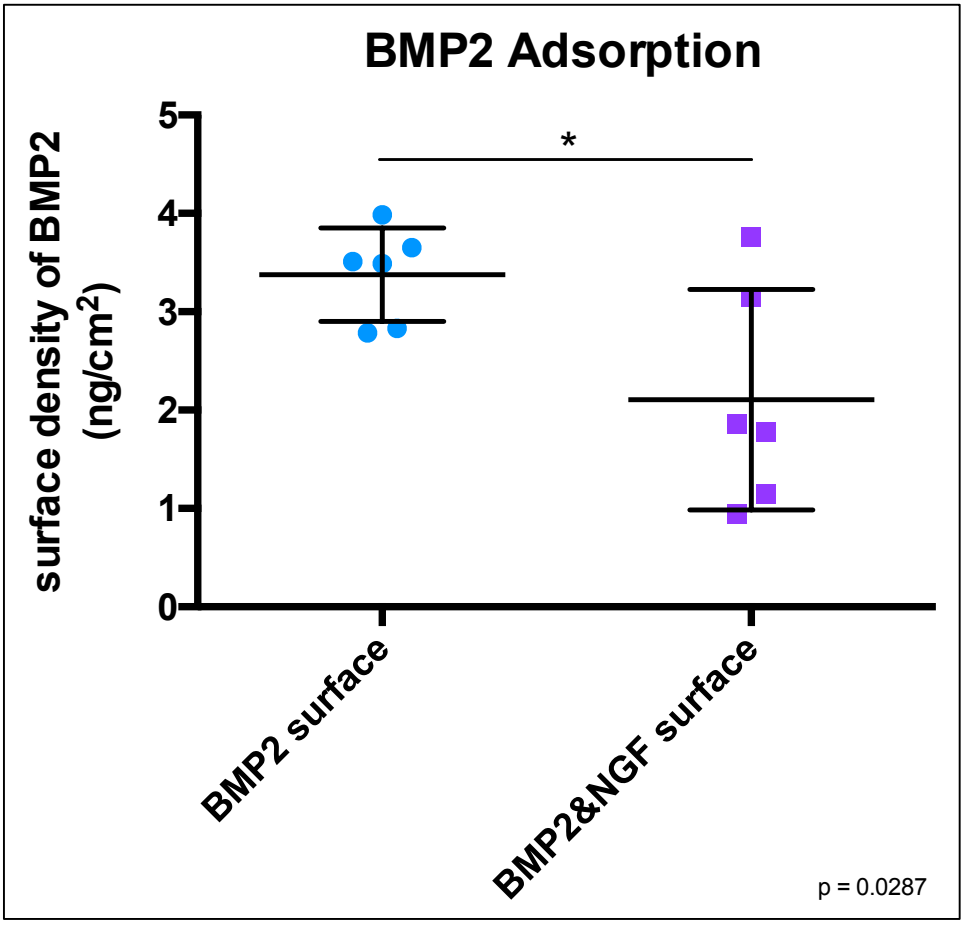

Figure 3-2 The surface density of BMP-2 on PEA + FN surfaces.
BMP-2 adsorption on 12 PEA + FN surfaces was quantified when 25 ng/mL of BMP-2 solution was adsorbed alone or in a 1:1 volume ratio with NGF. The concentration of BMP-2 in the supernatant was determined using a standard curve, and the value was deducted from the concentration of the original sample, to give the surface density of BMP-2 on each surface. n=6. Graph shows mean +/- SD. stats *=p<0.05 by Kruskal-Wallis. Data indicates BMP-2 is adsorbed onto PEA + FN substrates when supplied alone or in a mix with NGF.

3.4.3 NGF Adsorption of PEA Surfaces

A sandwich ELISA was also carried out to quantitatively determine the ability of NGF to bind to PEA + FN surfaces when it was supplied alone, and in a 1:1 concentration ratio with BMP-2 (Figure 3-3). NGF was adsorbed on its own at 25 ng/mL and a NGF/BMP-2 mix solution was prepared using an equal volume of each GF, when the GFs were each at a concentration of 25 ng/mL.

The results indicated that NGF adsorbs onto PEA + FN surfaces when supplied on its own, or in a mix with BMP-2. In addition, as would be expected, the results suggested that there is a greater surface density of NGF on NGF only surfaces, compared to surfaces when NGF and BMP-2 were co-adsorbed.

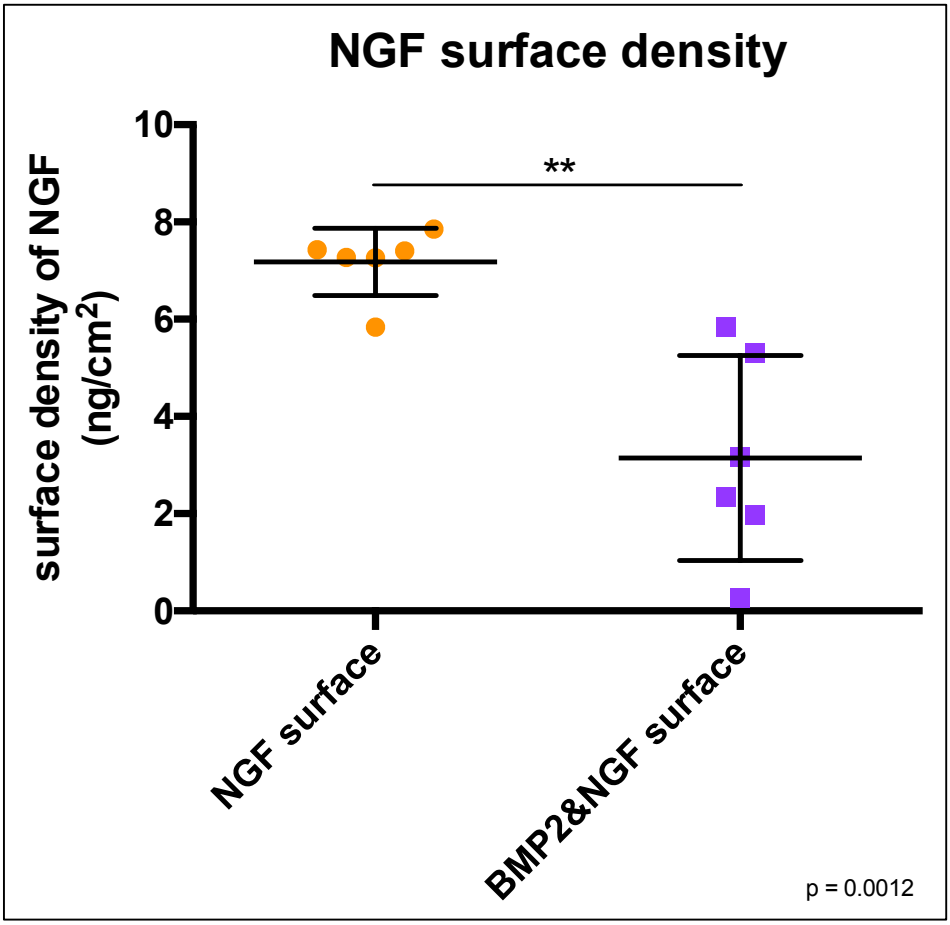

Figure 3-3 The surface density of NGF on PEA + FN surfaces.
NGF adsorption on 12 PEA + FN surfaces was quantified when 25 ng/mL of NGF solution was adsorbed alone or in a 1:1 volume ratio with BMP-2. The concentration of NGF in the supernatant was determined using a standard curve, and the value was deducted from the concentration of the original sample, to give the surface density of NGF on each surface. n=6. Graph shows mean +/- SD. stats *=p<0.05, ** =p<0.01 by Kruskal-Wallis. Data indicates NGF is adsorbed onto PEA + FN substrates when supplied alone or in a mix with BMP-2.

3.4.4 Elastic Modulus of Collagen Gels

In order to determine the stiffness of the collagen gel intended for use in this model, rheology was used to determine the elastic modulus of 6 collagen gels, wherein three batches (A-C) were split into two technical replicates, A and B. Results are shown in Figure 3-4.

The results suggested that the elastic modulus of the collagen gels intended for use in this model ranged from 25 to 45, and further indicated that gels from the same batch had a similar elastic modulus. It is possible that the slight changes in the storage/elastic modulus values reported here, in gels of the same batch, may have arisen from the addition of the gel to the wells occurring at slightly different times. The difference in storage/elastic modulus that existed between gels made in different batches is likely to have arisen from small differences in the volume of NaOH added to the gel mixture, resulting from differing perceptions of the colour change (Section 2.4.4).

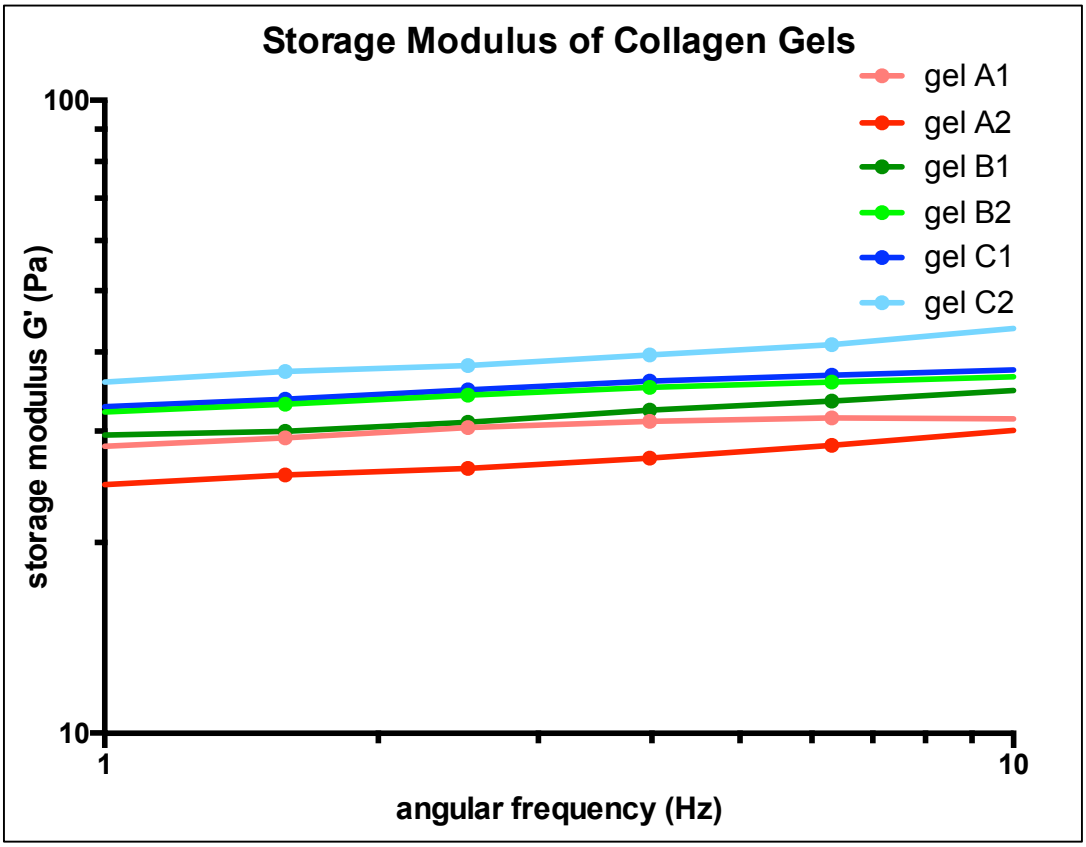

Figure 3-4 Storage modulus of collagen gels
The storage modulus of 6 collagen gels, prepared from 3 batches (A-C) with 2 technical replicates was carried out. The graph shows the range of storage modulus (G') values obtained, representing the elastic modulus when the angular frequency range is between 1 and 10 Hz. Units = Pa. Data indicates an elastic modulus range of collagen gels from 25 to 45 Pa.

3.4.5 Young's Modulus of Collagen Gels

The values obtained from rheology experiments used to determine the storage modulus of the collagen gels intended for use in this model were further used to determine the Young's modulus of the collagen gels. The Young's modulus for each gel tested at angular frequencies between 1 and 10 Hz were determined using Hooke's Law (E = 3G'), where E represents the Young's modulus, and G' refers to the storage modulus values previously obtained, and shown in Figure 3-4 (Greenleaf et al., 2003).

The results shown in Figure 3-5 suggested that the collagen gels intended for use within this HSC niche model had a mean Young's modulus of around 100 Pa (Metzger et al., 2014). This implied that the gel would have a beneficial effect within the model, as it would mimic the stiffness and 3D character of the natural bone marrow niche (Metzger et al., 2014, Sobotková et al., 1988).

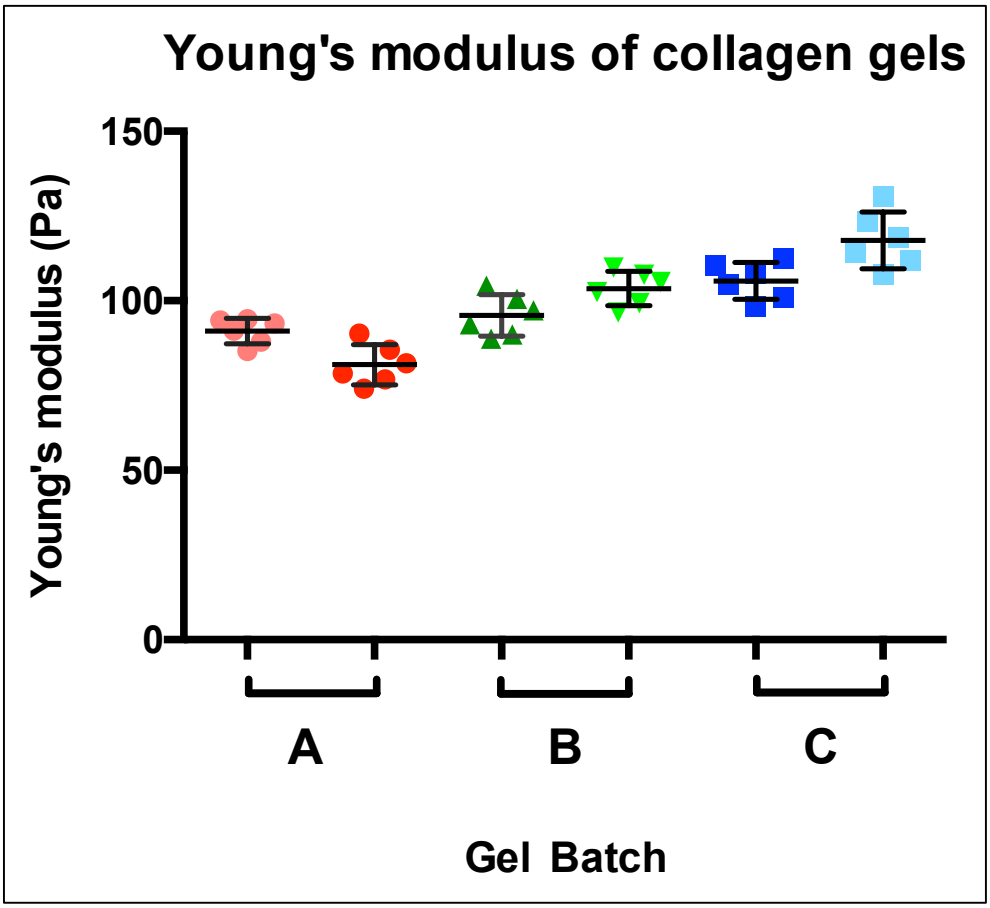

Figure 3-5 The Young's modulus of collagen gels
Elastic modulus values for two technical replicates within three batches of collagen gels (A-C) were obtained using rheology to determine storage modulus values, and then using Hooke's Law (E = 3G') to calculate the Young's modulus. (assuming a Poisson's ratio of 0.5). n=6. Graph shows mean +/- SD. Data indicates a Young's modulus of collagen gels to be around 100 Pa.

3.5 Discussion

This chapter describes the characterisation of the materials involved in an *in vitro* HSC niche model using PEA + FN + GF surfaces as the foundation, with a collagen gel to mimic the stiffness and enhance the characteristics of the niche. The stiffness of the collagen gel was tested using rheology, to ensure that it was comparable to the stiffness of the natural HSC niche in the bone marrow (Figure 3-5). In addition, PEA surfaces with an absorbed layer of FN were characterised by AFM to confirm the presence of FN networks, indicative of fibrillogenesis. These PEA + FN surfaces were also supplied with a solution of BMP-2, NGF or BMP-2&NGF mixed together, and the absorption and surface density of these growth factors were determined using sandwich ELISAs.

Rheology is a commonly used method to test the stiffness of gels. Due to gels being complex solids, their viscosity is not a fixed value (Krieger and Dougherty, 1959). Rather, it is dependent on the degree of shear to which they are exposed (Brady and Bossis, 1985). The bone marrow is a soft material with a reported Young's modulus of approximately 100 Pa, and previous work in the field of biomaterials has shown that culturing MSCs with gels of such stiffness can enhance osteogenic differentiation, as is desired in this model (Sobotková et al., 1988, Metzger et al., 2014, Winer et al., 2008). Results show that the collagen gels intended for using in this HSC niche model had an elastic modulus of between 25 and 45 Pa. Obtaining these values allowed for Young's modulus values to be calculated using Hooke's law, which identified the Young's modulus of the gels as ~100 Pa (Figure 3-5) (Fung, 2013, Greenleaf et al., 2003). This result suggested that the collagen type I gels had similar physical properties to the *in vivo* niche, indicating that the model may regulate the HSCs and MSCs similarly to the body. In order to improve the results, it would be advantageous to test a greater number of collagen gels, using more technical replicates to determine if the differences observed within the same batch do result from differences in pipetting time.

The use of AFM allowed for the imaging of several different areas of multiple PEA and PMA + FN coated coverslips, as shown in Figure 3-1. A similar network conformation of FN was observed on each PEA + FN coverslip, in each of the 4 areas scanned. However, a different conformation of FN was observed in each

area of the 4 PMA + FN coverslips scanned. On PMA + FN coverslips, the network conformation of FN was never observed, confirming published results showing that the fibrillogenesis occurring on PEA coverslips does not occur on PMA + FN coverslips. Although the approach was robust, it would have been beneficial to scan more regions of a greater number of coverslips to ensure that results were consistent over a larger sample size.

Concurrent with the results obtained from the AFM experiments, the use of ELISAs to determine the surface density of GFs bound to PEA + FN surfaces, showed that GFs are able to bind to PEA + FN surfaces (Figure 3-2, Figure 3-3). This suggested that the GF binding domain of the FN is exposed on PEA + FN surfaces – a characteristic of FN fibrillogenesis. Both the BMP-2 and NGF ELISA experiments demonstrated that the GFs are able to bind to PEA + FN surfaces, as the concentration of the GFs in the supernatant following a 2-hour incubation of the GFs on the PEA + FN surfaces was less than that of the solution initially supplied to the surfaces. In the BMP-2 surface density/adsorption experiment, it was promising to observe that significantly less BMP-2 was adsorbed when supplied in a BMP-2&NGF mix, than when BMP-2 was supplied alone in solution. This observation implied that some of the GF binding sites on the FN molecules were being occupied by NGF, when the BMP-2 and NGF were supplied together. The results shown in Figure 3-3 from the NGF surface density/absorption experiment support this hypothesis, in that these results also showed that significantly less NGF was bound when NGF was supplied in an NGF&BMP-2 mix solution. This suggested that some of the GF binding sites on the FN were being occupied by BMP-2. Although these results were promising and supported the hypothesis that GFs can bind to PEA + FN surfaces, even when more than one GF was adsorbed at once, the range of surface density values in both ELISA experiments was quite large. To overcome this, it would have been beneficial to have used more than 12 PEA + FN surfaces per ELISA. It would also be advantageous to repeat this experiment using PEA surfaces obtained from different polymerisation batches, to determine if batch variability may influence the surface density of GFs on PEA + FN surfaces. Finally, it is important to acknowledge that the maximum GF surface density value obtained in the BMP-2 experiment was 3.98 ng/cm^2, whereas the maximum value obtained in the NGF experiment was 7.85 ng/cm^2. Despite efforts being made to ensure a high level

of consistency in the preparation of materials for these ELISA experiments, these values were considerably different and could be down to differences in room temperature or batch variability between the surfaces and FN or GF solutions used. To investigate if this variability is down to error, repetition of the experiments using the same BMP-2&NGF combined solution supernatant for both ELISAs, at the same time on the same day, with samples from the same batch of PEA would provide some insight as to why this difference in GF surface density was apparent.

Further to expanding sample sizes and improving on aforementioned methods, knowledge and understanding of how the GFs bind to PEA + FN surfaces could be enhanced by carrying out gold labelled antibody staining of PEA + FN + GF surfaces. It is possible to use an anti-BMP-2 antibody in conjunction with a secondary antibody that is labelled with a gold nanoparticle (Llopis-Hernández et al., 2016). These nanoparticles could be observed using phase AFM images to show the exact binding location of BMP-2 molecules to FN fibrils in the PEA networks. Additional experiments that would have been useful to carry out in order to confirm previous findings and assumptions about GFs and FN adsorbed on PEA surfaces, include using a blocking antibody to block the FN III^{12-14} repeat region, which is responsible for the GF binding. Using a blocking antibody on this region and comparing the surface density of GFs on unblocked FN molecules to normal FN molecules on PEA would clarify the likelihood of non-specific binding.

In conclusion, the results discussed in this chapter provided a foundation for the construction of an HSC niche model based on PEA + FN that also incorporated the use of a collagen type I gel. The results obtained demonstrated that a collagen type I gel with an elastic modulus comparable to that of the natural bone marrow could be made in the lab. Further, the results showed that when a layer of FN is adsorbed onto PEA coated glass coverslips, a network conformation of FN could be clearly observed. This network conformation was indicative of a well-published phenomenon known as FN fibrillogenesis, which is associated with the exposure of the cell adhesion and GF binding domains of FN. Further results suggested that the GF binding domain is exposed, as it has been shown that BMP-2 and NGF can be adsorbed on to PEA + FN surfaces either independently or together.

CHAPTER 4

Chapter 4 Stromal Layer Characterisation

4.1 Introduction

4.1.1 The role of a stromal layer in a PEA + FN HSC niche model

It is known that incorporation of a stromal layer into HSC niche models is one of the easiest and most successful means of inducing HSC survival, maintenance and proliferation (Dexter, 1982, Leisten et al., 2012). Such stromal layers may consist of MSCs, OBs or both. In order to understand the basic nature of HSC niche models, it is important to characterise the stromal layer and to determine its nature in terms of MSC and OB phenotype. While each cell type has been shown to be beneficial on its own in the design of HSC niche models, design of a model incorporating both MSCs and OBs would be advantageous, as both cell types secrete a unique profile of HSC maintenance factors, critical for the development of a successful HSC niche model (Méndez-Ferrer et al., 2010, Calvi et al., 2003).

4.1.2 MSCs in HSC niche models

The role of MSCs in HSC niche models is well characterised, and it is known that MSCs support HSCs in the niche primarily via the expression of HSC maintenance factors (Méndez-Ferrer et al., 2010). As a result, it is important to consider this significant role of MSCs in the design of HSC niche models. In order to ensure that MSCs are able to retain their phenotype when incorporated into HSC niche models, it is necessary to ensure that MSC marker expression is retained throughout the culture period of the model.

MSCs that are positive for nestin expression are considered to be one of the most important MSC populations for maintenance of the HSC niche, because nestin^{+} MSCs express high levels of HSC maintenance genes (Méndez-Ferrer et al., 2010, Pinho et al., 2013). In addition, HSC niche models that incorporate MSCs should have expression of other MSC markers checked, to consider other populations of MSCs. For example, STRO-1 is an established MSC marker, and although STRO-1 expression decreases gradually with MSC expansion, STRO-1 positive MSCs have been shown to have HSC supportive roles (Ning et al., 2011). Thus, it is important to also consider STRO-1 expression in MSCs incorporated into HSC

niche models (Kolf et al., 2007). Similarly, it is also important to consider other MSC markers that are associated with the International Society of Cellular Therapy human MSC identification criteria. Despite nestin and STRO-1 expression being important in the characterisation of MSC phenotype in HSC niche models, analysis of other markers such as ALCAM may help to provide further insight into the phenotype of MSCs in HSC niche models (Nakamura et al., 2010b).

The stromal layer incorporated into the PEA + FN + GF niche models associated with this thesis will be developed by seeding STRO-1^+ MSCs on to PEA + FN + GF substrates, and culturing the cells for 21 days. Although some evidence exists to suggest that PEA + FN surfaces may act to maximise retention of the MSC phenotype, it is hypothesised that long-term culture of the MSCs combined with the incorporation of GFs such as BMP-2 may result in some osteogenic differentiation of the MSCs. In order to ascertain if the MSC phenotype can be retained, the expression of MSC markers will be assessed after 21 days of culture. The expression of nestin, STRO-1 and ALCAM in MSCs cultured on control and PEA + FN surfaces, in four different media types will be assessed using in cell western (ICW).

4.1.3 OBs in HSC niche models

Similarly to MSCs, OBs are a well-characterised HSC niche supportive cell type (Arai et al., 2004, Calvi et al., 2003). Known to function principally in the endosteal niche in the bone marrow, OBs have been shown to secrete high levels of a unique profile of HSC maintenance factors (Lévesque et al., 2010, Nakamura et al., 2010a). Thus, it is important to consider their role in HSC niche models, as their unique HSC maintenance factor expression profile is likely valuable, particularly if it can be produced in conjunction with the HSC maintenance factor expression profile of MSCs.

As mentioned, this chapter will assess the ability of PEA + FN + GF substrates to support production of HSC maintenance factors, and it is hypothesised that the greatest and most valuable production of these HSC maintenance factors will come from a model incorporating both MSCs and OBs (Méndez-Ferrer et al., 2010, Calvi et al., 2003, Zhang et al., 2003). To this end, this chapter aims to investigate the potential of an HSC niche model based on PEA + FN + GFs to

induce osteogenesis while maintaining MSC character of the stromal layer. It is hypothesised that using PEA + FN + BMP-2 will help to induce osteogenic differentiation of some of the model's STRO-1^+ MSCs. To test this hypothesis, and to compare the potential effects of other growth factors and control surfaces on inducing a degree of osteogenesis while maintaining MSC phenotype, the expression of OCN and OPN in MSCs will be determined after 21 days using ICW, in four possible media types.

4.1.4 Expression of HSC maintenance factors in HSC niche models

Numerous proteins and molecules are postulated to act as HSC maintenance factors in the literature (Calvi et al., 2003, Ding et al., 2012, De Ugarte et al., 2003). However, certain proteins are particularly well characterised and have been extensively studied. For example, SCF is known to exist in secreted and transmembrane forms. Throughout life, HSCs have been shown to express the same levels of expression of the SCF receptor, c-KIT, and SCF has been shown to increase the survival, self-renewal and maintenance of HSCs cultured *in vitro (Ema et al., 2000, Walasek et al., 2012)*. Although c-KIT receptor expression levels remain the same on HSCs throughout life, it is important to note that HSCs have been shown to become less sensitive to SCF; adult HSCs require six times the concentration of SCF to induce maximum survival when compared to foetal HSCs (Zhang and Lodish, 2008). Thus, it is important to assess the ability of the stromal layers of HSC niche models to secrete SCF. As the model associated with this thesis is aimed towards culturing adult HSCs, it is important to select a PEA + FN substrate that allows for maximal expression of SCF from the stromal layer. ICW will be carried out to determine the expression of transmembrane SCF in the stromal layer, after 21 days, in four different media types.

In addition to SCF, VCAM-1 is another important HSC maintenance factor. This protein is a cell adhesion molecule and is particularly important for facilitating the attraction to, and binding of, HSCs to MSCs and OBs (Kopp et al., 2005, Jung et al., 2005). In theory, the incorporation of high levels of VCAM-1 into a HSC niche model would allow the HSCs to localise closely with the stromal layer, thus enhancing the accessibility of HSCs to beneficial regulatory signals from the stromal layer. Thus, this chapter also aims to use ICW to assess the effect of

different substrate and media types on the expression of VCAM-1 from cells of the stromal layer.

Although ICW can be effectively used to analyse the effects of different surface and media types on transmembrane SCF and VCAM-1 expression, ELISAs can also be used as a means of investigating the effects of changing media and surface types on the secretion of soluble HSC maintenance factors. CXCL-12 and THPO are also well-characterised HSC maintenance factors, known to attract and maintain HSCs in the *in vivo* bone marrow niche, respectively (Greenbaum et al., 2013, Yoshihara et al., 2007). Development of an HSC niche model that encourages the stromal layer to express high levels of these proteins would be particularly advantageous, as their presence would encourage homing of HSCs towards the stromal layer, while also encouraging HSC maintenance and proliferation (Table 1-5). In particular, high levels of THPO are desirable, as THPO has been shown to have a synergistic role with other growth factors, and may enhance the effects of the other GFs in the model (Qian et al., 2007).

4.2 Aims and Objectives

The aim of this chapter of the thesis is to determine the potential of PEA + FN + GF substrates and four different media types to induce the following, within a 21-day HSC niche model:

- maintenance of the expression of MSC markers STRO-1, ALCAM and nestin
- maximal expression of OB markers OCN and OPN
- maximal expression of HSC maintenance factors SCF, VCAM-1, CXCL-12 and THPO

The reasoning for testing four different media types is that standard lab DMEM supplemented with 10% FBS was used in initial tests to determine if the surface types were sufficient to induce changes in the expression of OB markers and HSC maintenance markers, while maintaining MSC marker expression. Upon obtaining promising results, the media type was more carefully considered, as it is known that HSCs do not respond well to culture in serum-containing medium. Unlike

HSCs, MSCs are dependent on serum in the media, and so it was decided that a serum-containing medium would be used for days 1-14 of the culture, and that on day 15 when the HSCs would be added to the culture, the media would be changed to a media more suitable for HSCs. It was initially recommended that the day 15 to 21 cultures were carried out using a serum free medium supplemented with 5 GFs (5 GF media). However, the cost of this medium combined with promising results obtained by collaborators suggested a similar, if not better, effect on HSC survival could be observed using only 3 GFs in the media, but at different concentrations (3 GF media). Further to this, results from collaborative laboratories working on HSC niche models suggested that using 2% serum, preferably from humans rather than bovine, would also help to humanise the model and make the effects of the PEA + FN + GF surfaces more apparent. In summary, the four different media types shown in Figure 4-1 were tested sequentially.

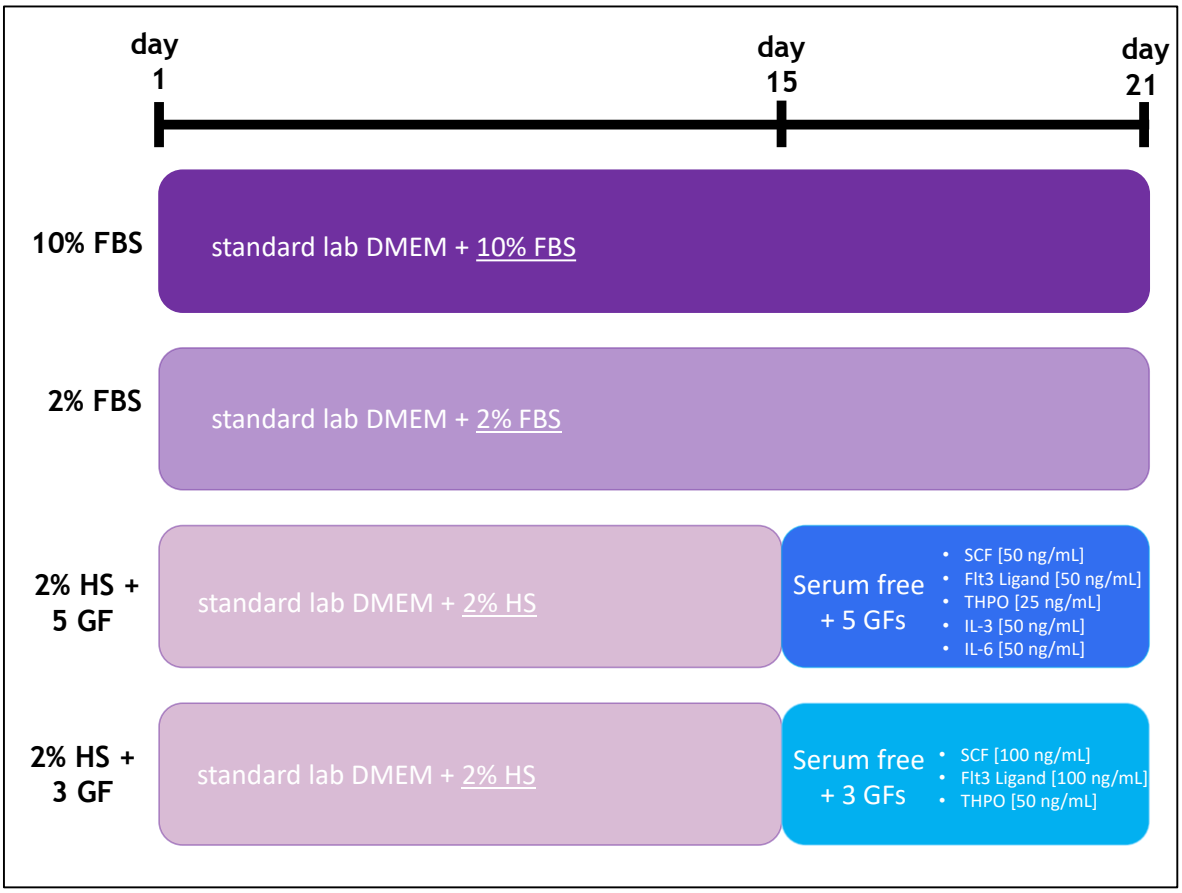

Figure 4-1 Cell culture media timeline
MSCs were cultured for 21 days in 4 different media types prior to being tested in stromal layer characterisation experiments. Media types 1 and 2 used the same media throughout the culture period, whereas media types 3 and 4 used a human serum-containing medium until day 15, when this media type was exchanged for a serum free media type, supplemented with either 3 or 5 GFs. FBS = foetal bovine serum. HS = human serum.

4.3 Materials and Methods

4.3.1 Collagen gel function

Determining how the collagen gels described in Chapter 3 may fit into this model was challenging, as work from collaborators suggested that the collagen gel may act to induce the differentiation of HSCs. The presence of the collagen gel would also make harvesting the HSCs a more challenging task. In order to reduce the complexity of this multifaceted model, it was decided that the collagen gel would be present in the models from day 3 to day 14, allowing time for the stromal layer to respond to it. On day 15, the gel was lifted out of the well, which did not affect the confluent layer of cells; from days 15 onwards of the cell culture, the collagen gel was not present.

4.3.2 In Cell Western^{TM} (ICW) Assay

Following cell culture, cells were fixed and permeabilised using the cell fixation and permeabilisation solutions outlined in section 2.2. Each sample was then incubated with LiCOR Odyssey Blocking Buffer for 1.5 hours. Primary antibodies were prepared in blocking buffer (1:100) and 150 µl of antibody solution was added to each well containing a coverslip and cells, in a 24-well plate. The primary antibody solution was left to incubate overnight at 4 ^{o}C, and the following day, each well was washed three times with (0.1% Tween-20/PBS), with each wash being left on the samples for 5 minutes. Secondary antibody/CellTag solutions were prepared to comprise: secondary antibodies diluted in blocking buffer (1:800); CellTag diluted in blocking buffer (1:500); 0.2% Tween-20. Wash buffer was removed from each well and 150 µl of secondary antibody/CellTag solution was added to each well and left to incubate for 1 hour at room temperature on a platform rocker. The secondary antibody/CellTag solution was removed and the wash step was repeated for a total of 3 x 5 minute washes. Following the last wash, the wash solution was removed completely and each coverslip was transferred to a new 24-well plate to ensure samples were as dry as possible for accuracy during the imaging step.

Samples were scanned with detection in the 800 nm channel for detection of the protein of interest and in the 700 nm channel for detection of the CellTag

fluorescence (indicative of cell number). Analysis was carried out by normalising the fluorescence units associated with the abundance of the protein of interest to the fluorescence units associated with the CellTag fluorescence units. Once the 800nm/700nm values were calculated, all values for samples were normalised to glass.

4.3.3 Immunostaining

Cells were fixed, as outlined in section 2.2. Cells were then permeabilised for 4 minutes at 4 ^{o}C using 150 µl of permeabilisation buffer, per well of a 24 well plate. The permeabilisation solution was removed, and primary antibodies were diluted 1:50 in PBS/BSA, and left to incubate for overnight at 4 ^{o}C, with 150 µl per well of a 24-well plate. The primary antibody mixes were removed, and cells were washed three times, using 300 mL of wash buffer (0.5% Tween-20/PBS). Following the wash step, samples were incubated with a secondary antibody solution (biotin-conjugated anti-rabbit/mouse secondary antibody diluted 1:50 in PBS/BSA) at 150 µl per well, at 4 ^{o}C overnight. The following day, the wash step was repeated and 150 µl of fluorescein streptavidin solution (diluted 1:50 in PBS/BSA) was added to each well. The plate was incubated for 30 minutes at 4 ^{o}C, in the dark. The wash step was repeated and samples were mounted onto glass coverslips using mounting medium containing 4', 6-diamidino-2-phenylindole (DAPI), before being used in fluorescence microscopy.

4.3.4 Fluorescence Microscopy

Immunostained samples were imaged using an inverted microscope (Axiovert 200M; Zeiss, Germany) linked to a CCD camera (QImaging, Canada) or a QCapture camera (QImaging, Canada). Greyscale images were acquired corresponding to the different filters, and these were converted to RGB colour format using FIJI software. Composite images were produced by overlaying the coloured greyscale images.

4.3.5 Scanning Electron Microscopy (SEM)

SEM was used to obtain high magnification images of STRO-1^{+} MSCs. Cells were cultured for 21 days, and then fixed in the wells of the 24-well culture plate, with 1.5 % glutaraldehyde, buffered in 0.1 M sodium cacodylate for 1 hour at 4

°C. The cells were post-fixed in 1 % osmium tetroxide in 0.1 M sodium cacodylate buffer, and then stained using uranyl acetate. An ethanol drying series using 30%, 50%, 70%, 90% ethanol, followed by dried absolute ethanol was used, and a final dehydration using hexamethyldisilizane was carried out. Once the hexamethyldisilizane was removed, samples were placed in a dessicator and left overnight to allow for further drying. The next day, samples were attached to aluminium stubs with double-sided conductive carbon tape and sputter coated with gold-palladium to a thickness of 15-20 nm (Polaron SC515 SEM coater). Images were acquired using a JEOL JSM 6400 Scanning Electron Microscope, in conjunction with Olympus Scandium Software, with kind assistance from Margaret Mullin (University of Glasgow).

4.3.6 MTT Assay

STRO-1$^+$ cells were cultured for 7 days in a 24-well plate at 37 °C and 5 % CO_2. On day 7, 200 µl of MTT dye solution (Sigma-Aldrich, UK) was added to each well. The plate was incubated for 4 hours at 37 °C and 5 % CO_2, and then the media was removed and 200 µl of DMSO was added to each well to solubilise the fomazan crystals inside the cells. The plate was transferred to a shaker and was incubated for a further 5 minutes at room temperature. The liquid was removed from the wells and transferred to a 96 well plate with DMSO used as a blank. Absorbance at 550 nm was detected using a microplate reader.

4.3.7 Flow Cytometry Staining

Following 21 days of culture in the systems, MSCs were removed from surfaces in the wells of 24-well plates following a 20-minute incubation with accutase at 37 °C. The cell suspension within each well was transferred to a FACS tube, and 1ml of FACS buffer at 4 °C was added. The tubes were centrifuged for 5 minutes at 400 g, and the cell pellets were re-suspended in 500 µl of FACS buffer. The cell suspensions were split into two tubes, and centrifuged for 5 minutes at 400 g. Cell pellets were then re-suspended in an antibody mix containing CD29, CD13, CD90, CD73, CD105, CD166, CD31 diluted 1:50 in FACS buffer and CD44 diluted 1:250. Cells were incubated for 30 minutes on ice and in the dark, before being centrifuged for 5 minutes at 400 g. Cells were finally re-suspended in 200 µl of

FACS buffer. Flow cytometry was carried out using an ATTUNE XDP (Thermo Fisher) flow cytometer and resulting data was analysed using FlowJo software.

4.3.8 T Cell Suppression Assay

MSCs were cultured for 21 days, and at the end of this culture period, T cells were added and co-cultured for a further 5 days to determine the capacity of the MSCs to suppress T cell proliferation.

Peripheral blood mononuclear cells (PBMCs) were isolated from peripheral blood, donated by healthy volunteers with full ethical consent. The PBMCs were isolated using Ficoll-Hypaque density gradient centrifugation, and the number of PBMCs added to each well of a 24-well plate was calculated to ensure a 1:2 ratio of MSCs to PBMCs. To ensure this was carried out accurately, an average of the cell number of 3 wells featuring MSCs cultured on a particular substrate type was taken, and used to give the mean number of MSCs per substrate type.

Prior to adding the PBMCs to the wells, the PBMCs cells were stained using carboxyfluorescein succinimidyl ester (CFSE) (ThermoFisher, UK). After calculating the number of cells to be added to each well, the cells were centrifuged for 5 minutes at 400 g. Cells were re-suspended in 1x PBS, and CFSE was added at a concentration of 1:1000 (CFSE:PBS). Cells were incubated in the CFSE/PBS mix for 20 minutes at 37 ^{o}C, before 250 µl of culture medium was added and cells were incubated for a further 5 minutes. The cells were centrifuged for 5 minutes at 400 g and the supernatant was discarded before they were re-suspended in the appropriate volume of fresh culture medium. A positive control was set up, where the T cells were maximally stimulated using phorbol 12-myristate 12-acetate (PMA) (Sigma-Aldrich, UK) at a concentration of 50 ng/ml, and IL-2 at a concentration of 50 ng/ml.

PBMCs were added to model wells containing MSCs (n=4) and were cultured for 5 days. On the 5th day, the non-adherent cells were harvested from the wells and allowed to flow through 70 µm nylon mesh cell separation filters (ThermoFisher, UK). 1ml of 1x PBS was added to wash remaining cells through the filter. Cell suspensions were centrifuged for 5 minutes at 400g, and were re-suspended in 500 µl of FACS buffer. Flow cytometry was used to identify peaks of CFSE

staining, indicative of the number of T cell divisions. This was carried out using an ATTUNE XDP (Thermo Fisher) flow cytometer and resulting data was analysed using FlowJo software.

The gating strategy used in FlowJo was based around the number of cells present within each peak, representing each cell division of the T cells, and is shown in Figure 4-2.

Following identification of the number of cells that underwent each division, the proliferation index was calculated as the sum of the cells in all generations divided by the calculated number of original parent cells (Holmgren et al., 1995, Smits et al., 2005).

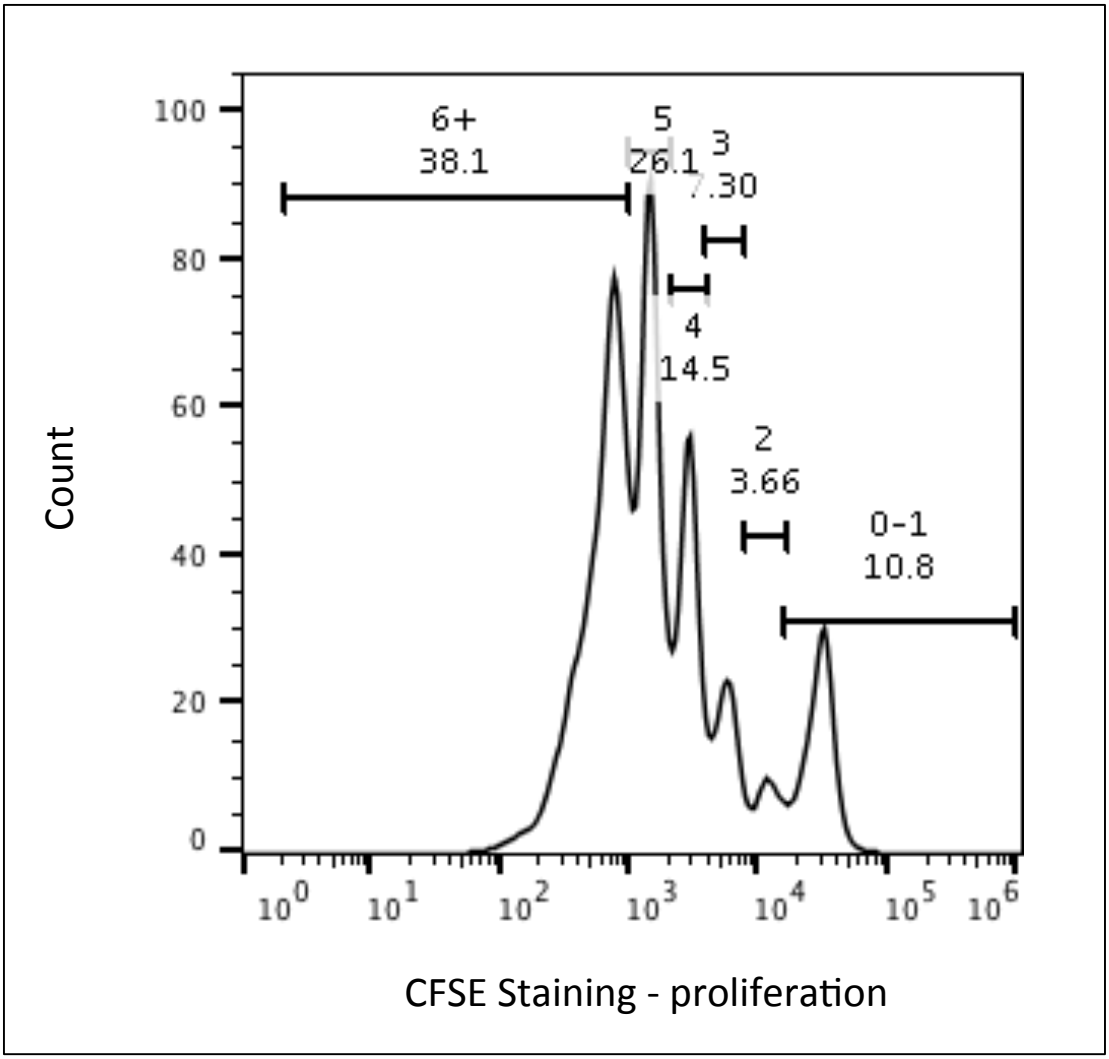

Figure 4-2 Suppression assay CFSE gating strategy
To determine the number of cells in each model that had undergone proliferation, and how many divisions had occurred, CFSE staining was carried out in T cells that were left to culture for 5 days in models containing MSCs. At the end of the culture, T cells were analysed using flow cytometry and the above gating strategy was employed to identify how many divisions T cells had undergone.

4.4 Results

4.4.1 STRO-1$^+$ MSC morphology is unaffected by substrates

In order to assess the basic effects of cell culture on PEA + FN substrates, STRO-1$^+$ MSCs were cultured on PEA + FN and PEA + FN + GF surfaces, and their morphology was compared to that of cells cultured on control surfaces of glass and glass + FN (Figure 4-3).

The results obtained from the SEM images suggested that the cell morphology of STRO-1$^+$ MSCs was similar when cultured on PEA + FN surfaces or PEA + FN + GF substrates, to that of cells cultured on control Glass + FN surfaces. Unusual artefacts resembling filopodia were observed in all 5000x magnification images. Imaging of additional samples that were dried in the same way, compared to others that were not, suggested that these artefacts resulted from the drying process.

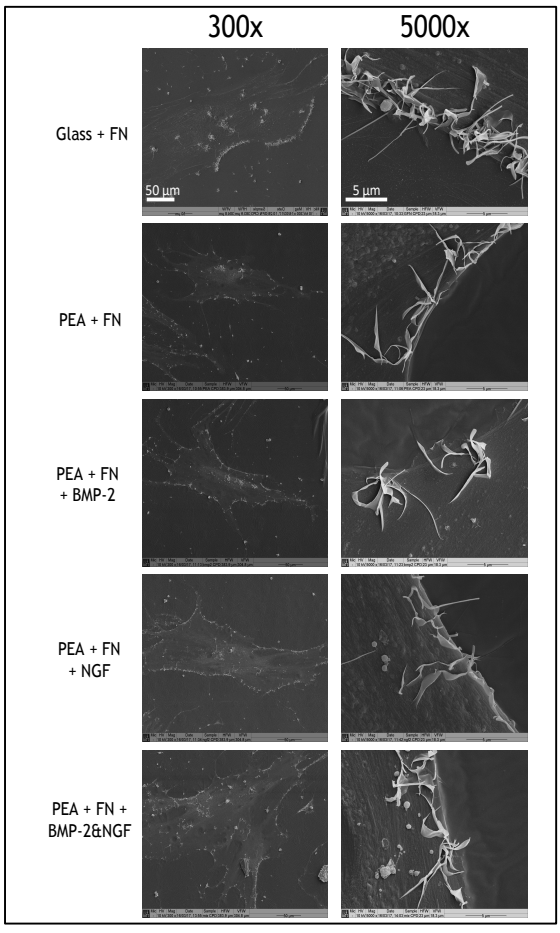

Figure 4-3 SEM Images of STRO-1+ Cells on Substrates
SEM images were obtained at 300x and 5000x magnification on PEA + FN surfaces, with a Glass + FN control. Cell morphology appears similar irrespective of different culture substrates. Data indicates a similar MSC morphology irrespective of culture substrate.

4.4.2 STRO-1 protein expression results in 10% FBS media

4.4.2.1 MSC marker expression

To determine if PEA + FN + GF substrates alter the expression levels of MSC markers relative to controls, STRO-1$^+$ cells were cultured on PEA + FN + GF and control substrates, and fixed after 21 days before being stained with ICW antibodies for ALCAM, STRO-1 and Nestin. The abundance of the protein of interest was normalised to cell number, giving a relative fluorescence (RF) value. Fold changes relative to glass were then calculated (Figure 4-4).

The results shown in Figure 4-4 showed that levels of nestin and STRO-1 expression in STRO-1$^+$ cells were not statistically different when the cells are cultured on PEA + FN or PEA + FN + GF surfaces, compared to controls. ALCAM expression appeared to be reduced in cells cultured on PEA + FN + NGF surfaces, yet these ALCAM expression levels were not statistically different to those found in cells cultured on the other tested substrates.

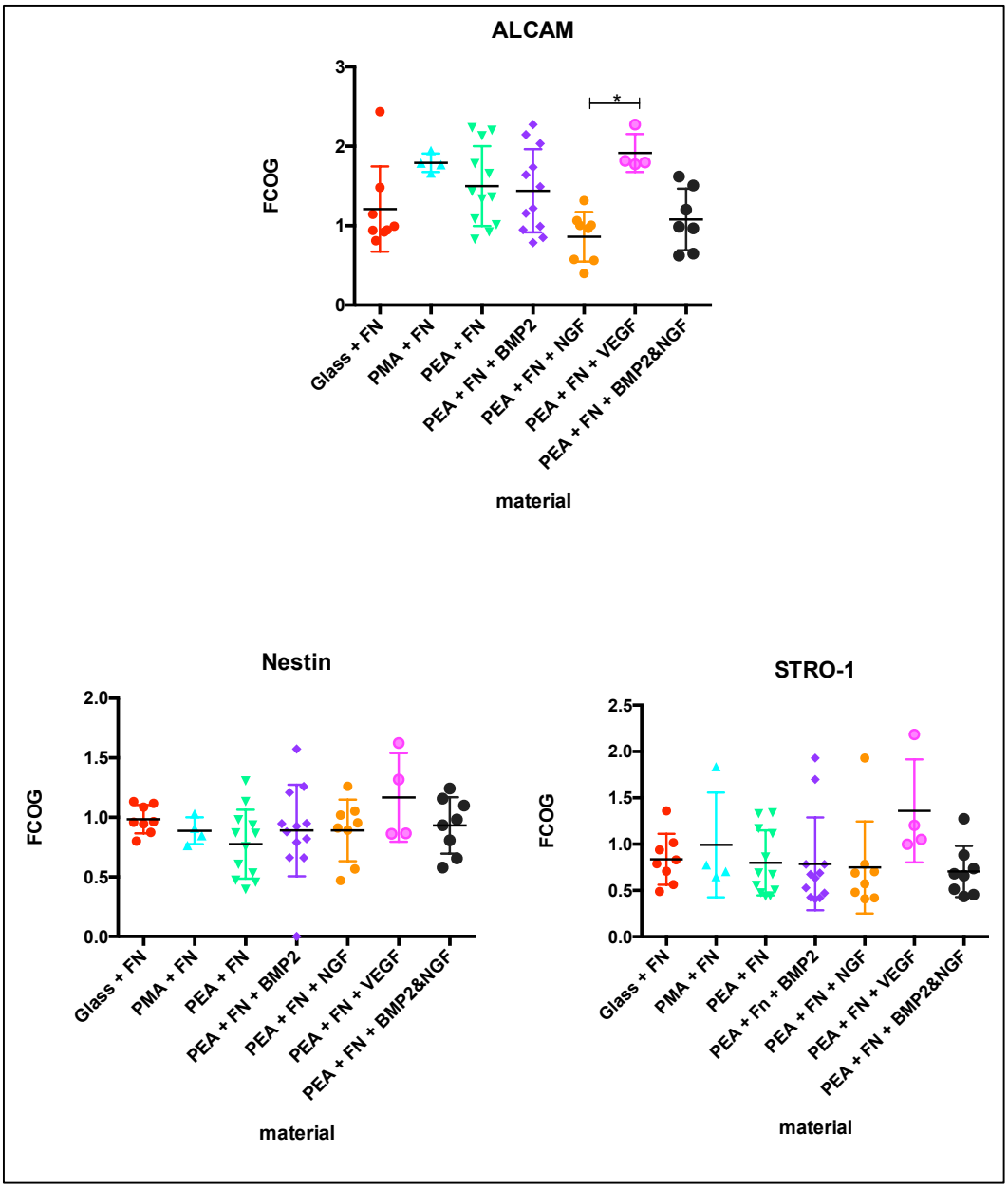

Figure 4-4 ICW results for MSC marker expression after 21 days
ICW was carried out to determine the effect of culturing STRO-1$^+$ cells on PEA + FN, and control surfaces, on the expression of MSC markers, ALCAM, nestin and STRO-1$^+$. Fluorescence values relative to the protein of interest were normalised to cell number. Fold change values over glass (FCOG) are reported. n ≥ 3. PMA+FN & PEA + FN + VEGF = 1 biological replicate; all other surfaces = 3 biological replicates. Graph shows mean +/- SD. *=p<0.05, **=p<0.01 by Kruskal-Wallis. Data generally indicates that substrate type has no statistically significant effect on the expression of MSC markers.

4.4.2.2 Osteogenesis marker expression

To assess the ability of PEA + FN + BMP-2 substrates to stimulate osteogenic differentiation in STRO-1$^+$ MSCs, cells were culture for 21 days and were stained with ICW antibodies for OCN and OPN. The abundance of the protein of interest was normalised to cell number, giving a relative fluorescence (RF) value. Fold changes relative to glass were then calculated (Figure 4-5).

The results obtained suggested that the PEA + FN + BMP-2 surfaces were not sufficient to induce a statistically significant increase in the BMP-2 expression in STRO-1$^+$ cells after 21 days of culture in the 10% FBS media.

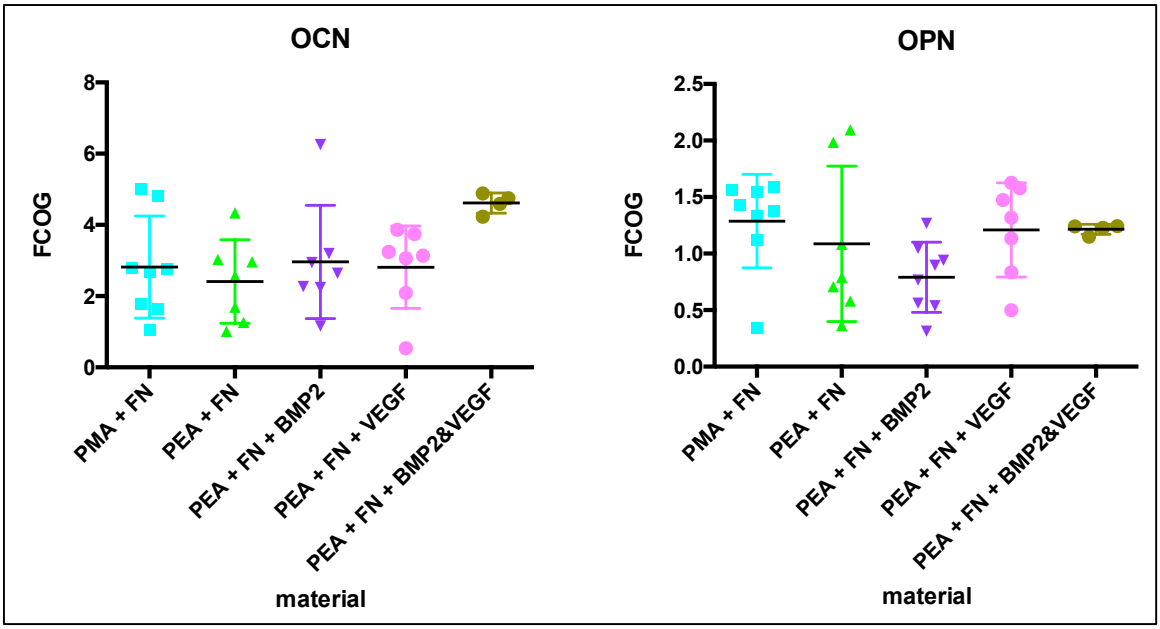

Figure 4-5 ICW results indicative of osteogenesis after 21 days
ICW was carried out to determine the potential of PEA + FN + BMP-2 surfaces to stimulate osteogenic differentiation of STRO-1$^+$ cells are 21 days of culture in DMEM supplemented with 10% FBS. Antibodies against OCN and OPN were used and fluorescence values relative to the protein of interest were normalised to cell number. Fold changes over glass (FCOG) are reported. n ≥ 3. 2 biological replicates were used. Graph shows mean +/- SD. Data suggest that substrate type has no statistically significant effect on the expression of osteogenesis markers.

4.4.2.3 HSC maintenance factor expression

To determine if PEA + FN surfaces could induce an increase in the expression levels of HSC maintenance factors relative to controls, STRO-1$^+$ cells were cultured on PEA + FN and control surfaces, and fixed after 21 days before being stained with ICW antibodies for SCF and VCAM-1. The abundance of the protein of interest was normalised to cell number, giving a relative fluorescence (RF) value. Fold changes relative to glass were then calculated (Figure 4-6).

The results of the ICW analyses shown above suggested that PEA + FN + GF surfaces were capable of enhancing SCF expression in STRO-1$^+$ cells. Notably, the PEA + FN + BMP-2&NGF surface appeared to be the strongest candidate for incorporation into an HSC niche model, as this surface induced a significantly higher expression of SCF in cells than the PEA + FN + BMP-2 surface alone. The VCAM-1 results suggested that the PEA + FN surfaces had less of a statistically

significant impact on VCAM-1 expression. However, it was interesting to note that the PEA + FN + All4 surface where BMP-2, NGF, PDGF and VEGF were adsorbed together onto the surface induced a statistically higher expression of VCAM-1 compared to controls.

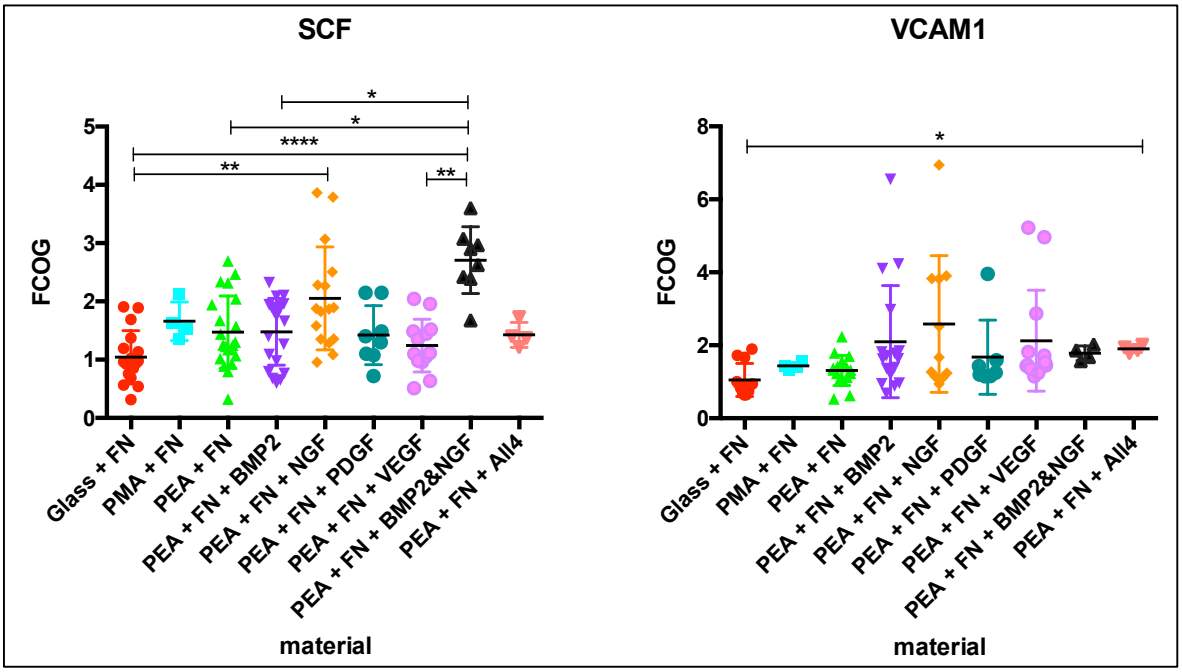

Figure 4-6 ICW results for SCF and VCAM-1 expression after 21 days
Graphs show results of ICW experiments carried out to assess changes in SCF and VCAM-1 expression in STRO-1$^+$ cells cultured for 21 days on substrates in DMEM supplemented with 10% FBS. Antibodies against SCF and VCAM-1 were used and fluorescence values relative to the protein of interest were normalised to cell number. Fold change values over glass (FCOG) are reported. PEA + FN + All4 represents PEA + FN surfaces with a combination of BMP2, NGF, PDGF and VEGF adsorbed. n ≥ 3. (*SCF results* – PEA + FN, PEA + FN + BMP2 = 5 biological replicates; Glass + FN, PEA + FN + NGF = 4 biological replicates; PEA + FN + VEGF = 3 biological replicates; PEA + FN + PDGF = 2 biological replicates; PMA + FN, PEA + FN + All4 = 1 biological replicate) (VCAM-1 results – PEA + FN, PEA + FN + BMP2 = 4 biological replicates; Glass + FN, PEA + FN + NGF, PEA + FN + VEGF = 3 biological replicates; PEA + FN + PDGF = 2 biological replicates; PMA + FN, PEA + FN + All4 = 1 biological replicate). Graph shows mean +/- SD. *=p<0.05, **=p<0.01, ***=p<0.001, ****=p<0.0001, by ANOVA. Data indicates that the addition of GFs to PEA + FN substrates enhances expression of HSC maintenance factors SCF & VCAM-1.

4.4.3 Niche protein expression results in 2% FBS media

As is shown in chapter section 4.4.2, the PEA + FN + GF surfaces are capable of enhancing expression of the critical HSC maintenance factor, SCF, while maintaining MSC marker expression and osteogenesis marker expression. It was hypothesised that the subtle differences observed in osteogenesis marker expression may be made clearer by reducing the concentration of serum in the

media, as this contains high concentrations of varying growth factors that may swamp or drown-out the effect of the GF surfaces. Thus, it was deemed worthwhile to investigate if reducing the concentration of serum leads to more clear-cut differences in ability of the PEA + FN + GF surfaces to induce an HSC niche supporting phenotype in STRO-1^+ MSCs.

In addition, to increase n numbers to consistently be 4 and reduce the cost, size and scale of experiments, it was decided that future work would focus exclusively on BMP-2 and NGF GFs, as these GFs appeared to considerably increase SCF expression in STRO-1^+ cells cultured on these substrates, making them the most suitable HSC niche model substrate candidates.

4.4.3.1 MSC marker expression (2% FBS media)

To determine if reducing the serum concentration in the media affects the expression of MSC markers, ALCAM, nestin and STRO-1, ICW was carried out after 21 days of culture in DMEM supplemented with 2% FBS. The fold change over glass values for the niche model candidate surfaces are shown in Figure 4-7.

The results obtained supported previous results shown in Figure 4-4, where expression levels of nestin and STRO-1 were not significantly up-regulated or down-regulated in response to cell culture on any of the tested substrates. Although the previous results showed a statistically significant decrease in ALCAM expression in cells cultured on PEA + FN + NGF substrates, the results shown here suggested that the surface alone is not sufficient to induce such statistically significant differences.

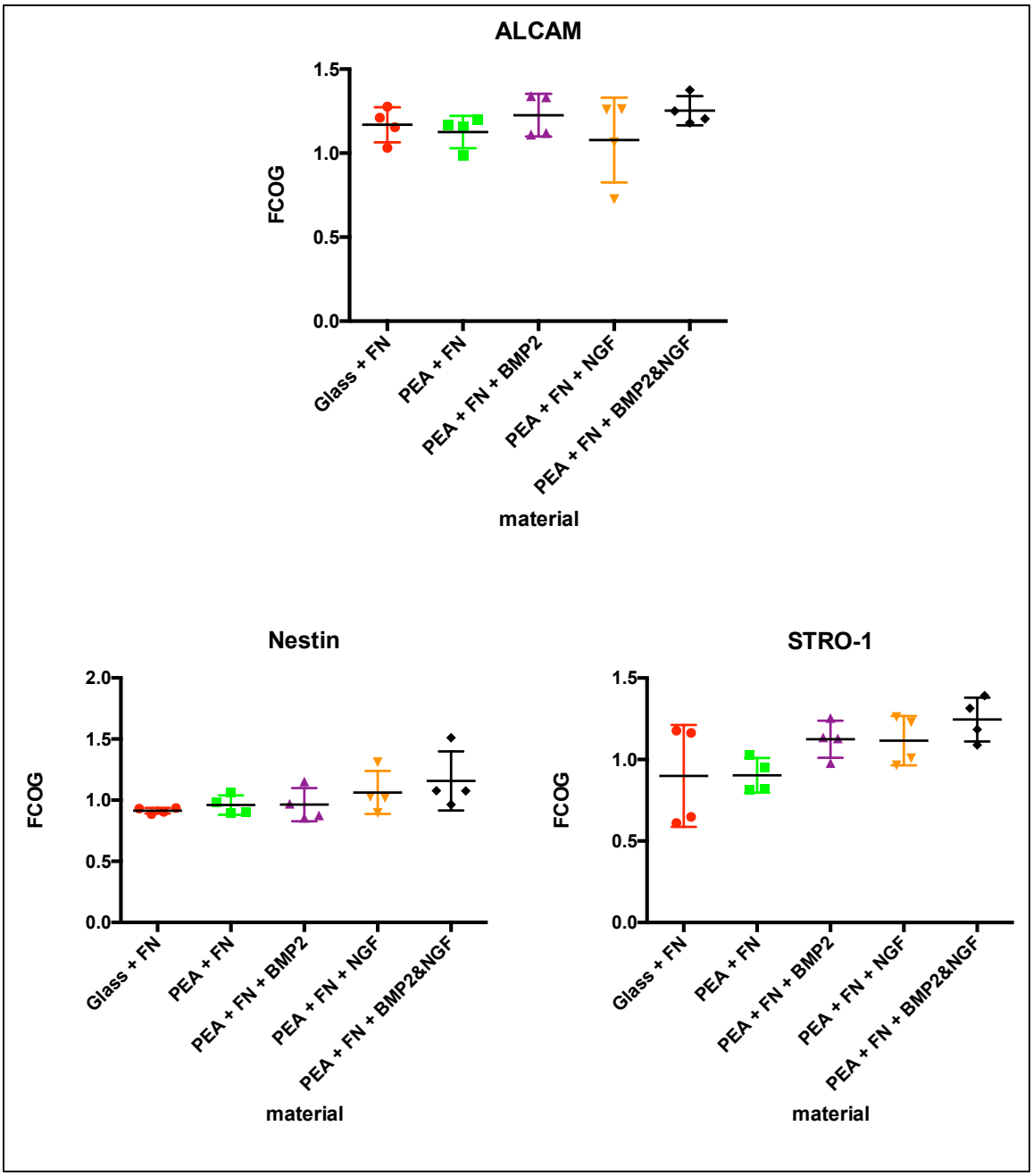

Figure 4-7 ICW results for MSC marker expression in 2% FBS media
ICW was carried out to determine whether reducing the concentration of FBS in the media to 2% would result in changes in the expression levels of MSC markers, ALCAM, nestin and STRO-1 being observed in cells cultured on different potential niche model substrates. Fold change values over glass (FCOG) are reported. n = 4. 1 biological replicate. Graph shows mean +/- SD. Data indicates that substrate type has no statistically significant effect on the expression of MSC markers.

4.4.3.2 Osteogenesis marker expression (2% FBS media)

In order to assess the capacity of PEA + FN + BMP-2 surfaces to induce a greater level of osteogenesis in STRO-1$^+$ cells cultured for 21 days when the serum concentration was reduced to 2%, ICW was carried out to determine protein level changes in OCN and OPN. The fold change over glass values for the niche model candidate surfaces are presented in Figure 4-8.

The results shown in Figure 4-8 suggested that expression of OCN and OPN was highest on PEA + FN + BMP-2 substrates. The mean fold change over glass values indicative of OCN and OPN expression for cells on PEA + FN + BMP-2&NGF substrates also appeared to be slightly higher than on controls, yet to a lesser extent. This was likely to be down to NGF occupying some of the GF binding sites, and therefore there being fewer binding sites occupied by BMP-2 on these combined GF substrates.

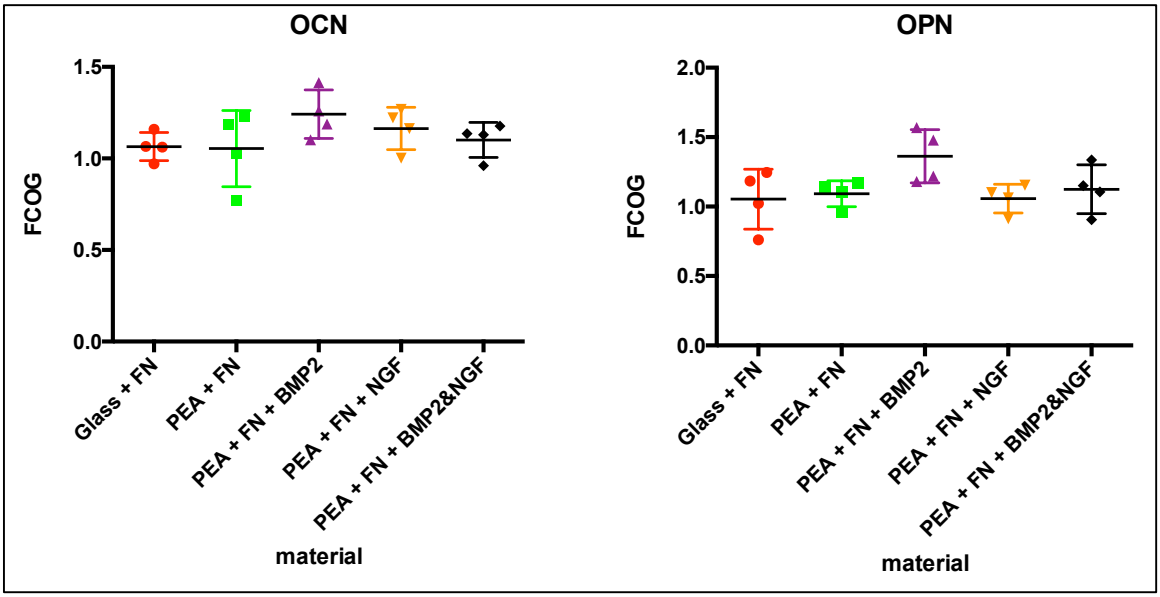

Figure 4-8 ICW results indicative of osteogenesis in 2% FBS media
STRO-1$^+$ cells were cultured for 21 days on different niche model candidate substrates, and ICW was carried out to determine if different PEA + FN substrates have the capacity to support increased expression levels of osteogenesis markers, OCN and OPN, when cultured in media supplemented with 2% FBS. Fold change values over glass (FCOG) are reported. n = 4. 1 biological replicate. Graph shows mean +/- SD. Data indicates that culture on PEA + FN + BMP-2 substrates enhances expression of osteogenic differentiation markers.

4.4.3.3 HSC maintenance factor expression (2% FBS media)

ICW was used to determine if reducing the concentration of FBS in the media to 2% was sufficient to allow the action of the PEA + FN bound GFs to accentuate the differences in SCF and VCAM-1 expression in STRO-1$^+$ cells cultured on different substrates, as observed in Figure 4-6. The fold change over glass values for the niche model candidate surfaces are presented in Figure 4-9.

The SCF data shown in Figure 4-9 suggested that SCF expression levels were greatest on PEA + FN + GF substrates. While this result is not statistically significant, it is important to note that the result observed supported the SCF data shown in Figure 4-6, and provided additional evidence to suggest that PEA + FN + GF substrates could be valuable in HSC niche models.

The data above also provided evidence to suggest that PEA + FN + NGF surfaces may act to support enhanced expression levels of VCAM-1 in STRO-1$^+$ cells cultured in media supplemented with 2% FBS. A increase in VCAM-1 expression relative to controls was observed in Figure 4-6, and so further results existed to support the use of PEA + FN + GF surfaces in HSC niche models.

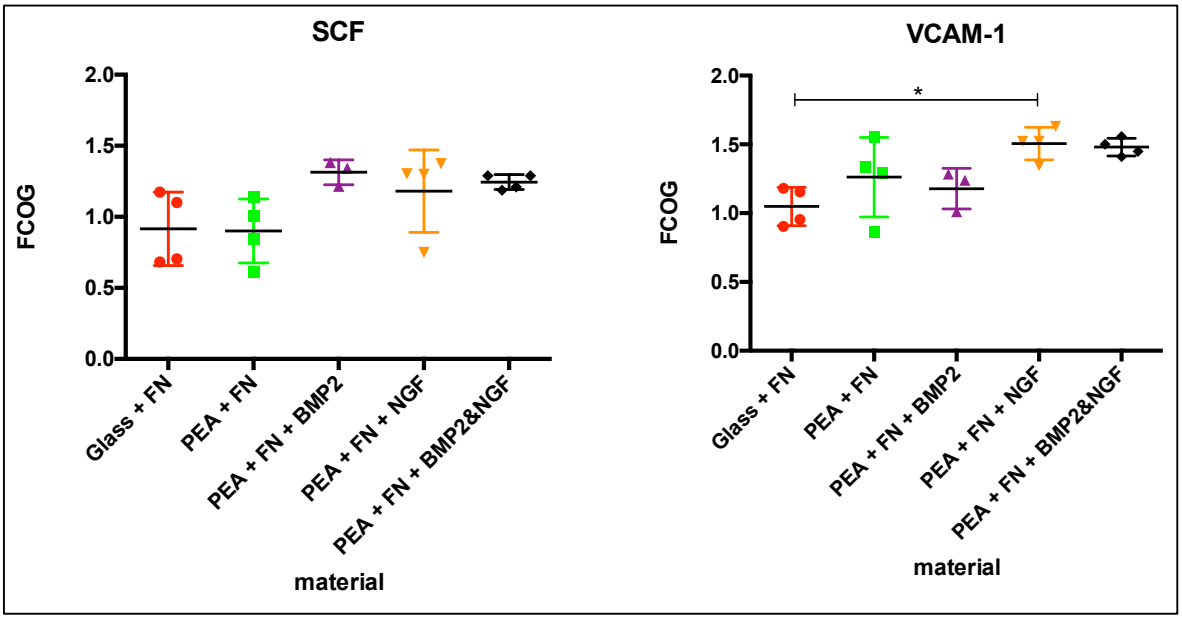

Figure 4-9 ICW results for SCF and VCAM-1 expression in 2% FBS media
STRO-1$^+$ cells were cultured for 21 days on different niche model candidate substrates, and ICW was carried out to determine if different PEA + FN substrates have the capacity to support increased expression levels of expression of HSC maintenance factors, SCF and VCAM-1, when cultured in media supplemented with 2% FBS. Fold change values over glass are reported. n = 4. 1 biological replicate. Graph shows mean +/- SD. *=p<0.05 by Kruskal-Wallis. Data indicates that culture on GF-containing substrates increases expression of HSC maintenance factors.

4.4.4 Niche protein expression results in 2% human serum media for 14 days and 5GF media for 7 days

The promising results obtained and shown in sections 4.4.2 and 4.4.3 encouraged further investigation into the potential of PEA + FN + GF surfaces within HSC niche models. As further research into models containing these surfaces progressed, it was important to take the likelihood of such models to support HSC survival into consideration. As the models are intended for use with human cells, it was advised by collaborators that the FBS in the media was exchanged for human serum, and cells were cultured in media containing 2% HS for 14 days, before being switched to an HSC-supportive media (referred to as 5GF media) for days 14-21 of culture. To ensure that the change in media composition did not affect the viability of STRO-1^+ cells, an MTT assay was carried out. Results shown in Figure 4-10 suggested that there was no statistically significant impact on cell viability, and so ICW was carried out to assess how this culture method affects the behaviour of STRO-1^+ MSCs cultured on the substrate types, with regards to the expression of MSC and HSC maintenance factors, ICW was carried out as per sections 4.4.2 and 4.4.3.

4.4.4.1 STRO-1$^+$ cell viability in varying serum concentrations and types

An MTT assay was carried out after 3,7 and 14 days of cell culture to determine the effect of changing the concentration and type of serum in the media on STRO-1$^+$ cell viability (Figure 4-10)

The results suggested that culturing cells in 10% FBS, 2% FBS or 2% HS induced no statistically significant differences in the viability of STRO-1$^+$ cells cultured for 3, 7 or 14 days. This result proposed that using a reduced concentration of human serum as opposed to FBS would have no impact on the basic health of the MSCs used within an HSC niche model.

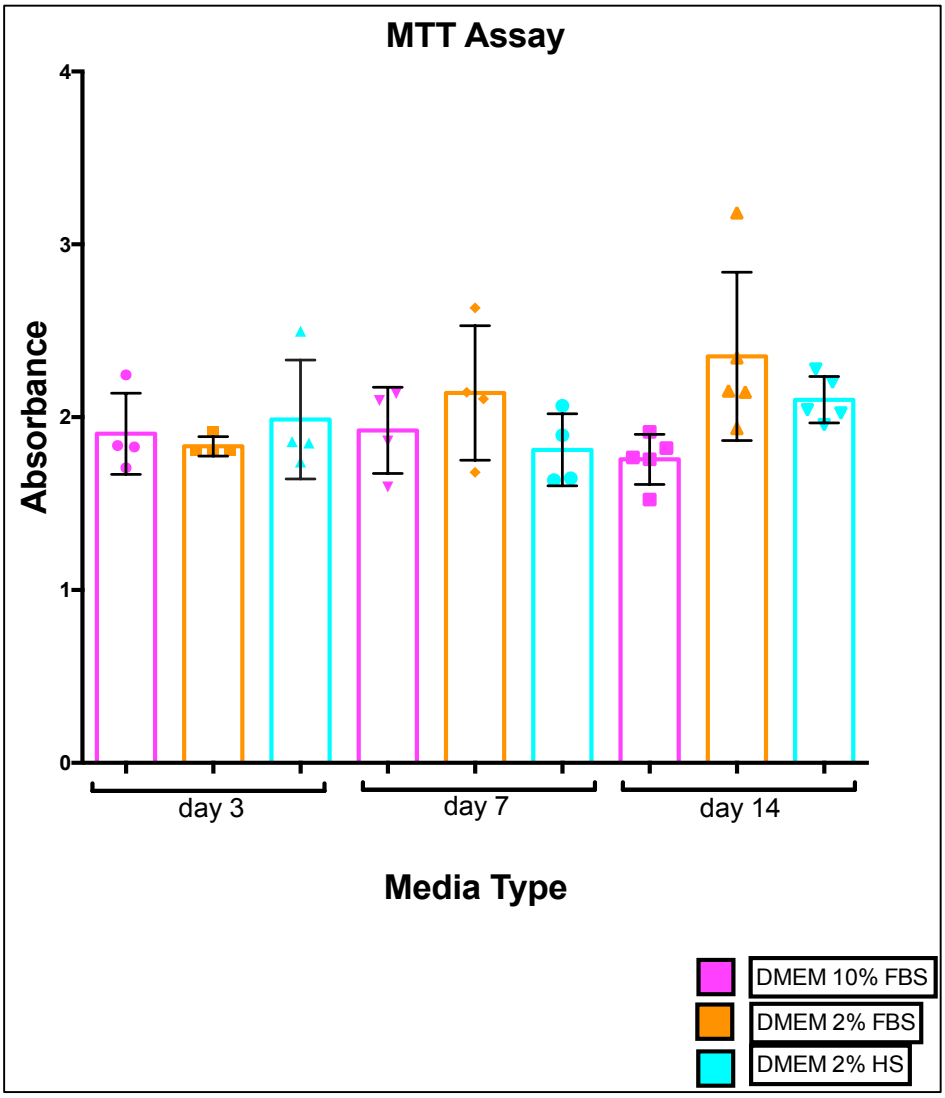

Figure 4-10 STRO-1 cell viability in media with different serum type and concentration
STRO-1$^+$ cells were cultured for 3, 7 and 14 days in DMEM supplemented with 10% FBS, 2% FBS or 2% human serum (HS), and their viability was determined using an MTT assay. Graph shows mean +/- SD. Data indicates that MSC viability is not affected, over time, by the media formulation used.

4.4.4.2 MSC marker expression (HS and 5GF media)

ICW was carried out to determine if culturing STRO-1$^+$ MSCs in DMEM supplemented with 2% HS for days 1-14 and then 5GF media for days 15-21 produced similar results to those observed in Figure 4-4 and Figure 4-7, whereby the expression of MSC markers STRO-1 and nestin is not statistically different in cells cultured on the different substrate types. The fold change over glass values for the niche model candidate surfaces are presented in Figure 4-11.

The results suggested that use of DMEM supplemented with 2% HS for the first 14 days of cell culture and then the use of 5GF media for days 15-21 of the culture did not induce any statistically significant differences in the expression levels of ALCAM, nestin or STRO-1 in cells cultured on the different niche substrate types (as observed in Figure 4-7).

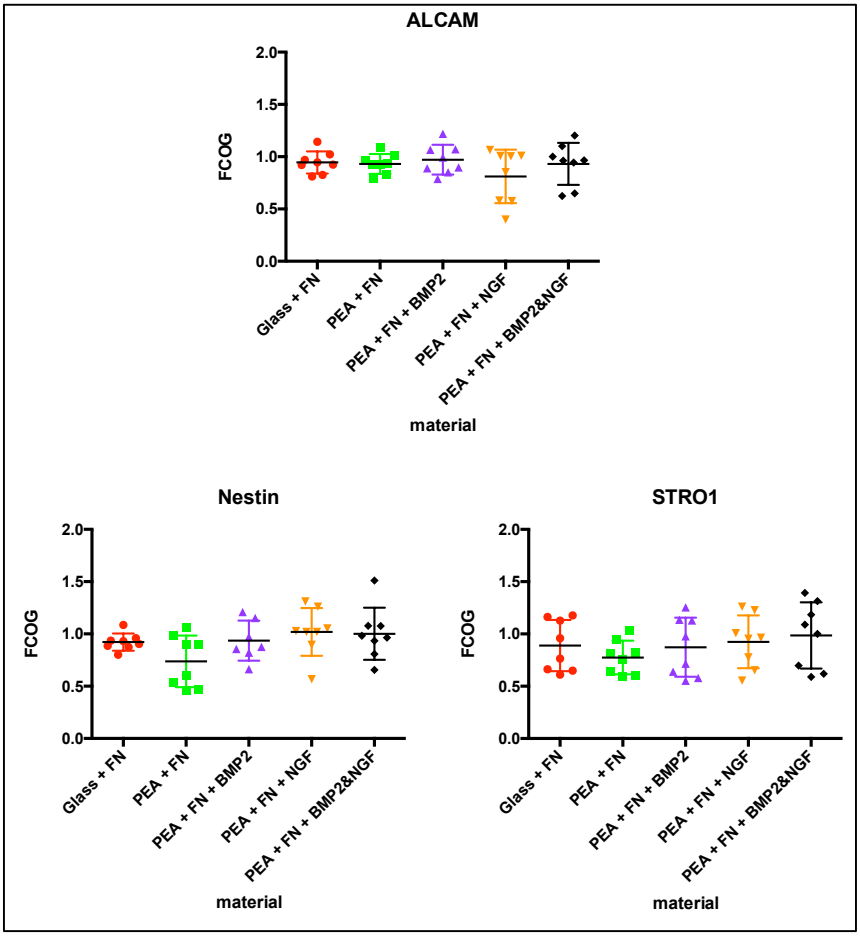

Figure 4-11 ICW results for MSC marker expression in 2% HS and 5GF media
ICW was carried out to determine if culture of STRO-1$^+$ MSCs on different niche model candidate substrates altered the expression levels of MSC markers, ALCAM, nestin and STRO-1 after 14 days of culture in DMEM supplemented with human serum and then 7 days of culture in 5GF media. Fold change values over glass (FCOG) are reported. n = 4. 2 biological replicates. Graph shows mean +/- SD. Data indicates that expression of MSC markers is not affected by cell culture on the different substrates tested.

4.4.4.3 HSC maintenance factor expression (HS and 5GF media)

ICW was carried out to determine if culturing STRO-1$^+$ cells in DMEM supplemented with 2% HS for 14 days, and then 5GF media for days 15-21 of culture produced similar results to those observed in Figure 4-6 and Figure 4-9, whereby PEA + FN + GF surfaces appear to enhance expression of SCF and VCAM-1, relative to controls (Figure 4-12).

SCF was maximally expressed in cells cultured on PEA + FN + BMP-2&NGF substrates in this media type. Although the results were not statistically significant, SCF expression observed here was similar to that observed in Figure 4-6 and Figure 4-9, wherein PEA substrates, notably the PEA + FN + BMP-2&NGF substrate, induced the highest expression levels of SCF in STRO-1$^+$ cells.

Interestingly, using DMEM supplemented with 2% HS for 14 days of cell culture and then 5GF media, potentiated the subtle differences in the expression of VCAM-1 in cells cultured on different substrates that are shown in Figure 4-6 and Figure 4-9. As with the SCF result shown, the VCAM-1 result suggested that the PEA + FN + BMP-2&NGF substrate is the best for maximising VCAM-1 expression in STRO-1$^+$ cells cultured in this media type.

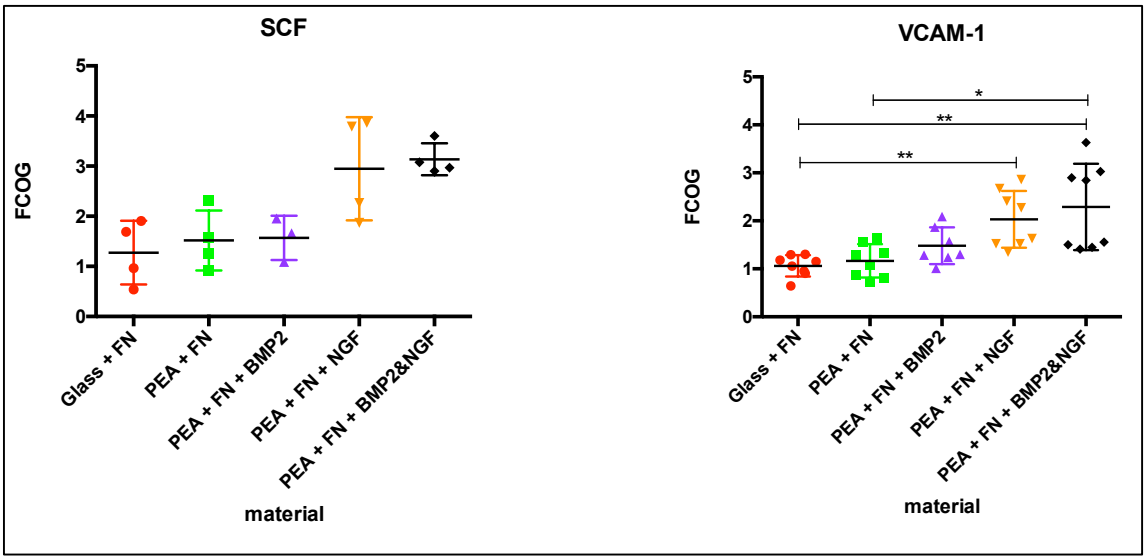

Figure 4-12 ICW results for SCF and VCAM-1 expression in 2% HS and 5GF media
ICW was carried out to determine if culture of STRO-1$^+$ MSCs on different niche model candidate substrates altered the expression levels of HSC maintenance factors, SCF and VCAM-1 after 14 days of culture in DMEM supplemented with human serum and then 7 days of culture in 5GF media. Fold change values over glass (FCOG) are reported. n = 4. 2 biological replicates. Graph shows mean +/- SD. *=p<0.05, **=p<0.01 by Kruskal-Wallis. Data indicates that PEA + FN + BMP-2&NGF substrates may optimally enhance the expression of HSC maintenance factors, SCF & VCAM-1.

4.4.5 Niche protein expression results in 2% human serum media for 14 days and 3GF media for 7 days

The results from section 4.4.4 show that MSC marker expression can be maintained and SCF and VCAM-1 expression can be maximised on PEA + FN + BMP-2&NGF surfaces. In addition, these results also imply that using a medium containing 2% HS for 14 days of culture and then a serum-free media suited to HSCs for days 15 to 21 of culture supports this phenotype in STRO-1^+ cells. Taking these observations into consideration, it was decided that this media formulation would be well suited for use in an HSC niche model. However, additional work from collaborators found that using 3GF media for the culture of HSCs was just as effective as using 5GF media. Thus, in order to reduce the cost associated with model development, it was decided that use of the 3GF media would be worth investigating. To this end, ICW was carried out to determine if using 3GF media from days 15 to 21 affected the previously observed expression differences, whereby MSC marker expression was maintained and OCN, OPN, SCF and VCAM-1 expression levels were maximised on PEA + FN + GF substrates.

4.4.5.1 MSC marker expression (HS and 3GF media)

ICW was carried out to determine if culturing STRO-1^+ MSCs in DMEM supplemented with 2% HS for days 1-14 and then 3GF media for days 15-21 produced similar results to those observed in Figure 4-4, Figure 4-7 and Figure 4-11, whereby STRO-1 and nestin expression is not statistically different in cells cultured on different substrates. In addition, ALCAM expression was considered, as an ideal model would also maintain ALCAM expression in cells cultured on all substrate types (Figure 4-13).

The graphs suggested that there were no statistically significant differences in the expression levels of ALCAM, nestin or STRO-1 between cells cultured on the different substrates in 2% HS media for 14 days and then 3GF media for 7 days. The results obtained here correlated with those previously obtained for different media types, and suggested that the different substrate types had no profound effect on the expression levels of these MSC markers in STRO-1^+ cells.

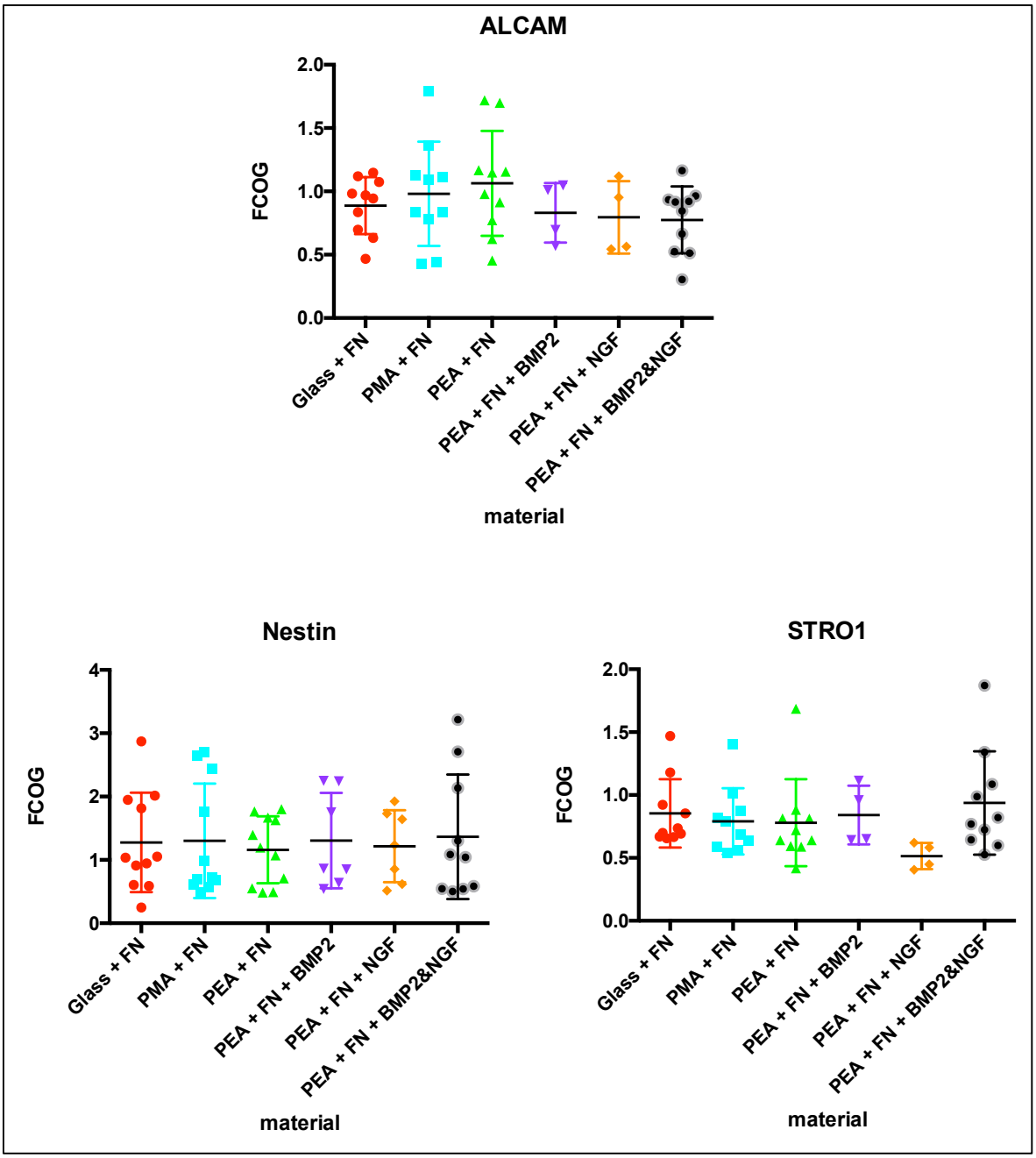

Figure 4-13 ICW results for MSC marker expression in 2% HS and 3GF media
ICW was carried out to determine if culture of STRO-1^{+} MSCs on different niche model candidate substrates altered the expression levels of MSC markers, ALCAM, nestin and STRO-1 after 14 days of culture in DMEM supplemented with human serum and then 7 days of culture in 3GF media. Fold change values over glass (FCOG) are reported. n ≥ 3. Glass + FN, PMA + FN, PEA + FN, PEA + FN + BMP-2&NGF = 3 biological replicates. PEA + FN + BMP-2 & PEA + FN + NGF ≥ 1 biological replicate. Graph shows mean +/- SD. Data indicates that MSC marker expression is not affected by the substrate used in the HSC niche models.

4.4.5.2 Osteogenesis marker expression (HS and 3GF media)

To investigate the hypothesis that PEA + FN + BMP-2 or PEA + FN + BMP-2&NGF substrates would induce the greatest expression of osteogenesis markers in STRO-1$^+$ cells cultured on these substrates, ICW was carried out to determine if this hypothesis was true for cells cultured in media containing 2% HS for 14 days and 3GF media for days 15 to 21 of culture (Figure 4-14).

The graphs suggested that levels of OCN expression in STRO-1$^+$ cells was not statistically different when the cells were cultured on the different substrates in this media formulation. However, fitting with the hypothesis, the results suggested that OPN expression was highest in cells cultured on PEA + FN + BMP-2 substrates and PEA + FN + BMP-2&NGF substrates. OPN is associated with a more primitive phenotype, while OCN is associated with a more mature phenotype (Aubin et al., 1995). Consequently, these results suggested that the PEA + FN + GF surfaces and this culture method collectively induced the formation of a primitive OB phenotype in some cells, which could be of great value to this HSC niche model (Nilsson et al., 2005).

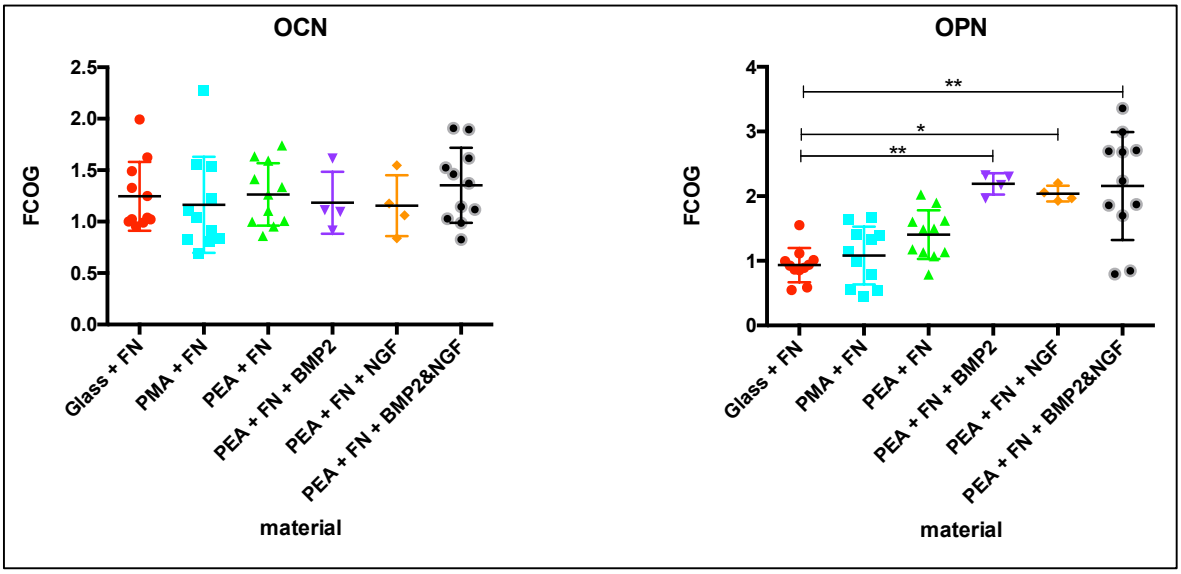

Figure 4-14 ICW results indicative of osteogenesis in 2% HS and 3GF media
STRO-1$^+$ cells were cultured on different niche model candidate substrates, and ICW was carried out to determine if different PEA + FN substrates have the capacity to support increased expression levels of osteogenesis markers, OCN and OPN, when cultured in media supplemented with 2% HS for days 1-14 and then 3GF media for days 15-21. Fold change values over glass (FCOG) are reported. n ≥ 3. Glass + FN, PMA + FN, PEA + FN and PEA + FN + -&NGF = 3 biological replicates. PEA + FN + BMP2 and PEA + FN + NGF = 1 biological replicate. Graph shows mean +/- SD. *=p<0.05, **=p<0.01 by Kruskal-Wallis. Data suggests that OPN expression is highest on substrates with BMP-2 bound.

4.4.5.3 HSC maintenance factor expression (HS and 3GF media)

ICW was carried out to determine if similar differences in SCF and VCAM-1 expression to those observed in Figure 4-12 remained when STRO-1$^+$ cells were cultured in DMEM supplemented with 2% HS for 14 days and then 3GF media for days 15-21, rather than in 5GF media for days 15-21 (Figure 4-15).

The results obtained for the relative expression levels of SCF were similar to those shown in Figure 4-12, in that PEA + FN + GF substrates appeared to induce greater expression of SCF relative to control substrates. Interestingly, in this media type, it appeared that the PEA + FN + NGF and PEA + FN + BMP-2&NGF substrates induced a statistically significant increase in SCF expression, relative to the gold standard glass + FN substrate, suggesting that these substrates and this media formulation had strong potential within an HSC niche model.

The data obtained for VCAM-1 expression in cells cultured on the different substrates was also somewhat similar to that shown in Figure 4-12, in that the PEA + FN + GF surfaces seemed to induce a marginal increase in VCAM-1 expression in cells cultured on these surfaces, relative to controls. However, it should be noted that this change was not statistically significant.

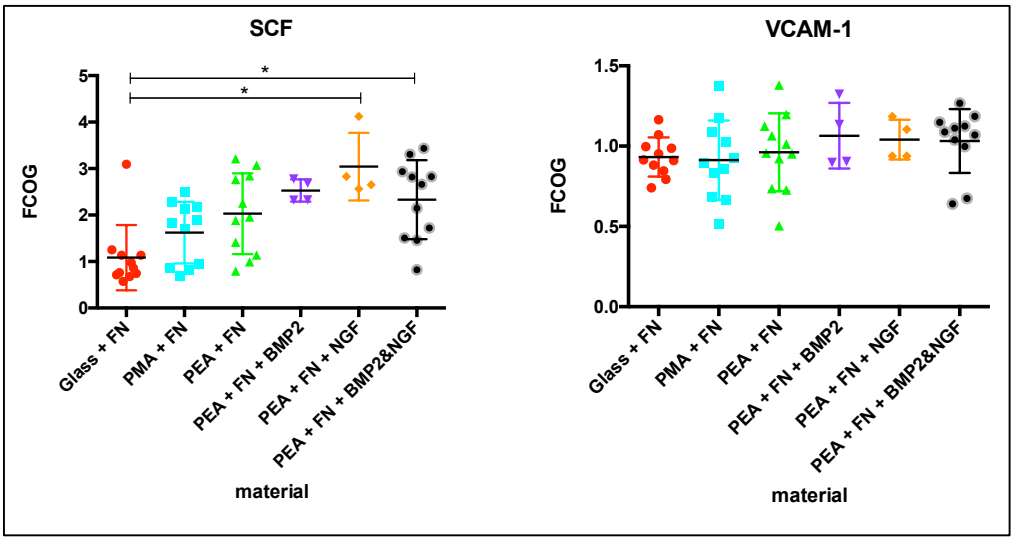

Figure 4-15 ICW results for SCF and VCAM-1 expression in 2% HS and 3GF media
ICW was carried out to determine if culture of STRO-1$^+$ MSCs on different niche model candidate substrates altered the expression levels of HSC maintenance factors, SCF and VCAM-1 after 14 days of culture in DMEM supplemented with human serum and then 7 days of culture in 3GF media. Fold change values over glass (FCOG) are reported. n ≥ 3. Glass + FN, PMA + FN, PEA + FN and PEA + FN + BMP2&NGF = 3 biological replicates. PEA + FN + BMP2 and PEA + FN + NGF = 1 biological replicate. Graph shows mean +/- SD. *=p<0.05, **=p<0.01 by Kruskal-Wallis. Data indicates that SCF expression is enhanced on substrates with NGF bound.

4.4.6 Flow cytometry analysis of additional MSC marker expression in 2% HS and 3GF media

The results shown in Figure 4-4, Figure 4-7, Figure 4-11 and Figure 4-13 suggest that there are no reproducible, statistically significant differences in the expression levels of nestin or STRO-1 between cells cultured on the candidate niche model substrates tested. In addition, the results observed were consistent despite 4 different media compositions tested. To minimise experiment size, cost and complexity, work here on focused on using only PEA + FN + BMP-2&NGF substrates representing the PEA + FN + GF group, as this substrate appeared to produce cell populations with a phenotype most favourable within an HSC niche model.

In order to assess the effect of culture on the expression of additional MSC markers, flow cytometry was carried out using antibodies against CD166 (ALCAM) CD105, CD90, CD29 and CD13, to determine what percentage of total cell number expressed each marker type (Figure 4-16).

The results suggested that there were no major reductions in the expression of the MSC markers tested in cells cultured on the PEA + FN + BMP-2&NGF substrates, relative to controls. It was particularly interesting to see an apparent rise in the expression of CD166 (ALCAM) in cells cultured on the PEA + FN + BMP-2&NGF substrates, as the result shown in Figure 4-13 indicated that ALCAM expression may be reduced in cells cultured on PEA + FN + BMP-2&NGF substrates. However, it was important to note that the flow cytometry protocol followed in this experiment required approximately 30 000 cells per test, and so 3 wells of $1x10^4$ cells were pooled per sample, meaning the overall n number was one. Thus, it would be important to repeat this experiment several times more before a valid conclusion could be made.

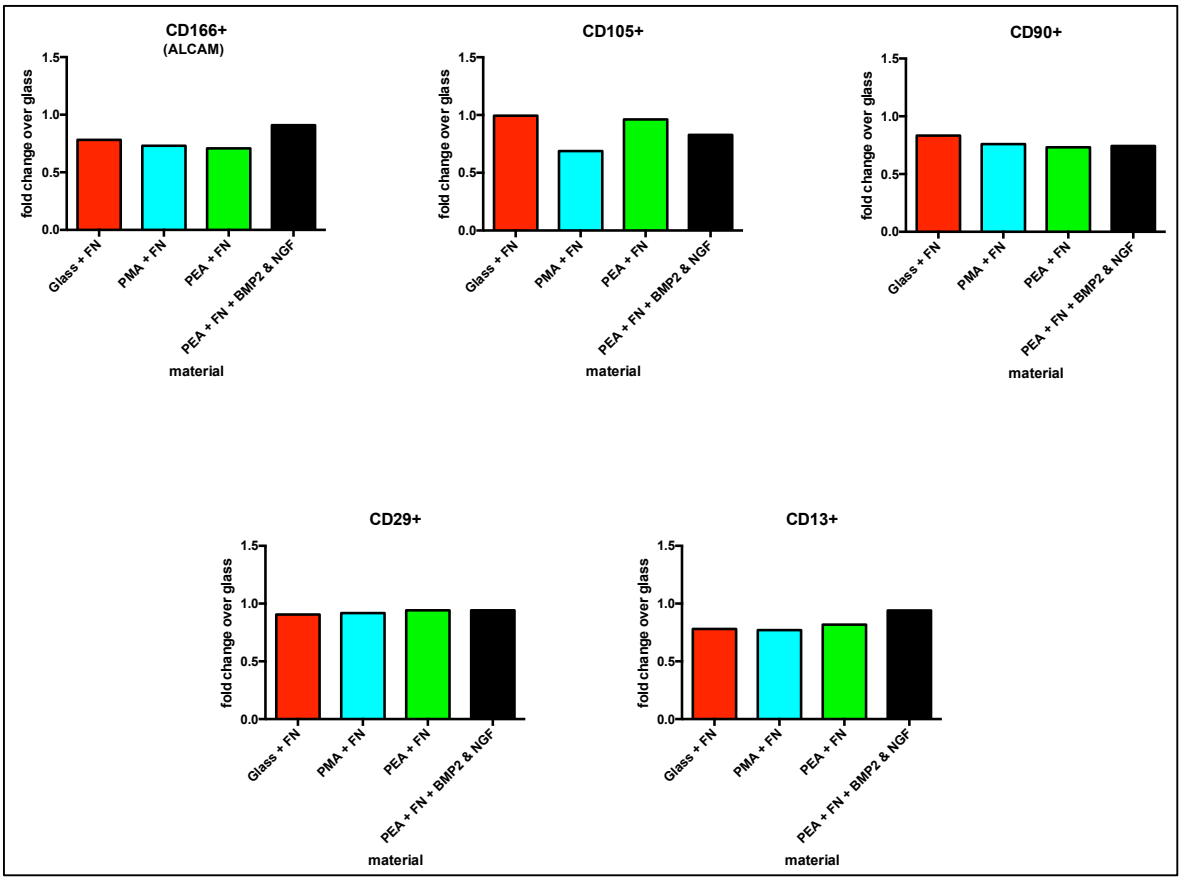

Figure 4-16 Flow cytometry results for MSC marker expression in 2% HS and 3GF media
Flow cytometry was carried out to assess the effect of STRO-1$^+$ cell culture on different niche model candidate substrates, in 2% HS and 3GF media for 21 days. 3 samples of approximately 1 x 10^4 cells were pooled per substrate type, per protein test, and cells were stained with antibodies against CD166, CD105, CD90, CD29 and CD13. The percentage of the total cell number expressing each marker was determined using FlowJo software and fold change over glass values are reported. n=1. Data indicates that MSC marker expression is not reduced in models featuring GF-containing substrates.

4.4.7 Assessing MSC function using T cell suppression assay

As shown in Figure 4-4, Figure 4-7, Figure 4-11, Figure 4-13 and Figure 4-16, the expression of MSC markers was not affected when STRO-1$^+$ MSCs were cultured on any of the niche model candidate substrates tested. However, other results presented in this chapter suggested that a degree of osteogenesis was occurring when cells were cultured in models containing PEA + FN + BMP-2 and PEA + FN + BMP-2&NGF substrates. This suggested that the MSC character of STRO-1$^+$ cells cultured in models containing these substrates may be less, and would be replaced by some osteogenic character. In order to further test the results suggesting MSC phenotype is not affected by culture in models containing osteogenesis-promoting substrates, a T cell suppression assay was carried out.

The T cell suppressive character of MSCs derived from the bone marrow is considered to be a key characteristic of MSCs (Bloom et al., 2015). Thus, T cells were stained with CFSE dye and added to MSCs cultured for 21 days in HSC niche models, and were cultured for 5 days to determine the capacity of the MSCs to suppress T cell proliferation. The proliferation index, indicative of how well T cells proliferate, was calculated and the results are shown in Figure 4-17 (Gorgoulis et al., 2005, Gattinoni et al., 2011).

The results indicated that MSCs cultured in models featuring PMA + FN substrates and PEA + FN + BMP-2&NGF substrates had the best capacity to suppress T cell proliferation. It was particularly interesting to observe that the only niche model substrate that induced a statistically lower level of T cell proliferation to the stimulated control, was the PEA + FN + BMP-2&NGF substrate, as this observation suggested that while some osteogenesis may occur in models comprising this substrate, the substrate does not lessen the stem cell character of the MSCs cultured on it.

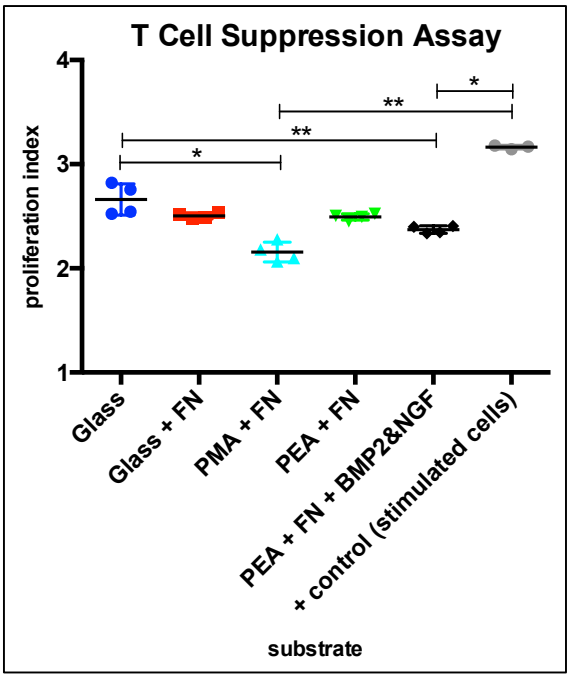

Figure 4-17 Proliferation index of T cells cultured with MSCs from HSC niche models
CFSE staining of T cells was carried out after culture for 5 days in HSC niche models featuring MSCs cultured on different niche model candidate substrates in 2% HS media for 14 days and 3GF media for the 7 days following. n=4. Flow cytometry and analysis using FlowJo software were used to determine the number of cells in each division generation and the number of original parent cells. The proliferation index was calculated by dividing the sum of T cells in all generations by the number of parent cells. Positive controls comprise T cells stimulated with PMA and IL-6, cultured in the absence of MSCs. Graph shows mean +/- SD. *=p<0.05, **=p<0.01 by Kruskal-Wallis. Data indicates that MSCs maintain their ability to suppress T cells when cultured on PEA + FN + BMP-2&NGF substrates.

4.4.8 CXCL-12 secretion from STRO-1$^+$ cells cultured on niche model candidate substrates in varying media compositions

In addition to using ICW to assess the effect of cell culture in different media types, and on different substrates, on the expression of cell surface markers, an ELISA for CXCL-12 was carried out to determine the effect of these changes on CXCL-12 secretion from the STRO-1$^+$ cells comprising the stromal layer of the developing HSC niche model.

4.4.8.1 Analysis of CXCL-12 ELISA data from STRO-1$^+$ cells cultured in DMEM supplemented with 10% FBS

An ELISA was used to determine the effect of cell culture on different candidate niche model substrates in DMEM supplemented with 10% FBS. 3 technical replicates for each substrate were analysed and their concentrations were determined following interpolation of a standard curve. The mean concentration of CXCL-12 in the media of cells cultured on each substrate type was determined, and fold change values over glass were calculated (Figure 4-18).

The results suggested that there were no statistically significant differences in the secretion of CXCL-12 from cells cultured on different substrates or at different time points. The results of the ICW analyses suggested that reducing the concentration of serum in the media potentiated the effect of the GFs on the PEA + FN + GF surfaces (sections 4.4.2, 4.4.3, 4.4.4 & 4.4.5). Consequently, it is possible that the high concentration of FBS in the media here was diminishing the differences in protein level expression resulting from culture on the substrates, in terms of the secretion of CXCL-12 from STRO-1$^+$ cells. In accordance with model development and these observations, it was decided that this work would be repeated with a lower concentration of serum in the media.

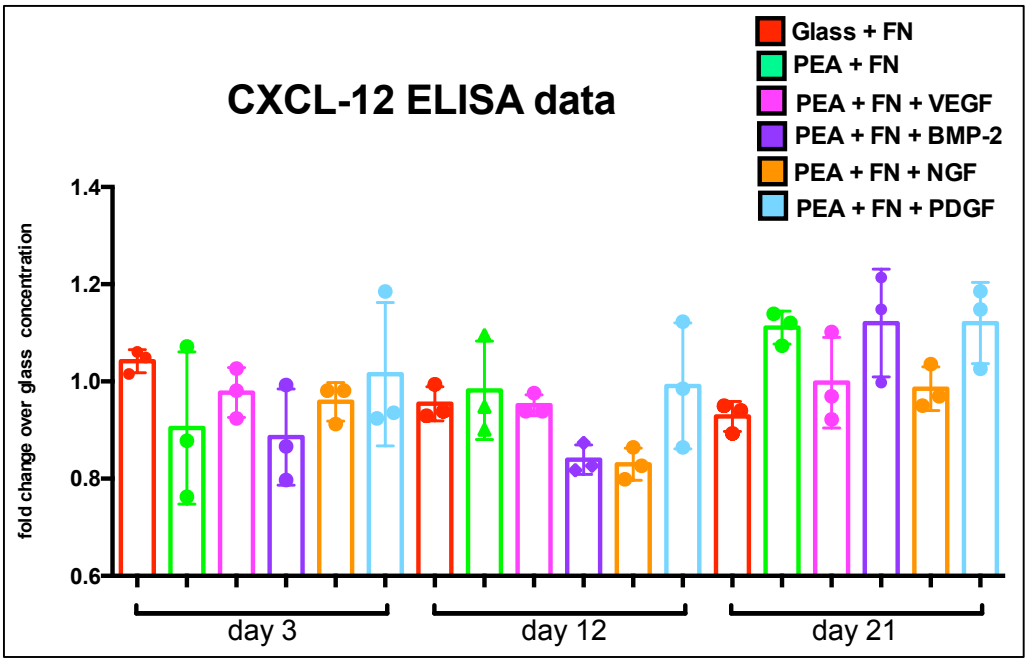

Figure 4-18 CXCL-12 ELISA data from culture in DMEM supplemented with 10% FBS
An ELISA was carried out to determine the concentration of CXCL-12 in the media supernatant of STRO-1$^+$ cells cultured in DMEM supplemented with 10% FBS. Media was collected from days 0-3, 9-12 and 18-21 and the concentration was determined following interpolation of a standard curve. The mean concentration of CXCL-12 in the media of cells cultured on each substrate type was calculated, and is reported as a fold change over glass. n=3. Graph shows mean +/- SD. Data indicates that the different substrates have no statistically significant effect on the expression of CXCL-12 in MSCs cultured in 10% FBS media.

4.4.8.2 Analysis of CXCL-12 ELISA data from STRO-1$^+$ cells cultured in DMEM supplemented with 2% HS then 3GF media

To determine the effect of reducing the concentration of serum from 10% to 2%, and switching from FBS to HS followed by 3GF media, at day 14 (to mimic the point of HSC addition) a second CXCL-12 ELISA was carried out to determine the concentration of CXCL-12 in the media supernatants of HSC niche models within a 24-well plate. At the time when this experiment was carried out, it had previously been decided that the PEA + FN + GF samples that would be considered would be only PEA + FN + BMP-2, PEA + FN + NGF and PEA + FN + BMP-2&NGF, as these samples induced the greatest expression levels of HSC maintenance factors and OPN in cells cultured in media supplemented with 2% HS then 3GF media for days 15-21 (Figure 4-19).

The data shown in Figure 4-19 suggested that cells cultured between days 0-3 and days 9-12 on the PEA + FN + BMP-2 substrates secreted the highest mean levels of CXCL-12. However, for cells cultured from days 18-21, it is apparent

that those on PEA + FN + NGF and PEA + FN + BMP-2&NGF substrates appeared to secrete the highest levels of CXCL-12 – these substrates appeared to induce an average of a five-fold increase in CXCL-12 secretion. This result suggested that culture of the STRO-1$^+$ cells for 21 days is a good length of culture, as the HSCs would not be added until the end of the culture at day 15. Further, this result indicated that this timing would expose the HSCs to maximal levels of CXCL-12 secreted from the stromal layer. In addition, this result also suggested that the PEA + FN + GF substrates maximally induced secretion of CXCL-12 from the stromal layer, fitting well with previous findings shown in Figure 4-12 and Figure 4-15, whereby the PEA + FN + GF substrates induce maximal expression of SCF and VCAM-1.

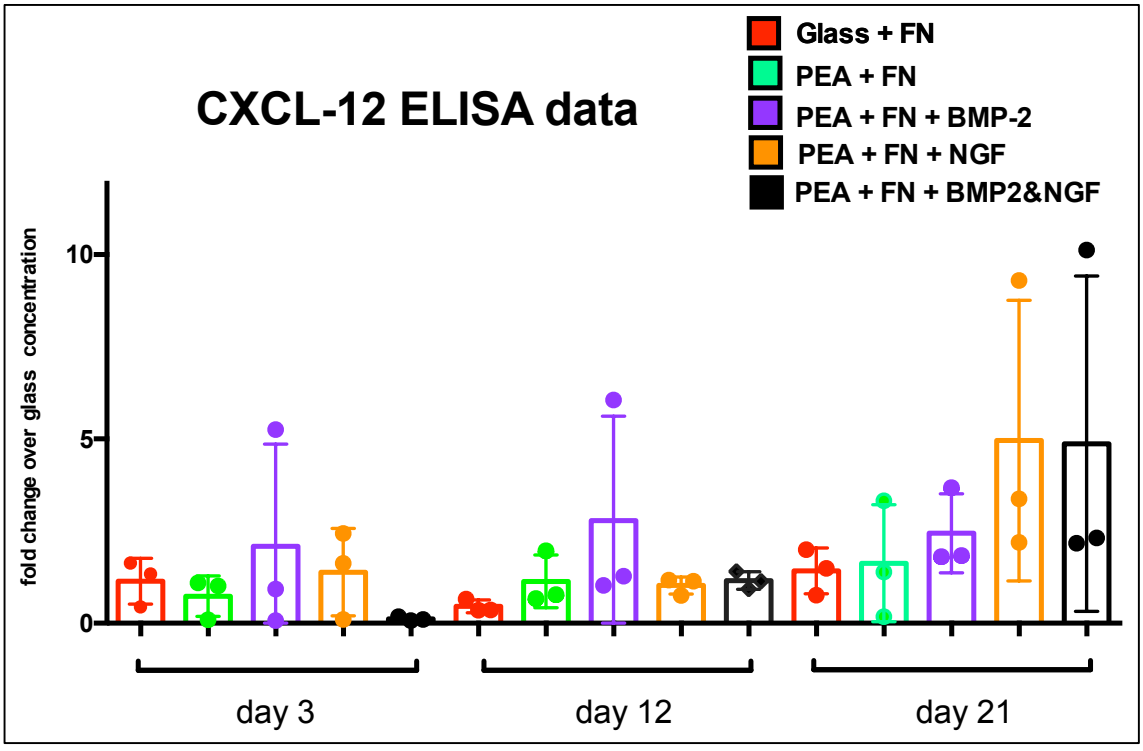

Figure 4-19 CXCL-12 ELISA data from culture in DMEM supplemented with 2% HS
An ELISA was carried out to determine the concentration of CXCL-12 in the media supernatant of STRO-1$^+$ cells cultured in DMEM supplemented with 2% HS until day 14, then 3GF media from day 15-21. Media was collected from days 0-3, 9-12 and 18-21 and the concentration was determined following interpolation of a standard curve. The mean concentration of CXCL-12 in the media of cells cultured on each substrate type was calculated, and is reported as a fold change over glass. n=3. Graph shows mean +/- SD. The results indicate that cells cultured on substrates containing BMP-2 alone or with NGF have the greatest expression levels of CXCL-12.

4.4.9 THPO secretion from STRO-1$^+$ cells cultured on niche model candidate substrates in varying media compositions

In addition to using ICW to assess the effect of cell culture in different media types, and on different substrates, on the expression of cell surface markers, an ELISA for THPO was carried out to determine the effect of these changes on THPO secretion.

4.4.9.1 Analysis of THPO ELISA data from STRO-1$^+$ cells cultured in DMEM supplemented with 10% FBS

An ELISA was used to determine the effect of cell culture on different candidate niche model substrates in DMEM supplemented with 10% FBS. 3 technical replicates for each substrate were analysed and their concentrations were determined following interpolation of a standard curve. The mean concentration of THPO in the media of cells cultured on each substrate type was determined, and fold change values over glass were calculated (Figure 4-20).

The results obtained from the THPO ELISA suggested that cells cultured on PEA + FN + BMP-2 surfaces secreted the highest levels of THPO at all time points. It was particularly interesting to observe that there was an approximately 7.5-fold increase relative to glass in THPO secretion from cells cultured on PEA + FN + BMP-2 substrates after 21 days. These results were expected, as it is known that THPO is secreted from cells of the osteoblastic lineage, and the BMP-2 that is present on the PEA + FN + BMP-2 substrates is likely to induce osteogenic differentiation of the STRO-1$^+$ cells, particularly after 21 days of culture.

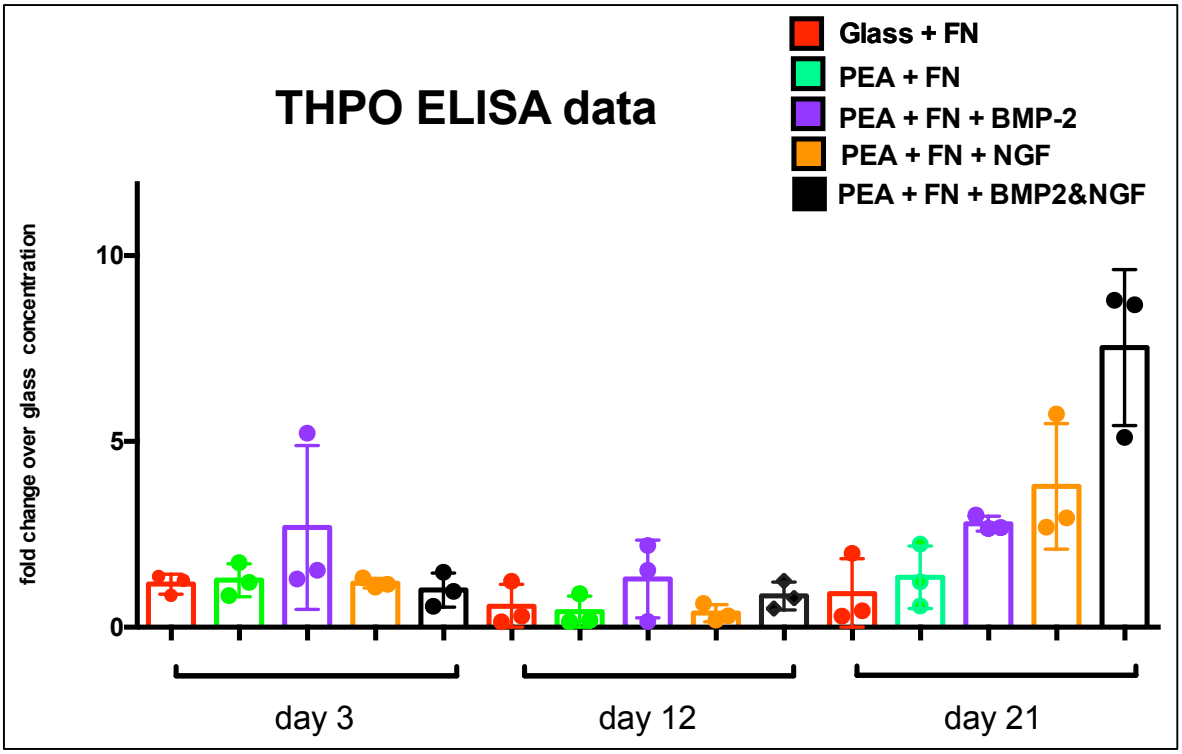

Figure 4-20 THPO ELISA data from culture in DMEM supplemented with 10% FBS
An ELISA was carried out to determine the concentration of THPO in the media supernatant of STRO-1$^+$ cells cultured in DMEM supplemented with 10% FBS. Media was collected from days 0-3, 9-12 and 18-21 and the concentration was determined following interpolation of a standard curve. The mean concentration of THPO in the media of cells cultured on each substrate type was calculated, and is reported as a fold change over glass. n=3. Graph shows mean +/- SD. Data indicates that GF substrates maximally enhance THPO expression in MSCs.

4.4.9.2 Analysis of THPO ELISA data from STRO-1$^+$ cells cultured in DMEM supplemented with 2% HS then 3GF media

Based on the results shown in Figure 4-20, it was decided that the secretion of THPO in response to culture on different niche candidate substrates should also be determined for cells cultured in DMEM supplemented with 2% HS then 3GF media, as opposed to 10% FBS. Thus, an ELISA was carried out using 3 technical replicates per substrate type, and the concentration of THPO in the media was determined following interpolation of a standard curve. The mean concentration of THPO in the media of cells cultured on each substrate type was determined and fold change values over glass were calculated (Figure 4-21).

The results shown in Figure 4-21 had less dramatic increases in the fold change over glass concentration of THPO in the media. However, it was apparent that a similar result to that shown in Figure 4-20 was observed; the PEA + FN + GF surfaces generally induced the stromal layer to secrete a larger quantity of

THPO into the media, when compared to controls. It was particularly promising to see a similar result at day 21, whereby PEA + FN + BMP-2 and PEA + FN + BMP-2&NGF substrates induced higher secretion of THPO compared to all controls. This suggested that the BMP-2 present on the substrates was acting to stimulate osteogenic differentiation, in turn stimulating THPO secretion. Thus, further results highlighting the potential of PEA + FN + GF surfaces within HSC niche models existed, and the benefit of using a 21 day culture was also shown again.

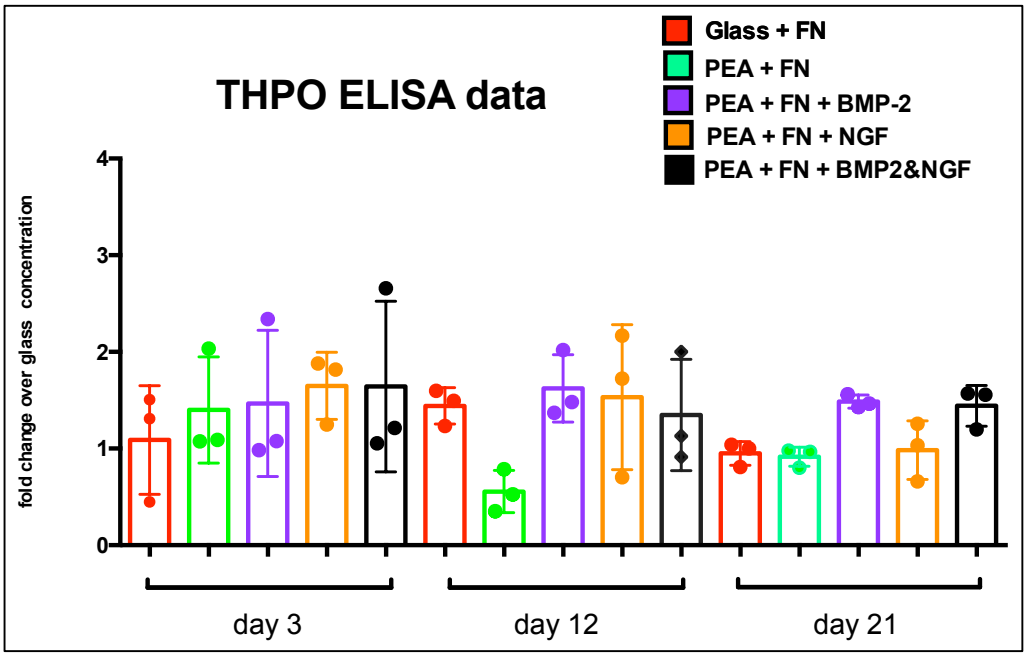

Figure 4-21 THPO ELISA data from culture in DMEM supplemented with 2% HS
An ELISA was carried out to determine the concentration of THPO in the media supernatant of STRO-1$^+$ cells cultured in DMEM supplemented with 2% HS until day 14, then 3GF media from days 15-21. Media was collected from days 0-3, 9-12 and 18-21 and the concentration was determined following interpolation of a standard curve. The mean concentration of THPO in the media of cells cultured on each substrate type was calculated, and is reported as a fold change over glass. n=3. Graph shows mean +/- SD. Data indicates that substrates featuring GFs may enhance THPO expression in MSCs.

4.4.10 Cell number analyses

The results shown in sections 4.4.8 and 4.4.9 indicate that higher levels of CXCL-12 and THPO were found in the media of STRO-1$^+$ cells cultured on niche model candidate substrates comprising PEA + FN + GFs, after 21 days. However, in order to determine if this greater concentration of CXCL-12 or TPO is resulting from the cells responding to the substrate by proliferating, it is necessary to calculate the number of cells present on each substrate type (thus determining if the increased concentrations are arising from an increased number of cells on these substrates).

In order to assess the influence of the niche model candidate substrates used in sections 4.4.8 and 4.4.9, the results of all ICWs carried out were reviewed, and the values obtained from the 700 nm channel, which indicates cell number, were taken. The fold change values over the mean glass values for each ICW analysis carried out were determined, and then fold change over glass fluorescence units were analysed (Figure 4-22).

The results indicated that the PEA + FN substrate resulted in the greatest expansion in STRO-1$^+$ cell number over a 21 day culture period. This result was encouraging, as it suggested that the increased concentration of CXCL-12 and THPO in the media supernatant of cells cultured on PEA + FN + GF surfaces (as shown in sections 4.4.8 and 4.4.9) was not arising as a result of these surface types inducing higher levels of cell expansion relative to PEA + FN controls. Rather, the result shown here suggested that the greater levels of CXCL-12 and THPO present in the media supernatant of STRO-1$^+$ cells cultured on PEA + FN + GF substrates was arising a result of cellular responses to the substrates.

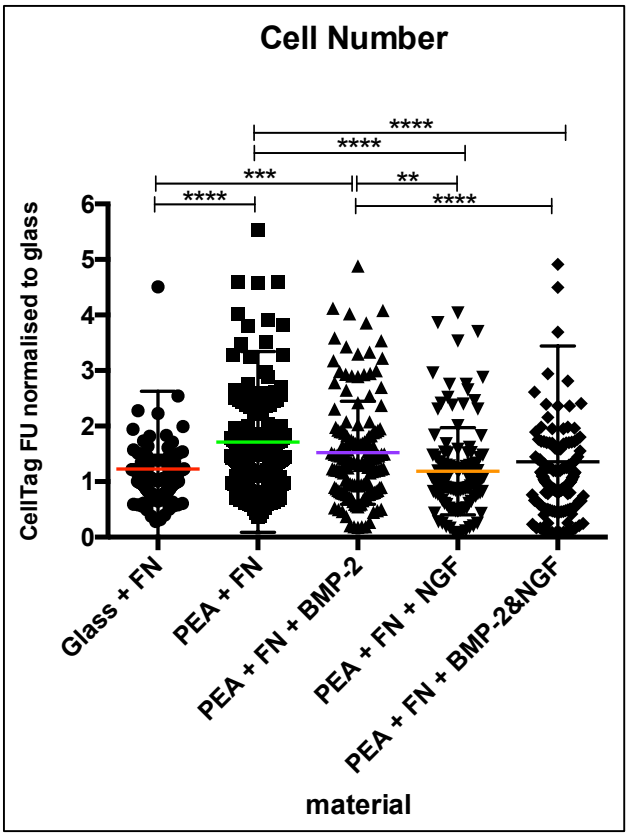

Figure 4-22 Cell number analysis after 21 days of culture on niche model candidate substrates
In order to assess the effect of cell culture on the niche model candidate substrates on total cell number, STRO-1$^+$ cells were cultured for 21 days and stained with CellTag 700 fluorescent dye. The fluorescence units obtained were normalised to the mean value obtained for glass substrates. Following the collection of fold change over glass values for cells from different donors, values were plotted on a graph and analysed using a non-parametric Kruskal-Wallis test. n ≥ 3. 11 biological replicates. Graph shows mean +/- SD. *=p<0.05, **=p<0.01, ***=p<0.001, ****=p<0.0001, by ANOVA. Data indicates that MSCs proliferate most on the PEA + FN substrate type.

4.5 Discussion

The bone marrow HSC niche is a complex environment, and HSC survival and proliferation is dependent on a range of regulatory signals from multiple cell types (Calvi et al., 2003, Méndez-Ferrer et al., 2010). In order to design an HSC niche model that can mimic the natural bone marrow niche as closely as possible, it is important to strive to develop a model that incorporates multiple regulatory signals. In the previous chapter, it was shown that BMP-2 and NGF can be bound, both independently and together, to PEA + FN substrates. It was hypothesised that BMP-2 bound to PEA + FN may act to stimulate a degree of osteogenic differentiation of MSCs, leading to the expression of valuable HSC maintenance factors produced by osteoblast cells (Figure 1-5). In addition, it was also hypothesised that the STRO-1$^+$ MSCs in the model may respond positively to stimulation by NGF, enhancing the secretion of HSC maintenance

factors from MSCs, as is postulated to occur in the bone marrow. This chapter described how GFs, notably BMP-2 and/or NGF, adsorbed on PEA + FN substrates could modulate the behaviour or STRO-1$^+$ cells, resulting in expression of an HSC niche-like phenotype.

4.5.1 Discussion of MSC phenotype

SEM image results demonstrated that STRO-1$^+$ cells cultured on PEA + FN + GF substrates have a similar morphology to STRO-1$^+$ cells cultured on Glass + FN controls. This suggested that the different substrate types are equally as good at supporting MSC spreading and viability. However, to further investigate the potential of different niche model candidate substrates to support MSCs, these cells were cultured for 21 days in media supplemented with 10% FBS, before ICW was carried out to test for maintenance in the expression of MSC markers. The results showed no statistically significant differences in the expression of ALCAM, nestin or STRO-1 in cells cultured on PEA + FN + GF substrates, when compared to controls (Figure 4-4). This suggested that the PEA + FN + GF substrates maintain a similar population of MSCs as controls; PEA + FN + GF substrates were good candidate niche model substrates for generating HSC maintenance factors from these MSC populations. However, further development of the model involved reducing the concentration of serum in the media to 2% FBS for 21 days, and later reducing the length of serum-present culture from 21 days to 14 days. The results obtained throughout testing these different media compositions showed that no statistically significant differences in the expression of these MSC markers was found amongst cells cultured in different media types, indicating that the media type used in the model was not a concern in terms of MSC marker expression (Figure 4-7, Figure 4-11 and Figure 4-13). The flow cytometry results shown in Figure 4-16 validated the ICW results, and supported the observation that cell culture on the different niche candidate model substrates did not affect expression of MSC cell surface markers.

Although the ICW and flow cytometry results indicated that the expression of MSC markers in STRO-1$^+$ cells cultured in the HSC niche models was not affected by substrate type, a T cell suppression assay was also carried out to determine if this classic aspect of MSC character was affected by culture on any of the substrates. Interestingly, the PEA + FN + BMP-2&NGF substrate optimally

suppressed T cells, showing that MSCs cultured on this substrate had the best MSC character. This finding is not what was expected; it was expected that the osteogenesis occurring on this substrate type would slightly reduce the MSC character (McMurray et al., 2011). Nevertheless it was interesting and future work should focus on repeating this experiment using MSCs from different donors and at different passages to determine the effect of these variables on the results.

In order to strengthen the data obtained, it would have been advantageous to carry out PCR to validate the results obtained and presented from ICW and flow cytometry. In addition, given more time, it would have been valuable to test cells from a larger pool of donors, ensuring that a minimum of 3 biological replicates were used with all substrate and also all media formulations, to give a more robust analysis.

4.5.2 Discussion of osteogenic phenotype

While the development of an HSC niche model that has a stromal layer with a maintained expression of MSC markers is desirable, it is also favourable for the model to include expression of some osteogenesis markers, which indicate the presence of an osteoblast population, known for secreting a valuable profile of HSC maintenance factors (Calvi et al., 2003). To this end, ICW was also carried out to test for changes in the expression levels of two osteogenesis markers, OCN and OPN. The first ICW experiment aimed to determine the osteogenic potential of the PEA + FN + GF surfaces was carried out in DMEM supplemented with 10% FBS, and although the results obtained did not show any statistically significant increases in the expression of OCN or OPN, results suggested that OCN levels may be higher in cells cultured on PEA + FN + BMP-2&VEGF substrates (Figure 4-5). Further development of the model resulted in the testing of cells cultured on substrates with a reduced concentration of FBS in the media (2% FBS). It was anticipated that this reduction in serum concentration would increase the BMP-2 responsiveness of the stromal cells (Osyczka et al., 2009). Accordingly, this reduction in the concentration of serum appeared to result in an increase in the expression of OCN and OPN in PEA + FN + BMP-2 substrates relative to controls, compared to the result obtained for cell cultures in 10% FBS media (Figure 4-8). This increased in osteogenesis marker expression, relative to

controls, in cells on PEA + FN + BMP-2 substrates would be expected, and it was hypothesised that the difference may have arisen from fewer GFs being present in the serum, allowing the cells to become more responsive to the BMP-2 on the substrate (Osyczka et al., 2009). Towards the end of the model development, it was noted that when the HSCs would be added to the model, they would require culture in a serum-free medium. It had been decided that the MSCs would be cultured for 14 days, and that the HSCs would be added on day 15. Thus, DMEM supplemented with 2% human serum (preferable to FBS as this model is a human HSC niche model) would be used until day 14 of the culture, and then a serum-free media supplemented with 3GFs would be used for culture from days 15 to 21. ICW was also carried out to test the effect of this culture method on OCN and OPN expression, and the results suggested that this media formulation resulted in cells cultured on all PEA + FN + GF substrates to have statistically significant increases in OPN expression (Figure 4-14). Notably, the PEA + FN + BMP-2&NGF substrates induced the highest expression of OPN, and also slightly higher levels of OCN relative to controls. As OPN is a more primitive marker of osteogenesis, this results suggests that cell culture on the PEA + FN + BMP-2&NGF substrate, in 2% HS then 3GF media, results in the formation of a population of immature OBs.

It would be beneficial to carry out PCR to validate the results and statistically significant increases in osteogenesis marker expression observed with the PEA + FN + BMP-2 and PEA + FN + BMP-2&NGF substrates. It is known that BMP-2 signalling occurs through activation of the SMAD pathway, and so comparison of levels of phosphorylated SMAD 1 and 5 to total SMAD 1 and 5 could also be carried out, using ICW, to show that BMP-2 signalling is higher on PEA + FN + BMP-2 substrates (Lee et al., 2003).

As the results indicate that OPN expression is more greatly increased than OCN expression on these substrates, relative to controls, indicating a primitive OB population, alkaline phosphatase expression could also be determined. It would be interesting to do this over time to determine if there is a particular time at which the alkaline phosphatase expression is particularly apparent, as this would provide information regarding the time point at which most of the osteogenesis is occurring.

4.5.3 Discussion of HSC maintenance factor expression results

As the principal aim of this chapter was to determine the capacity of PEA + FN + GF substrates to enhance the expression of HSC maintenance factors in STRO-1$^+$ MSCs, ICW was also used to quantitatively analyse changes in the expression of membrane-bound SCF and VCAM-1. Initial experiments using media supplemented with 10% FBS showed statistically significant increases in SCF expression when cells were cultured on PEA + FN + BMP-2&NGF substrates, relative to glass and PEA + FN controls (Figure 4-6). This appeared to be maintained when cells were cultured in a media containing a lower concentration of serum (Figure 4-9). However, the statistically significant increases relative to controls were no longer present in the results. Repetition of this experiment using 2% HS media followed by 5GF media also failed to produce statistically significant results (Figure 4-12). Yet, the results suggested that cell culture on the PEA + FN + BMP-2&NGF substrate generates the greatest fold increase (approximately 3 to 4 fold) in SCF expression relative to controls. Interestingly, the statistically significant increases in SCF expression on PEA + FN + NGF and PEA + FN + BMP-2&NGF substrates were apparent in the 2% HS and 3GF media culture, suggesting that this media type is optimal for generating consistent increases in SCF expression for cells cultures on these surface types, relative to controls. VCAM-1 expression tended to be highest on PEA + FN + NGF and PEA + FN + BMP-2 and NGF substrates. However, the results often lack the same degree of statistical significance as the SCF results, suggesting that the niche model candidate substrates tested here may induce some increases in VCAM-1 expression, but work more efficiently to enhance SCF expression.

As before, the results obtained via ICW regarding SCF and VCAM-1 expression could be validated using PCR. As SCF is also partly secreted, it would be interesting to carry out an ELISA monitoring the secretion of SCF from the stromal layer over time. The results could provide insight into how much SCF is secreted and how much is retained in the membrane-bound form, and it may be the case that certain substrates induce a greater expression of soluble SCF than others.

The results from the ELISAs carried out revealed a number of important aspects of this model. Firstly, it is important to note that reducing the concentration of

serum in the media from 10% to 2% made subtle differences apparent, which indicated that cells cultured on PEA + FN + BMP-2 surfaces consistently secreted more CXCL-12 relative to controls (Figure 4-19, Figure 4-21). In addition, the results for the CXCL-12 ELISA from cells cultured in 2% serum indicated that approximately five-fold more CXCL-12 was detected in the media of cells cultured between days 18 and 21 on PEA + FN + NGF and PEA + FN + BMP-2&NGF substrates. It should be noted that these increases were not arising from a statistically greater number of cells being present on these substrates (Figure 4-22). These observations highlighted the benefit of using a 21 day model, and also the PEA + FN + GF substrates. Interestingly, the THPO ELISA results suggested that reducing the concentration of serum reduces the fold increases generated by PEA + FN + GF substrates for media collected between days 18 and 21 (Figure 4-20, Figure 4-21). However, it is promising to observe that PEA + FN + GF substrates generally induced the secretion of a greater concentration of THPO from cells, relative to controls. In brief, the ELISA results indicated two important points: the PEA + FN + NGF or PEA + FN + BMP-2&NGF substrate was best for CXCL-12 expression and the PEA + FN + BMP-2 substrate was best for THPO expression; the lower concentration of serum required by a model aimed towards HSC culture was favourable in terms of inducing high levels of CXCL-12 expression.

There were considerable differences in the results obtained for the CXCL-12 and THPO ELISAs in media containing 10% serum in the media and 2% serum in the media. Consequently, repetition of the CXCL-12 and THPO ELISAs would be advantageous to determine the consistency of results. Collecting media supernatants from more than 3 samples would also provide a better average of the results, allowing for more valid conclusions to be drawn.

4.5.4 Chapter conclusions

Taking the results of this chapter into consideration, is has been important to deduce which one of the PEA + FN + GF substrates tested would be preferable for use in later experiments using HSCs. This was important for three main reasons:

1. It would be too demanding of the PEA supplier to provide large quantities of PEA for the testing of substrates loaded with BMP-2, NGF, PDGF, VEGF and all possible combinations with an n number of at least 3.

2. Use of all aforementioned GFs and combinations was very costly, particularly with n numbers great enough for effective analysis.

3. It would was too difficult to obtain large enough numbers of HSCs to incorporate into n ≥ 3 of each substrate type, and to costly to culture such high numbers.

The results of this chapter generally highlighted the value of using NGF and BMP-2, especially when combined. Thus, it was decided that PEA + FN + BMP-2&NGF would be the substrate of choice for use in further development and testing of this model. Further, it was decided that the media of choice for future work would be DMEM supplemented with 2% HS for 14 days and then 3GF media for days 14 to 21 of the cell culture. The reasoning for this choice was as follows:

1. HSCs require serum-free media for survival, and so it was deemed important to have as little serum in the media prior to their addition to the model.

2. 3GF media was recommended to us as optimal for HSC culture by collaborators.

3. 3GF media is more cost-effective than 5GF media.

4. 2% HS media followed by 3GF media induces statistically significant increases in the expression of OPN and SCF for cells cultured on the PEA + FN + BMP-2&NGF substrate of choice.

5. The PEA + FN + BMP-2&NGF substrate was able to allow all aforementioned points while also maintaining similar levels of expression of MSC markers in MSCs, and also enhancing MSC characteristics (such a T cell suppression) relative to controls.

CHAPTER 5

Chapter 5 Metabolomic Analysis of MSCs

5.1 Introduction

5.1.1 Metabolomics

Metabolomics can be referred to as the scientific study of chemical processes involving metabolites, where the term metabolites relates to the small molecule intermediates and products of metabolism (Daviss, 2005, Tyagi et al., 2010). Metabolomics has also been explained as being a non-biased identification and quantification of all metabolites present within a biological system (Fiehn, 2002). In terms of common metabolite extraction methods, metabolomics simply allows for the identification of small molecules present within cells at a given time, thus providing insight into the cellular processes that have taken place at that precise point in time (McNamara et al., 2012). It is important to note that the metabolomic profile reflects the culture of the cells, and so the metabolomic profile of cells cultured under different conditions, but with metabolites extracted at the same point in time, may be compared to give an indication of how the culture differences affect the metabolomic profile and the general response of cells (Tsimbouri et al., 2012).

While targeted methods of metabolomics looking specifically at changes in the abundance of particular metabolites exist, untargereted metabolomic approaches also exist (Tautenhahn et al., 2012a, Römisch-Margl et al., 2012). The benefit of using untargeted metabolomics is that it allows for analysis of the entire complement of metabolites, known as the metabolome, and is thus capable of identifying key metabolites that vary under certain conditions (Dunn et al., 2013).

5.1.2 Metabolomic Pathways of Relevance

Metabolomics generates a wealth of data, and has been criticised as often producing too much (Daviss, 2005). Thus, in order to draw valid conclusions from large-scale metabolomic data sets, it is important to consider key metabolic pathways that may be of significance and relevance to research.

5.1.2.1 Amino acid metabolism

Understanding the effects of different culture methods on amino acid metabolism is important, as a high abundance of amino acids in cells is associated with increased levels of protein synthesis and enhanced levels of differentiation (Sampath et al., 2008). While this basic correlation is important, it should also be noted that amino acids can also act as powerful signalling molecules that can regulate a diverse range of cell functions including stem cell self-renewal, proliferation and differentiation (Zhao et al., 2012, Tjabringa et al., 2008). For example, arginine and proline are involved in producing nitric oxide, which is in turn a requirement of polyamine biosynthesis (Wang et al., 2015). The mammalian polyamines produced may be putrescine, spermidine or spermine, and are positively charged (Childs et al., 2003). The charge of these molecules allows them to bind to acidic sites on RNA and DNA, making polyamines known transcription regulators of regulatory genes such as c-Myc and c-Jun (Liu et al., 2006, Xiao et al., 2007). Polyamines can also affect proteins, and are known to influence kinases and phosphatases (Yoshida et al., 2004). Since the initial discovery of these roles of polyamines, further research has shown a general role of polyamine production in enhancing osteogenic differentiation of adipose-derived stem cells (Tjabringa et al., 2008). Thus, considering amino acid metabolism in research associated with cellular differentiation is important.

5.1.2.2 Carbohydrate metabolism

One of the other most commonly analysed pathways in stem cell metabolomics is that associated with carbohydrate metabolism and respiration (Meissen et al., 2012, Turner et al., 2008). Generally, it is accepted that enhanced carbohydrate metabolism, associated with increased oxidative phosphorylation, occurs when active stem cells to undergo differentiation (Varum et al., 2011, Houghton, 2006). Conversely, it is accepted that quiescent stem cells are less metabolically active than their cycling counterparts (Chung et al., 2007). This hypothesis was proven true in 2007, when Chung and colleagues showed that disrupting the respiratory chain in embryonic stem cells impedes differentiation into cardiomyoctyes, while engagement of the system enhances differentiation. Since then, the relevance of understanding carbohydrate metabolism in a diverse

range of stem cells, including HSCs and MSCs, has been acknowledged, as the metabolomic profile provides a direct indication of cellular differentiation (Simsek et al., 2010).

5.1.2.3 Lipid metabolism

Alongside amino acid and carbohydrate metabolic pathways, lipid metabolic pathways are also of considerable significance when considering their impact on cell fate. For example, several studies reported in the 1990s showed that addition of a particular metabolite to cell cultures could enhance cell differentiation (Kliewer et al., 1995, Okazaki et al., 1990). The mechanisms underlying this stimulation of differentiation vary depending on the lipid and cell type being considered. However, it has been shown that prostaglandins are physiologically active lipid compounds that act similarly to hormones. These prostaglandins stimulate peroxisome proliferator-activated receptor γ (PPAR-γ), and stimulate adipogenic differentiation of murine fibroblasts (Kliewer et al., 1995).

In research published in 2016, Alakpa et al showed that MSC differentiation down the osteogenic lineage could be controlled using hydrogels of different stiffness (Alakpa et al., 2016). In addition to this, the authors showed that specific lipids, lysophosphatidic acid and cholesterol sulfate, were depleted following differentiation of cells down the chondrogenic and osteogenic differentiation lineages, respectively. The group suggest that this arose as a result of these particular metabolites being used up in the differentiation process. Thus, it is important to consider that use of metabolomics to identify the depletion of particular lipids may be valuable in supporting other results that indicate differentiation.

5.1.3 Metabolomics and MSCs in bioengineering

Previous studies have shown that cell phenotype is linked to their metabolic profile; stem cells have been shown to be metabolically inactive, while differentiating cells have been identified as having heightened metabolic activity (Yanes et al., 2010, Chung et al., 2007). Further, it has been shown that

the changes present within the metabolism occur rapidly as stem cells begin to differentiate (Reyes et al., 2006).

Metabolomics has been particularly useful in understanding the effect of MSCs in bioengineering applications. For example, it has been shown that MSCs cultured on functionalised 15 nm nanopillar structures on titania have an 'active' phenotype, with upregulation of metabolites associated with differentiation down the osteogenic lineage (McNamara et al., 2011). The potential of bioengineering applications was further highlighted when it was shown that surfaces with nanoscale features could retain the stem cell phenotype of MSCs after a long 8-week culture (McMurray et al., 2011). In this study, it was reported that cells expressing a stem cell phenotype possess more unsaturated metabolites, compared to differentiating controls. These results correlate well with the findings of Yanes et al., and both groups of authors propose that such unsaturated metabolites are important for maintaining the chemical plasticity of cells, and act to regulate differentiation by controlling redox status (Yanes et al., 2010, McMurray et al., 2011).

It is understood that human MSCs express higher levels of glycolysis enzymes and lower levels of oxidative phosphorylation proteins, when compared to OBs (Chen et al., 2008). This suggests that MSCs are more dependent on low energy yielding glycolysis and less dependent on high energy yielding oxidative phosphorylation. Taking this and the aforementioned points into consideration, is important to note that metabolomics can be used in two main ways that relate to this thesis: to indicate if a cell population is metabolically similar to that of stem cells; to indicate if a cell population is metabolically similar to that of differentiated cells.

5.2 Aims and Objectives

The aim of this chapter of the thesis is to use untargeted metabolomics to further investigate how the changes in MSC phenotype arising from culture in different HSC niche models (as outlined in Chapter 4) affect the cells at the metabolomic level.

To this end, metabolites were extracted from STRO-1$^+$ cells cultured on Glass + FN, PMA + FN, PEA + FN and PEA + FN + BMP-2&NGF substrates, for 21 days. Days 1-14 of the cell culture was in DMEM containing 2% human serum, and days 15-21 were in '3GF' serum free media.

Amino acid, carbohydrate and lipid pathways are commonly studied in metabolomics (Butte, 2000, Brown et al., 2016). Consequently, this chapter uses untargeted metabolomics and data processing software to extract metabolite information associated with each of these pathways and to draw conclusions relating to the effect of the niche model candidate substrates on the regulation of STRO-1$^+$ MSCs.

5.3 Materials and Methods

5.3.1 Sample Preparation

The media supernatant in wells of a 24-well plate representing HSC niche models was removed and the cells on the substrates were washed once using 500 µl of 1x PBS at 4 ^oC. 500 µl of a cold methanol-chloroform solution (1:3:1 ratio of chloroform: methanol: water) was added to each well of the plate, and the plate was sealed using parafilm. The plate was incubated at 4^oC on a rotary shaker for 1 hour. Blanks were prepared by adding the same volume of methanol-chloroform solution to wells of a 24-well plate with substrates that had been treated in the same way as all other substrates during the culture period, but in the absence of cells.

Following the 1-hour incubation, the resulting solutions were transferred to reaction tubes and centrifuged at 1300 rpm for 3 minutes, in order to isolate cell debris. The supernatants were transferred to fresh reaction tubes, and 50 µl of solution from each tube was transferred to a fresh tube, creating a pooled sample for quality control purposes. All samples were stored at -80 ^oC, until they were subjected to liquid chromatography by the Glasgow Polyomics facility at the University of Glasgow.

n=3 for each substrate was used.

5.3.2 Liquid Chromatography Mass Spectrometry (LCMS)

The LCMS stage of this work was carried out by staff at the metabolomics facility within Glasgow Polyomics, headed by Dr. Karl Burgess.

LCMS allows for the isolation of individual metabolites from the mixture produced in each sample, and separates the metabolites prior to their isolation relative to their mass:charge (m/z) ratio. An UltiMate 3000 RSLC featuring a 20 mm x 2.1 mm ZIC-pHILIC analytical column running at 300 µl/min, coupled to an Orbitrap Q-Exactive (Thermo Fisher) was used. Standards comprising known metabolites were also processed in this way, and their respective retention times in the chromatography column were used to identify sample metabolites.

5.3.3 Data Analysis

The raw data obtained from the LCMS stage was processed using XCMS to allow for peak picking (Tautenhahn et al., 2012a, Tautenhahn et al., 2012b). An IDEOM/MzMatch excel interface was generated by the staff at the Glasgow Polyomics facility, with kind assistance from Gavin Blackburn, University of Glasgow. This IDEOM interface allowed for the putative identification of metabolites, in conjunction with the Kyoto Encyclopaedia of Genes and Genomes (KEGG) database (Kanehisa et al., 2011). Files relating to amino acid, carbohydrate and lipid metabolism were exported from the IDEOM interface and were further processed using Metaboanalyst for further analysis including the generation of heatmaps and principal component analysis (PCA) plots (Xia et al., 2012).

5.4 Results

Half of the results reported in this section are presented in the form of heatmaps, to allow for the easy visualisation of fold changes in the abundance of metabolites involved in amino acid, carbohydrate and lipid metabolic pathways. In each heatmap, the metabolites are ranked from hot (associated with darker red colours and increased abundance) to cold (associated with darker blue colours and decreased abundance).

The other results presented in this chapter are in the form of principal component analysis (PCA) plots, which show scatter plots indicative of variance within data sets (van den Berg et al., 2006, Bro and Smilde, 2014). Metabolic differences are shown by separation of clusters within the scatter plots.

5.4.1 The effect of niche models on amino acid metabolism

In order to determine the effect of the different substrates tested within HSC niche models featuring DMEM supplemented with 2% HS until day 14, and 3GF media from days 15-21, on amino acid metabolism, metabolites were extracted on day 21 and processed as outlined in section 5.3. The results are shown in Figure 5-1 and Figure 5-2.

The results shown in Figure 5-1 indicated that the abundance of amino metabolites was lowest on PEA + FN + BMP-2&NGF substrates, relative to controls. This indicated that cells cultured on control substrates had a more quiescent phenotype, while cells cultured on the PEA + FN + BMP-2&NGF substrates appeared to demonstrate a divergent phenotype, indicative of osteogenic differentiation. This hypothesis fitted well with the conclusions drawn earlier in this thesis, whereby the PEA + FN + BMP-2&NGF substrate optimally enhanced osteogenic differentiation.

Figure 5-2 showed that the greatest variation existed within the Glass + FN data set, and indicated that the least variation existed within cells from the PEA + FN + BMP-2&NGF data set. This result was encouraging as it suggested that having the GFs bound to the PEA + FN substrate gave a better homogeneity of the metabolomic amino acid profile of the stromal layer.

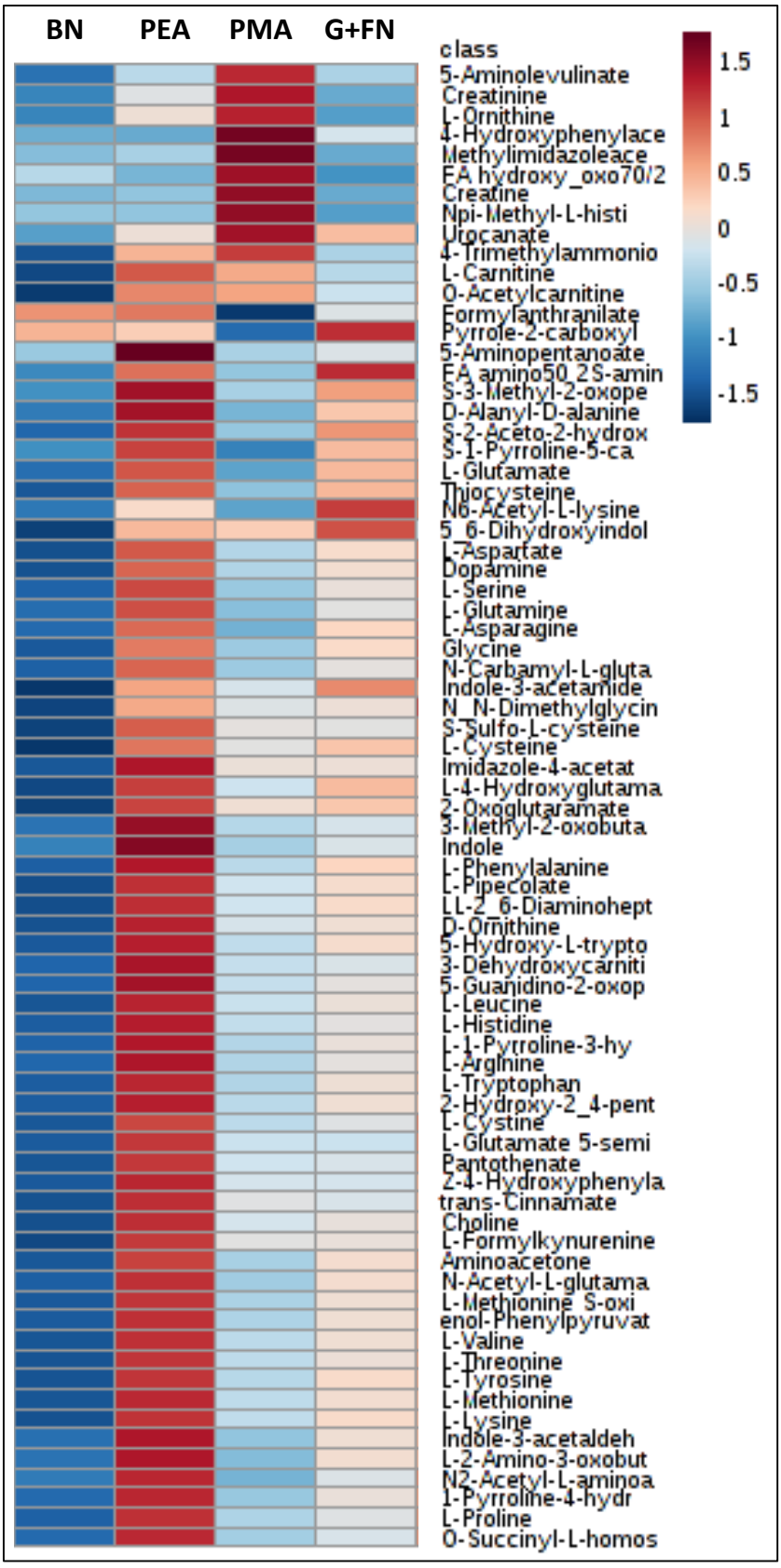

Figure 5-1 Amino acid metabolite profile of MSCs on HSC niche model substrates
Metabolites associated with amino acid metabolism in STRO-1 $^{+}$ MSCs were analysed after 21 days of culture in HSC niche models featuring different substrates. BN = average of PEA + FN + BMP-2&NGF substrates; PEA = average of PEA + FN substrates; PMA = average of PMA + FN substrates; G+FN = average of glass + FN substrates. n=3. Blue colours are indicative of fold decreases in metabolite abundance. Red colours are indicative of fold increases in metabolite abundance. Data indicates that amino acid metabolites are lowest in MSCs cultured on PEA + FN + BMP-2&NGF substrates

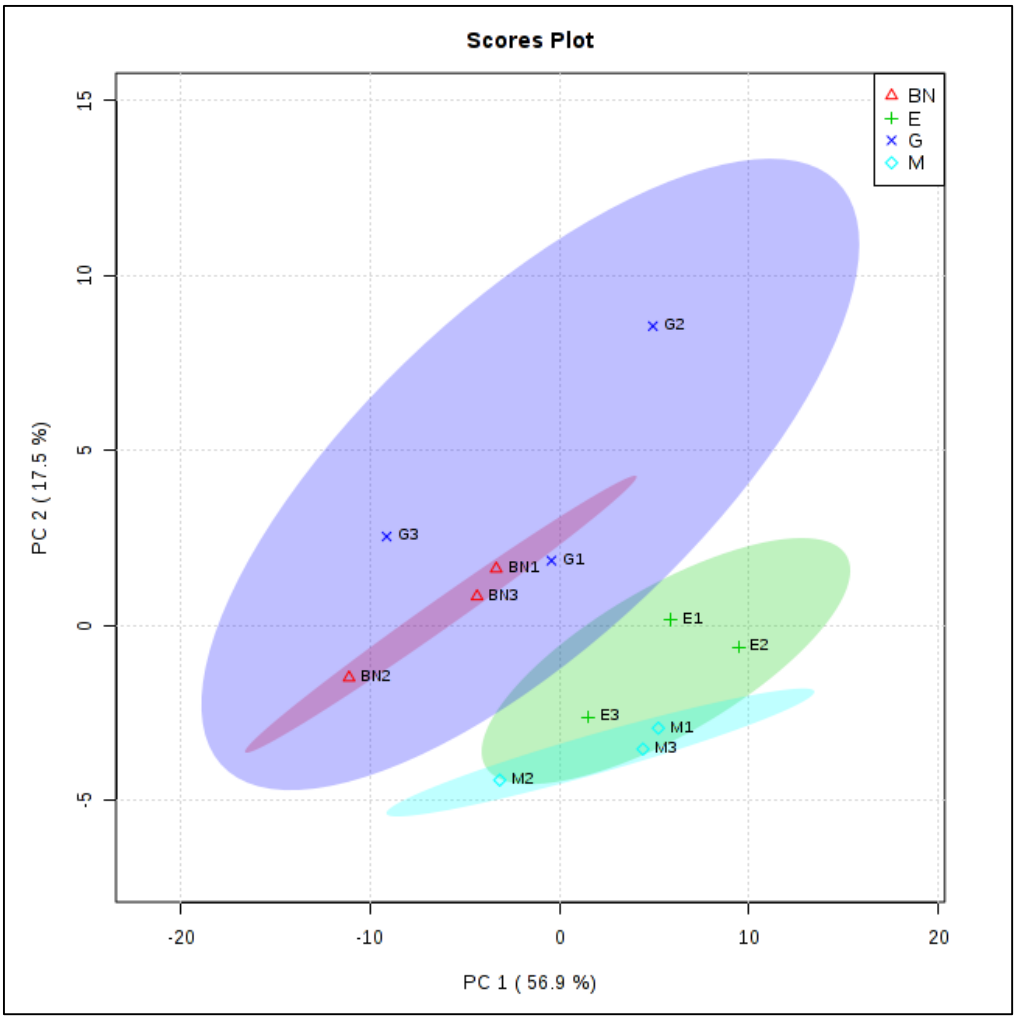

Figure 5-2 PCA plot of amino acid metabolites detected in MSCs cultured in HSC niche models containing glass + FN, PMA + FN, PEA + FN and PEA + FN + BMP-2&NGF substrates Data sets were obtained from putative amino acid metabolites identified from STRO-1$^+$ MSCs cultured in HSC niche models containing different substrate types for 21 days. G = Glass + FN; M = PMA + FN; E = PEA + FN; BN = PEA + FN + BMP-2&NGF. Points represent individual samples of each substrate type. n=3. Ellipses represent the spatial borders associated with each substrate type, to a 95% confidence interval. Data indicates that the greatest variation in amino acid metabolite abundance exists within MSCs cultured on glass substrates.

The effect of niche models on carbohydrate metabolism

In a bid to assess if the metabolite profile of PEA + FN + BMP-2&NGF substrates was distinct to that of controls, differences in the abundance of metabolites associated with carbohydrate metabolism in STRO-1$^+$ cells cultured in HSC niche models with different substrates were determined after 21 days of culture. Results are shown in Figure 5-3 and Figure 5-4.

The results shown in Figure 5-3 indicated that PEA + FN + BMP-2&NGF substrates had the lowest abundance of carbohydrates present, relative to controls. As before, this result indicated that cells cultured on control substrates had a more

quiescent phenotype. Conversely, this observation also suggested that the divergent phenotype observed in cells cultured on PEA + FN + BMP-2&NGF substrates was resulting from osteogenic differentiation. This result correlated well with those described in Chapter 4, wherein it was hypothesised that the PEA + FN + BMP-2&NGF substrate induced osteogenic differentiation.

The PCA plot shown in Figure 5-4 illustrated that the greatest variation in carbohydrate metabolite profile existed within MSCs cultured on PEA + FN + BMP-2&NGF substrates. It was apparent that the least variation within a group existed within cells cultured on PMA + FN substrates. This result was interesting and suggested that while the PEA + FN + BMP-2&NGF substrates may have induced homogeneity in terms of amino acid metabolite variation, this substrate did not have the same effect on carbohydrate metabolite variation.

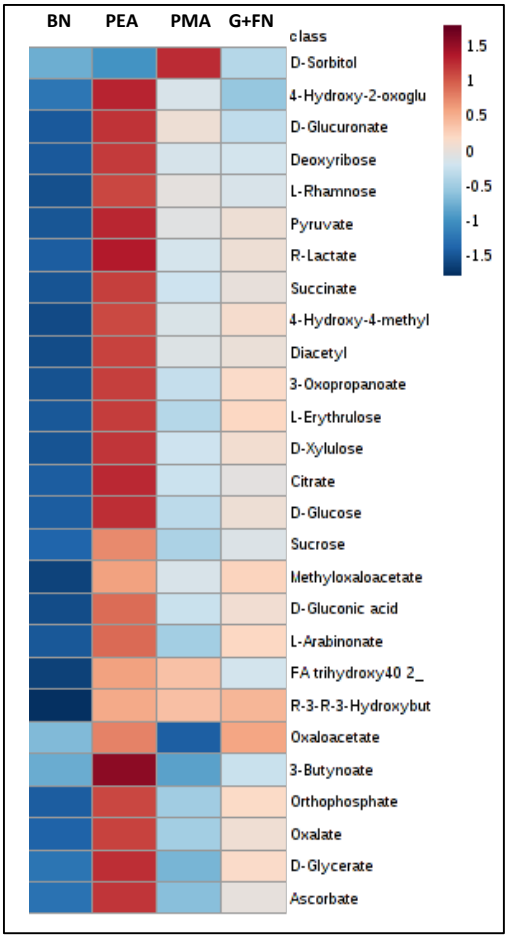

Figure 5-3 Carbohydrate metabolite profile of MSCs on HSC niche model substrates
Metabolites associated with carbohydrate metabolism in STRO-1 $^{+}$ MSCs were analysed after 21 days of culture in HSC niche models featuring different substrates. BN = average of PEA + FN + BMP-2&NGF substrates; PEA = average of PEA + FN substrates; PMA = average of PMA + FN substrates; G+FN = average of glass + FN substrates. n=3. Blue colours are indicative of fold decreases in metabolite abundance. Red colours are indicative of fold increases in metabolite abundance. Data indicates that carbohydrate metabolites are lowest in MSCs cultured on PEA + FN + BMP-2&NGF substrates

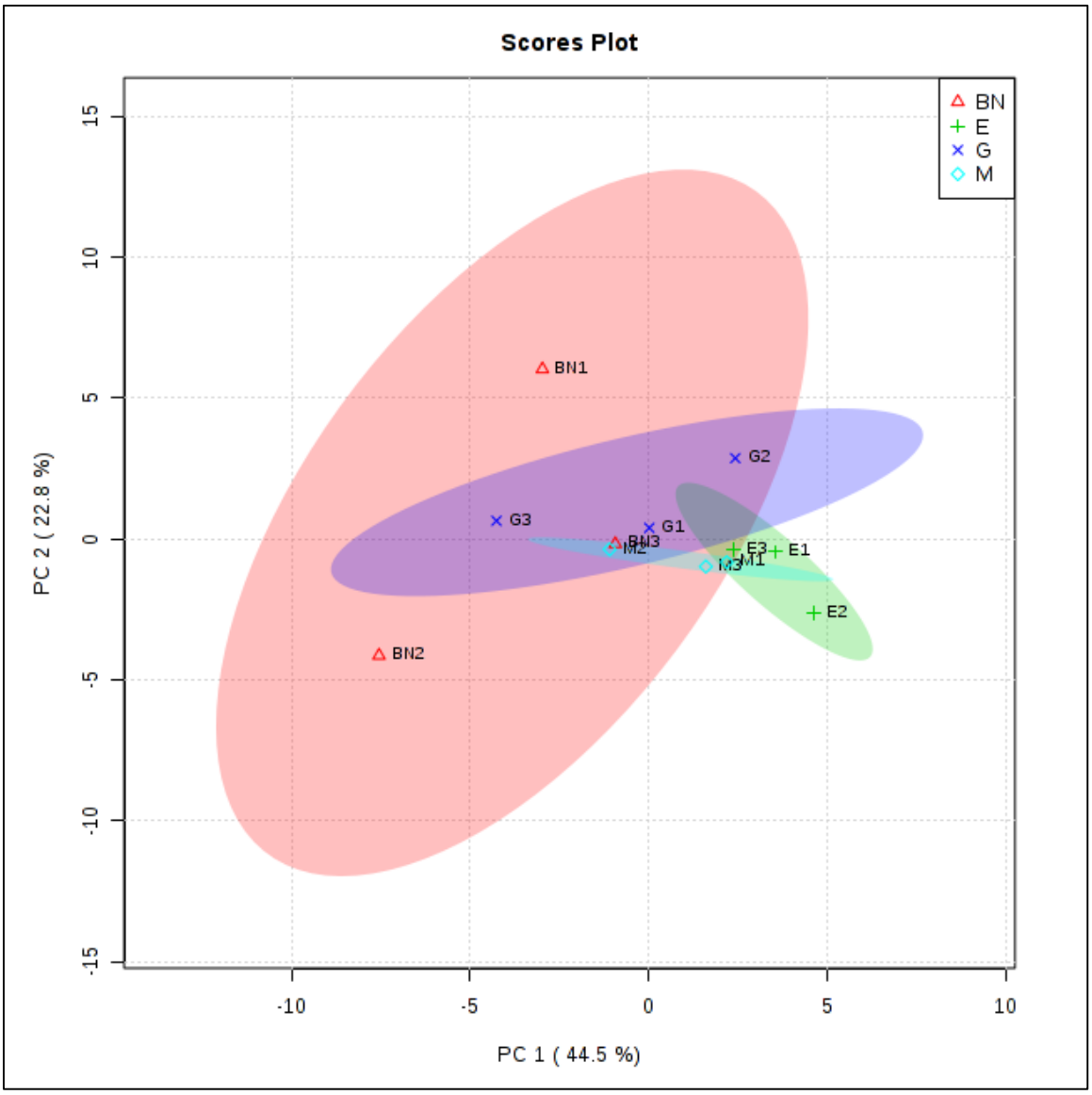

Figure 5-4 PCA plot of carbohydrate metabolites detected in MSCs cultured in HSC niche models containing glass + FN, PMA + FN, PEA + FN and PEA + FN + BMP-2&NGF substrates Data sets were obtained from putative carbohydrate metabolites identified from STRO-1$^+$ MSCs cultured in HSC niche models containing different substrate types for 21 days. G = Glass + FN; M = PMA + FN; E = PEA + FN; BN = PEA + FN + BMP-2&NGF. Points represent individual samples of each substrate type. n=3. Ellipses represent the spatial borders associated with each substrate type, to a 95% confidence interval. Data indicates that the greatest variation in amino acid metabolite abundance exists within MSCs cultured on PEA + FN + BMP-2&NGF substrates.

5.4.2 The effect of niche models on lipid metabolism

The abundance of lipid metabolites present within STRO-1$^+$ cells cultured on different HSC niche model substrates was determined in order to determine if the osteogenesis indicated to exist of PEA + FN + BMP-2&NGF substrates (Chapter 4) altered the putative lipid metabolite profile. Results are presented in Figure 5-5 and Figure 5-6.

The results shown in Figure 5-5 suggested that the abundance of lipid metabolites was generally lowest in cells cultured in HSC niche models that incorporated PEA + FN + BMP-2&NGF substrates. This generally low abundance of lipid metabolites indicated that cells cultured on control substrates had a quiescent phenotype, while the divergent data set associated with cells cultured on PEA + FN + BMP-2&NGF substrates was likely to be indicative of a less quiescent, more metabolically active osteogenic differentiation phenotype. This observation was in accordance with the findings of Alakpa et al; it was likely that this had arisen as the lipid metabolites were used up in the differentiation process (Alakpa et al., 2016). In particular, it was apparent that there was a much lower abundance of diethanolamine present in cells cultured on the PEA + FN + BMP-2&NGF substrate type, compared to controls. This was indicative of diethanolamine being consumed in the differentiation process associated with the PEA + FN + BMP-2&NGF substrate. However, future work should seek to investigate the significance of this further.

The results of the PCA analysis shown in Figure 5-6 indicated that the PMA + FN and PEA + FN + BMP-2&NGF substrates functioned particularly well to induce homogeneity of lipid metabolites present within MSCs. Conversely, the PCA plot illustrated that the glass + FN substrate allowed for a greater variation in the abundance of metabolites present.

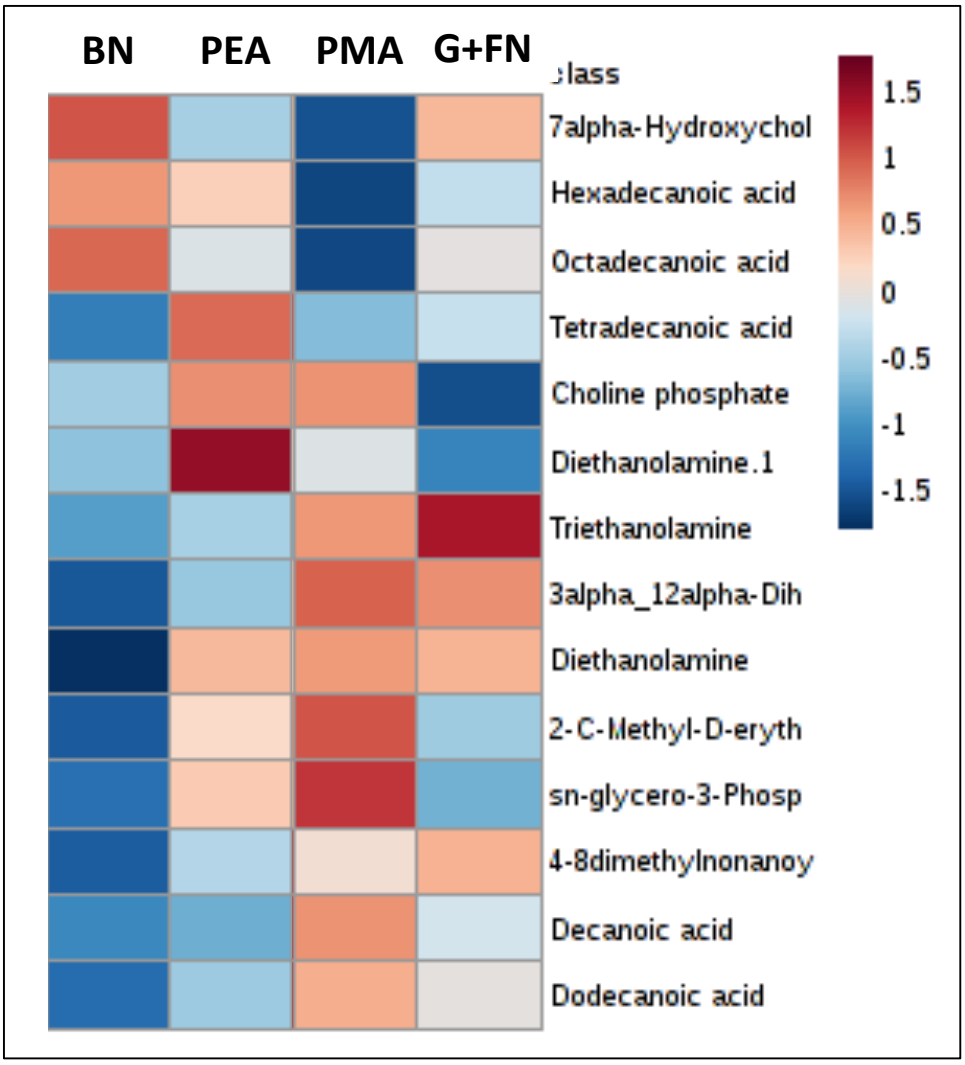

Figure 5-5 Lipid metabolite profile of MSCs on HSC niche model substrates
Metabolites associated with lipid metabolism in STRO-1 $^{+}$ MSCs were analysed after 21 days of culture in HSC niche models featuring different substrates. BN = average of PEA + FN + BMP-2&NGF substrates; PEA = average of PEA + FN substrates; PMA = average of PMA + FN substrates; G+FN = average of glass + FN substrates. n=3. Blue colours are indicative of fold decreases in metabolite abundance. Red colours are indicative of fold increases in metabolite abundance. Data indicates that lipid metabolites are generally lowest in MSCs cultured on PEA + FN + BMP-2&NGF substrates

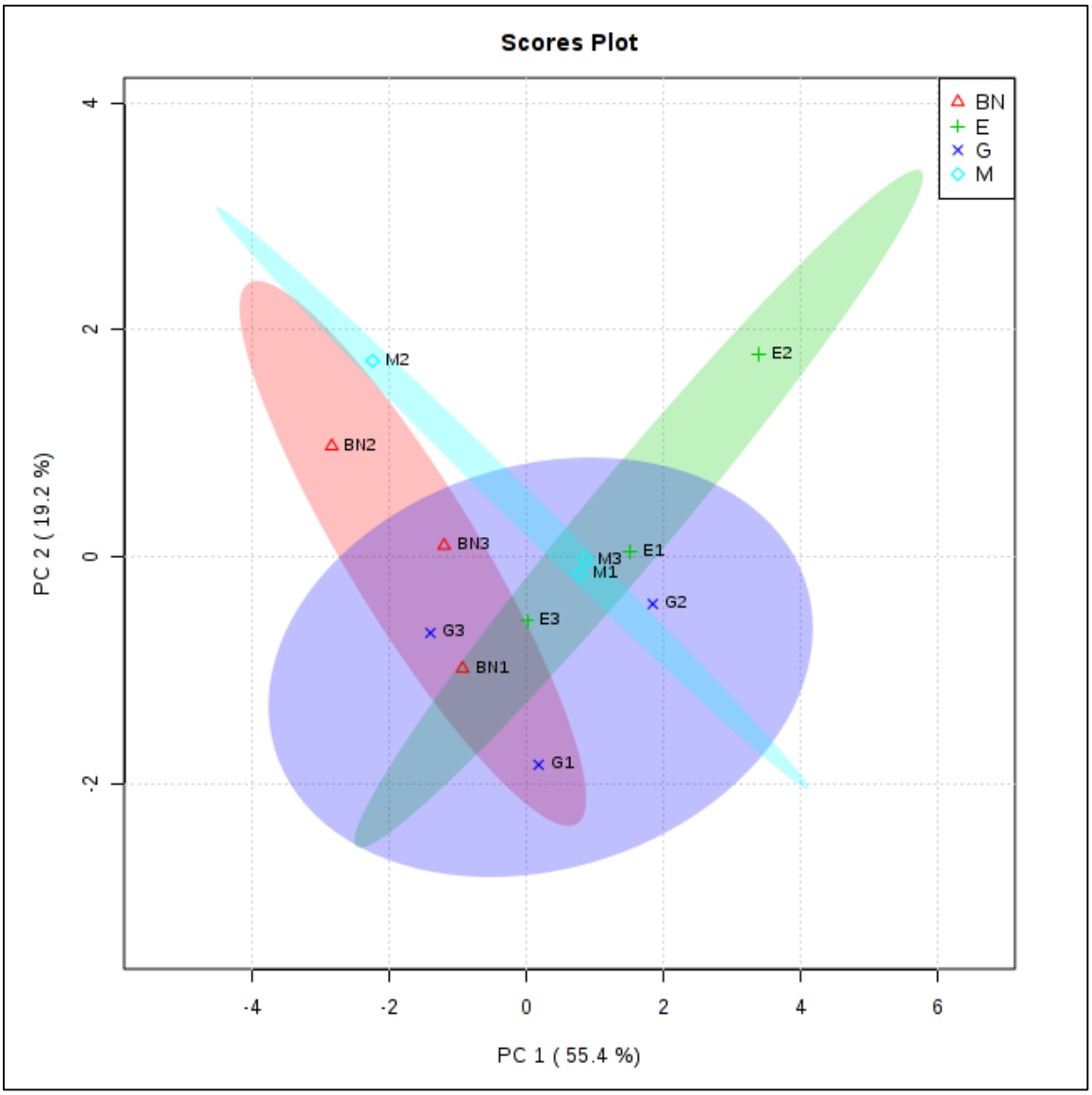

Figure 5-6 PCA plot of lipid metabolites detected in MSCs cultured in HSC niche models containing glass + FN, PMA + FN, PEA + FN and PEA + FN + BMP-2&NGF substrates
Data sets were obtained from putative lipid metabolites identified from STRO-1$^+$ MSCs cultured in HSC niche models containing different substrate types for 21 days. G = Glass + FN; M = PMA + FN; E = PEA + FN; BN = PEA + FN + BMP-2&NGF. Points represent individual samples of each substrate type. n=3. Ellipses represent the spatial borders associated with each substrate type, to a 95% confidence interval. Data indicates that the greatest variation in amino acid metabolite abundance exists within MSCs cultured on glass substrates.

5.5 Discussion

The aim of this chapter was to assess the effect of culture on HSC niche model substrates on the abundance of metabolites present within STRO-1$^+$ MSCs. In particular, this chapter aimed to investigate the potential of models featuring the PEA + FN + BMP-2&NGF substrate to induce expression of metabolite profiles that are associated with the osteogenic differentiation phenotype suggested by the results presented in Chapter 4.

The heat map results associated with the amino acid metabolite profile indicated that cells cultured on PEA + FN + BMP-2&NGF substrates had lower levels of amino acids present within them, when compared to cells grown on control substrate types. This suggested that protein synthesis, associated with cellular differentiation was occurring, and consequently the results shown in Figure 5-1 provided further evidence to support the role of PEA + FN + BMP-2&NGF substrates in HSC niche models. Similarly, the carbohydrate metabolite profile shown in Figure 5-3 suggested that MSCs cultured in models featuring PEA + FN + BMP-2&NGF substrates were the most metabolically active, and were likely to be undergoing differentiation (Chung et al., 2007). Finally, the lipid metabolite profile results were less clear, but also suggested that most lipid metabolites were lowest in abundance in cells cultured on PEA + FN + BMP-2&NGF substrates, relative to controls. As heightened lipid metabolism is also associated with differentiation, this result also highlighted the likely osteogenic differentiation happening in models with this substrate type (Alakpa et al., 2016).

The PCA plots presented in this chapter illustrated that the different substrates had varying capacities to regulate variation in the abundance of metabolites associated with amino acid, carbohydrate and lipid metabolism. It appeared that the PEA + FN + BMP-2&NGF substrate of interest was particularly good at promoting homogeneity and reducing variation associated with amino acid and lipid metabolite abundance. This was important as it implied that certain results were more reliable than others; the relatively small variation within the PEA + FN and PEA + FN + BMP-2&NGF groups shown in Figure 5-2 meant that the results presented in the heatmap of amino acid metabolism were more reliable. In other words, the distinct heat map differences in amino acid metabolism were likely to be indicative of true differences. It should also be noted that in all three PCA plots presented, the ellipses representing PEA + FN and PEA + FN + BMP-2&NGF substrates had very few regions of overlap, again suggesting that the metabolic profile of cells cultured on GF substrates were distinct to those only on PEA + FN substrates. In the context of this HSC niche model design, this was important as it suggested that the GFs have an important role to play and that GF substrates were markedly different to PEA + FN controls.

The results shown in this chapter indicate that the growth factors present on the PEA + FN substrates alter the metabolomic profile of the cells present in the stromal layer. In my opinion, the metabolomic profiles of cells cultured on GF substrates have a clear distinction to those cultured on FN only substrates, concurrent with findings already published by numerous groups relating to different cell types having different metabolomic profiles (Okazaki et al., 1990, Kliewer et al., 1995, Alakpa et al., 2016). The results from this chapter indicated that the increased expression of OCN and OPN on PEA + FN + BMP-2 substrates relative to controls and presented in chapter 4 truly represent an increased osteogenic phenotype arising from the BMP-2. However, to further investigate the effect of GFs on the metabolomic profiles of cells, it would be interesting to consider the effects of different GFs and to carry out similar analyses considering other HSC niche model candidate GFs such as VEGF and PDGF.

Although the results presented in this chapter were promising in validating the results presented in Chapter 4 of this thesis, whereby it seemed apparent that there were distinct differences in the state of MSCs cultured on the different niche model candidate substrates, it is important to stress the need for further metabolomics analyses to validate the conclusions drawn. Firstly, it would be important to increase the n numbers tested, to get a clearer and more accurate picture of what was occurring at the metabolite level. In addition, it would be advantageous to carry out metabolomics analyses with MSCs obtained from different donors to test for donor variability. Finally, it should also be noted that carrying out metabolomics analyses at different time points throughout the cell culture would provide a clearer insight into when the majority of osteogenesis occurs within these HSC niche models.

CHAPTER 6

Chapter 6 HSC Characterisation

6.1 Introduction

6.1.1 Characterisation of the classic HSC phenotype

CD34 is the most commonly used antigen in the identification and isolation of HSC populations in humans (Terstappen et al., 1991). In addition, exclusion of CD38 is commonly used for HSC identification, as expression of CD38 is associated with more differentiated haematopoietic cell types (Notta et al., 2010). Thus, the main aim of this chapter is to determine how effectively candidate niche models with different substrates and media formulations act, in terms of favouring maintenance of the classic $CD34^+CD38^-$ HSC phenotype. To this end, flow cytometry was used in 5 different experiments, using HSCs from 5 different donors, with the aim of drawing a general conclusion as to which surface type and media formulation allowed for the greatest numbers of $CD34^+CD38^-$ cells to be present in each model after 5 days of culture, when $CD34^+CD38^-$ cells were added to MSC cultures (as outlined in Figure 4-1).

6.1.2 The relevance of $CD34^+CD38^+$ and $CD34^-CD38^+$ progenitors

Although the $CD34^+CD38^-$ phenotype is regarded as the classic HSC phenotype, variations in the levels of expression of these two cell surface antigens also exist in the form of $CD34^+CD38^+$ and $CD34^-CD38^+$ (Engelhardt et al., 2002, Wang et al., 2004a). These phenotypes are associated with less primitive multipotent haematopoietic progenitors; $CD34^+CD38^+$ and $CD34^+CD38^-$ cells represent cell types that are further down the haematopoietic hierarchy (Figure 1-2, Table 1-1) (Chao et al., 2008, Morrison and Weissman, 1994). Although $CD34^+CD38^+$ and $CD34^-CD38^+$ cells are considered to be more differentiated than the classic $CD34^+CD38^-$ HSC, these cell types are generally regarded as multipotent progenitors, and thus have the capacity to also differentiate into cells of lymphoid, myeloid and erythroid lineages, meaning these cell types would also be valuable within HSC niche models (Dahlberg et al., 2011, Schuster et al., 2012, Osawa et al., 1996). Consequently, an additional aim of this chapter is to determine the potential of the niche models to induce expression of $CD34^+CD38^+$ and $CD34^-CD38^+$ phenotypes after 5 days of culture.

6.1.3 Commitment of progenitors to differentiation lineages

All three of the aforementioned $CD34^+CD38^-$, $CD34^+CD38^+$ and $CD34^-CD38^+$ cell types have the capacity to undergo differentiation, producing cells of the lymphoid, myeloid and erythroid lineages (Miyamoto et al., 2002). Although evidence is shown in previous chapters suggesting that the PEA + FN + BMP-2&NGF substrate may act favourably in conjunction with the stromal layer and 2% HS and 3GF media formulation to support maintenance and expansion of haematopoietic multipotent progenitors, it is also important to consider that the HSC niche is dynamic, and that the models may cause the $CD34^+CD38^-$ cells added at day 15 to further progress towards differentiating beyond the $CD34^+CD38^+$ and $CD34^+CD38^-$ phenotypes. Therefore, while the main aims of this chapter are to determine the capacity of the developed niche models to induce maintenance and expansion of the progenitor cells, this chapter also aims to determine whether the models affect commitment of these progenitor cells to the lymphoid, myeloid and erythroid differentiation lineages. To determine if this were the case, flow cytometry was also carried out to compare the expression levels of CD7, CD36 and CD41a, which are indicative of lymphoid, erythroid and myeloid commitment, respectively, in cells of each progenitor type.

6.2 Aims and Objectives

The results shown in Chapter 4 outline that use of DMEM supplemented with 2% HS for 14 days, followed by use of 3GF media for days 15-21 of cell culture, represents the media formulation that best suited the development of this model in terms of inducing the most favourable phenotype in MSCs and cost. However, it is important to note that as this work progressed, additional advice from collaborators paired with the results shown in this chapter led to the use of 3 media formulations in the HSC addition phase of the model, as outlined in Figure 6-1. In addition, it was concluded that culturing HSCs for 7 days may prove to be too long, as collaborators observed that the cells tend to differentiate by that point in standard culture, and the effect of the models may not be strong enough to overcome this. Therefore, a shorter culture period of 5 days was decided to be appropriate for these preliminary experiments where HSCs were added into the models.

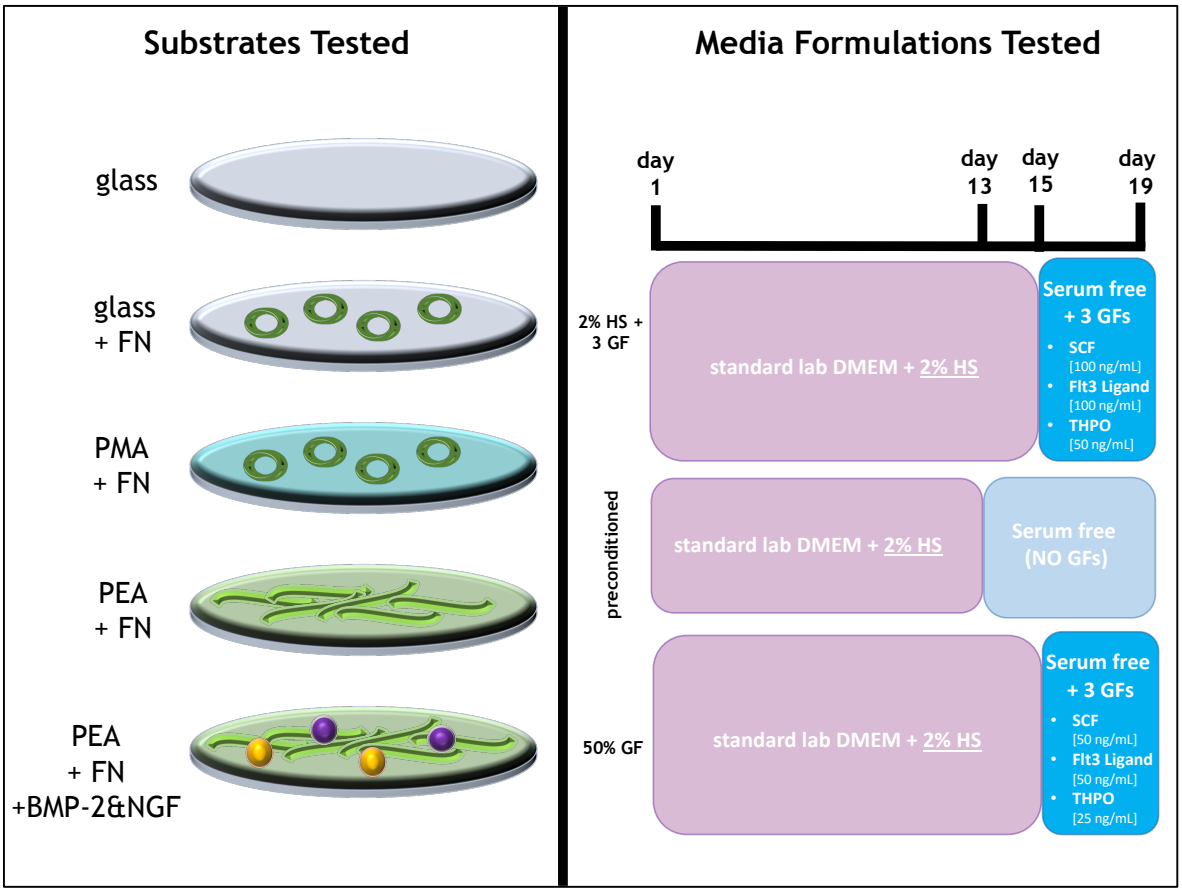

Figure 6-1 Substrates and media formulations used in HSC culture experiments
The results shown in this chapter were obtained using models testing the effect of one of 5 different substrates (glass, glass + FN, PMA + FN, PEA + FN and PEA + FN + BMP-2&NGF), where green circles indicate globular fibronectin and green fibrils represent network fibronectin. Media formulations tested; '2% HS + 3GF' where 3 GFs were used in the HSC culture period; preconditioned media where no GFs were used; 50% GF media where 3GFs at 50% of the concentration in the 3GF media were used for the duration of the HSC culture period.

This chapter will address the results associated with each of the haematopoietic multipotent progenitors, $CD34^{+}CD38^{-}$, $CD34^{+}CD38^{+}$ and $CD34^{-}CD38^{+}$, in terms of:

- the portion of the total cell number expressing each phenotype after 5 days of culture

- the portion of the total progenitor number expressing: CD7 (indicative of cells preparing to commit to the lymphoid lineage); CD36 (indicative of cells preparing to commit to the erythroid lineage); CD41a (indicative of cells preparing to commit to the myeloid lineage)

6.3 Materials and Methods

6.3.1 HSC culture

HSCs were obtained commercially from CalTag MedSystems, UK. They were stored at -80 ^{o}C in liquid nitrogen until required. When the cells were required, the vial of cells was transported from the -80 ^{o}C freezer, and immediately transferred to a 37 ^{o}C water bath, where it was left for 3 minutes to ensure defrosting. Cells were transferred to a 15 mL falcon tube, and 10 mL of SFM base media was added to the tube. The cell suspension was centrifuged for 10 minutes at 400 g, and the cell pellet was re-suspended in 2mL of 3GF or 5 GF media depending on the media type being used for the rest of the experiment. Cells were counted using a haemocytometer and trypan blue, and then the remaining cell suspension was transferred to a central well of a 6 well plate and left overnight in an incubator at 37 ^{o}C and 5% CO_2.

Cells were seeded the day after being brought up from frozen. Seeding of the HSCs involved their addition to the model outlined in Chapter 4, where a layer of stromal cells had been cultured for 15 days. The HSCs were counted on this day, and the cell suspension was transferred from the central well of a 6 well plate to a 15 ml falcon tube. 20 µl of cells were taken from the well and transferred to a reaction tube for phenotyping via FLOW cytometry. The appropriate volume of serum-free media was added to the remaining volume of cell suspension, to allow for the cells to be seeded at 5 x 10 ^{4} cells per well of a 24 well plate. As these cells are non-adherent, it was not possible to change the media once the HSCs were added to the model wells containing the polymer-coated coverslip, MSCs and HSCs. Thus, once the HSCs were added to the wells, they remained in the plate for 5 days.

6.3.2 Flow cytometry

6.3.2.1 Flow cytometry staining

After the 5-day culture of HSCs, 5 µl of cell suspension was drawn from each well and transferred to a reaction tube, for use as a ‘cell only’ FLOW cytometry control. The cell suspension within each well was transferred to a FACS tube, and 1ml of FACS buffer at 4 ^{o}C was added. The tubes were centrifuged for 5

minutes at 400 g, and the cell pellets were re-suspended in 500 µl of FACS buffer. The cell suspensions were split into two tubes, and centrifuged for 5 minutes at 400g. Cell pellets were then re-suspended in either antibody mix A or antibody mix B, where cells would be stained for differentiation or progenitor markers, respectively.

Table 6-1 Flow cytometry antibody mixes

Fluorophore	Tube A CD numbers	Tube B CD numbers
FITC	41a	Lin
PE	34	34
Cy5		
Cy7	38	38
APC	36	
APC-Cy7	45	
BV421	7	

Cells were incubated with the above antibodies for 30 minutes, in the dark and on ice. The samples were centrifuged for 5 minutes at 400 g, and were then re-suspended in 200 µl of FACS buffer. Each sample was stored on ice and kept in a box for a maximum of 1 hour before being processed through a BD FACSCanto II FLOW cytometer.

6.3.2.2 Flow cytometer usage

Cells were run in a BD FACSCanto II analyser. Unstained controls were used to set the voltage for each of the 6 channels used, and isotype controls for each channel were used with cells as negative controls, allowing for the non-specific background signal to be differentiated from the specific antibody signal.

Table 6-2 FLOW cytometry antibody list

Cell Surface Marker	Fluorophore	Supplier
lineage (LIN) cocktail	FITC	BD Biosciences, UK
CD34	PE	BD Biosciences, UK
CD38	Cy7	BD Biosciences, UK
CD45	A7	BD Biosciences, UK
CD7	BV-241	BD Biosciences, UK
CD36	APC	BD Biosciences, UK
CD41a	FITC	BD Biosciences, UK
mouse isotype control	FITC	BD Biosciences, UK
mouse isotype control	PE	BD Biosciences, UK
mouse isotype control	Cy7	BD Biosciences, UK
mouse isotype control	A7	BD Biosciences, UK
mouse isotype control	BV-241	BD Biosciences, UK
mouse isotype control	APC	BD Biosciences, UK

6.3.2.3 Flow cytometry compensation

In order to correct for any spectral overlap, UltraComp eBeads™ were used to perform fluorescence compensation. 1 drop of the beads was added to 100 μL of FACS buffer in a reaction tube, and 1 μL of each antibody was added. The reaction tubes were stored on ice and in the dark for 30 minutes, before the mixtures were each centrifuged at 600 g for 5 minutes. The pellets were re-suspended in 200 μL of FACS buffer and the samples were run separately in the cytometer in the compensation set up. The spectral overlap settings were set automatically, by the accompanying software.

6.3.2.4 Flow cytometry gating strategy and data analysis

Gating strategy work was carried out using FlowJo™ software with kind assistance from Ewan Ross, the University of Glasgow. The first step in the gating strategy was to use a forward scatter area (FSC-A) versus side scatter area (SSC-A) plot to identify the population of viable cells (Figure 6-2a). From this plot, an additional plot of FSC-A versus forward scatter width (FSC-W) was produced, in order to identify the single cells and exclude any doublets (Figure 6-2b).

The single cell population was then used to identify the lineage negative population of cells, from which the $CD34^{+}CD38^{-}$, $CD34^{+}CD38^{+}$ and $CD34^{-}CD38^{+}$ cell populations could be identified (Figure 6-2c, Figure 6-2d).

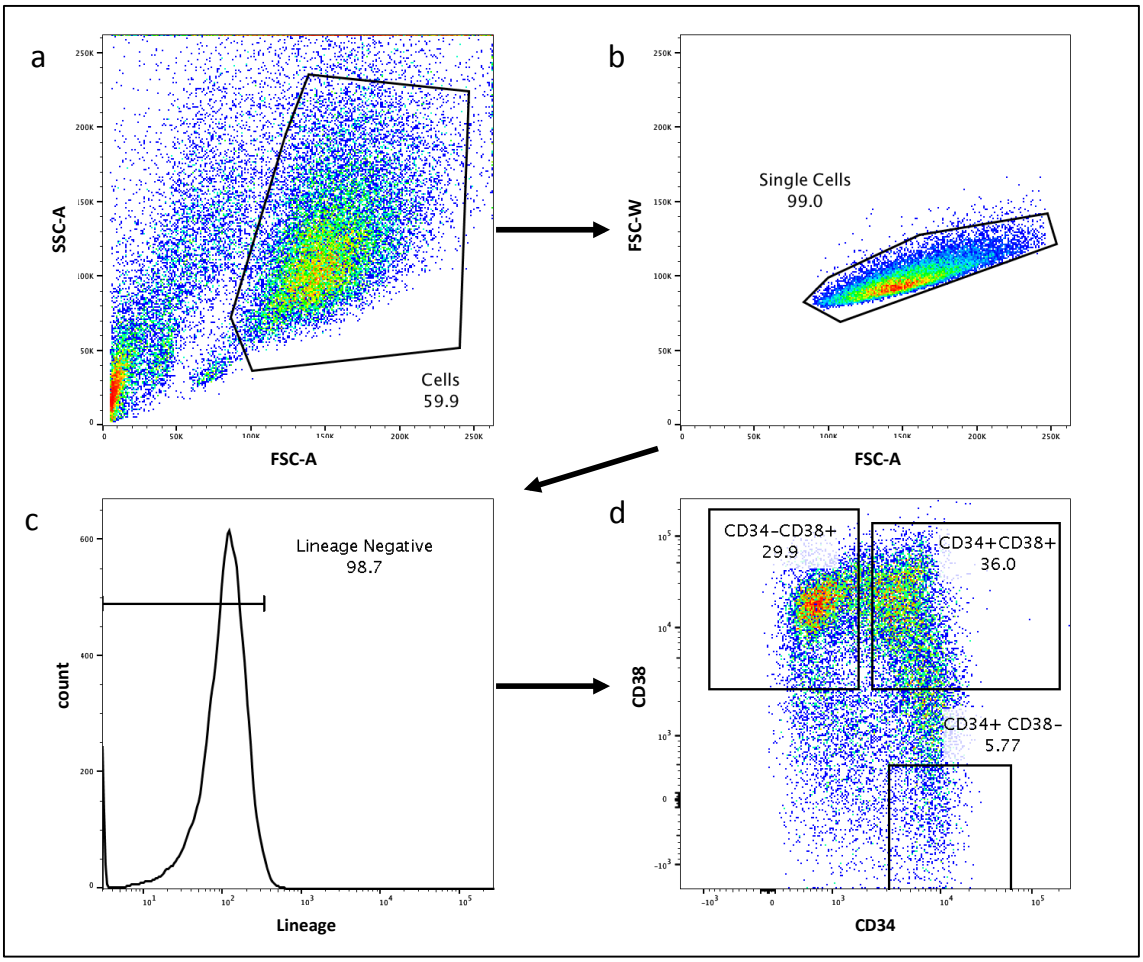

Figure 6-2 Flow cytometry gating strategy for progenitor identification
Sample data is from models featuring PEA + FN + BMP-2&NGF substrates and containing 3GF media. a = forward scatter versus side scatter plot, for identification of a viable cell population; b = single cell population with doublet exclusion; c = application of gating on the lineage negative cell population ; d = identification of progenitors.

The gating strategy for determining the percentage of cells expressing CD7, CD36 and CD41a, within each of the $CD34^{+}CD38^{-}$, $CD34^{+}CD38^{+}$ and $CD34^{-}CD38^{+}$ populations, is outlined in Figure 6-3. This gating strategy allowed for the determination of the exact number of cells expressing CD7, CD36 and CD41a within each population type, which was then converted to a percentage of the total cell number within each population subset.

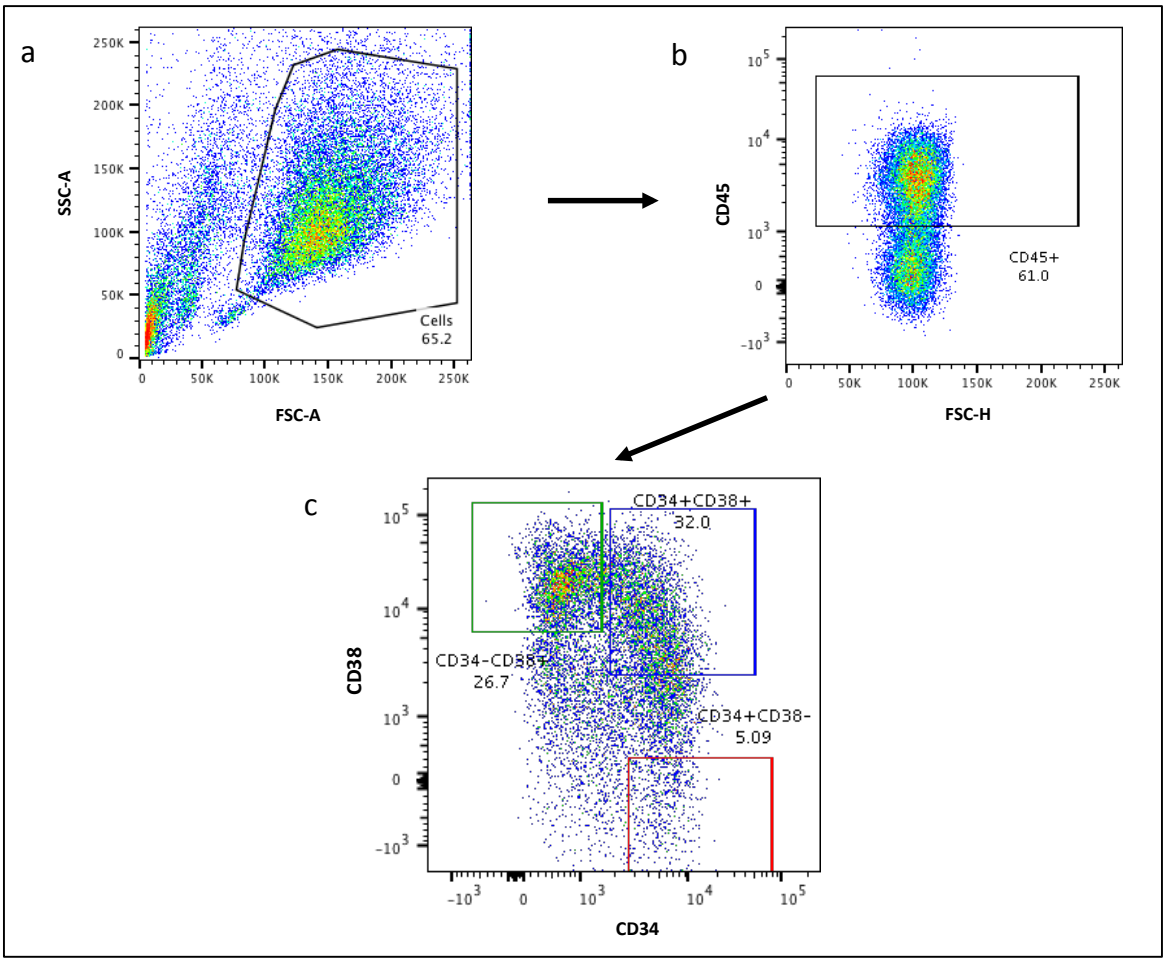

Figure 6-3 Flow cytometry gating strategy for progenitor populations associated with differentiation analyses
Sample data is from models featuring PEA + FN + BMP-2&NGF substrates and containing 3GF media. a = forward scatter versus side scatter plot, for identification of a viable cell population; b = application of gating on $CD45^{+}$ population; c = identification of progenitors

Following the identification of the $CD34^{+}CD38^{-}$, $CD34^{+}CD38^{+}$ and $CD34^{-}CD38^{+}$ populations, expression of CD7, CD36 and CD41a was determined. Cells were considered positive for each marker type if the expression levels were to the right of the lines marked in Figure 6-4, Figure 6-5 and Figure 6-6.

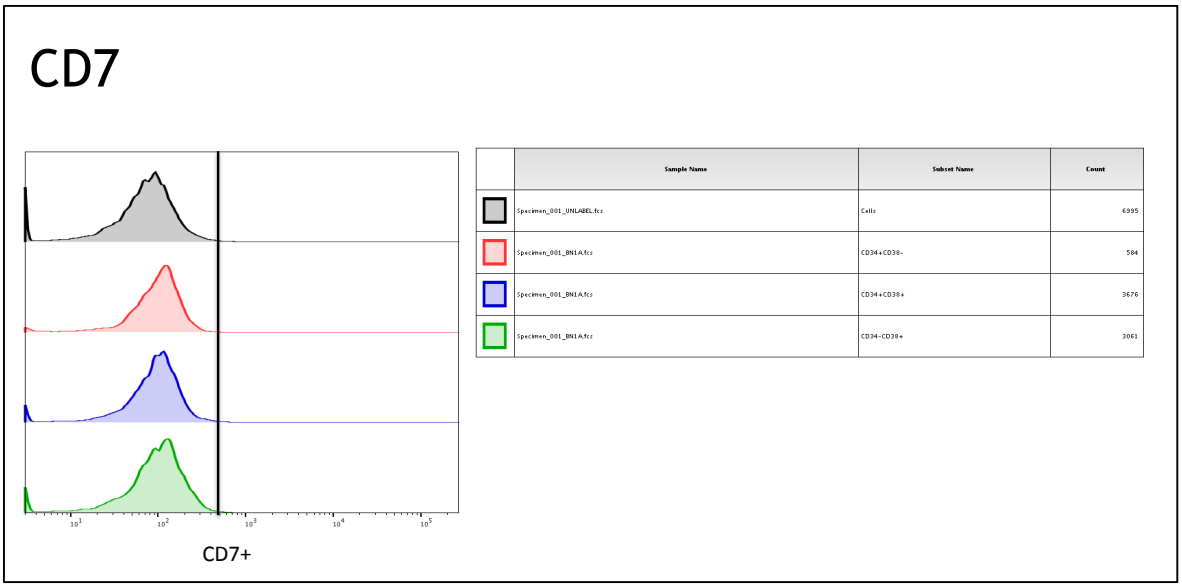

Figure 6-4 Gating strategy for CD7+ populations
Sample data is from models featuring PEA + FN + BMP-2&NGF substrates and containing 3GF media. Cells positive for CD7 were tested for in each $CD34^{+}CD38^{-}$, $CD34^{+}CD38^{+}$ and $CD34^{-}CD38^{+}$ populations, using unstained cells as negative controls. y axes are indicative of cell count. Cells to the right of the vertical black line indicate positive expression.

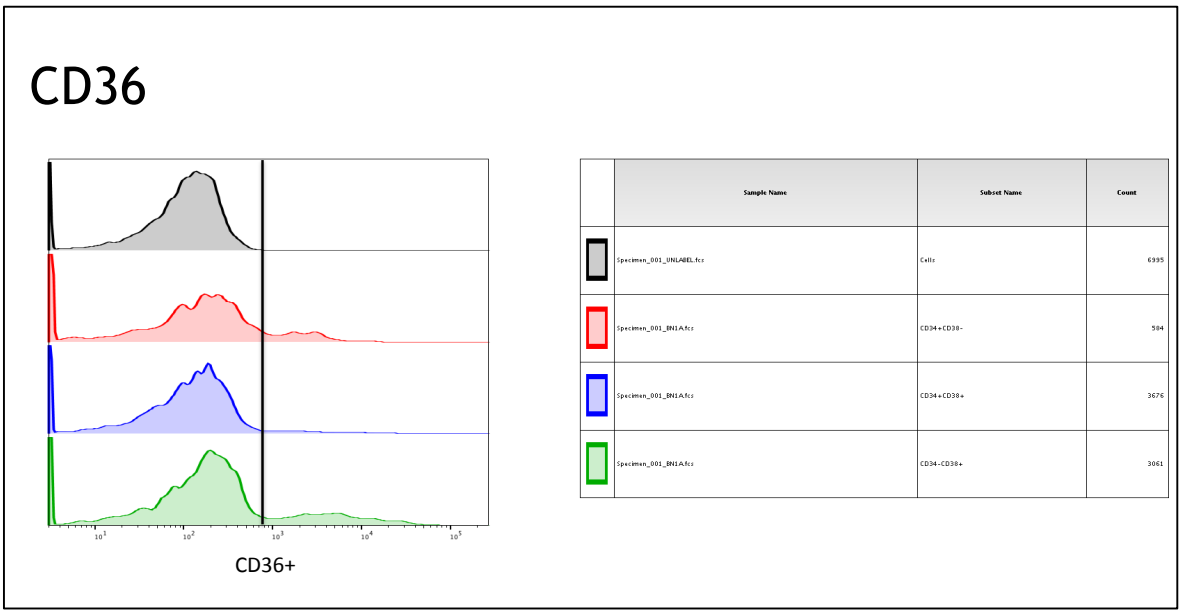

Figure 6-5 Gating strategy for CD36+ populations
Sample data is from models featuring PEA + FN + BMP-2&NGF substrates and containing 3GF media. Cells positive for CD36 were tested for in each $CD34^{+}CD38^{-}$, $CD34^{+}CD38^{+}$ and $CD34^{-}CD38^{+}$ populations, using unstained cells as negative controls. y axes are indicative of cell count. Cells to the right of the vertical black line indicate positive expression.

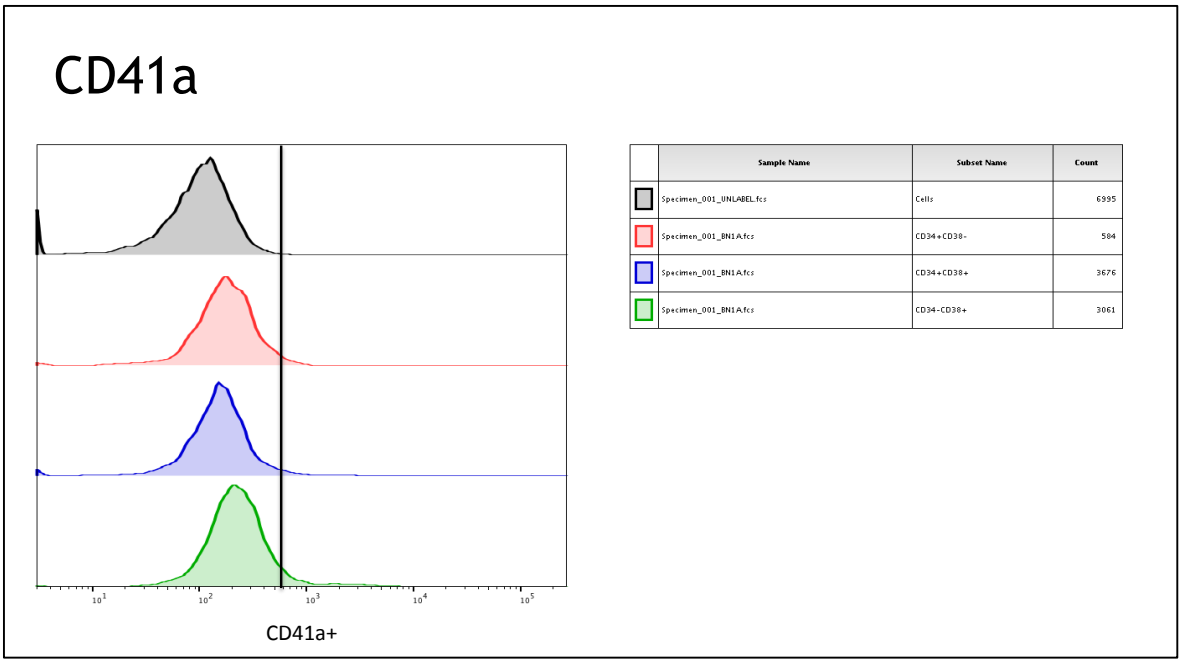

Figure 6-6 Gating strategy for CD41a+ populations
Sample data is from models featuring PEA + FN + BMP-2&NGF substrates and containing 3GF media. Cells positive for CD41a were tested for in each $CD34^{+}CD38^{-}$, $CD34^{+}CD38^{+}$ and $CD34^{-}CD38^{+}$ populations, using unstained cells as negative controls. y axes are indicative of cell count. Cells to the right of the vertical black line indicate positive expression.

6.3.2.5 Statistical Analyses

Statistical analyses were carried out as outlined in section 2.5. However, statistically significant differences are only marked on the graphs in this chapter if the differences exist between models that had the same cell cultures in them; statistically significant differences are marked for models where MSCs and HSCs were co-cultured in both analysed models, but not between models where HSCs were cultured in one but MSCs and HSCs were co-cultured in the other analysed model.

6.4 Results

6.4.1 $CD34^+CD38^-$ cells in candidate models

6.4.1.1 Retention of the $CD34^+CD38^-$ phenotype in candidate models

In order to determine the capacity of the niche model candidate substrates to support retention of a $CD34^+CD38^-$ cells, these cells were cultured for 5 days in models using each substrate type and a stromal layer cultured in one of the three media types outlined in Figure 6-1. However, it should be noted that additional controls were used, where HSCs were cultured alone, in the absence of the stromal layer (indicated by (H) next to the substrate name on the x axes of Figure 6-7). Models with the MSC stromal layer and HSCs are marked (M+H).

The results in Figure 6-7a showed that the presence of MSCs in HSC niche models resulted in increased numbers of cells with the $CD34^+CD38^-$ phenotype existing after 5 days of culture. Interestingly, there were no statistically significant differences in the number of cells with the $CD34^+CD38^-$ phenotype between models using the PEA + FN + GF substrates and those using the controls. It was hypothesised that this may have been due to the concentration of GFs in the 3GF media dampening the effects of the GFs on the surfaces, thus it was decided to repeat the experiment using preconditioned media (with no GFs present) (Figure 6-7b).

Unexpectedly, the results in Figure 6-7b indicated that the $CD34^+CD38^-$ phenotype is optimally expressed when HSCs are cultured alone in the models. This may have arisen from the HSCs binding to the FN and responding to it by differentiating (Yoder and Williams, 1995). However, this result is the opposite of what the literature suggests, whereby MSCs are strongly favoured within HSC niche models (Leisten et al., 2012, Fajardo-Orduña et al., 2015). Consequently, it was decided that the experiment should be repeated again, and that the concentration of GFs used in the 3GF media should be halved, as a means of understanding if this type of media may act to still support HSC life, while providing a greater opportunity for the effect of the GFs on the substrates to take effect.

The experiments associated with the results shown in Figure 6-7a & b were repeated using 50%GF media three times, with three different HSC and three different MSC donors (Figure 6-7 c, d & e). The results shown in Figure 6-7c suggested that the PEA + FN surface optimally supports maintenance of the $CD34^{+}CD38^{-}$ phenotype in this media type, and allows for a statistically significant increase, relative to glass controls. However, this experiment was repeated, using the same media formulation, it can be observed that this small difference was reproducible for the results shown in Figure 6-7d, but not for Figure 6-7e.

In a bid to consider all data shown in Figure 6-7, and draw a general conclusion about the effect of the surfaces regardless of the media type, the values obtained for each experiment were collated and Figure 6-7f was produced. This graph proposed that the substrate type used within these models had no significant effect on the expression of the $CD34^{+}CD38^{-}$ phenotype in HSCs.

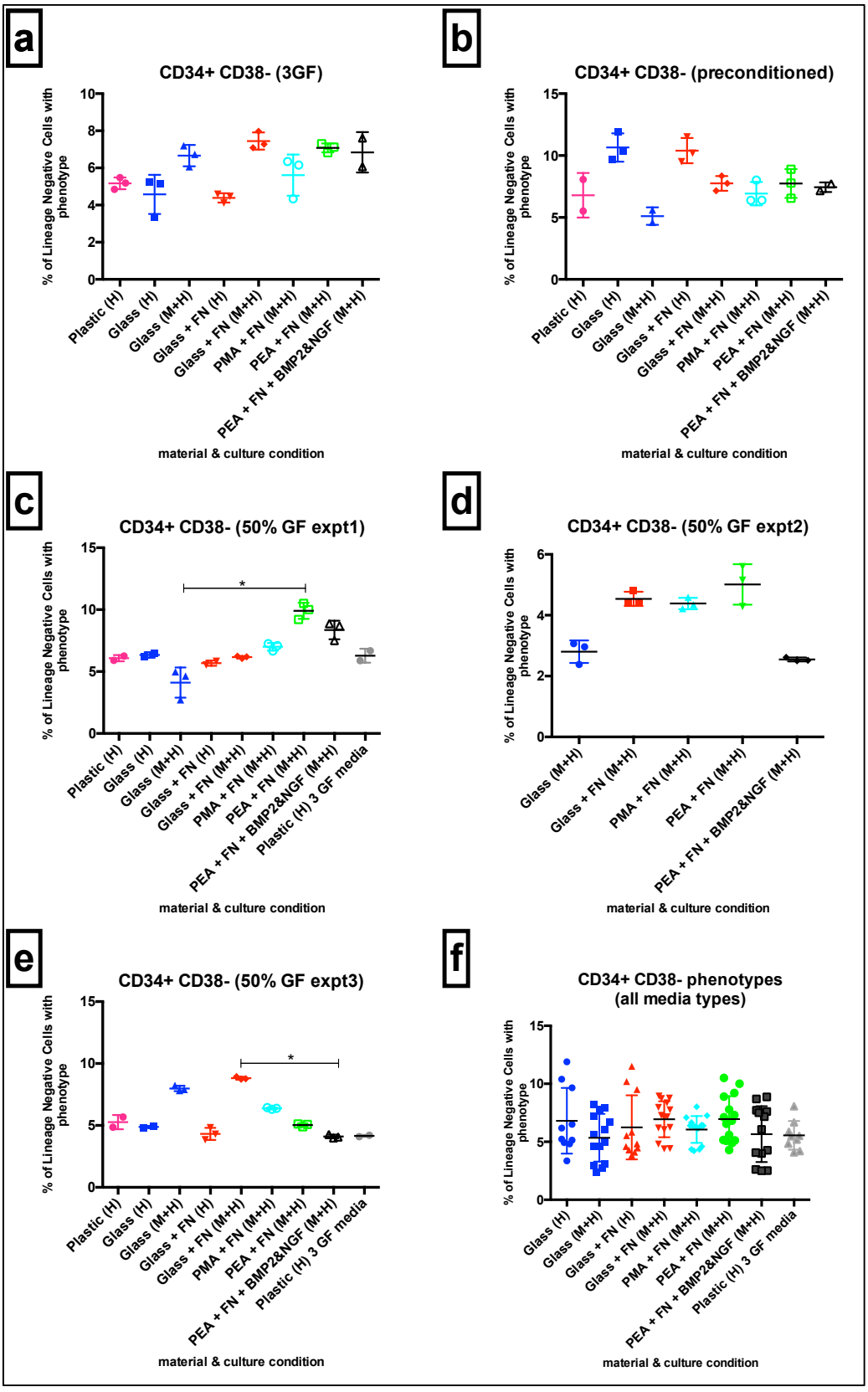

Figure 6-7 CD34+CD38- populations in niche models using different substrates & media types.

Graphs show the percentage of lineage negative cells expressing the $CD34^{+}CD38^{-}$ HSC phenotype after cell culture for 5 days in models with different substrates. (H) = HSC only negative control. (M+H) = MSCs + HSCs in a co-culture. a = culture in 3GF media; b = culture in preconditioned medium; c,d & e = culture in 50%GF medium, from 3 separate donors; f = results from all media types collated. Graphs show mean +/- SD. *=p<0.05, **=p<0.01, ***=p<0.001, ****=p<0.0001, by Kruskal-Wallis. $CD34^{+}CD38^{-}$ phenotype is enhanced by the presence of MSCs within models

6.4.1.2 $CD34^+CD38^-$ commitment to the lymphoid lineage

Although the results shown in section 6.4.1.1 suggest that the substrates and media types tested to feature within the designed HSC niche models do not generate significant and consistent effects on the $CD34^+CD38^-$ phenotype, further analyses were carried out to determine if these variables affected the expression of CD7 (indicative of lymphoid commitment) within cells of the $CD34^+CD38^-$ population. The results are presented in Figure 6-8.

The graph shown in Figure 6-8a showed that only a very low proportion of $CD34^+CD38^-$ cultured in all models with any substrate type expressed CD7, suggesting that progression towards lymphoid commitment was generally low at the 5-day culture time point. The spread of the data points implied that n numbers should be greater in order make any differences more apparent.

Figure 6-8b showed results associated with models using preconditioned media types. Although the differences in CD7 expression in cells in different models lacked statistical significance, it was interesting to observe that when MSCs were present, the expression of CD7 was generally lower. This observation correlated well with the results presented in Figure 6-7, as those results showed that models with stromal layers generally enhanced maintenance of the more primitive $CD34^+CD38^-$ progenitor phenotype. This result may have arisen from expression of markers associated with differentiation down different haematopoietic lineages. In addition, it is important to note that CD7 expression was lowest in the 'Plastic (H) 3 GF media' where HSCs were cultured in 3 GF media. This suggested that having GFs in the media acted to prevent commitment to the lymphoid lineage.

Graphs in Figure 6-8c, d & e represent three repetitions of the same experiment using 50% GF media, but with HSCs and MSCs from 3 different donors. A similar difference was observed in graphs c & d, whereby CD7 expression appeared to be lower in models containing MSCs and FN-containing substrates. This result correlated well with that observed in Figure 6-7c & d, as that figure showed that models containing MSCs and FN-containing substrates acted to maintain the primitive $CD34^+CD38^-$ progenitor population. This difference was not observed in Figure 6-8e, suggesting donor variability affected the potency of the models.

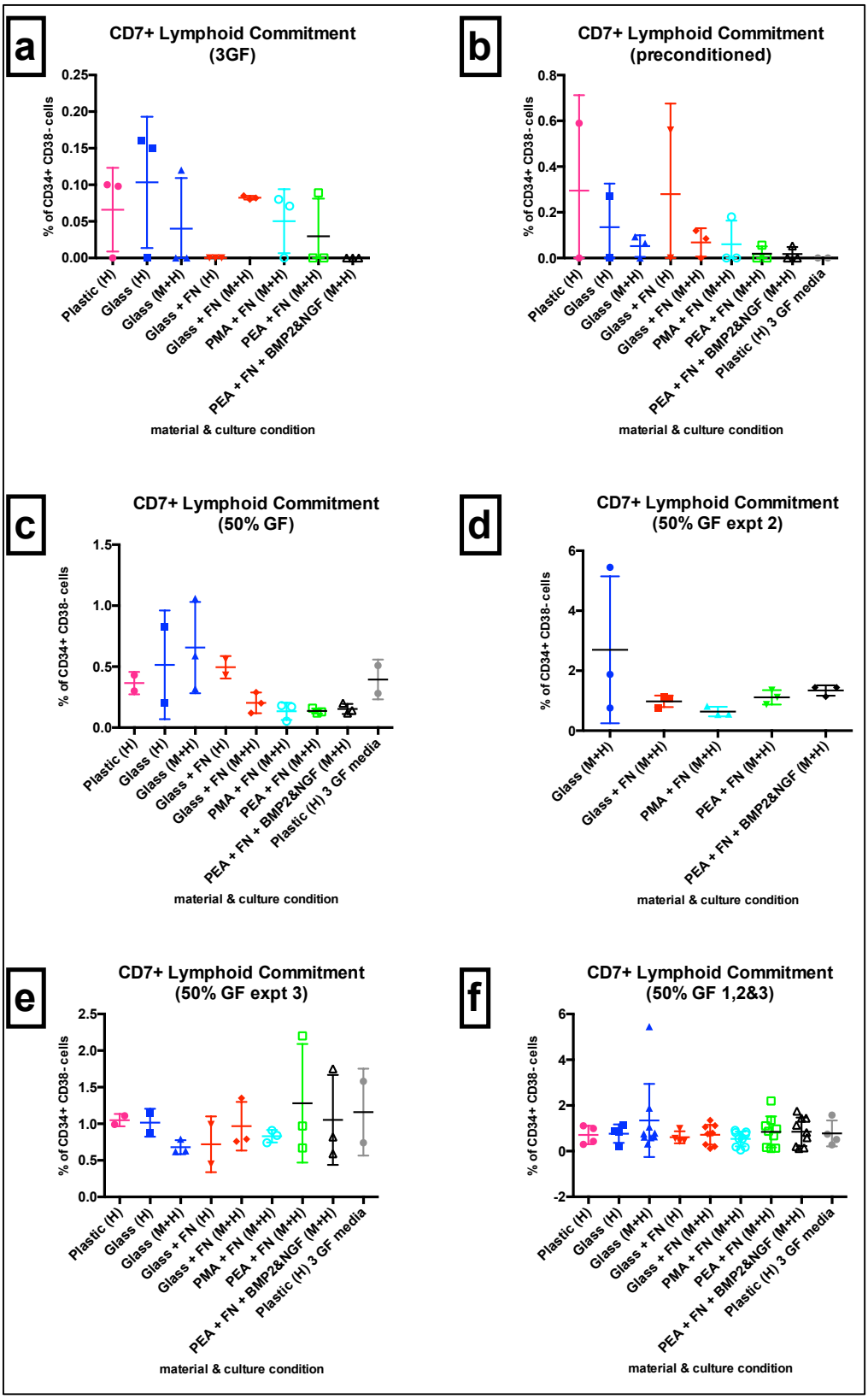

Figure 6-8 CD34+CD38-CD7+ populations in niche models using different substrate and media types

Graphs show the percentage of $CD34^{+}CD38^{-}CD45^{+}$ cells expressing CD7 (associated with lymphoid lineage commitment) after cell culture for 5 days in models with different substrates and media types. (H) = HSC only negative control. (M+H) = MSCs + HSCs in a co-culture. a = culture in 3GF media; b = culture in preconditioned medium; c,d & e = culture in 50%GF medium from 3 separate donors; f = results from all media types collated. Graphs show mean +/- SD. *=p<0.05, **=p<0.01, ***=p<0.001, ****=p<0.0001, by Kruskal-Wallis. Data indicates that HSC niche models have no statistically significant effect on the expression of CD7 within the $CD34^{+}CD38^{-}$ population.

6.4.1.3 $CD34^+CD38^-$ commitment to the erythroid lineage

Analysis of CD36 expression was carried out to determine the capacity of the different candidate niche model substrates, and different media formulations, to support the progression of $CD34^+CD38^-$ cells towards the erythroid differentiation lineage. The results are shown in Figure 6-9.

Figure 6-9a suggested that there were no significant differences in the expression of CD36 in $CD34^+CD38^-$ cells cultured on different niche model candidate substrates in the 3GF media type. It was interesting to observe that the percentage of $CD34^+CD38^-$ cells expressing CD36 increased to around 8% when the GF-free preconditioned media was used with preconditioned media and many substrates (Figure 6-9b). This indicated that the concentration of GFs in the 3GF media may have suppressed lineage commitment and helped to maintain primitive progenitor populations of HSCs within these models.

Although Figure 6-9c, d & e represented three repetitions of the same experiment using 50% GF media, but with cells from different donors, the results were markedly variable. This stressed that donor variability affected the potency of the models. However, observation of Figure 6-9f (where all results irrespective of media type have been collated) indicated that there are no prominent differences or statistically significant results indicating that CD36 expression within the $CD34^+CD38^-$ population was affected by the substrates in the model.

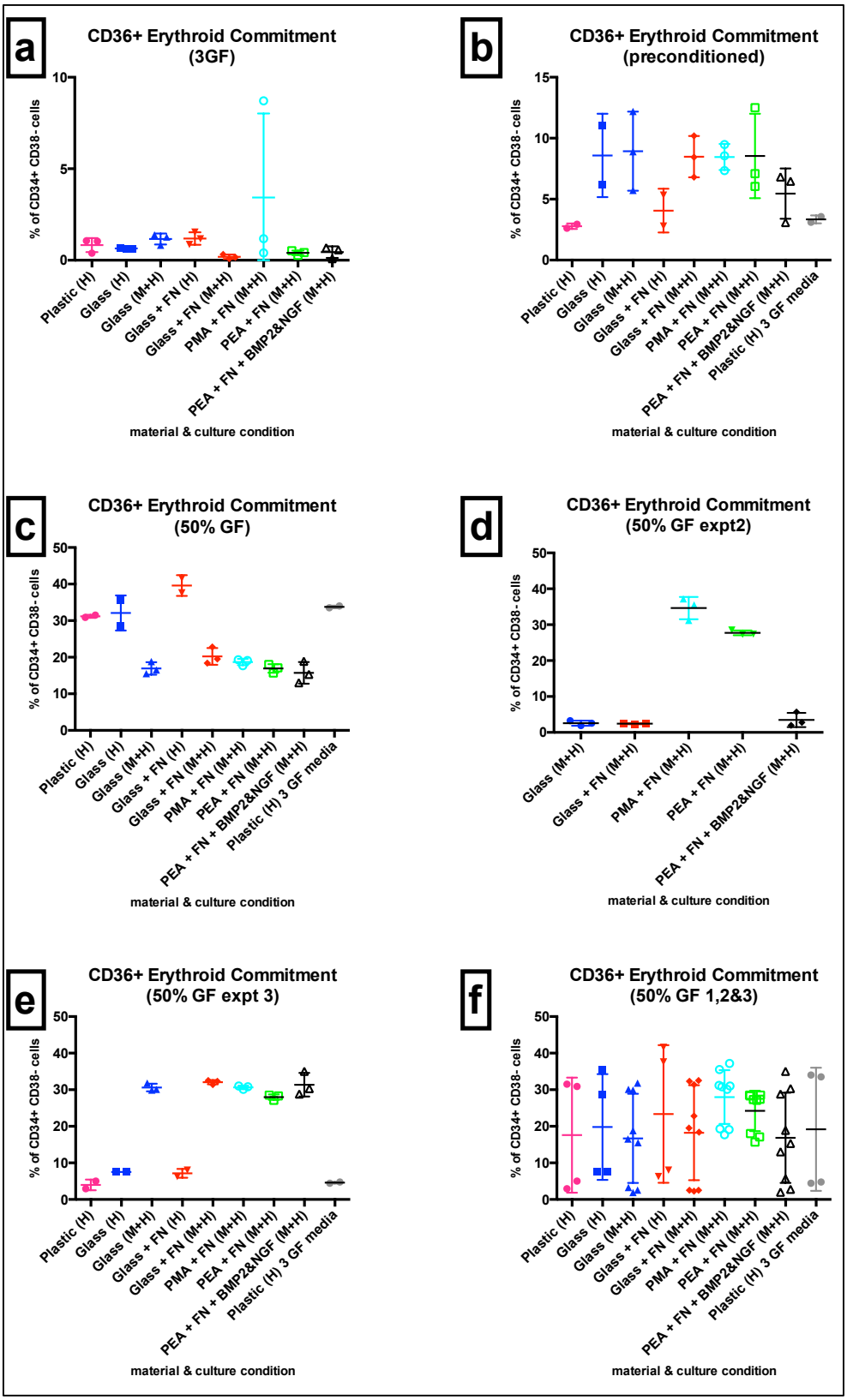

Figure 6-9 CD34+CD38-CD36+ populations in niche model candidate systems using different substrate and media types.
Graphs show the percentage of $CD34^{+}CD38^{-}$ $CD45^{+}$ cells expressing CD36 (associated with erythroid lineage commitment) after cell culture for 5 days in models with different substrates and media types. (H) = HSC only negative control. (M+H) = MSCs + HSCs in a co-culture. a = culture in 3GF media; b = culture in preconditioned medium; c,d & e = culture in 50%GF medium, from 3 separate donors; f = results from all media types collated. Graphs show mean +/- SD. *=p<0.05, **=p<0.01, ***=p<0.001, ****=p<0.0001, by Kruskal-Wallis. Data indicates that HSC niche models have no statistically significant effect on the expression of CD36 within the $CD34^{+}CD38^{-}$ population.

6.4.1.4 $CD34^+CD38^-$ commitment to the myeloid lineage

Further analysis of the $CD34^+CD38^-$ population was carried out to determine the effects of different niche model candidate substrates and media formulations on the expression of CD41a, indicative of progression of $CD34^+CD38^-$ cells towards differentiation down the myeloid lineage. The results are presented in Figure 6-10.

The data shown in Figure 6-10a suggested that the presence of MSCs and substrates containing FN within niche models can acted favourably to reduce the number of cells expressing a $CD41a^+$ phenotype within the $CD34^+CD38^-$ population, when HSCs were cultured in the 3GF media. The same difference was not observed in Figure 6-10b, when the experiment was repeated but with media changed to preconditioned media. However, it was interesting to note that the PEA + FN + GF surface produced some of the lowest numbers of cells with CD41a expression, in both media types. This suggested that the BMP-2 and NGF may function to maintain low levels of CD41a expression.

Graphs in Figure 6-8c, d & e represented three repetitions of the same experiment using 50% GF media, but with HSCs and MSCs from 3 different donors. Interestingly, a similar result was observed in graphs c & e, whereby CD41a expression was at its lowest in $CD34^+CD38^-$ cells cultured in models containing a stromal layer/HSC co-culture. However, the same subtle difference was not observed in graph d, where there were considerable differences in the expression of CD41a between cells cultured in models with the PMA + FN and PEA + FN substrates, compared to controls. It was important to note that in Figure 6-10b, c & e, the number of $CD34^+CD38^-$ cells expressing CD41a is similar in the 'Plastic (H)' models where HSCs are cultured alone in the 50% GF media and also in the 'Plastic (H) 3 GF media' models, where the cells are cultured in the 3 GF media. This showed that the media type was not what was affecting the CD41a expression profile of these cells, rather it may have been donor cell variability, or the effect of the substrates on the stromal layer.

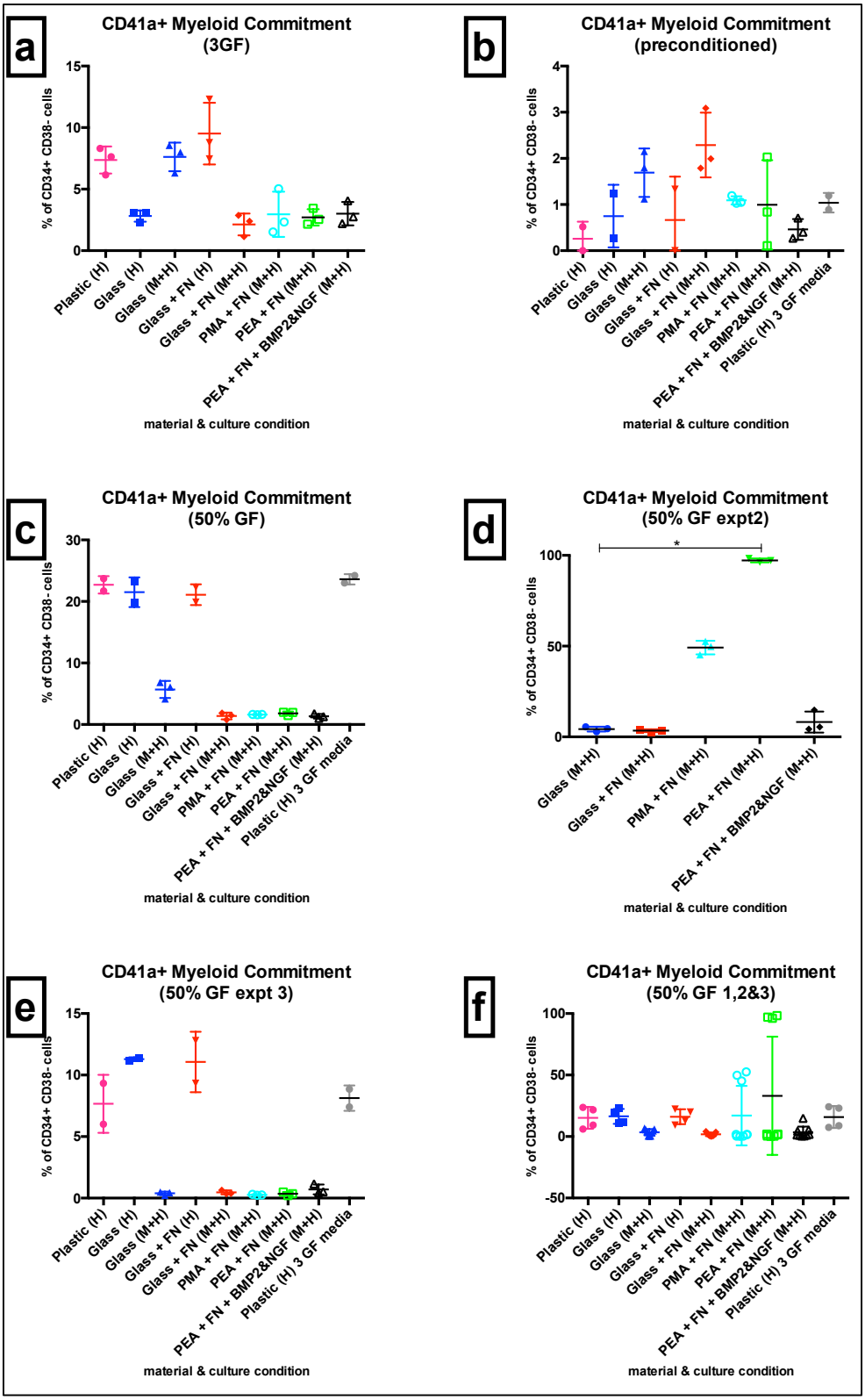

Figure 6-10 CD34+CD38- populations in niche models using different substrates and media types

Graphs show the percentage of $CD34^{+}CD38^{-}$ $CD45^{+}$ cells expressing CD41a (associated with myeloid lineage commitment) after cell culture for 5 days in models with different substrates and media types. (H) = HSC only negative control. (M+H) = MSCs + HSCs in a co-culture. a = culture in 3GF media; b = culture in preconditioned medium; c,d & e = culture in 50%GF medium, from 3 separate donors; f = results from all media types collated. Graphs show mean +/- SD. *=p<0.05, **=p<0.01, ***=p<0.001, ****=p<0.0001, by Kruskal-Wallis. Data indicates that HSC niche models have no statistically significant effect on the expression of $CD34^{+}CD38^{-}$ population.

6.4.2 $CD34^+CD38^+$ cells in candidate models

6.4.2.1 Expression of the $CD34^+CD38^+$ phenotype in candidate models

Although the $CD34^+CD38^-$ phenotype was the most important phenotype to regard in the development of this HSC niche model, similar analyses as those shown in section 6.4.1 were carried out regarding the $CD34^+CD38^+$ population of cells existing within the models after 5 days of culture. To first determine the effect of the models on the number of cells with the $CD34^+CD38^+$ phenotype, flow cytometry was carried out, using cells from 5 different donors in 5 different experiments. Results are presented in Figure 6-11.

Figure 6-11a & b indicated that there were no statistically significant differences in the percentage of lineage negative cells expressing the $CD34^+CD38^+$ phenotype in models using the different substrate types, with either the 3GF or preconditioned media types. Interestingly, while the results were repeats of the same experiment, Figure 6-11c & e both also show no statistically significant differences, while Figure 6-11d does. Observation of the data presented in Figure 6-11d indicated that the PEA + FN surface optimally supported the $CD34^+CD38^+$ phenotype. However, it should be noted that the percentage of lineage negative cells with the $CD34^+CD38^+$ phenotype was markedly higher than it was in all other experiments. The collated data shown in Figure 6-11f confirmed that there were no statistically significant differences between models with the different substrates within them.

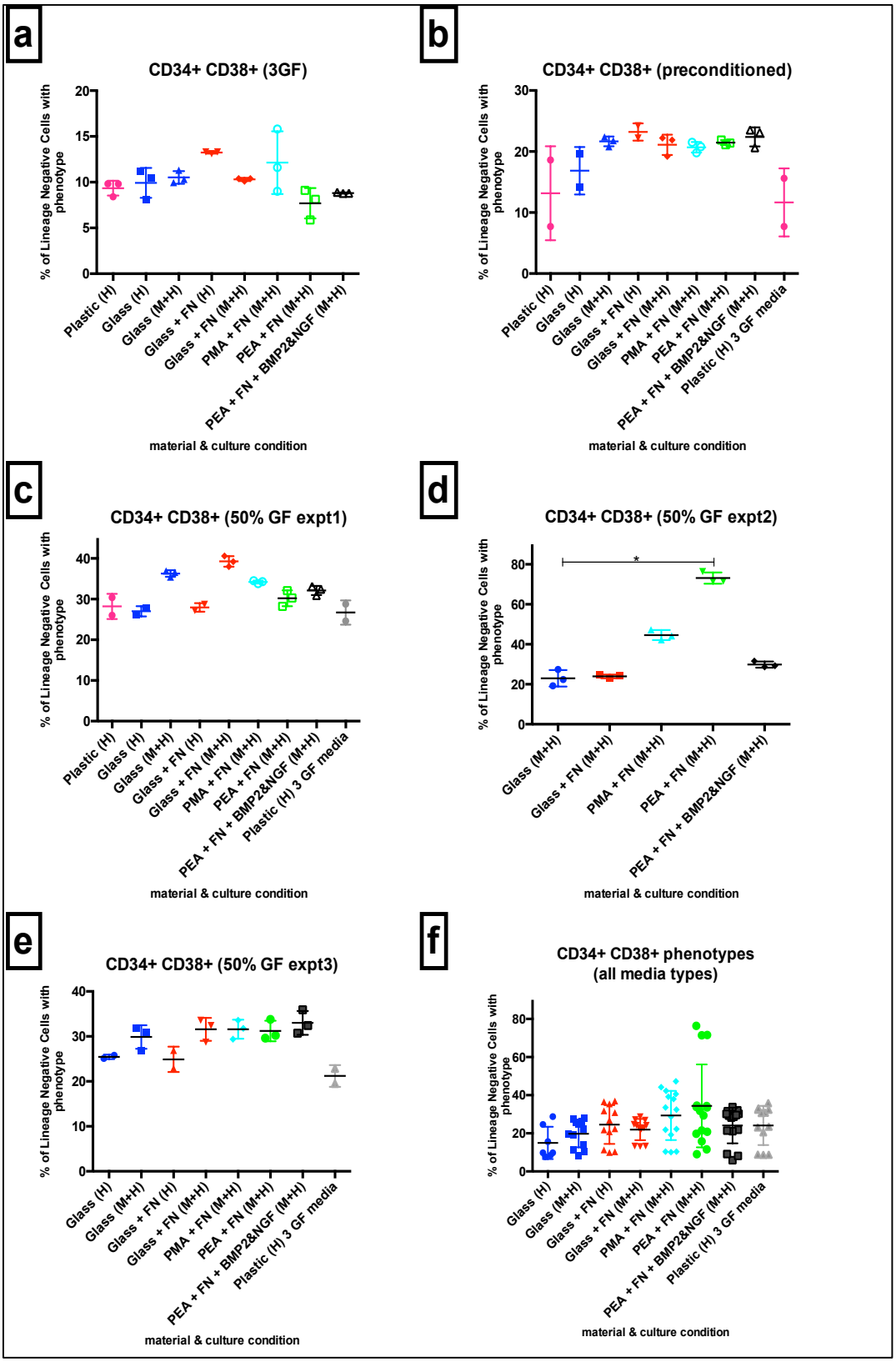

Figure 6-11 CD34+CD38+ populations in niche models using different substrates and media types

Graphs show the percentage of lineage negative cells expressing the $CD34^{+}CD38^{+}$ progenitor phenotype after cell culture for 5 days in models with different substrates. (H) = HSC only negative control. (M+H) = MSCs + HSCs in a co-culture. a = culture in 3GF media; b = culture in preconditioned medium; c,d & e = culture in 50%GF medium, from 3 separate donors; f = results from all media types collated. Graphs show mean +/- SD. *=p<0.05, **=p<0.01, ***=p<0.001, ****=p<0.0001, by Kruskal-Wallis. Data indicates that HSC niche models have no statistically significant effect on the expression of the $CD34^{+}CD38^{+}$ phenotype.

6.4.2.2 $CD34^+CD38^+$ commitment to the lymphoid lineage

Although the results shown in section 6.4.2.1 suggest that the substrates and media types tested to feature within the designed HSC niche models do not generate significant and consistent effects on the $CD34^+CD38^-$ phenotype, further analyses were carried out to determine if these variables affected the expression of CD7 (indicative of lymphoid commitment) within cells of the $CD34^+CD38^+$ population. Results are presented in Figure 6-12.

The graphs shown in Figure 6-12 showed that, regardless of the media type used within the models, the different substrates did not induce any statistically significant differences in the percentage of $CD34^+CD38^+$ cells expressing CD7. It was particularly interesting to observe that the percentages of $CD34^+CD38^+$ cells with the CD7 phenotype in different models varied between the experiments shown in Figure 6-12c, d & e, despite each experiment using the same media formulation and the same batch of substrates. This stressed that cells from different donors behave differently, as the cells are the only variable within these experiments.

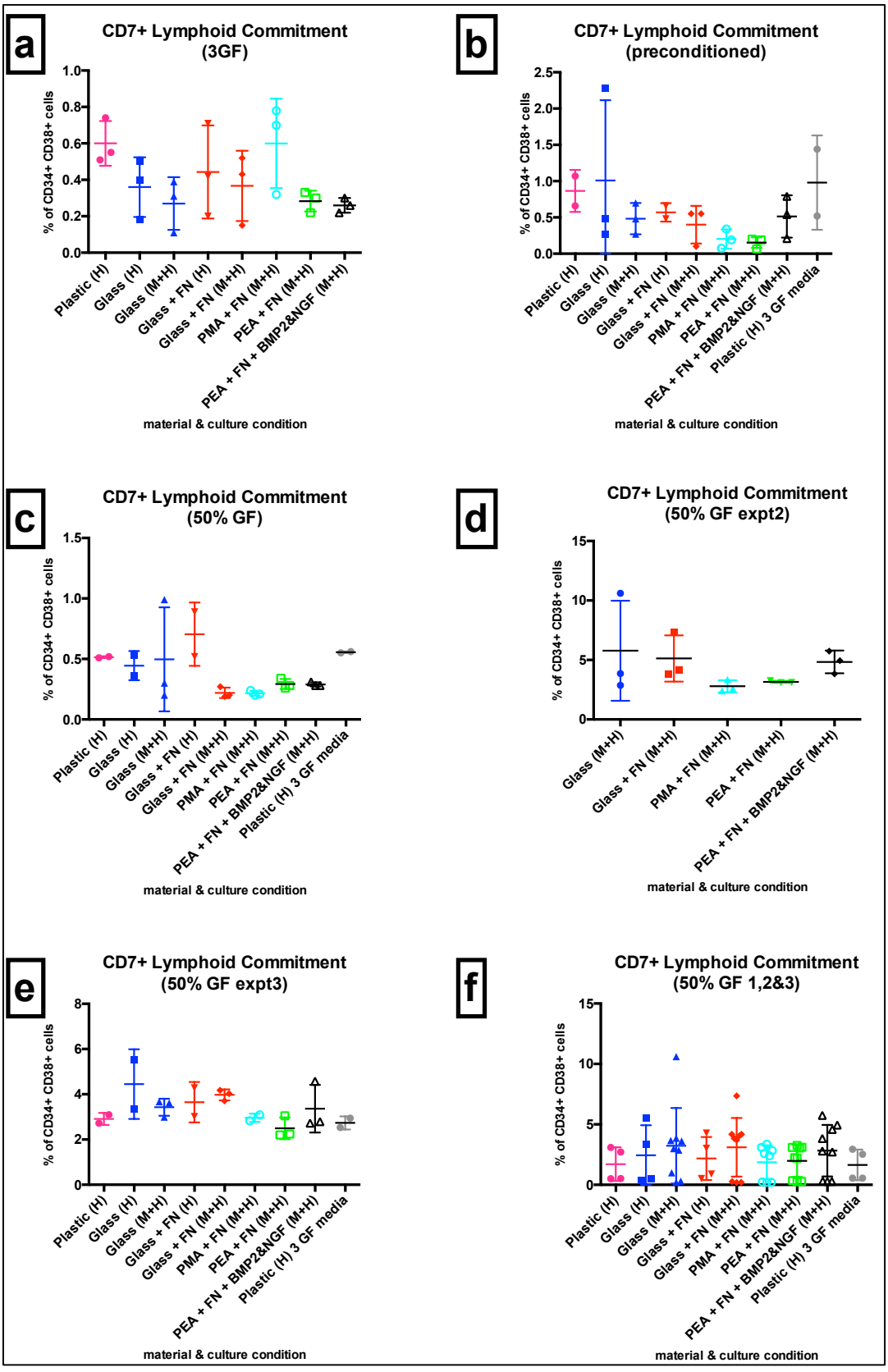

Figure 6-12 CD34+CD38+CD7+ populations in niche models using different substrate and media types

Graphs show the percentage of $CD34^{+}CD38^{+}$ $CD45^{+}$ cells expressing CD7 (associated with lymphoid lineage commitment) after cell culture for 5 days in models with different substrates and media types. (H) = HSC only negative control. (M+H) = MSCs + HSCs in a co-culture. a = culture in 3GF media; b = culture in preconditioned medium; c,d & e = culture in 50%GF medium from 3 separate donors; f = results from all media types collated. Graphs show mean +/- SD. Data indicates that HSC niche models have no statistically significant effect on the expression of CD7 within the $CD34^{+}CD38^{+}$ population

6.4.2.3 $CD34^+CD38^+$ commitment to the erythroid lineage

In order to determine if the different substrates and media types tested have the capacity to affect the likelihood of $CD34^+CD38^+$ cells expressing CD36 (indicative of commitment towards the erythroid differentiation lineage), flow cytometry was carried out five times, as before, using cells from 5 different donors. Results are given in Figure 6-13.

The results shown in Figure 6-13 suggest that there were no reproducible, statistically significant differences in the percentage of $CD34^+CD38^+$ expressing CD36 as a result of responses to the tested substrates in the different media types tested. However, it was important to observe that in Figure 6-13b and c, when the preconditioned and 50% GF media formulations were used, respectively, the models with co-cultures featuring a stromal layer and HSCs generally had a reduction in the percentage of $CD34^+CD38^+$ cells expressing CD36, relative to HSC only controls. This stressed the benefit of including the stromal layer within the model, as it appeared to suppress progress to erythroid lineage commitment. In turn, this result supported the general opinion in the literature, where evidence exists to suggest that co-cultures of HSCs and stromal layers work effectively to maintain a more primitive phenotype in HSCs (Dexter, 1982, Leisten et al., 2012). In addition, it is important to note that experiments using the 50% GF media generally resulted in a higher expression of CD36 within the $CD34^+CD38^+$ population, particularly when compared to the experiment using 3GF media. This highlighted the importance of carefully considering the media type when designing an HSC niche model.

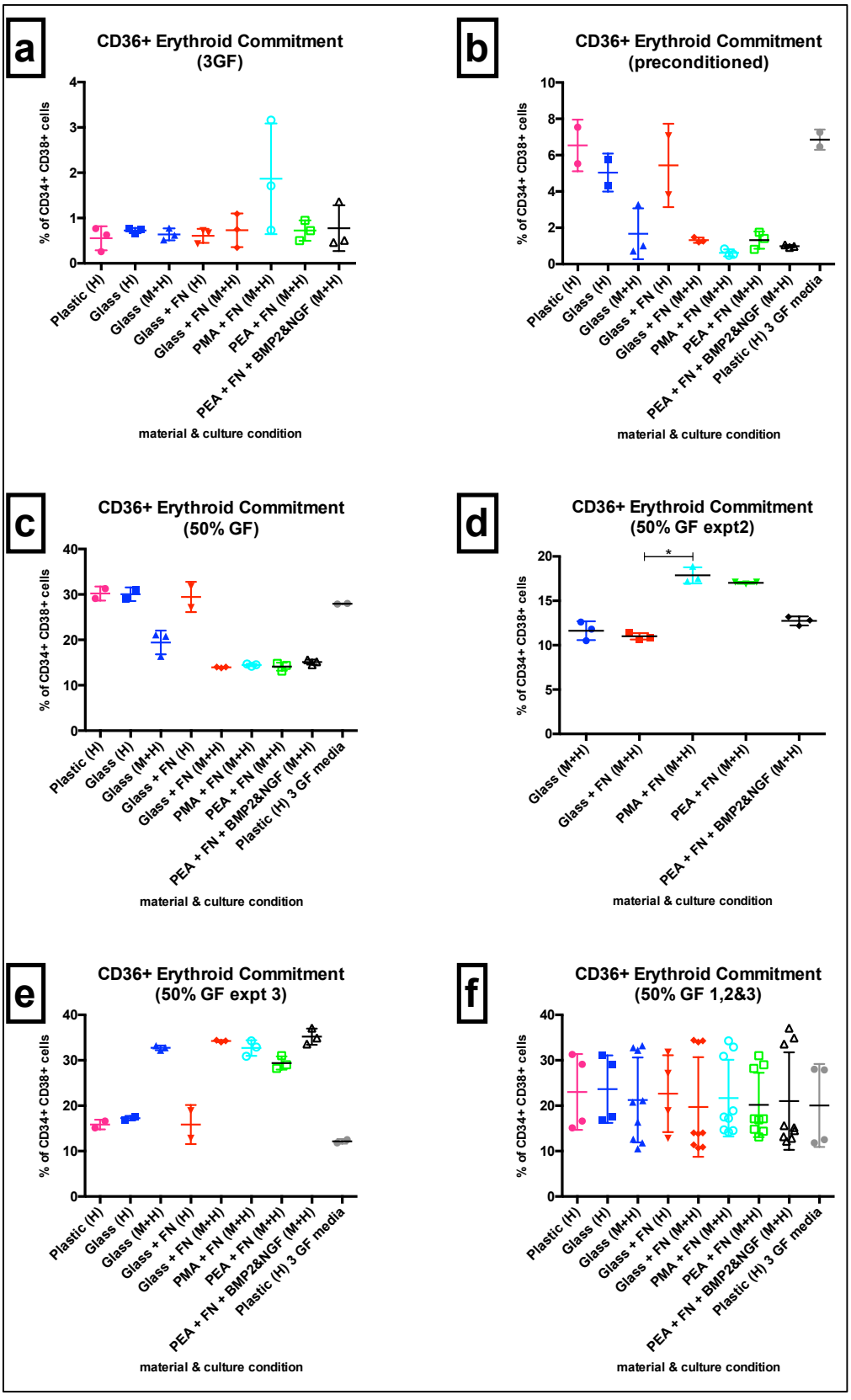

Figure 6-13 CD34+CD38+CD36+ populations in niche models using different substrates and media types

Graphs show the percentage of $CD34^{+}CD38^{+}CD45^{+}$ cells expressing CD36 (associated with erythroid lineage commitment) after cell culture for 5 days in models with different substrates and media types. (H) = HSC only negative control. (M+H) = MSCs + HSCs in a co-culture. a = culture in 3GF media; b = culture in preconditioned medium; c,d & e = culture in 50%GF medium from 3 separate donors; f = results from all media types collated. Graphs show mean +/- SD. Data indicates that HSC niche models have no statistically significant effect on the expression of CD36 within the $CD34^{+}CD38^{+}$ population.

6.4.2.4 $CD34^+CD38^+$ commitment to the myeloid lineage

To assess the capacity of the different substrates and media types tested to affect the likelihood of $CD34^+CD38^+$ cells expressing CD41a (indicative of myeloid lineage commitment), flow cytometry was carried out testing cells from 5 different donors in 5 separate experiments. Results are presented in Figure 6-14.

The results shown in Figure 6-14 indicated that there were no reproducible, statistically significant differences in the percentage of $CD34^+CD38^+$ cells expressing CD41a as a result of responses to the tested substrates in the different media types tested. However, it was intriguing to observe that in Figure 6-14b, c & e, CD41a expression was generally lower in models containing a stromal layer/HSC co-culture on PEA + FN and/or GF substrates, irrespective of media type. Although this chapter shows results indicating that the HSC/stromal layer co-culture helped to reduce expression of lineage commitment markers, this result also suggested that the PEA + FN and/or GF substrates may also suppress differentiation and lineage commitment.

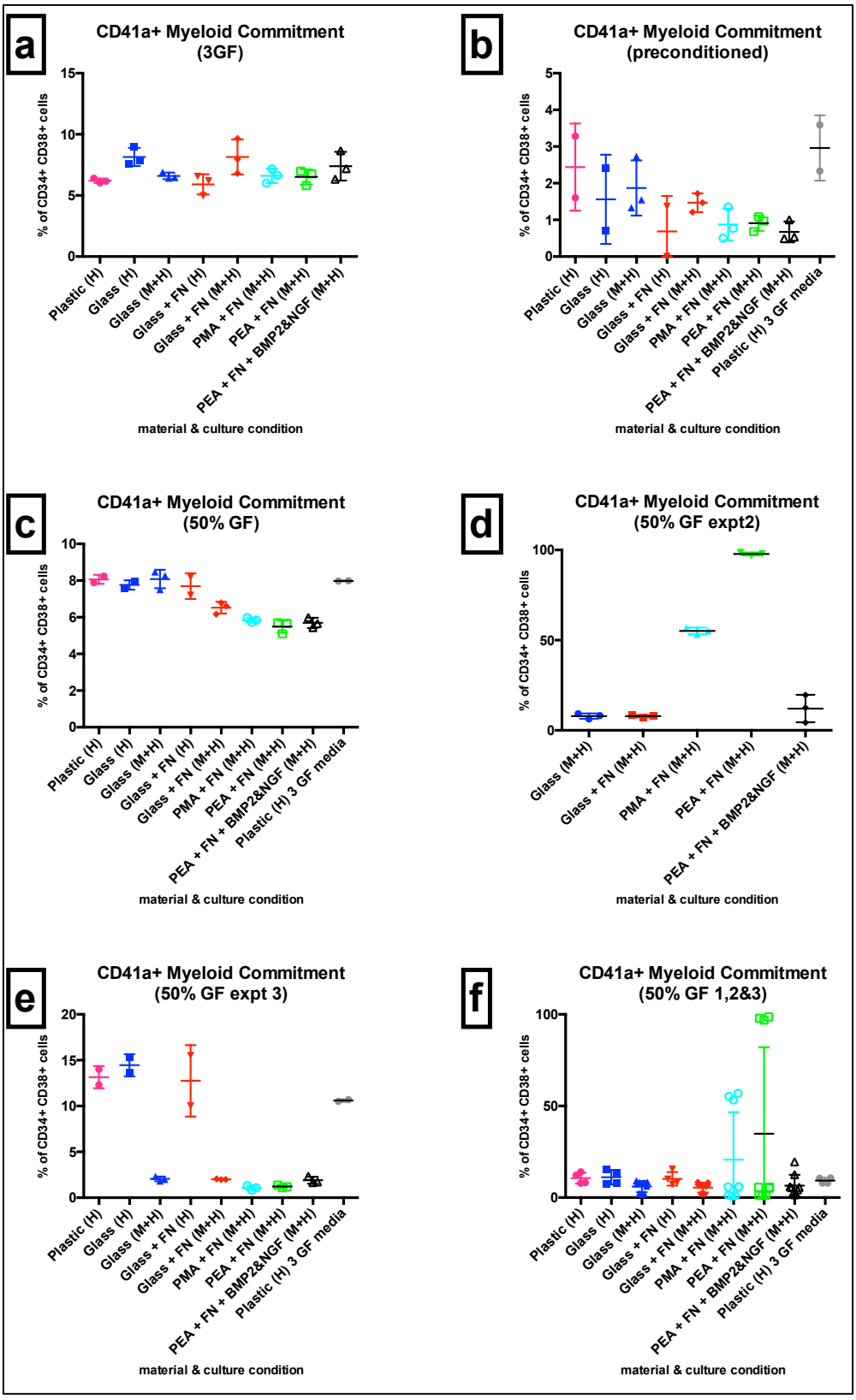

Figure 6-14 CD34+CD38+CD41a+ populations in niche models using different substrates and media types

Graphs show the percentage of $CD34^{+}CD38^{+}CD45^{+}$ cells expressing CD41a (associated with myeloid lineage commitment) after cell culture for 5 days in models with different substrates and media types. (H) = HSC only negative control. (M+H) = MSCs + HSCs in a co-culture. a = culture in 3GF media; b = culture in preconditioned medium; c, d & e = culture in 50%GF medium, from 3 separate donors; f = results from all media types collated. Graphs show mean +/- SD. Data indicates that HSC niche models have no statistically significant effect on the expression of CD41a within the $CD34^{+}CD38^{+}$ population.

6.4.3 $CD34^{-}CD38^{+}$ cells in candidate models

6.4.3.1 Expression of the $CD34^{-}CD38^{+}$ phenotype in candidate models

Flow cytometry analyses were carried out regarding the $CD34^{-}CD38^{+}$ population of cells existing within the models after 5 days of culture. To first determine the effect of the models on the number of cells with the $CD34^{-}CD38^{+}$ phenotype, flow cytometry was carried out, using cells from 5 different donors in 5 different experiments. The results are shown in Figure 6-15.

From the results presented in Figure 6-15, it was deduced that there were no reproducible, statistically significant differences in the percentages of $CD34^{-}$ $CD38^{+}$ cells present in models with different substrates cultured in the different possible media types. This was somewhat encouraging as it suggested that models containing PEA substrates did not influence cells that lie between the important $CD34^{+}CD38^{-}$ population of cells and the differentiated cells associated with the haematopoietic hierarchy (section 1.2.1). This finding implied that the models were either suited to influencing very primitive or highly differentiated cell types, which is of greater economical and clinical value (Krause et al., 1996, Gajkowska et al., 2006, Maruyama et al., 2016).

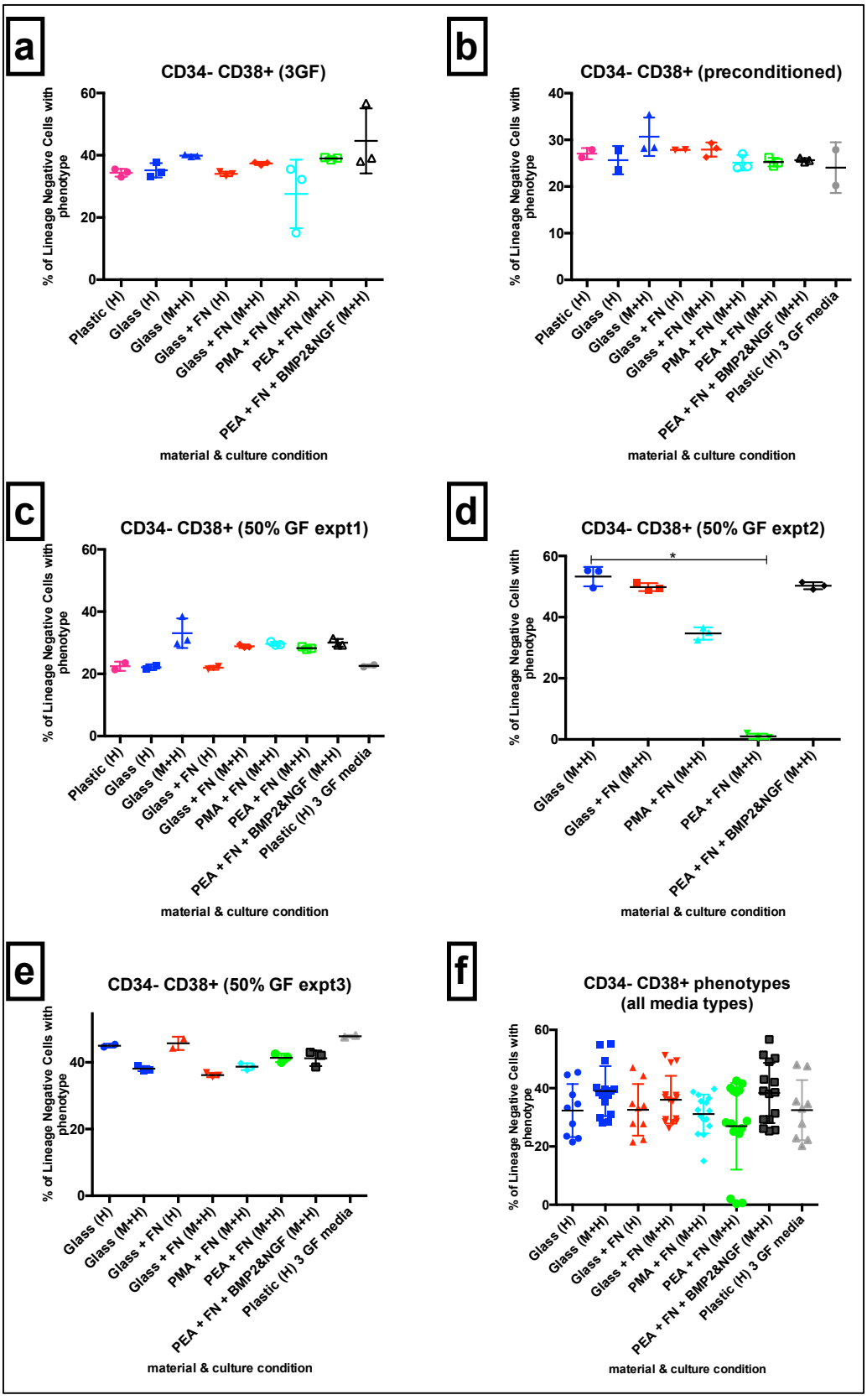

Figure 6-15 CD34-CD38+ populations in niche models using different substrates and media types

Graphs show the percentage of lineage negative cells expressing the $CD34^{-}CD38^{+}$ phenotype after cell culture for 5 days in models with different substrates. (H) = HSC only negative control. (M+H) = MSCs + HSCs in a co-culture. a = culture in 3GF media; b = culture in preconditioned medium; c, d & e = culture in 50%GF medium, from 3 separate donors; f = results from all media types collated. Graphs show mean +/- SD. *=p<0.05 by Kruskal-Wallis. Data indicates that HSC niche models have no statistically significant effect on the expression of the $CD34^{-}CD38^{+}$ phenotype

6.4.3.2 $CD34^{-}CD38^{+}$ commitment to the lymphoid lineage

Despite results shown in Figure 6-15 suggesting that the substrates and media formulations used within the niche models had little effect on the numbers of $CD34^{-}CD38^{+}$ cells present after 5 days of culture, flow cytometry was also used to determine if expression of CD7 within this population was affected by these variables. The results are presented in Figure 6-16.

From the results shown in Figure 6-16, some subtle differences existed within the data presented in graphs a, b, c & e. These subtle differences indicated that models with a stromal layer/HSC co-culture, and either PMA or PEA substrates, acted to reduce differentiation and the progression of cells towards the lymphoid lineage. This difference was not apparent in Figure 6-16d, but it was possible that this unusual result has arisen from variation in the cells from the donor.

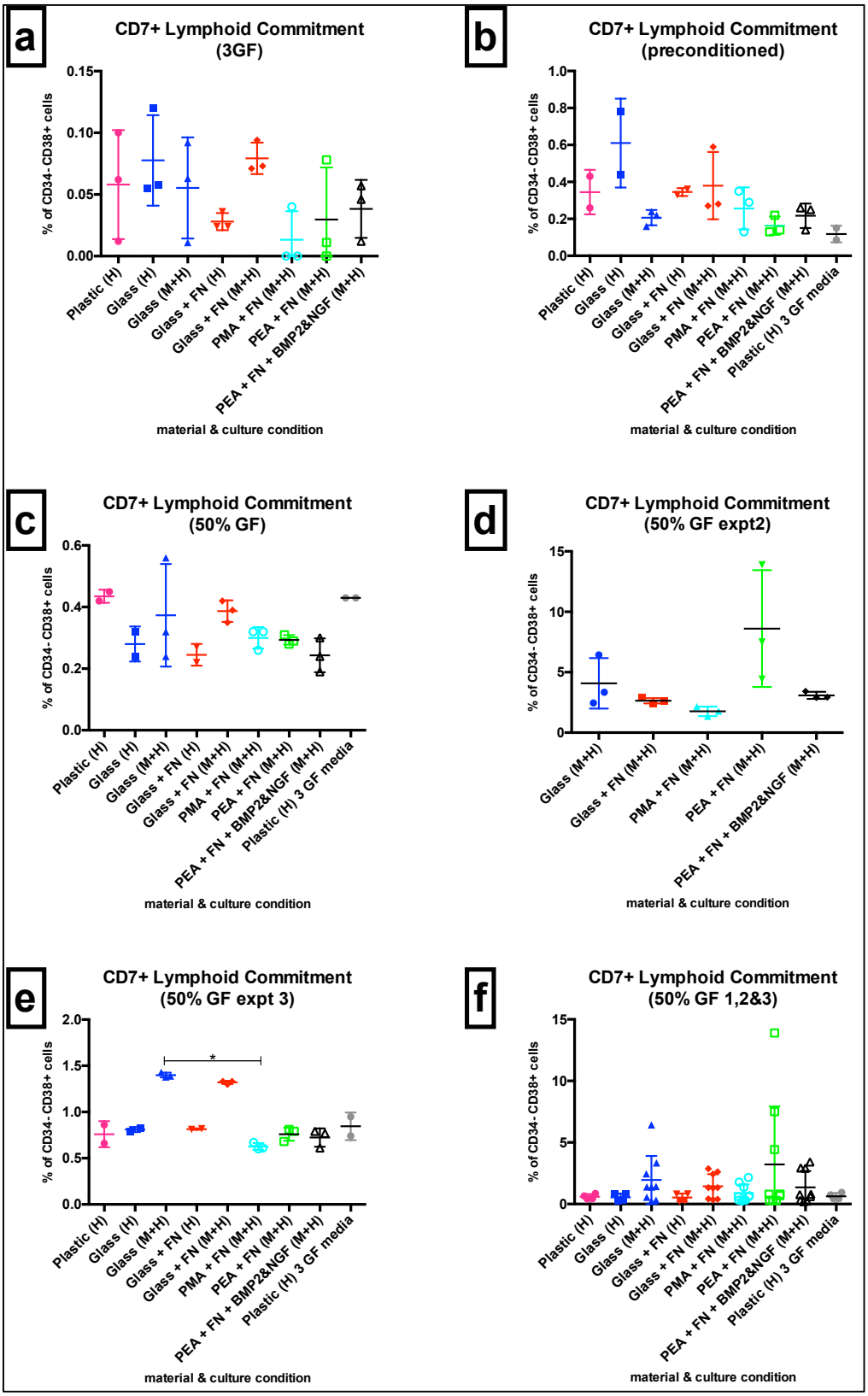

Figure 6-16 CD34-CD38+CD7+ populations in niche models using different substrates and media types

Graphs show the percentage of $CD34^{-}CD38^{+}CD45^{+}$ cells expressing CD7 (associated with lymphoid lineage commitment) after cell culture for 5 days in models with different substrates and media types. (H) = HSC only negative control. (M+H) = MSCs + HSCs in a co-culture. a = culture in 3GF media; b = culture in preconditioned medium; c,d & e = culture in 50%GF medium from 3 separate donors; f = results from all media types collated. Graphs show mean +/- SD. *=p<0.05 by Kruskal-Wallis. Data indicates that HSC niche models have no statistically significant effect on the expression of CD7 within the $CD34^{-}CD38^{+}$ population.

6.4.3.3 $CD34^{-}CD38^{+}$ commitment to the erythroid lineage

To further investigate if progression towards lineage commitment within the $CD34^{-}CD38^{+}$ population is affected by cell culture in the different niche models designed in this work, flow cytometry was carried out to assess expression of CD36 within this population, as CD36 expression is associated with commitment to the erythroid lineage. The results are shown in Figure 6-17.

It was apparent from Figure 6-17 that there were no reproducible, statistically significant differences in the expression of CD36 within the $CD34^{-}CD38^{+}$ population, when HSCs were cultured in models containing different candidate niche model substrates and media of different formulations.

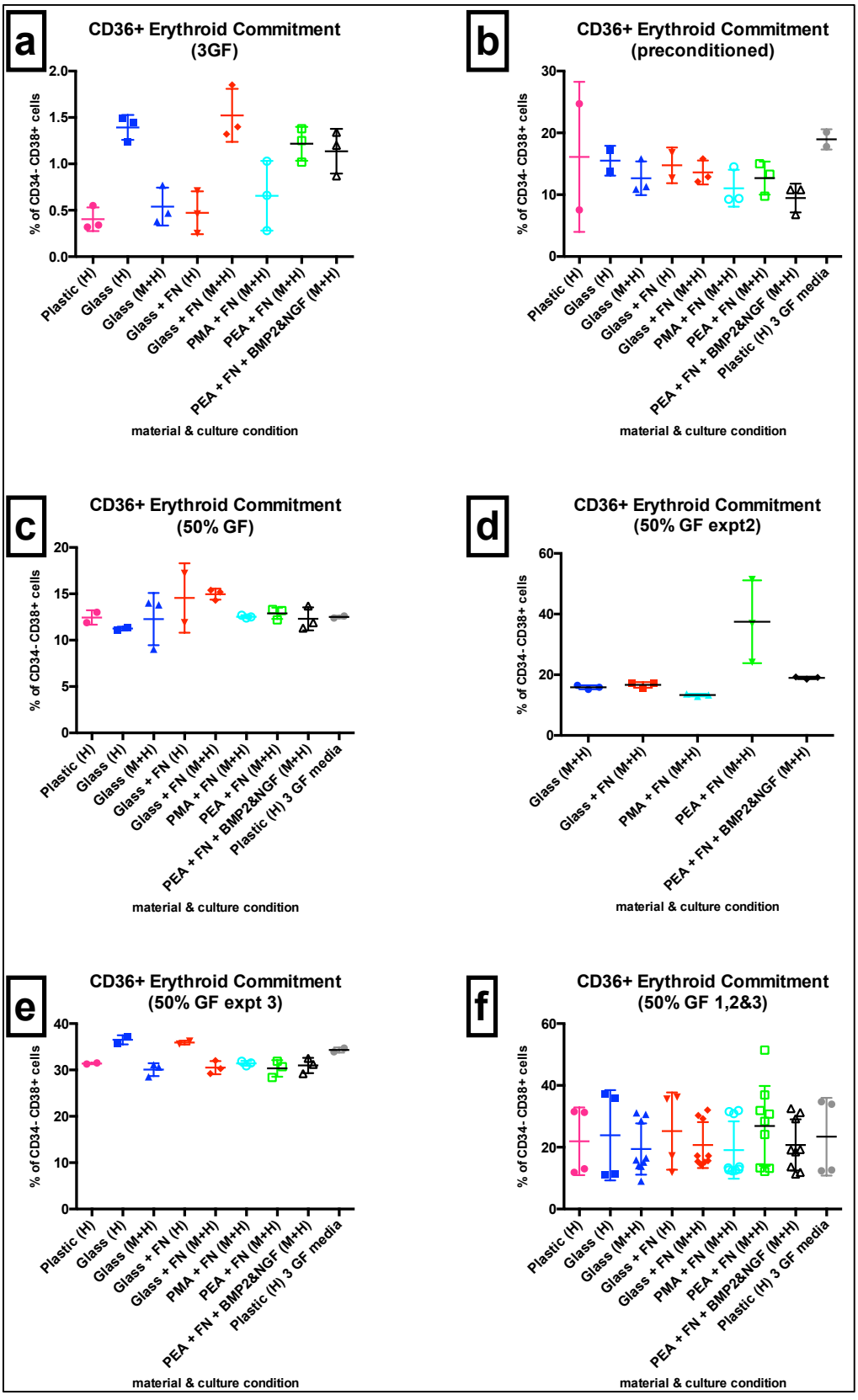

Figure 6-17 CD34-CD38+CD36+ populations in niche models using different substrates and media types

Graphs show the percentage of $CD34^{-}CD38^{+}$ $CD45^{+}$ cells expressing CD36 (associated with erythroid lineage commitment) after cell culture for 5 days in models with different substrates and media types. (H) = HSC only negative control. (M+H) = MSCs + HSCs in a co-culture. a = culture in 3GF media; b = culture in preconditioned medium; c,d & e = culture in 50%GF medium from 3 separate donors; f = results from all media types collated. Graphs show mean +/- SD. Data indicates that HSC niche models have no statistically significant effect on the expression of CD36 within the $CD34^{-}CD38^{+}$ population.

6.4.3.4 $CD34^{-}CD38^{+}$ commitment to the myeloid lineage

To determine if HSC culture within models containing different candidate niche model substrates and media of different formulations affects commitment of cells in the $CD34^{-}CD38^{+}$ population towards the myeloid lineage, flow cytometry was carried out to assess expression of CD41a. The results are presented in Figure 6-18.

The results presented in Figure 6-18 demonstrated that subtle differences apparent, irrespective of the media formulation used. These small differences can be found in Figure 6-18a, b, c & e, and suggested that when PMA or PEA substrates were used with a stromal layer/HSC co-culture, commitment towards the myeloid lineage was reduced, relative to controls.

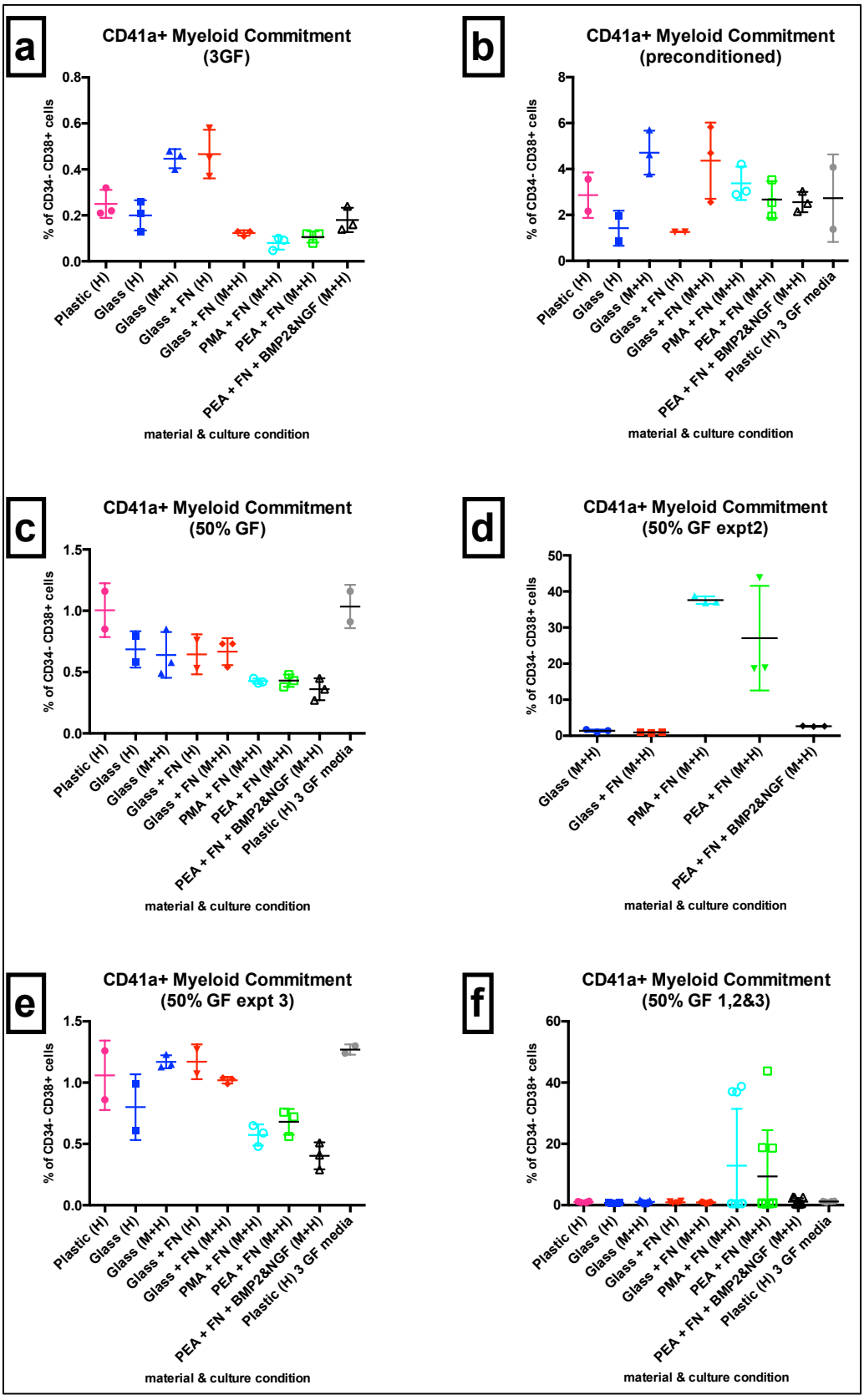

Figure 6-18 CD34-CD38+CD41a+ populations in niche models using different substrates and media types

Graphs show the percentage of $CD34^{-}CD38^{+}CD45^{+}$ cells expressing CD41a (associated with myeloid lineage commitment) after cell culture for 5 days in models with different substrates and media types. (H) = HSC only negative control. (M+H) = MSCs + HSCs in a co-culture. a = culture in 3GF media; b = culture in preconditioned medium; c, d & e = culture in 50%GF medium, from 3 separate donors; f = results from all media types collated. Graphs show mean +/- SD. Data indicates that HSC niche models have no statistically significant effect on the expression of CD41a within the $CD34^{-}CD38^{+}$ population.

6.5 Discussion

6.5.1 $CD34^+CD38^-$ phenotype retention & lineage commitment

The most commonly accepted phenotype for HSCs is the $CD34^+CD38^-$ phenotype (Terstappen et al., 1991, Notta et al., 2010). Thus, the main aim of this chapter was to assess the capacity of HSC niche models containing PEA + FN + BMP-2&NGF substrates, and a co-culture of stromal layer cells with HSCs, to maintain the $CD34^+CD38^-$ phenotype of HSCs after 5 days of culture in such models. The results relating to this principal aim are shown in Figure 6-7. These results confirmed that models using a stromal layer/HSC co-culture were advantageous in maintaining expression of the $CD34^+CD38^-$ phenotype after 5 days of culture. Generally, there were no reproducible, statistically significant differences in the expression of the $CD34^+CD38^-$ phenotype after the culture when cells were in models using the different substrates. However, Figure 6-7c showed that the PEA + FN substrate may have had the capacity to induce an increase in the maintenance of this phenotype, when used in conjunction with the 50% GF media. It should be noted that this experiment was carried out three times using HSCs and stromal layer cells from different donors, and that the results were different each time despite all other variables being kept constant. This highlighted the issues associated with using cells from different donors, and also stressed the need for this work to be repeated several more times before a valid conclusion can be drawn regarding the capacity of the substrates and media formulations tested to influence the $CD34^+CD38^-$ phenotype.

Although the primary aim of this chapter was to investigate the capacity of the models to support the maintenance of the $CD34^+CD38^-$ phenotype after 5 days of culture, cells with this phenotype also have the capacity to express cell surface markers that are indicative of how they will commit to certain differentiation lineages (Reinhold et al., 1993). Consequently, this chapter also aimed to determine if the different models tested were able to affect expression of CD7 (associated with lymphoid commitment), CD36 (associated with erythroid commitment) and CD41a (associated with myeloid commitment) (Reinhold et al., 1993, Lapillonne et al., 2010, De Luca et al., 2009). Figure 6-8 showed flow cytometry results relating to CD7 expression within the $CD34^+CD38^-$ phenotype, and suggested that generally, the PEA + FN + BMP-2&NGF substrate worked best

to reduce differentiation and progression towards the lymphoid lineage. The results relating to erythroid commitment are shown in Figure 6-9, where CD36 expression within the $CD34^+CD38^-$ population was monitored using flow cytometry. The results showed no reproducible, statistically significant differences in expression of CD36 in the $CD34^+CD38^-$ population after culture in the models. However, out of the stromal layer/HSC co-culture models, cells cultured in models with PEA + FN + BMP-2&NGF substrates generally tended to have the lowest expression levels of CD36. This indicated that perhaps HSCs in models featuring this substrate type were more primitive and less committed to differentiation. Finally, Figure 6-10 showed results relating to expression of CD41a and commitment to the myeloid lineage. These results stressed the importance of using a stromal layer/HSC co-culture, by showing that commitment to this differentiation lineage was reduced in co-culture models. In turn, this implied that there is a more primitive phenotype in cells in the co-culture models. It should be noted that Figure 6-10b & d indicated that the PEA + FN + BMP-2&NGF substrates optimally reduced commitment to the myeloid lineage, which also suggested that this substrate type may actively suppress differentiation. However, this result was not reproducible and this observation stressed the need for repetition of this before clear conclusions can be effectively reached.

6.5.2 $CD34^+CD38^+$ phenotype development & lineage commitment

While the $CD34^+CD38^-$ phenotype is the most desirable to maintain within an HSC niche model, the development of models that maintain the $CD34^+CD38^+$ phenotype could also be of good worth, as these cells can still differentiate in accordance with the haematopoietic hierarchy (Table 1-1, Figure 1-3) (Chao et al., 2008). Although the main aim of this thesis was to develop a model that could maximise maintenance of the $CD34^+CD38^-$ phenotype, the differentiation potential of cells with the $CD34^+CD38^+$ phenotype could also be valuable in the development of a different sort of HSC niche-associated model, wherein the focus may be to add HSCs and encourage their differentiation. Thus, flow cytometry was also used to investigate the effect of the models on expression of the $CD34^+CD38^+$ phenotype. Figure 6-11 showed how cell culture within models with different substrates and media types influences expression of the $CD34^+CD38^+$ phenotype. Generally, this figure indicated that there were no

statistically significant and reproducible differences in $CD34^+CD38^+$ expression levels in the different models. In certain cultures (Figure 6-11a, c & e), it was apparent that the PEA + FN + BMP-2&NGF substrate with a co-culture of HSCs and the stromal layer, acted to reduce the expression of the $CD34^+CD38^+$ phenotype relative to controls. While this result was promising in that it indicated that the cells are either more primitive, and higher up in the haematopoietic hierarchy, or that the cells are more differentiated (and so the surface may be useful for a differentiation model), the difference was not always reproducible.

As with the $CD34^+CD38^-$ haematopoietic progenitor phenotype, cells expressing the $CD34^+CD38^+$ phenotype can also commit to several differentiation lineages. Thus, flow cytometry was used to investigate the numbers of $CD34^+CD38^+$ cells expressing CD7, CD36 and CD41a, indicative of their commitment to the lymphoid, erythroid and myeloid lineages, respectively. Figure 6-12 showed flow cytometry results relating to CD7 expression within the $CD34^+CD38^+$ phenotype, and indicated that generally, PMA + FN and PEA + FN substrates were the most effective at minimising CD7 expression in $CD34^+CD38^+$ populations. However, it should be noted this was a slight difference, rather than a statistically significant result. Figure 6-13 showed the results associated with CD36 expression, and indicated that in certain experiments (Figure 6-13b & c), culture of HSCs in models featuring the stromal layer/HSC co-culture helped to minimise CD36 expression, relative to controls. It was apparent that this arose irrespective of the substrate included in the model. Finally, Figure 6-14 displayed results associated with CD41a expression in the $CD34^+CD38^+$ population. These results lack statistical significance. However, small differences were apparent in Figure 6-14a, b, c & e, where models featuring the PEA + FN and PEA + FN + BMP-2&NGF substrates were among those with the lowest expression levels of CD41a in the $CD34^+CD38^+$ population. Collectively, the results of this lineage commitment marker analysis suggested that lineage commitment in the $CD34^+CD38^+$ population was minimised in models containing the PEA + FN or PEA + FN + BMP-2&NGF substrates.

6.5.3 $CD34^{-}CD38^{+}$ phenotype development & lineage commitment

This chapter also assessed the effect of HSC culture in models containing different substrates and media compositions, on inducing expression of the $CD34^{-}CD38^{+}$ phenotype. Figure 6-15 showed that no statistically significant differences in the expression of the $CD34^{-}CD38^{+}$ phenotype were apparent after a 5-day culture of HSCs in the different models. This result indicated that any potential effects of the models on HSC phenotype lay in altering the expression of more primitive cells (such as the $CD34^{+}CD38^{-}$ or $CD34^{+}CD38^{+}$ progenitors) or more differentiated cells, which have already made commitment to differentiation lineages. To determine if such differentiated cells were likely to have arisen from the $CD34^{-}CD38^{+}$ population, flow cytometry experiments assessed expression of CD7, CD36 and CD41a. No reproducible, statistically significant differences were observed relating to the expression of any of these three markers, when cells were cultured in different models, relative to controls. However, results observed in Figure 6-18 indicated that the PMA + FN, PEA + FN and PEA + FN + BMP-2&NGF substrates have some capacity to suppress commitment to the myeloid lineage.

6.5.4 Chapter conclusions

The aim of this chapter was to use flow cytometry to demonstrate the effect that different niche model substrates and media types have on the expression of haematopoietic phenotypes, when $CD34^{+}CD38^{-}$ cells were cultured within models for 5 days. To this end, expression cell surface markers associated with three different progenitor populations, $CD34^{+}CD38^{-}$, $CD34^{+}CD38^{+}$ and $CD34^{-}CD38^{+}$, was determined. In addition, expression of CD7, CD36 and CD41a within each of these populations was determined, as these markers are indicative of progression towards lineage commitment.

Results shown in Chapter 4 suggest that the use of PEA + FN + BMP-2&NGF substrates in HSC niche models may act to: maintain expression of MSC markers; induce expression of early osteogenesis marker, OPN; enhance expression of HSC maintenance factors. Taken together, it was hypothesised that this substrate may act to maintain expression of haematopoietic progenitor phenotypes of HSCs cultured in such models. However, each figure shown in this chapter failed

to show and statistically significant and reproducible results, indicating that while the PEA + FN + BMP-2&NGF substrate may act to induce an HSC niche like phenotype in MSCs, the strength of this model was not sufficient to impact the HSC phenotype, or any other HSC progenitor phenotype, after 5 days of culture. The results also showed that the substrates did not induce statistically significant differences in the expression of lineage commitment markers. However, it should be noted that while differences in results tend to lack statistical significance, there were subtle differences that were apparent within this chapter, and these subtle differences should be considered if future work is carried out using the substrates and media formulations tested in this work. Key highlights from this chapter to note include:

1. In terms of maintaining the $CD34^{+}CD38^{-}$ phenotype, the PEA + FN substrate appeared to be most beneficial when used in conjunction with 50% GF media for the duration of the HSC culture

2. Expression of CD36, associated with commitment to the erythroid lineage, was often lower in $CD34^{+}CD38^{-}$ cells cultured in models featuring PEA + FN + BMP-2&NGF substrates and a stromal layer of cells

3. Expression of CD41a, associated with commitment to the myeloid lineage, was shown to be considerably lower within each of the three tested progenitor population groups when cells were cultured in models featuring fibronectin and a co-culture of HSC and stromal layer of cells.

4. PEA + FN + BMP-2&NGF substrates used in models with a co-culture of HSCs and a stromal layer, acted to reduce the expression of the $CD34^{+}CD38^{+}$ phenotype relative to controls.

Although the points above are important to consider, to improve the quality of results shown in this chapter and test more thoroughly for statistically significant results, the experiments could be improved in a number of ways as outlined in Table 6-3 Methods for improving future HSC work

Table 6-3 Methods for improving future HSC work

Method of Improvement	Reasoning
Increasing n number of models using HSCs from the same donor	The experiments in this chapter only allowed for n=2 in many cases, impacting statistical significance.
Increasing n number of experiments using each media type	Time restrictions only allowed for 5 cell cultures to be carried out in this work. For fairness, n=3 of each media type would be carried out.
Using stromal cells and HSCs from the same two donors to test the effects different media types	Acquiring more cells from the same donor would allow for donor cell variability to be ruled out, as multiple experiments could be carried out using cells from the same donors.
Using stromal cell/HSC combinations from different donors to test the effect of the surfaces with the same media type	Using the stromal cells from one donor while keeping the media formulation constant and changing only the HSC donor would allow for the true effect of HSC donor variability to be assessed. This would also allow for the consistency of the effect of the substrates to be assessed.
Testing additional media types	While this chapter aimed to determine the best media type for HSC culture, a clear conclusion could not be made. Increasing n numbers may help to produce conclusions. However, testing other media types may be of value. This may be carried out by increasing or decreasing the concentration of GFs included in the 3GF media. Additional GFs may also be tested (such as IL-3 an IL-6).
Testing different HSC culture time points	The results presented within this chapter relate only to HSC culture for 5 days. It is possible that the models may elicit their effects before or after this culture period, and thus lesser and longer periods of culture should be assessed.
Testing additional differentiation markers	While, CD7, CD36 and CD41a were interesting to study. Analysis of additional markers such as CD3 representing T cells may be of interest (Smith et al., 1989).

It is important to note that HSCs were difficult to revive, or to obtain from donors at the precise 15-day time point involved with this model. In addition, the cost of commercial HSCs was very high. This resulted in only experiments using low n numbers being feasible, which directly impacted on the statistics. In order to make this work more economically viable and statistically reliable, further work should seek to investigate the effect of using MSCs seeded onto candidate substrates more closely to the time of HSC addition. Having a less precise or closer time point for the addition of the HSCs would make retrieving cells from bone marrow donors more achievable, eliminating the need for expensive commercial HSCs, in turn making models more economically viable.

CHAPTER 7

Chapter 7 Discussion

7.1 General Discussion

HSCs are highly valued stem cells, in terms of their rarity and ability to be used for a diverse range of clinical applications (Bensinger et al., 2001). However, their fast rate of differentiation means that maintaining and expanding populations of HSCs in the lab is challenging (Dexter, 1982). To overcome this, a considerable portion of the scientific community is committed to designing biomimetic HSC niche models that will allow for the *in vitro* culture and expansion of HSCs in the lab (Huang et al., 2016, Wuchter et al., 2016). It is recognised that HSCs are maintained as stem cells as a result of regulatory signals sent from various other cell types in the *in vivo* bone marrow niche (Ding et al., 2012, Calvi et al., 2003). To this end, a reasonable approach to designing effective, novel HSC niche models is one where the presence and function of more than one support cell type Is present.

Taking into account the already well-documented role of MSCs in HSC niche models, this thesis aimed to design and develop an *in vitro* HSC niche model comprising MSCs and also OBs, with an appropriate media formulation that could support the maintenance of HSCs. With this aim, PEA + FN substrates were used as a foundation for the model, as it has been shown that these substrates can induce a degree of osteogenesis when BMP-2 is tethered to the FN, while also supporting maintenance of an MSC population (Llopis-Hernández et al., 2016, Rico et al., 2016a).

ELISA results showed that it is possible to bind BMP-2 and NGF to PEA + FN substrates at the same time. This co-adsorption of GFs produced a novel biomaterial, which comprised the foundation of the HSC niche model developed in this work. To make the physical properties of this *in vivo* model more biomimetic of the human BM niche, a collagen type I gel was used, and was shown to have a Young's modulus comparable to that existing in nature (Sobotková et al., 1988, Metzger et al., 2014). Finally various media compositions were tested to suit the specific needs of the MSC/stromal layer of cells that were cultured on the PEA + FN + GF substrates, as well as the HSCs.

7.1.1 Utilising PEA substrates and collagen gels in HSC niche models

The ability of FN to undergo a phenomenon known as fibrillogenesis in response to PEA surfaces, forming a network of FN fibrils, has been well studied (Rico et al., 2009, Rico et al., 2016b). However, to verify this, AFM was carried out to allow for the visualisation of FN networks on PEA surfaces. The result obtained showed that FN fibrils appear on PEA surfaces, but not on control surfaces. Additional work had shown that BMP-2 can be bound to PEA + FN (Llopis-Hernández et al., 2016). However, there was a lack of studies relating to the binding of other GFs. In order to determine if more than one GF could be tethered to PEA + FN substrates, ELISAs were carried out, and showed that both BMP-2 and NGF could be bound to PEA + FN substrates, when adsorbed together or independently. Rheology experiments provided evidence to suggest that collagen type I gels produced in house had a similar Young's modulus to the liquid phase of the bone marrow. Taken together, these results indicated that PEA + FN + GF substrates and collagen gels were promising foundations for the development of a controlled, *in vitro* HSC niche model, wherein GFs may regulate and control the phenotype of cells while the collagen gel could act to mimic the physical properties of the natural niche.

7.1.2 Characterising MSC phenotype in models comprising PEA substrates and growth factors

In order to characterise the effect of culturing STRO-1$^+$ MSCs on PEA + FN + GF substrates for 21 days, ICW was carried out to determine the effect of the substrates on the phenotype of MSCs. ICW assessed the effect of the substrates on expression of: MSC markers (ALCAM, nestin and STRO-1); osteogenesis markers (OCN and OPN); HSC maintenance factors (SCF and VCAM-1). However, the composition of the cell culture media was changed in addition to the substrates the cells were cultured on. Initial tests used standard lab DMEM supplemented with 10% FBS to determine if the substrates induced any phenotypic effects. While no statistically significant differences in the expression of MSC or osteogenesis markers between cells cultured on PEA + FN + GF substrates compared to controls were observed, it was observed that SCF expression was significantly higher in cells cultured on PEA + FN + NGF and PEA +

FN + BMP-2 substrates, relative to controls. In particular, it was intriguing to note that SCF expression was significantly higher on PEA + FN + BMP-2&NGF substrates, compared to substrates where BMP-2 was adsorbed alone. This promising result suggested that PEA + FN + GF substrates had the capacity to enhance expression of HSC maintenance factors in MSCs. However, the results did not correlate well with results published that suggested that PEA + FN + BMP-2 substrates enhance osteogenesis marker expression in MSCs. Thus, further experiments were carried out with a reduced concentration of serum in the media, to determine if the effects of the substrates may be potentiated. After testing the effects of media supplemented with 2% FBS, advice from collaborators suggested that supplementing with 2% HS would be more effective and reliable, and also suggested that switching to a serum-free media for the duration of the prospective HSC culture period would be appropriate. Thus, additional media formulations were tested, and results suggested that PEA + FN + NGF and PEA + FN + BMP-2&NGF substrates and the use of DMEM supplemented with 2% HS for days 1-14 of the cell culture, and then serum-free media supplemented with 3GFs (3GF media) for days 15-21, resulted in statistically significant increases in OPN and SCF expression in MSCs, relative to controls. In addition, use of these substrates maintained expression of MSC markers, relative to controls, which suggested that use of these substrates in models featuring the aforementioned media formulation, actively supports an HSC niche phenotype in MSCs.

The ability of the PEA + FN + BMP-2&NGF substrates to enhance osteogenesis but not alter the expression of MSC markers in STRO-1^+ cells was intriguing, as it would be expected that the enhanced osteogenesis would reduce the proportion of MSCs present in models featuring this substrate type. In order to validate ICW results, a T cell suppression assay was carried out. It was observed that MSCs cultured in models with PEA + FN + BMP-2&NGF substrates were the most effective at suppressing T cell proliferation, and thus these cells appeared to have the strongest evidence of classically-acting MSCs on them; the PEA + FN + BMP-2&NGF substrate did not affect the maintenance of MSC populations within HSC niche models.

Although ICW results indicated that SCF expression could be maximised in cells cultured on PEA + FN + GF substrates, these results only reflected upon cell surface proteins. In order to test the effect of MSC culture on these substrates on the expression of soluble HSC maintenance factors, ELISAs were carried out to test the concentration of CXCL-12 and THPO found in the media supernatant at three time points throughout the 21-day cell culture. In the 2% HS media followed by 3GF media, mean CXCL-12 secretion was highest in cells cultured on PEA + FN + BMP-2 substrates at the start and middle of the culture. Yet, PEA + FN + NGF and PEA + FN + BMP-2&NGF substrates induced highest CXCL-12 secretion at day 21. THPO ELISA results suggested that PEA + FN + GF substrates also induced optimal secretion of THPO. Collectively, the ELISA results also showed evidence to support the use of PEA + FN + GF substrates in HSC niche models.

The results presented in this thesis indicated that the PEA + FN + BMP-2&NGF substrate optimally induced expression of proteins associated with the HSC niche phenotype in MSCs. This result can be thus generalised as:

- Expression of MSC markers ALCAM, nestin and STRO-1 were maintained at similar levels on PEA + FN + BMP-2&NGF substrates and on controls.

- Expression of early osteogenesis marker, OPN, was highest on PEA + FN + BMP-2 and PEA + FN + BMP-2&NGF substrates.

- Expression of HSC maintenance factors were higher on PEA + FN + BMP-2&NGF substrates.

7.1.3 Metabolomic changes in MSCs cultured in HSC niche models

Collectively, the results presented in Chapter 4 support findings presented by Llopis-Hernandez et al., whereby the BMP-2 bound to PEA + FN substrates was capable of inducing a degree of osteogenic differentiation in MSCs (Llopis-Hernández et al., 2016). However, the differences observed using ICW did not always show reproducible statistically significant differences in the expression of osteogenesis markers, OCN and OPN, between cells cultured in models featuring

the PEA + FN + BMP-2&NGF substrate, and those in models with just PEA + FN substrates. To further investigate the effect of culturing MSCs within models comprising these substrates, metabolomics was carried out. It was hypothesised that the metabolomic profiles of MSCs cultured on PEA + FN + BMP-2&NGF substrates may be distinct to those of MSCs cultured on PEA + FN substrates, as the osteogenesis occurring would be likely to affect key metabolites associated with amino acid, carbohydrate and lipid metabolism (Tjabringa et al., 2008, Chung et al., 2007, Alakpa et al., 2016). Analysis of the aforementioned metabolomic profiles suggested that the hypothesis was true, and heatmap analyses illustrated that cells cultured in models featuring the PEA + FN + BMP-2&NGF substrate type generally had fewer metabolites than controls. The results of these metabolomic analyses indicated that:

- Amino acid metabolism was heightened in MSCs cultured on PEA + FN + BMP-2&NGF substrates, and this is likely to have arisen due to the enhanced levels of protein synthesis that accompany differentiation (Tjabringa et al., 2008).

- Carbohydrate metabolism was heightened in MSCs cultured on PEA + FN + BMP-2&NGF substrates, and is likely to be indicative of heightened respiration, associated with enhanced metabolic activity and differentiation (Chung et al., 2007).

- Lipid metabolism was also enhanced when MSCs are cultured on PEA + FN + BMP-2&NGF substrates, which may also be indicative of osteogenesis (Alakpa et al., 2016).

In addition to the heat map analyses, PCA plots were used to show metabolite variation within cells cultured on each substrate type, and it was apparent that the ellipses representing metabolite variation in cells cultured on PEA + FN substrates had minimal regions of overlap with cells cultured on PEA + FN + BMP-2&NGF substrates, suggesting that the metabolomic profiles of cells cultured on these substrates were distinct.

7.1.4 Responses of HSCs to HSC niche models

Although the true phenotype of HSCs is disputed in the literature, the general opinion in the field is that cells with the $CD34^+CD38^-$ phenotype are regarded as HSCs (Hao et al., 1995, da Silva et al., 2010). However, it is acknowledged that other haematopoietic progenitors exist, such as those expressing $CD34^+CD38^+$ and the $CD34^-CD38^+$ phenotypes. $CD34^+CD38^+$ cells may represent multipotent or oligopotent progenitors, such as common myeloid progenitors or common lymphoid progenitors, still capable of forming all cells of the haematopoietic system (Chao et al., 2008). However, evidence does exist showing that potential oligopotent progenitors can be distinguished from their multipotent parental cells; oligopotent progenitors do not generate colony-forming unit-cells (CFU-C) for as long as $CD34^+CD38^-$ cells *in vitro* (Hao et al., 1995). In addition, $CD34^+CD38^+$ cells have been reported to be capable of *in vivo* repopulation of murine haematopoietic cells for 12 weeks, while multipotent $CD34^+CD38^-$ populations can repopulate for at least 20 weeks (Hogan et al., 2002). While $CD34^-CD38^+$ cells are the most differentiated of the three aforementioned progenitor types, evidence also exists in the literature, which shows that these cells have extensive lymphoid and myeloid repopulating abilities (Wang et al., 2003). Taking the aforementioned points into consideration, it is evident that there is not yet a clear-cut phenotypic definition of an HSC, and so it may be of value to consider each of these putative progenitor phenotypes when developing an HSC niche model.

To this end, the principal aim of Chapter 6 of this thesis was to test the models designed earlier in the thesis, in a bid to determine if models comprising the PEA + FN + BMP-2&NGF substrates could maintain/expand each of the progenitor types more effectively than models containing control substrates. Further, an additional aim of this work was to determine if models featuring PEA + FN + BMP-2&NGF substrate encouraged or restricted expression of markers associated with differentiation down the lymphoid, erythroid and myeloid lineages, within each progenitor population. These experiments were carried out on five separate occasions, using HSCs and MSCs from different donors each time. In three of these cases, the same media type was used (50% GF media), on one occasion 3GF media was used, and on one occasion, preconditioned media was used. The reasoning for this was that the 50% GF media gave far better retention

of the $CD34^{+}CD38^{-}$ phenotype in PEA + FN + BMP-2&NGF models relative to controls in the first trial, and so the work was repeated twice more to test the reproducibility of the results associated with using 50% GF media in the model.

The results showed that no reproducible, statistically significant differences in the expression of $CD34^{+}CD38^{-}$, $CD34^{+}CD38^{+}$ or $CD34^{-}CD38^{+}$ phenotypes were observed between cells cultured in models containing the PEA + FN + BMP-2&NGF substrates compared to controls. However, it was interesting to observe that on two of the three occasions where the 50% GF media was used, models featuring PEA + FN substrates contained the highest expression of $CD34^{+}CD38^{-}$ cells. Although the results presented in Chapter 4 suggested that the PEA + FN + BMP-2&NGF substrate may be most effective in supporting the $CD34^{+}CD38^{-}$ phenotype, it was encouraging to note this subtle difference whereby PEA + FN substrates were most effective. Although time restrictions limited further investigation into why this may be the case, it is known that adherent cells, such as those of the stromal layer, secrete FN during their culture (Den Braber et al., 1998, Midwood et al., 2004). It is therefore possible that the stromal layer of cells on the PEA + FN substrates secreted FN, which responded to the PEA and FN fibrils already present on the substrates, producing new fibrils. It is likely that the new FN also adopted a network conformation, allowing room for binding of additional GFs in the media or secreted by the cells (Llopis-Hernández et al., 2016). In order to test the likelihood of this, it would be interesting quantify the amount of FN present on the surfaces before and after the 19-day cell culture using ELISAs (Ohh et al., 1998). Assuming more FN was present, it would then also be beneficial to attempt test the conformation of the new FN. This could be attempted using AFM or FRET (Baneyx et al., 2001). Although the results lack reproducibility, the ability of the PEA + FN surface to generate an increase in the number of cells with the $CD34^{+}CD38^{-}$ phenotype is interesting and does suggest that there may be potential for the use of this substrate in an HSC niche model geared towards expanding populations of HSCs.

Considering the results associated with the expression of lineage commitment markers within each of the three progenitor populations, it was apparent that expression of: CD7 (associated with lymphoid commitment), CD36 (associated with erythroid commitment) and CD41a (associated with myeloid commitment)

were not statistically higher or lower in models containing PEA + FN and/or GFs, relative to controls. However, it should be acknowledged that some subtle differences existed, and that these provided some insight into how the model currently works, and how it may be improved. For example, key points to consider include:

- Within the $CD34^{+}CD38^{-}$ population, PEA + FN/PEA + FN + BMP-2&NGF substrate models did not contain a greater or lesser proportion of cells expressing CD7, CD36 or CD41a compared to controls where MSCs and HSCs are co-cultured. This suggested the MSCs were eliciting a controlling response and that the PEA substrates are not influencing HSC differentiation. This stressed the benefits of including a stromal layer of MSCs in models and the lack of effect on differentiation is encouraging in terms of developing a primitive HSC model.

- In all 3 progenitor types, expression of CD41a in haematopoietic cells cultured in PEA + FN + BMP-2&NGF models was often lower than it is in controls, irrespective of media type, even when MSCs also featured in the models. This implied that the PEA + FN + BMP-2&NGF substrate induced the stromal layer to respond in a way that limited HSC commitment to the myeloid lineage, without enhancing/driving commitment down the erythroid or lymphoid lineages.

- The use of MSCs and HSCs from different donors in different experiments affected results, and in order to obtain a more reliable set of results, future work should envisage to use cells from the same donors when testing additional variables such as the effect or substrates or media compositions.

7.2 Thesis Conclusion

The research presented in this thesis described the stages taken in the design, characterisation and testing of an *in vitro* HSC niche model using PEA surfaces. It has been shown that PEA surfaces can have a layer of FN adsorbed on them, which induced the formation of FN networks on PEA + FN substrates. It has also

been shown that these substrates can have GFs such as BMP-2 and NGF bound to them, following adsorption of the GFs either independently or together.

The development of this *in vitro* HSC niche model also considered the importance of a 3D system, and so the use of a collagen type I gel was tested. Results identified the collagen type I gels as having a similar Young's modulus as the HSC-occupied region of the human bone marrow. Consequently, this gel was also used within the model, albeit only for the time before the HSCs were added, in a bid to minimise complexity of this preliminary work.

Following the design and development of the models material components, this thesis then sought to characterise the response of a stromal layer of cells, comprising STRO-1^+ cells seeded at day 1, to the different PEA + FN based substrates after 21 days. The results of this characterisation work led to the PEA + FN + BMP-2&NGF substrate being deemed the most likely to induce an HSC niche phenotype in MSCs; results showed it was able to maintain expression of MSC markers, enhance expression of early osteogenesis markers and also enhance expression of HSC maintenance factors. Work carried out in the later parts of this thesis assessed the effects of only these GFs bound to PEA, and not the other GFs such as VEGF and PDGF, which were also tested in the stromal layer characterisation work.

The apparent advantages of using PEA + FN + BMP-2&NGF substrates in HSC niche model development led to the use of metabolomics, in a bid to understand what was occurring metabolically in STRO-1^+ cells as they responded to this substrate type. The results of the metabolomics analyses correlated well with the results from the ICW work, and also suggested that the MSCs cultured in models featuring PEA + FN + BMP-2&NGF substrates are most metabolically active (indicative of differentiation), in terms of amino acid, carbohydrate and lipid metabolism.

The final section of this thesis focused on testing the ability of models featuring the PEA + FN + BMP-2&NGF substrate to maintain phenotypes associated with HSCs and haematopoietic progenitors. Although the results did not show any reproducible, statistically significant differences in the maintenance of such phenotypes, slight differences were evident that stressed the benefit of using

the stromal layer within the model, and also that suggested PEA surfaces may be useful for enhancing HSC expansion, depending on the donor cells used. Finally, the results also showed differences, which indicated that PEA + FN + BMP-2&NGF substrates reduced expression of CD41a, indicative of commitment to the myeloid lineage.

In summary, this thesis demonstrated that it is possible to use PEA + FN substrates as a platform for constructing HSC niche models featuring substrate-bound GFs. In addition, it showed that the resulting PEA + FN + GF substrates can be used to maximise the expression of an HSC niche-supportive phenotype in MSCs. However, it also showed that donor cell variability is an issue of paramount importance, and that while the models induce an HSC-supportive MSC phenotype, the expression of the proteins associated with that phenotype is not always sufficient to overcome donor cell variability issues; in certain cases the models were able to expand HSC populations, but not always.

7.3 Overview relating this thesis to related studies

The results presented in this thesis correlated, to an extent, with other findings and results published in the field. For example, various models have been created wherein a combination of topographical features, ECM proteins and GFs exist with the capability of modulating MSC phenotype (Dalby et al., 2007, Salmeron-Sanchez et al., 2011, Fourel et al., 2016, Llopis-Hernández et al., 2016). Concurrent with these publications, the PEA + FN + BMP-2 +/- NGF also acted to stimulate a degree of osteogenic differentiation in STRO-1^+ MSCs (Chapters 3 & 4). The same PEA + FN + BMP-2&NGF substrates were also able to induce cells to express a distinct metabolomic profile, relative to PEA + FN controls, providing further evidence to suggest the induction of an osteogenic phenotype as a result of the substrate (Chapter 5) (Alakpa et al., 2016). Finally, a wealth of data also exists to show that the presence of a stromal layer of MSCs and/or OBs acts to maximise HSC maintenance and minimise HSC differentiation (chapter 6) (Dexter, 1982, Moore et al., 1997, Weisel et al., 2006).

However, it should be noted that the results presented in chapter 6 indicate that the substrates are not able to promote the same degree of HSC phenotype

maintenance as similar models (Leisten et al., 2012, Wuchter et al., 2016). Thus, considering means of improving the model is important.

7.4 Recommendations for Future Model Development

The research carried out during the development of this novel *in vitro* HSC niche model has identified the potential of PEA + FN substrates in a new area of bioengineering. However, further development of this model, or use of these substrates in a similar way, will require further study. Suggestions of what this further study may involve are outlined below:

- Investigation into the possibility of adsorbing more GFs to PEA + FN substrates at one time. Time limitations only allowed for the testing of a limited number of combinations, and it should be stressed that the results relating to the phenotypic effect of culturing MSCs on PEA + FN substrates with 4 growth factors adsorbed were different to those obtained when 2 growth factors were used at once. Further research into the different combinations of GFs would be of value to making the models more biomimetic.

- Investigation of the possibility of adsorbing the GFs that are currently supplied to HSCs in the 3GF media formulation on to PEA + FN substrates. This may elicit sustained signalling and reduce the costs of model testing (Fan et al., 2007).

- Use of MSCs from the same donor and at the same passage, to test the effect of different substrates and media types. Donor cell variability will have inevitably skewed some of the data presented in this thesis, and the only way of truly determining the optimal media for maximising a niche-like phenotype in MSCs would be to use cells from the same donor, at the same passage.

- Full characterisation of the response of MSCs cultured in DMEM supplemented with 2% HS for 14 days and then 50% GF for 5 days. (ICW, ELISA, MTT).

- Use of HSCs from the same donor in multiple experiments carried out at the same time, testing the effects of different media compositions. The work presented in this thesis allowed for only a few different media formulations to be used, but titrating the growth factors featured in the 3GF media to determine an optimal concentration for HSC culture would be highly advantageous to the progression of this work.

- Testing of the ability to add, and effectively retrieve, HSCs from the models when the collagen gel remained for the duration of the cell culture. The effect of the collagen gel should also be compared to controls where the collagen gel is absent.

- Testing different lengths of HSC culture period

- Testing the HSCs retrieved from culture within the models in colony-forming cell assays (Sarma et al., 2010).

- The addition of different cell types to the model. A wealth of evidence exists to support a role of CAR cells and sympathetic nerve cells in the HSC niche (Kunisaki et al., 2013a, Katayama et al., 2006). Thus, assessing the potential of PEA + FN substrates to enhance the HSC supportive phenotype of these cells would be of great interest. It should be noted that these cells may be integrated into the model independently or more than one could be cultured in a stromal layer on the PEA + FN substrates.

- Greater investigation into the differentiation potential of HSC cultures developed in the improved models; it could be the case that models developed in the aforementioned ways may alter the differentiation capacities of the haematopoietic cells included in them. While the main aim of this thesis was to expand HSCs in culture, it could be advantageous to develop models in which differentiation of HSCs to form particular specialised haematopoietic cells is maximised.

7.5 Future Potential of HSC Niche Models & Clinical Relevance

While it is apparent that there are limitations to the model described in this thesis, evidence is presented that highlights the potential of the use of PEA + FN + GF substrates for stimulating the expression of an HSC niche like phenotype in MSCs. Thus, it is plausible that the work of this thesis may facilitate future HSC niche model development that can be used to benefit the scientific and medical communities in the ways outlined below.

Using HSC niche models to expand populations of HSCs would be of tremendous clinical value; HSCs are required in vast quantities for HSC transplants, and allogeneic transplants are often depended upon for the treatment of diseases including leukaemia and thalassaemia. However, less than 30% of patients are able to find a suitable donor (Copelan, 2006). Developing means of isolating and harvesting healthy HSCs from patients and then expanding their HSCs in the lab would overcome this problem, and would allow a greater percentage of patients to receive treatment. In addition, this would reduce the time spent finding an appropriate donor and the financial strain on the healthcare services, as only one patient would require medical attention and there would be fewer associated travel costs. In addition to the aforementioned diseases, HSC expansion using an *in vitro* HSC niche model and autologous transplantation could also be used to improve chemotherapy treatments by replenishing the healthy immune cells in an effective way, following the immune system damage that is a side-effect of most chemotherapy programmes (Schmitz et al., 2002, Slavin et al., 1998).

Aside from using *in vitro* HSC niche model expansion of HSCs to facilitate medical treatments, the use of models in this way could also be used to model disease *in vitro*, allowing for a greater understanding of how diseased cells function, and also how effective a range of drugs are. Such drugs may be tested for how damaging they are to healthy HSCs, or equally models could be used to expand populations of leukaemic HSCs, meaning leukaemia drugs could be tested effectively. This would be a particularly useful as many current drug testing platforms associated with HSCs run using murine HSCs. While this has been a

useful means of drug testing to date, interspecies variation is undeniable, and results from human HSC studies would be more reliable (Goyama et al., 2015).

Another critical way in which an *in vitro* HSC niche model could be of value, would be in elucidating the mechanisms of haematopoiesis. Although knowledge of haematopoiesis is increasing, there are many unanswered questions relating to what signals cause key aspects of HSC function, such as self-renewal, proliferation and apoptosis. Unfortunately the current limitation to understanding these mechanisms is harvesting sufficient numbers of HSCs and also retaining them in their stem cell state as research proceeds (Rodriguez-Fraticelli et al., 2018). Developing an *in vitro* HSC niche model could overcome these problems, and could help in the understanding of HSC biology.

List of References

ACAR, M., KOCHERLAKOTA, K. S., MURPHY, M. M., PEYER, J. G., OGURO, H., JAIYEOLA, C., ZHAO, Z., LUBY-PHELPS, K. & MORRISON, S. J. 2015. Deep imaging of bone marrow shows non-dividing stem cells are mainly perisinusoidal. *Nature,* 526**,** 126.

AGGARWAL, S. & PITTENGER, M. F. 2005. Human mesenchymal stem cells modulate allogeneic immune cell responses. *Blood,* 105**,** 1815-1822.

AKASHI, K., TRAVER, D., MIYAMOTO, T. & WEISSMAN, I. L. 2000. A clonogenic common myeloid progenitor that gives rise to all myeloid lineages. *Nature,* 404**,** 193.

ALAKPA, E. V., JAYAWARNA, V., LAMPEL, A., BURGESS, K. V., WEST, C. C., BAKKER, S. C., ROY, S., JAVID, N., FLEMING, S. & LAMPROU, D. A. 2016. Tunable Supramolecular Hydrogels for Selection of Lineage-Guiding Metabolites in Stem Cell Cultures. *Chem,* 1**,** 298-319.

ANSELME, K. 2000. Osteoblast adhesion on biomaterials. *Biomaterials,* 21**,** 667-681.

ARAI, F., HIRAO, A., OHMURA, M., SATO, H., MATSUOKA, S., TAKUBO, K., ITO, K., KOH, G. Y. & SUDA, T. 2004. Tie2/Angiopoietin-1 Signaling Regulates Hematopoietic Stem Cell Quiescence in the Bone Marrow Niche. *Cell,* 118**,** 149-161.

ASHIKARI-HADA, S., HABUCHI, H., KARIYA, Y., ITOH, N., REDDI, A. H. & KIMATA, K. 2004. Characterization of growth factor-binding structures in heparin/heparan sulfate using an octasaccharide library. *Journal of Biological Chemistry,* 279**,** 12346-12354.

AUBIN, J., LIU, F., MALAVAL, L. & GUPTA, A. 1995. Osteoblast and chondroblast differentiation. *Bone,* 17**,** S77-S83.

AVERSA, F., TERENZI, A., TABILIO, A., FALZETTI, F., CAROTTI, A., BALLANTI, S., FELICINI, R., FALCINELLI, F., VELARDI, A. & RUGGERI, L. 2005. Full haplotype-mismatched hematopoietic stem-cell transplantation: a phase II study in patients with acute leukemia at high risk of relapse. *Journal of Clinical Oncology,* 2*3***,** 3447-3454.

AVRAHAM, H., COWLEY, S., CHI, S. Y., JIANG, S. & GROOPMAN, J. E. 1993. Characterization of adhesive interactions between human endothelial cells and megakaryocytes. *The Journal of clinical investigation,* 91**,** 2378-2384.

BALDRIDGE, M. T., KING, K. Y., BOLES, N. C., WEKSBERG, D. C. & GOODELL, M. A. 2010. Quiescent haematopoietic stem cells are activated by IFN-γ in response to chronic infection. *Nature,* 465**,** 793.

BALL, L. M., BERNARDO, M. E., ROELOFS, H., LANKESTER, A., COMETA, A., EGELER, R. M., LOCATELLI, F. & FIBBE, W. E. 2007. Cotransplantation of ex vivo–expanded mesenchymal stem cells accelerates lymphocyte recovery and may reduce the risk of graft failure in haploidentical hematopoietic stem-cell transplantation. *Blood,* 110**,** 2764-2767.

BALLESTER-BELTRÁN, J., CANTINI, M., LEBOURG, M., RICO, P., MORATAL, D., GARCÍA, A. J. & SALMERÓN-SÁNCHEZ, M. 2012. Effect of topological cues on material-driven fibronectin fibrillogenesis and cell differentiation. *Journal of*

Materials Science: Materials in Medicine, 23**,** 195-204.

BANEYX, G., BAUGH, L. & VOGEL, V. 2001. Coexisting conformations of fibronectin in cell culture imaged using fluorescence resonance energy transfer. *Proceedings of the National Academy of Sciences,* 98**,** 14464-14468.

BANSAL, R. & JAIN, A. 2015. Current overview on dental stem cells applications in regenerative dentistry. *Journal of natural science, biology, and medicine,* 6**,** 29.

BENSIDHOUM, M., CHAPEL, A., FRANCOIS, S., DEMARQUAY, C., MAZURIER, C., FOUILLARD, L., BOUCHET, S., BERTHO, J. M., GOURMELON, P. & AIGUEPERSE, J. 2004. Homing of in vitro expanded Stro-1-or Stro-1+ human mesenchymal stem cells into the NOD/SCID mouse and their role in supporting human CD34 cell engraftment. *Blood,* 103**,** 3313-3319.

BENSINGER, W. I., MARTIN, P. J., STORER, B., CLIFT, R., FORMAN, S. J., NEGRIN, R., KASHYAP, A., FLOWERS, M. E., LILLEBY, K. & CHAUNCEY, T. R. 2001. Transplantation of bone marrow as compared with peripheral-blood cells from HLA-identical relatives in patients with hematologic cancers. *New England Journal of Medicine,* 344**,** 175-181.

BHATIA, S., FRANCISCO, L., CARTER, A., SUN, C.-L., BAKER, K. S., GURNEY, J. G., MCGLAVE, P. B., NADEMANEE, A., O'DONNELL, M. & RAMSAY, N. K. 2007. Late mortality after allogeneic hematopoietic cell transplantation and functional status of long-term survivors: report

from the Bone Marrow Transplant Survivor Study. *Blood,* 110**,** 3784-3792.

BIRMINGHAM, E., NIEBUR, G. & MCHUGH, P. 2012. Osteogenic differentiation of mesenchymal stem cells is regulated by osteocyte and osteoblast cells in a simplified bone niche.

BLOOM, D. D., CENTANNI, J. M., BHATIA, N., EMLER, C. A., DRIER, D., LEVERSON, G. E., MCKENNA JR, D. H., GEE, A. P., LINDBLAD, R. & HEI, D. J. 2015. A reproducible immunopotency assay to measure mesenchymal stromal cell–mediated T-cell suppression. *Cytotherapy,* 17**,** 140-151.

BRADY, J. F. & BOSSIS, G. 1985. The rheology of concentrated suspensions of spheres in simple shear flow by numerical simulation. *Journal of Fluid Mechanics,* 155**,** 105-129.

BRAMONO, D. S., MURALI, S., RAI, B., LING, L., POH, W. T., LIM, Z. X., STEIN, G. S., NURCOMBE, V., VAN WIJNEN, A. J. & COOL, S. M. 2012. Bone marrow-derived heparan sulfate potentiates the osteogenic activity of bone morphogenetic protein-2 (BMP-2). *Bone,* 50**,** 954-964.

BRO, R. & SMILDE, A. K. 2014. Principal component analysis. *Analytical Methods,* 6**,** 2812-2831.

BROMBERG, O., FRISCH, B. J., WEBER, J. M., PORTER, R. L., CIVITELLI, R. & CALVI, L. M. 2012. Osteoblastic N-cadherin is not required for microenvironmental support and regulation of hematopoietic stem and progenitor cells. *Blood,* 120**,** 303-313.

BROWN, D. G., RAO, S., WEIR, T. L., O'MALIA, J., BAZAN, M., BROWN, R. J. & RYAN, E. P. 2016. Metabolomics and metabolic pathway networks

from human colorectal cancers, adjacent mucosa, and stool. *Cancer & metabolism,* 4**,** 11.

BURMAN, J., FRANSSON, M., TÖTTERMAN, T. H., FAGIUS, J., MANGSBO, S. M. & LOSKOG, A. S. 2013. T‐cell responses after haematopoietic stem cell transplantation for aggressive relapsing–remitting multiple sclerosis. *Immunology,* 140**,** 211-219.

BURT, R. K., BALABANOV, R., SNOWDEN, J. A., SHARRACK, B., OLIVEIRA, M. C. & BURMAN, J. 2018. Non-myeloablative hematopoietic stem cell transplantation (HSCT) is superior to disease modifying drug (DMD) treatment in highly active Relapsing Remitting Multiple Sclerosis (RRMS): interim results of the Multiple Sclerosis International Stem cell Transplant (MIST) Randomized Trial (S36. 004). AAN Enterprises.

BUTTE, N. F. 2000. Carbohydrate and lipid metabolism in pregnancy: normal compared with gestational diabetes mellitus–. *The American journal of clinical nutrition,* 71**,** 1256S-1261S.

CALVI, L., ADAMS, G., WEIBRECHT, K., WEBER, J., OLSON, D., KNIGHT, M., MARTIN, R., SCHIPANI, E., DIVIETI, P. & BRINGHURST, F. 2003. Osteoblastic cells regulate the haematopoietic stem cell niche. *Nature,* 425**,** 841-846.

CALVISI, D. F., LADU, S., GORDEN, A., FARINA, M., CONNER, E. A., LEE, J. S., FACTOR, V. M. & THORGEIRSSON, S. S. 2006. Ubiquitous activation of Ras and Jak/Stat pathways in human HCC. *Gastroenterology,* 130**,** 1117-1128.

CAO, L. & MOONEY, D. J. 2007. Spatiotemporal control over growth factor signaling for therapeutic

neovascularization. *Advanced drug delivery reviews,* 59**,** 1340-1350.

CAPLAN, A. I. 1991. Mesenchymal stem cells. *Journal of orthopaedic research,* 9**,** 641-650.

CAPLAN, A. I. 1994. The mesengenic process. *Clinics in plastic surgery,* 21**,** 429-435.

CARRAGEE, E. J., HURWITZ, E. L. & WEINER, B. K. 2011. A critical review of recombinant human bone morphogenetic protein-2 trials in spinal surgery: emerging safety concerns and lessons learned. *The Spine Journal,* 11**,** 471-491.

CARRERAS, E., BOIX, E., ROSENBERG, H. F., CUCHILLO, C. M. & NOGUÉS, M. V. 2003. Both aromatic and cationic residues contribute to the membrane-lytic and bactericidal activity of eosinophil cationic protein. *Biochemistry,* 42**,** 6636-6644.

CAVALCANTI- ADAM, E. A., AYDIN, D., HIRSCHFELD- WARNEKEN, V. C. & SPATZ, J. P. 2008. Cell adhesion and response to synthetic nanopatterned environments by steering receptor clustering and spatial location. *HFSP journal,* 2**,** 276-285.

CELSO, C. L., FLEMING, H. E., WU, J. W., ZHAO, C. X., MIAKE-LYE, S., FUJISAKI, J., CÔTÉ, D., ROWE, D. W., LIN, C. P. & SCADDEN, D. T. 2009. Live-animal tracking of individual haematopoietic stem/progenitor cells in their niche. *Nature,* 457**,** 92.

CHAO, M., SEITA, J. & WEISSMAN, I. Establishment of a normal hematopoietic and leukemia stem cell hierarchy. Cold Spring Harbor symposia on quantitative biology, 2008. Cold Spring Harbor Laboratory Press, sqb. 2008.73. 031.

CHEN, C. T., SHIH, Y. R. V., KUO, T. K., LEE, O. K. & WEI, Y. H. 2008. Coordinated changes of mitochondrial biogenesis and antioxidant enzymes during osteogenic differentiation of human mesenchymal stem cells. *Stem Cells,* 26**,** 960-968.

CHEN, X., SEVILLA, P. & APARICIO, C. 2013. Surface biofunctionalization by covalent co-immobilization of oligopeptides. *Colloids and Surfaces B: Biointerfaces,* 107**,** 189-197.

CHESHIER, S. H., MORRISON, S. J., LIAO, X. & WEISSMAN, I. L. 1999. In vivo proliferation and cell cycle kinetics of long-term self-renewing hematopoietic stem cells. *Proceedings of the National Academy of Sciences,* 96**,** 3120-3125.

CHILDS, A., MEHTA, D. & GERNER, E. 2003. Polyamine-dependent gene expression. *Cellular and Molecular Life Sciences CMLS,* 60**,** 1394-1406.

CHUA, K.-N., CHAI, C., LEE, P.-C., RAMAKRISHNA, S., LEONG, K. W. & MAO, H.-Q. 2007. Functional nanofiber scaffolds with different spacers modulate adhesion and expansion of cryopreserved umbilical cord blood hematopoietic stem/progenitor cells. *Experimental hematology,* 35**,** 771-781.

CHUA, P.-H., NEOH, K.-G., KANG, E.-T. & WANG, W. 2008. Surface functionalization of titanium with hyaluronic acid/chitosan polyelectrolyte multilayers and RGD for promoting osteoblast functions and inhibiting bacterial adhesion. *Biomaterials,* 29**,** 1412-1421.

CHUNG, S., DZEJA, P. P., FAUSTINO, R. S., PEREZ-TERZIC, C., BEHFAR, A. & TERZIC, A. 2007. Mitochondrial oxidative metabolism is required for

the cardiac differentiation of stem cells. *Nature Reviews Cardiology,* 4**,** S60.

CIVIN, C. I., STRAUSS, L., BROVALL, C., FACKLER, M., SCHWARTZ, J. & SHAPER, J. 1984. Antigenic analysis of hematopoiesis. III. A hematopoietic progenitor cell surface antigen defined by a monoclonal antibody raised against KG-1a cells. *The Journal of Immunology,* 133**,** 157-165.

CLARK, C., SAVANI, M., MOHTY, M. & SAVANI, B. 2016. What do we need to know about allogeneic hematopoietic stem cell transplant survivors? *Bone marrow transplantation,* 51**,** 1025.

CONNELLY, J. T., GAUTROT, J. E., TRAPPMANN, B., TAN, D. W.-M., DONATI, G., HUCK, W. T. & WATT, F. M. 2010. Actin and serum response factor transduce physical cues from the microenvironment to regulate epidermal stem cell fate decisions. *Nature cell biology,* 12**,** 711.

COPELAN, E. A. 2006. Hematopoietic stem-cell transplantation. *New England Journal of Medicine,* 354**,** 1813-1826.

DA SILVA, C. L., GONÇALVES, R., DOS SANTOS, F., ANDRADE, P. Z., ALMEIDA‐PORADA, G. & CABRAL, J. M. 2010. Dynamic cell–cell interactions between cord blood haematopoietic progenitors and the cellular niche are essential for the expansion of CD34+, CD34+ CD38− and early lymphoid CD7+ cells. *Journal of tissue engineering and regenerative medicine,* 4**,** 149-158.

DAHLBERG, A., DELANEY, C. & BERNSTEIN, I. D. 2011. Ex vivo expansion of human hematopoietic stem and progenitor cells. *Blood,* 117**,** 6083-6090.

DALBY, M. J., GADEGAARD, N. & OREFFO, R. O. C. 2014. Harnessing nanotopography and integrin-matrix interactions to influence stem cell fate. *Nat Mater,* 13**,** 558-569.

DALBY, M. J., GADEGAARD, N., TARE, R., ANDAR, A., RIEHLE, M. O., HERZYK, P., WILKINSON, C. D. & OREFFO, R. O. 2007. The control of human mesenchymal cell differentiation using nanoscale symmetry and disorder. *Nature materials,* 6**,** 997-1003.

DALBY, M. J., GARCÍA, A. J. & SALMERON-SANCHEZ, M. 2018. Receptor control in mesenchymal stem cell engineering. *Nature Reviews Materials,* 3**,** 17091.

DAVISS, B. 2005. Growing pains for metabolomics: the newest'omic science is producing results--and more data than researchers know what to do with. *The Scientist,* 19**,** 25-29.

DE LUCA, K., FRANCES-DUVERT, V., ASENSIO, M., IHSANI, R., DEBIEN, E., TAILLARDET, M., VERHOEYEN, E., BELLA, C., LANTHEAUME, S. & GENESTIER, L. 2009. The TLR1/2 agonist PAM 3 CSK 4 instructs commitment of human hematopoietic stem cells to a myeloid cell fate. *Leukemia,* 23**,** 2063.

DE UGARTE, D. A., ALFONSO, Z., ZUK, P. A., ELBARBARY, A., ZHU, M., ASHJIAN, P., BENHAIM, P., HEDRICK, M. H. & FRASER, J. K. 2003. Differential expression of stem cell mobilization-associated molecules on multi-lineage cells from adipose tissue and bone marrow. *Immunology letters,* 89**,** 267-270.

DEN BRABER, E., DE RUIJTER, J., GINSEL, L., VON RECUM, A. & JANSEN, J. 1998. Orientation of ECM protein deposition, fibroblast cytoskeleton,

and attachment complex components on silicone microgrooved surfaces. *Journal of Biomedical Materials Research: An Official Journal of The Society for Biomaterials, The Japanese Society for Biomaterials, and the Australian Society for Biomaterials,* 40**,** 291-300.

DEXTER, T. M. 1982. Stromal cell associated haemopoiesis. *Journal of Cellular Physiology,* 113**,** 87-94.

DI MAGGIO, N., PICCININI, E., JAWORSKI, M., TRUMPP, A., WENDT, D. J. & MARTIN, I. 2011. Toward modeling the bone marrow niche using scaffold-based 3D culture systems. *Biomaterials,* 32**,** 321-329.

DIGIUSTO, D. L., KRISHNAN, A., LI, L., LI, H., LI, S., RAO, A., MI, S., YAM, P., STINSON, S. & KALOS, M. 2010. RNA-based gene therapy for HIV with lentiviral vector–modified CD34+ cells in patients undergoing transplantation for AIDS-related lymphoma. *Science translational medicine,* 2**,** 36ra43-36ra43.

DING, L. & MORRISON, S. J. 2013. Haematopoietic stem cells and early lymphoid progenitors occupy distinct bone marrow niches. *Nature,* 495**,** 231.

DING, L., SAUNDERS, T. L., ENIKOLOPOV, G. & MORRISON, S. J. 2012. Endothelial and perivascular cells maintain haematopoietic stem cells. *Nature,* 481**,** 457.

DISCHER, D. E., MOONEY, D. J. & ZANDSTRA, P. W. 2009. Growth factors, matrices, and forces combine and control stem cells. *Science,* 324**,** 1673-1677.

DOMINICI, M., LE BLANC, K., MUELLER, I., SLAPER-CORTENBACH, I., MARINI, F., KRAUSE, D., DEANS, R., KEATING, A., PROCKOP, D. &

HORWITZ, E. 2006. Minimal criteria for defining multipotent mesenchymal stromal cells. The International Society for Cellular Therapy position statement. *Cytotherapy,* 8**,** 315-317.

DUNN, W. B., ERBAN, A., WEBER, R. J., CREEK, D. J., BROWN, M., BREITLING, R., HANKEMEIER, T., GOODACRE, R., NEUMANN, S. & KOPKA, J. 2013. Mass appeal: metabolite identification in mass spectrometry-focused untargeted metabolomics. *Metabolomics,* 9**,** 44-66.

ELLIS, S. J. & TANENTZAPF, G. 2010. Integrin-mediated adhesion and stem-cell-niche interactions. *Cell and tissue research,* 339**,** 121.

EMA, H., TAKANO, H., SUDO, K. & NAKAUCHI, H. 2000. In vitro self-renewal division of hematopoietic stem cells. *Journal of Experimental Medicine,* 192**,** 1281-1288.

ENDO, T. A., MASUHARA, M., YOKOUCHI, M., SUZUKI, R., SAKAMOTO, H., MITSUI, K., MATSUMOTO, A., TANIMURA, S., OHTSUBO, M. & MISAWA, H. 1997. A new protein containing an SH2 domain that inhibits JAK kinases. *Nature,* 387**,** 921.

ENGEL, E., MICHIARDI, A., NAVARRO, M., LACROIX, D. & PLANELL, J. A. 2008. Nanotechnology in regenerative medicine: the materials side. *Trends in biotechnology,* 26**,** 39-47.

ENGELHARDT, M., LÜBBERT, M. & GUO, Y. 2002. CD34+ or CD34−: which is the more primitive? *Leukemia,* 16**,** 1603.

ERICKSON, H. P. & CARRELL, N. 1983. Fibronectin in extended and compact conformations. Electron microscopy and sedimentation analysis. *Journal of Biological Chemistry,* 258**,** 14539-14544.

EVERCOOREN, B. V., KLEINMAN, H. K., OHNO, S., MARANGOS, P., SCHWARTZ, J. P. & DUBOIS-DALCQ, M. E. 1982. Nerve growth factor, laminin, and fibronectin promote neurite growth in human fetal sensory ganglia cultures. *Journal of neuroscience research,* 8**,** 179-193.

FAJARDO-ORDUÑA, G. R., MAYANI, H. & MONTESINOS, J. J. 2015. Hematopoietic Support Capacity of Mesenchymal Stem Cells: Biology and Clinical Potential. *Archives of Medical Research,* 46**,** 589-596.

FAN, V. H., AU, A., TAMAMA, K., LITTRELL, R., RICHARDSON, L. B., WRIGHT, J. W., WELLS, A. & GRIFFITH, L. G. 2007. Tethered epidermal growth factor provides a survival advantage to mesenchymal stem cells. *Stem cells,* 25**,** 1241-1251.

FENG, Q., CHAI, C., JIANG, X. S., LEONG, K. W. & MAO, H. Q. 2006. Expansion of engrafting human hematopoietic stem/progenitor cells in three-dimensional scaffolds with surface-immobilized fibronectin. *Journal of Biomedical Materials Research Part A,* 78**,** 781-791.

FERREIRA, M. S. V., JAHNEN-DECHENT, W., LABUDE, N., BOVI, M., HIERONYMUS, T., ZENKE, M., SCHNEIDER, R. K. & NEURS, S. 2012. Cord blood-hematopoietic stem cell expansion in 3D fibrin scaffolds with stromal support. *Biomaterials,* 33**,** 6987-6997.

FIEHN, O. 2002. Metabolomics—the link between genotypes and phenotypes. *Functional genomics.* Springer.

FISK, N. M., ROBERTS, I. A., MARKWALD, R. & MIRONOV, V. 2005. Can routine commercial cord

blood banking be scientifically and ethically justified? *PLoS Medicine,* 2**,** e44.

FOSSIEZ, F., DJOSSOU, O., CHOMARAT, P., FLORES-ROMO, L., AIT-YAHIA, S., MAAT, C., PIN, J.-J., GARRONE, P., GARCIA, E. & SAELAND, S. 1996. T cell interleukin-17 induces stromal cells to produce proinflammatory and hematopoietic cytokines. *Journal of Experimental Medicine,* 183**,** 2593-2603.

FOUREL, L., VALAT, A., FAUROBERT, E., GUILLOT, R., BOURRIN-REYNARD, I., REN, K., LAFANECHÈRE, L., PLANUS, E., PICART, C. & ALBIGES-RIZO, C. 2016. β3 integrin–mediated spreading induced by matrix-bound BMP-2 controls Smad signaling in a stiffness-independent manner. *J Cell Biol,* 212**,** 693-706.

FRENETTE, P. S., SUBBARAO, S., MAZO, I. B., VON ANDRIAN, U. H. & WAGNER, D. D. 1998. Endothelial selectins and vascular cell adhesion molecule-1 promote hematopoietic progenitor homing to bone marrow. *Proceedings of the National Academy of Sciences,* 95**,** 14423-14428.

FRIEDENSTEIN, A. J., CHAILAKHYAN, R. K., LATSINIK, N. V., PANASYUK, A. F. & KEILISS-BOROK, I. V. 1974. Stromal cells responsible for transferring the microenvironment of the hemopoietic tissues: cloning in vitro and retransplantation in vivo. *Transplantation,* 17**,** 331-340.

FUNG, Y.-C. 2013. *Biomechanics: mechanical properties of living tissues*, Springer Science & Business Media.

GAJKOWSKA, A., OLDAK, T., JASTRZEWSKA, M., MACHAJ, E., WALEWSKI, J., KRASZEWSKA, E. & POJDA, Z. 2006. Flow cytometric enumeration

of CD34+ hematopoietic stem and progenitor cells in leukapheresis product and bone marrow for clinical transplantation: a comparison of three methods. *Folia Histochemica et Cytobiologica,* 44**,** 53-60.

GATTAZZO, F., URCIUOLO, A. & BONALDO, P. 2014. Extracellular matrix: a dynamic microenvironment for stem cell niche. *Biochimica et Biophysica Acta (BBA)-General Subjects,* 1840**,** 2506-2519.

GATTINONI, L., LUGLI, E., JI, Y., POS, Z., PAULOS, C. M., QUIGLEY, M. F., ALMEIDA, J. R., GOSTICK, E., YU, Z. & CARPENITO, C. 2011. A human memory T cell subset with stem cell–like properties. *Nature medicine,* 17**,** 1290.

GONÇALVES, R., DA SILVA, C. L., CABRAL, J. M., ZANJANI, E. D. & ALMEIDA-PORADA, G. 2006. A Stro-1+ human universal stromal feeder layer to expand/maintain human bone marrow hematopoietic stem/progenitor cells in a serum-free culture system. *Experimental hematology,* 34**,** 1353-1359.

GORGOULIS, V. G., VASSILIOU, L.-V. F., KARAKAIDOS, P., ZACHARATOS, P., KOTSINAS, A., LILOGLOU, T., VENERE, M., DITULLIO JR, R. A., KASTRINAKIS, N. G. & LEVY, B. 2005. Activation of the DNA damage checkpoint and genomic instability in human precancerous lesions. *Nature,* 434**,** 907.

GOYAMA, S., WUNDERLICH, M. & MULLOY, J. C. 2015. Xenograft models for normal and malignant stem cells. *Blood***,** blood-2014-11-570218.

GRATWOHL, A., PASQUINI, M. C., ALJURF, M., ATSUTA, Y., BALDOMERO, H., FOEKEN, L., GRATWOHL, M., BOUZAS, L. F., CONFER, D. &

FRAUENDORFER, K. 2015. One million haemopoietic stem-cell transplants: a retrospective observational study. *The Lancet Haematology,* 2**,** e91-e100.

GREENBAUM, A., HSU, Y.-M. S., DAY, R. B., SCHUETTPELZ, L. G., CHRISTOPHER, M. J., BORGERDING, J. N., NAGASAWA, T. & LINK, D. C. 2013. CXCL12 in early mesenchymal progenitors is required for haematopoietic stem-cell maintenance. *Nature,* 495**,** 227.

GREENLEAF, J. F., FATEMI, M. & INSANA, M. 2003. Selected methods for imaging elastic properties of biological tissues. *Annual review of biomedical engineering,* 5**,** 57-78.

HABIBOVIC, P., YUAN, H., VAN DER VALK, C. M., MEIJER, G., VAN BLITTERSWIJK, C. A. & DE GROOT, K. 2005. 3D microenvironment as essential element for osteoinduction by biomaterials. *Biomaterials,* 26**,** 3565-3575.

HANOUN, M., MARYANOVICH, M., ARNAL-ESTAPÉ, A. & FRENETTE, P. S. 2015. Neural regulation of hematopoiesis, inflammation, and cancer. *Neuron,* 86**,** 360-373.

HAO, Q.-L., SHAH, A. J., THIEMANN, F. T., SMOGORZEWSKA, E. M. & CROOKS, G. 1995. A functional comparison of CD34+ CD38-cells in cord blood and bone marrow. *Blood,* 86**,** 3745-3753.

HAUG, J. S., HE, X. C., GRINDLEY, J. C., WUNDERLICH, J. P., GAUDENZ, K., ROSS, J. T., PAULSON, A., WAGNER, K. P., XIE, Y. & ZHU, R. 2008. N-cadherin expression level distinguishes reserved versus primed states of hematopoietic stem cells. *Cell stem cell,* 2**,** 367-379.

HE, X., MA, J. & JABBARI, E. 2008. Effect of grafting RGD and BMP-2 protein-derived peptides to a hydrogel substrate on osteogenic differentiation of marrow stromal cells. *Langmuir,* 24**,** 12508-12516.

HELFAND, M. 2013. Effectiveness and Harms of Recombinant Human Bone Morphogenetic Protein-2 in Spine Fusion. *Ann Intern Med,* 158**,** 890-902.

HESSE, E., SAITO, H., KIVIRANTA, R., CORREA, D., YAMANA, K., NEFF, L., TOBEN, D., DUDA, G., ATFI, A. & GEOFFROY, V. 2010. Zfp521 controls bone mass by HDAC3-dependent attenuation of Runx2 activity. *The Journal of cell biology,* 191**,** 1271-1283.

HIRAI, K., MORITA, Y., MISAKI, Y., OHTA, K., TAKAISHI, T., SUZUKI, S., MOTOYOSHI, K. & MIYAMOTO, T. 1988. Modulation of human basophil histamine release by hemopoietic growth factors. *The Journal of Immunology,* 141**,** 3958-3964.

HOGAN, C. J., SHPALL, E. J. & KELLER, G. 2002. Differential long-term and multilineage engraftment potential from subfractions of human CD34+ cord blood cells transplanted into NOD/SCID mice. *Proceedings of the National Academy of Sciences,* 99**,** 413-418.

HOLMGREN, L., O'REILLY, M. S. & FOLKMAN, J. 1995. Dormancy of micrometastases: balanced proliferation and apoptosis in the presence of angiogenesis suppression. *Nature medicine,* 1**,** 149.

HOOPER, A. T., BUTLER, J. M., NOLAN, D. J., KRANZ, A., IIDA, K., KOBAYASHI, M., KOPP, H.-G., SHIDO, K., PETIT, I. & YANGER, K. 2009. Engraftment and reconstitution of hematopoiesis

is dependent on VEGFR2-mediated regeneration of sinusoidal endothelial cells. *Cell stem cell,* 4**,** 263-274.

HORI, S., NOMURA, T. & SAKAGUCHI, S. 2003. Control of regulatory T cell development by the transcription factor Foxp3. *Science,* 299**,** 1057-1061.

HOSOKAWA, K., ARAI, F., YOSHIHARA, H., IWASAKI, H., HEMBREE, M., YIN, T., NAKAMURA, Y., GOMEI, Y., TAKUBO, K. & SHIAMA, H. 2010. Cadherin-based adhesion is a potential target for niche manipulation to protect hematopoietic stem cells in adult bone marrow. *Cell stem cell,* 6**,** 194-198.

HOUGHTON, F. D. 2006. Energy metabolism of the inner cell mass and trophectoderm of the mouse blastocyst. *Differentiation,* 74**,** 11-18.

HUANG, X., LI, C., ZHU, B., WANG, H., LUO, X. & WEI, L. 2016. Co‐cultured h BMSC s and HUVEC s on human bio‐derived bone scaffolds provide support for the long‐term ex vivo culture of HSC/HPC s. *Journal of Biomedical Materials Research Part A,* 104**,** 1221-1230.

HUTCHINGS, H., ORTEGA, N. & PLOUËT, J. 2003. Extracellular matrix-bound vascular endothelial growth factor promotes endothelial cell adhesion, migration, and survival through integrin ligation. *The FASEB Journal,* 17**,** 1520-1522.

IHLE, J. N., WITTHUHN, B. A., QUELLE, F. W., YAMAMOTO, K. & SILVENNOINEN, O. 1995. Signaling through the hematopoietic cytokine receptors. *Annual review of immunology,* 13**,** 369-398.

IVANOVA, N. B., DIMOS, J. T., SCHANIEL, C., HACKNEY, J. A., MOORE, K. A. & LEMISCHKA,

I. R. 2002. A stem cell molecular signature. *Science,* 298**,** 601-604.

JAENISCH, R. & YOUNG, R. 2008. Stem cells, the molecular circuitry of pluripotency and nuclear reprogramming. *Cell,* 132**,** 567-582.

JENSEN, F. B. 2004. Red blood cell pH, the Bohr effect, and other oxygenation- linked phenomena in blood O2 and CO2 transport. *Acta Physiologica,* 182**,** 215-227.

JING, D., FONSECA, A.-V., ALAKEL, N., FIERRO, F. A., MULLER, K., BORNHAUSER, M., EHNINGER, G., CORBEIL, D. & ORDEMANN, R. 2010. Hematopoietic stem cells in co-culture with mesenchymal stromal cells-modeling the niche compartments in vitro. *haematologica,* 95**,** 542-550.

JORGENSEN, I. & MIAO, E. A. 2015. Pyroptotic cell death defends against intracellular pathogens. *Immunological reviews,* 265**,** 130-142.

JUNG, Y., WANG, J., HAVENS, A., SUN, Y., WANG, J., JIN, T. & TAICHMAN, R. 2005. Cell-to-cell contact is critical for the survival of hematopoietic progenitor cells on osteoblasts. *Cytokine,* 32**,** 155-162.

KANEHISA, M., GOTO, S., SATO, Y., FURUMICHI, M. & TANABE, M. 2011. KEGG for integration and interpretation of large-scale molecular data sets. *Nucleic acids research,* 40**,** D109-D114.

KATAGIRI, T., YAMAGUCHI, A., IKEDA, T., YOSHIKI, S., WOZNEY, J. M., ROSEN, V., WANG, E. A., TANAKA, H., OMURA, S. & SUDA, T. 1990. The non-osteogenic mouse pluripotent cell line, C3H10T1/2, is induced to differentiate into osteoblastic cells by recombinant human bone morphogenetic protein-2. *Biochemical and*

biophysical research communications, 172**,** 295-299.

KATAYAMA, Y., BATTISTA, M., KAO, W.-M., HIDALGO, A., PEIRED, A. J., THOMAS, S. A. & FRENETTE, P. S. 2006. Signals from the Sympathetic Nervous System Regulate Hematopoietic Stem Cell Egress from Bone Marrow. *Cell,* 124**,** 407-421.

KENNEDY, M., FIRPO, M., CHOI, K., WALL, C., ROBERTSON, S., KABRUN, N. & KELLER, G. 1997. A common precursor for primitive erythropoiesis and definitive haematopoiesis. *Nature,* 386**,** 488.

KERN, S., EICHLER, H., STOEVE, J., KLÜTER, H. & BIEBACK, K. 2006. Comparative analysis of mesenchymal stem cells from bone marrow, umbilical cord blood, or adipose tissue. *Stem cells,* 24**,** 1294-1301.

KIEL, M. J., ACAR, M., RADICE, G. L. & MORRISON, S. J. 2009. Hematopoietic stem cells do not depend on N-cadherin to regulate their maintenance. *Cell stem cell,* 4**,** 170-179.

KIEL, M. J., IWASHITA, T., YILMAZ, Ö. H. & MORRISON, S. J. 2005. Spatial differences in hematopoiesis but not in stem cells indicate a lack of regional patterning in definitive hematopoietic stem cells. *Developmental biology,* 283**,** 29-39.

KLIEWER, S. A., LENHARD, J. M., WILLSON, T. M., PATEL, I., MORRIS, D. C. & LEHMANN, J. M. 1995. A prostaglandin J2 metabolite binds peroxisome proliferator-activated receptor γ and promotes adipocyte differentiation. *Cell,* 83**,** 813-819.

KÖHLER, G. & MILSTEIN, C. 1975. Continuous cultures of fused cells secreting antibody of predefined specificity. *Nature,* 256**,** 495.

KOLF, C. M., CHO, E. & TUAN, R. S. 2007. Mesenchymal stromal cells: biology of adult mesenchymal stem cells: regulation of niche, self-renewal and differentiation. *Arthritis research & therapy,* 9**,** 204.

KONDO, M., WEISSMAN, I. L. & AKASHI, K. 1997. Identification of clonogenic common lymphoid progenitors in mouse bone marrow. *Cell,* 91**,** 661-672.

KONTERMANN, R. E. 2011. Strategies for extended serum half-life of protein therapeutics. *Current opinion in biotechnology,* 22**,** 868-876.

KOPP, H.-G., AVECILLA, S. T., HOOPER, A. T. & RAFII, S. 2005. The bone marrow vascular niche: home of HSC differentiation and mobilization. *Physiology,* 20**,** 349-356.

KRAUSE, D. S., FACKLER, M. J., CIVIN, C. I. & MAY, W. S. 1996. CD34: structure, biology, and clinical utility [see comments]. *Blood,* 87**,** 1-13.

KRAUSE, D. S., THEISE, N. D., COLLECTOR, M. I., HENEGARIU, O., HWANG, S., GARDNER, R., NEUTZEL, S. & SHARKIS, S. J. 2001. Multi-organ, multi-lineage engraftment by a single bone marrow-derived stem cell. *Cell,* 105**,** 369-377.

KRIEGER, I. M. & DOUGHERTY, T. J. 1959. A mechanism for non- Newtonian flow in suspensions of rigid spheres. *Transactions of the Society of Rheology,* 3**,** 137-152.

KUNISAKI, Y., BRUNS, I., SCHEIERMANN, C., AHMED, J., PINHO, S., ZHANG, D., MIZOGUCHI, T., WEI, Q., LUCAS, D. & ITO, K. 2013a.

Arteriolar niches maintain haematopoietic stem cell quiescence. *Nature,* 502**,** 637-643.

KUNISAKI, Y., BRUNS, I., SCHEIERMANN, C., AHMED, J., PINHO, S., ZHANG, D., MIZOGUCHI, T., WEI, Q., LUCAS, D., ITO, K., MAR, J. C., BERGMAN, A. & FRENETTE, P. S. 2013b. Arteriolar niches maintain haematopoietic stem cell quiescence. *Nature,* 502**,** 637-643.

LANGER, R. & TIRRELL, D. A. 2004. Designing materials for biology and medicine. *Nature,* 428**,** 487.

LANSDORP, P., SUTHERLAND, H. & EAVES, C. 1990. Selective expression of CD45 isoforms on functional subpopulations of CD34+ hemopoietic cells from human bone marrow. *Journal of Experimental Medicine,* 172**,** 363-366.

LAPILLONNE, H., KOBARI, L., MAZURIER, C., TROPEL, P., GIARRATANA, M.-C., ZANELLA-CLEON, I., KIGER, L., WATTENHOFER-DONZE, M., PUCCIO, H. & HEBERT, N. 2010. Red blood cells generation from human induced pluripotent stem cells: perspectives for transfusion medicine. *Haematologica***,** haematol. 2010.023556.

LEE, M.-H., KWON, T.-G., PARK, H.-S., WOZNEY, J. M. & RYOO, H.-M. 2003. BMP-2-induced Osterix expression is mediated by Dlx5 but is independent of Runx2. *Biochemical and biophysical research communications,* 309**,** 689-694.

LEISTEN, I., KRAMANN, R., FERREIRA, M. S. V., BOVI, M., NEUSS, S., ZIEGLER, P., WAGNER, W., KNÜCHEL, R. & SCHNEIDER, R. K. 2012. 3D co-culture of hematopoietic stem and progenitor cells and mesenchymal stem cells in collagen scaffolds as a model of the hematopoietic niche. *Biomaterials,* 33**,** 1736-1747.

LEONARD, W. J. 2001. Role of Jak kinases and STATs in cytokine signal transduction. *International journal of hematology,* 73**,** 271.

LÉVESQUE, J., HELWANI, F. & WINKLER, I. 2010. The endosteal 'osteoblastic'niche and its role in hematopoietic stem cell homing and mobilization. *Leukemia,* 24**,** 1979.

LI, B., SHARPE, E. E., MAUPIN, A. B., TELERON, A. A., PYLE, A. L., CARMELIET, P., YOUNG, P. P., LI, B., SHARPE, E. E. & MAUPIN, A. B. 2006. VEGF and PlGF promote adult vasculogenesis by enhancing EPC recruitment and vessel formation at site of tumor neovascularization. *The FASEB Journal,* 20**,** 1495-1497.

LI, W., JOHNSON, S. A., SHELLEY, W. C., FERKOWICZ, M., MORRISON, P., LI, Y. & YODER, M. C. 2003. Primary endothelial cells isolated from the yolk sac and para-aortic splanchnopleura support the expansion of adult marrow stem cells in vitro. *Blood,* 102**,** 4345-4353.

LIN, F., ZHU, J., TONNESEN, M. G., TAIRA, B. R., MCCLAIN, S. A., SINGER, A. J. & CLARK, R. A. 2014. Fibronectin peptides that bind PDGF-BB enhance survival of cells and tissue under stress. *Journal of Investigative Dermatology,* 134**,** 1119-1127.

LIU, D. D., ZHANG, J. C., ZHANG, Q., WANG, S. X. & YANG, M. S. 2013. TGF-β/BMP signaling pathway is involved in cerium-promoted osteogenic differentiation of mesenchymal stem cells. *Journal of cellular biochemistry,* 114**,** 1105-1114.

LIU, L., GUO, X., RAO, J. N., ZOU, T., MARASA, B. S., CHEN, J., GREENSPON, J., CASERO, R. A. & WANG, J.-Y. 2006. Polyamine-modulated c-Myc

expression in normal intestinal epithelial cells regulates p21Cip1 transcription through a proximal promoter region. *Biochemical Journal,* 398**,** 257-267.

LLOPIS-HERNÁNDEZ, V., CANTINI, M., GONZÁLEZ-GARCÍA, C., CHENG, Z. A., YANG, J., TSIMBOURI, P. M., GARCÍA, A. J., DALBY, M. J. & SALMERÓN-SÁNCHEZ, M. 2016. Material-driven fibronectin assembly for high-efficiency presentation of growth factors. *Science Advances,* 2**,** e1600188.

LORD, B. I., TESTA, N. G. & HENDRY, J. H. 1975. The relative spatial distributions of CFUs and CFUc in the normal mouse femur. *Blood,* 46**,** 65-72.

LUCAS, D., SCHEIERMANN, C., CHOW, A., KUNISAKI, Y., BRUNS, I., BARRICK, C., TESSAROLLO, L. & FRENETTE, P. S. 2013. Chemotherapy-induced bone marrow nerve injury impairs hematopoietic regeneration. *Nature medicine,* 19**,** 695.

LUSTER, A. D. 1998. Chemokines—chemotactic cytokines that mediate inflammation. *New England Journal of Medicine,* 338**,** 436-445.

LUTOLF, M. P., GILBERT, P. M. & BLAU, H. M. 2009. Designing materials to direct stem-cell fate. *Nature,* 462**,** 433.

LUTTRELL, L. M., DAAKA, Y. & LEFKOWITZ, R. J. 1999. Regulation of tyrosine kinase cascades by G-protein-coupled receptors. *Current opinion in cell biology,* 11**,** 177-183.

MAJETI, R., PARK, C. Y. & WEISSMAN, I. L. 2007. Identification of a hierarchy of multipotent hematopoietic progenitors in human cord blood. *Cell stem cell,* 1**,** 635-645.

MARTINO, M. M. & HUBBELL, J. A. 2010. The 12th–14th type III repeats of fibronectin function as a highly promiscuous growth factor-binding domain. *The FASEB Journal,* 24**,** 4711-4721.

MARTINO, M. M., TORTELLI, F., MOCHIZUKI, M., TRAUB, S., BEN-DAVID, D., KUHN, G. A., MÜLLER, R., LIVNE, E., EMING, S. A. & HUBBELL, J. A. 2011. Engineering the growth factor microenvironment with fibronectin domains to promote wound and bone tissue healing. *Science translational medicine,* 3**,** 100ra89-100ra89.

MARUYAMA, H., KATAGIRI, T., KASHIWASE, K., SHIINA, T., SATO-OTSUBO, A., ZAIMOKU, Y., MARUYAMA, K., HOSOKAWA, K., ISHIYAMA, K. & YAMAZAKI, H. 2016. Clinical significance and origin of leukocytes that lack HLA-A allele expression in patients with acquired aplastic anemia. *Experimental hematology,* 44**,** 931-939. e3.

MCBEATH, R., PIRONE, D. M., NELSON, C. M., BHADRIRAJU, K. & CHEN, C. S. 2004. Cell shape, cytoskeletal tension, and RhoA regulate stem cell lineage commitment. *Developmental cell,* 6**,** 483-495.

MCMURRAY, R. J., GADEGAARD, N., TSIMBOURI, P. M., BURGESS, K. V., MCNAMARA, L. E., TARE, R., MURAWSKI, K., KINGHAM, E., OREFFO, R. O. & DALBY, M. J. 2011. Nanoscale surfaces for the long-term maintenance of mesenchymal stem cell phenotype and multipotency. *Nature materials,* 10**,** 637-644.

MCNAMARA, L. E., SJÖSTRÖM, T., BURGESS, K. E., KIM, J. J., LIU, E., GORDONOV, S., MOGHE, P. V., MEEK, R. D., OREFFO, R. O. & SU, B.

2011. Skeletal stem cell physiology on functionally distinct titania nanotopographies. *Biomaterials,* 32**,** 7403-7410.

MCNAMARA, L. E., SJÖSTRÖM, T., MEEK, R. D., OREFFO, R. O., SU, B., DALBY, M. J. & BURGESS, K. E. 2012. Metabolomics: a valuable tool for stem cell monitoring in regenerative medicine. *Journal of the Royal Society Interface,* 9**,** 1713-1724.

MEISSEN, J. K., YUEN, B. T., KIND, T., RIGGS, J. W., BARUPAL, D. K., KNOEPFLER, P. S. & FIEHN, O. 2012. Induced pluripotent stem cells show metabolomic differences to embryonic stem cells in polyunsaturated phosphatidylcholines and primary metabolism. *PloS one,* 7**,** e46770.

MENDELSON, A. & FRENETTE, P. S. 2014. Hematopoietic stem cell niche maintenance during homeostasis and regeneration. *Nature medicine,* 20**,** 833-846.

MÉNDEZ-FERRER, S., MICHURINA, T. V., FERRARO, F., MAZLOOM, A. R., MACARTHUR, B. D., LIRA, S. A., SCADDEN, D. T., MA'AYAN, A., ENIKOLOPOV, G. N. & FRENETTE, P. S. 2010. Mesenchymal and haematopoietic stem cells form a unique bone marrow niche. *Nature,* 466**,** 829-834.

METZGER, T. A., SHUDICK, J. M., SEEKELL, R., ZHU, Y. & NIEBUR, G. L. 2014. Rheological behavior of fresh bone marrow and the effects of storage. *Journal of the mechanical behavior of biomedical materials,* 40**,** 307-313.

MICHALLET, M., PHILIP, T., PHILIP, I., GODINOT, H., SEBBAN, C., SALLES, G., THIEBAUT, A., BIRON, P., LOPEZ, F. & MAZARS, P. 2000. Transplantation with selected autologous

peripheral blood CD34+ Thy1+ hematopoietic stem cells (HSCs) in multiple myeloma. *Experimental hematology, 2*8**,** 858-870.

MIDWOOD, K. S., WILLIAMS, L. V. & SCHWARZBAUER, J. E. 2004. Tissue repair and the dynamics of the extracellular matrix. *The international journal of biochemistry & cell biology,* 36**,** 1031-1037.

MIYAMOTO, T., IWASAKI, H., REIZIS, B., YE, M., GRAF, T., WEISSMAN, I. L. & AKASHI, K. 2002. Myeloid or lymphoid promiscuity as a critical step in hematopoietic lineage commitment. *Developmental cell,* 3**,** 137-147.

MOORE, K. A., EMA, H. & LEMISCHKA, I. R. 1997. In vitro maintenance of highly purified, transplantable hematopoietic stem cells. *Blood,* 89**,** 4337-4347.

MORRISON, S. J. & WEISSMAN, I. L. 1994. The long-term repopulating subset of hematopoietic stem cells is deterministic and isolatable by phenotype. *Immunity,* 1**,** 661-673.

MOULISOVÁ, V., GONZALEZ-GARCÍA, C., CANTINI, M., RODRIGO-NAVARRO, A., WEAVER, J., COSTELL, M., I SERRA, R. S., DALBY, M. J., GARCÍA, A. J. & SALMERÓN-SÁNCHEZ, M. 2017. Engineered microenvironments for synergistic VEGF–Integrin signalling during vascularization. *Biomaterials,* 126**,** 61-74.

NAKAMURA, S., MATSUMOTO, T., SASAKI, J.-I., EGUSA, H., LEE, K. Y., NAKANO, T., SOHMURA, T. & NAKAHIRA, A. 2010a. Effect of calcium ion concentrations on osteogenic differentiation and hematopoietic stem cell niche-related protein expression in osteoblasts. *Tissue Engineering Part A,* 16**,** 2467-2473.

NAKAMURA, Y., ARAI, F., IWASAKI, H., HOSOKAWA, K., KOBAYASHI, I., GOMEI, Y., MATSUMOTO, Y., YOSHIHARA, H. & SUDA, T. 2010b. Isolation and characterization of endosteal niche cell populations that regulate hematopoietic stem cells. *Blood*, blood-2009-08-239194.

NILSSON, S. K., JOHNSTON, H. M. & COVERDALE, J. A. 2001. *Spatial localization of transplanted hemopoietic stem cells: inferences for the localization of stem cell niches*.

NILSSON, S. K., JOHNSTON, H. M., WHITTY, G. A., WILLIAMS, B., WEBB, R. J., DENHARDT, D. T., BERTONCELLO, I., BENDALL, L. J., SIMMONS, P. J. & HAYLOCK, D. N. 2005. Osteopontin, a key component of the hematopoietic stem cell niche and regulator of primitive hematopoietic progenitor cells. *Blood,* 106, 1232-1239.

NING, H., LIN, G., LUE, T. F. & LIN, C.-S. 2011. Mesenchymal stem cell marker Stro-1 is a 75kd endothelial antigen. *Biochemical and biophysical research communications,* 413, 353-357.

NOHE, A., HASSEL, S., EHRLICH, M., NEUBAUER, F., SEBALD, W., HENIS, Y. I. & KNAUS, P. 2002. The mode of bone morphogenetic protein (BMP) receptor oligomerization determines different BMP-2 signaling pathways. *Journal of Biological Chemistry,* 277, 5330-5338.

NOTTA, F., DOULATOV, S. & DICK, J. E. 2010. Engraftment of human hematopoietic stem cells is more efficient in female NOD/SCID/IL-2Rgcnull recipients. *Blood*, blood-2009-10-249326.

OGAWA, M. 1993. Differentiation and proliferation of hematopoietic stem cells. *Blood,* 81, 2844-2853.

OHH, M., YAUCH, R. L., LONERGAN, K. M., WHALEY, J. M., STEMMER-RACHAMIMOV, A.

O., LOUIS, D. N., GAVIN, B. J., KLEY, N., KAELIN JR, W. G. & ILIOPOULOS, O. 1998. The von Hippel-Lindau tumor suppressor protein is required for proper assembly of an extracellular fibronectin matrix. *Molecular cell,* 1**,** 959-968.

OKAZAKI, T., BIELAWSKA, A., BELL, R. & HANNUN, Y. 1990. Role of ceramide as a lipid mediator of 1 alpha, 25-dihydroxyvitamin D3-induced HL-60 cell differentiation. *Journal of Biological Chemistry,* 265**,** 15823-15831.

OMATSU, Y., SUGIYAMA, T., KOHARA, H., KONDOH, G., FUJII, N., KOHNO, K. & NAGASAWA, T. 2010. The essential functions of adipo-osteogenic progenitors as the hematopoietic stem and progenitor cell niche. *Immunity,* 33**,** 387-399.

ORKIN, S. H. & ZON, L. I. 2008. Hematopoiesis: an evolving paradigm for stem cell biology. *Cell,* 132**,** 631-644.

ORLOWSKA, A., PERERA, P. T., AL KOBAISI, M., DIAS, A., NGUYEN, H. K. D., GHANAATI, S., BAULIN, V., CRAWFORD, R. J. & IVANOVA, E. P. 2017. The effect of coatings and nerve growth factor on attachment and differentiation of pheochromocytoma cells. *Materials,* 11**,** 60.

OSAWA, M., HANADA, K.-I., HAMADA, H. & NAKAUCHI, H. 1996. Long-term lymphohematopoietic reconstitution by a single CD34-low/negative hematopoietic stem cell. *Science,* 273**,** 242-245.

OSWALD, J., STEUDEL, C., SALCHERT, K., JOERGENSEN, B., THIEDE, C., EHNINGER, G., WERNER, C. & BORNHÄUSER, M. 2006. Gene-Expression Profiling of CD34+ Hematopoietic

Cells Expanded in a Collagen I Matrix. *Stem Cells,* 24**,** 494-500.

OSYCZKA, A. M., DAMEK-POPRAWA, M., WOJTOWICZ, A. & AKINTOYE, S. O. 2009. Age and skeletal sites affect BMP-2 responsiveness of human bone marrow stromal cells. *Connective tissue research,* 50**,** 270-277.

PANKOV, R. & YAMADA, K. M. 2002. Fibronectin at a glance. *Journal of cell science,* 115**,** 3861-3863.

PARK, C. W., KIM, K.-S., BAE, S., SON, H. K., MYUNG, P.-K., HONG, H. J. & KIM, H. 2009. Cytokine secretion profiling of human mesenchymal stem cells by antibody array. *International journal of stem cells,* 2**,** 59.

PASSWEG, J. R., BALDOMERO, H., BADER, P., BONINI, C., CESARO, S., DREGER, P., DUARTE, R. F., DUFOUR, C., FALKENBURG, J. F. & FARGE-BANCEL, D. 2015. Hematopoietic SCT in Europe 2013: recent trends in the use of alternative donors showing more haploidentical donors but fewer cord blood transplants. *Bone marrow transplantation,* 50**,** 476.

PEISTER, A., MELLAD, J. A., LARSON, B. L., HALL, B. M., GIBSON, L. F. & PROCKOP, D. J. 2004. Adult stem cells from bone marrow (MSCs) isolated from different strains of inbred mice vary in surface epitopes, rates of proliferation, and differentiation potential. *Blood,* 103**,** 1662-1668.

PETRAGLIA, F., FLORIO, P., NAPPI, C. & GENAZZANI, A. R. 1996. Peptide signaling in human placenta and membranes: autocrine, paracrine, and endocrine mechanisms. *Endocrine Reviews,* 17**,** 156-186.

PHELPS, E. A., LANDÁZURI, N., THULÉ, P. M., TAYLOR, W. R. & GARCÍA, A. J. 2010.

Bioartificial matrices for therapeutic vascularization. *Proceedings of the National Academy of Sciences,* 107**,** 3323-3328.

PINHO, S., LACOMBE, J., HANOUN, M., MIZOGUCHI, T., BRUNS, I., KUNISAKI, Y. & FRENETTE, P. S. 2013. PDGFRα and CD51 mark human nestin+ sphere-forming mesenchymal stem cells capable of hematopoietic progenitor cell expansion. *Journal of Experimental Medicine,* 210**,** 1351-1367.

PSALTIS, P., PATON, S., SEE, F., ARTHUR, A., MARTIN, S., ITESCU, S., WORTHLEY, S., GRONTHOS, S. & ZANNETTINO, A. 2010. Enrichment for STRO- 1 expression enhances the cardiovascular paracrine activity of human bone marrow- derived mesenchymal cell populations. *Journal of cellular physiology,* 223**,** 530-540.

QIAN, H., BUZA-VIDAS, N., HYLAND, C. D., JENSEN, C. T., ANTONCHUK, J., MÅNSSON, R., THOREN, L. A., EKBLOM, M., ALEXANDER, W. S. & JACOBSEN, S. E. W. 2007. Critical role of thrombopoietin in maintaining adult quiescent hematopoietic stem cells. *Cell stem cell,* 1**,** 671-684.

RAGNI, E., VIGANO, M., REBULLA, P., GIORDANO, R. & LAZZARI, L. 2013. What is beyond a qRT-PCR study on mesenchymal stem cell differentiation properties: how to choose the most reliable housekeeping genes. *Journal of cellular and molecular medicine,* 17**,** 168-180.

RANGASWAMI, H., BULBULE, A. & KUNDU, G. C. 2006. Osteopontin: role in cell signaling and cancer progression. *Trends in cell biology,* 16**,** 79-87.

RATNER, B. D., HOFFMAN, A. S., SCHOEN, F. J. & LEMONS, J. E. 2004. *Biomaterials science: an introduction to materials in medicine*, Elsevier.

REINHOLD, U., ABKEN, H., KUKEL, S., MOLL, M., MÜLLER, R., OLTERMANN, I. & KREYSEL, H.-W. 1993. CD7-T cells represent a subset of normal human blood lymphocytes. *The Journal of Immunology,* 150**,** 2081-2089.

REYA, T., DUNCAN, A. W., AILLES, L., DOMEN, J., SCHERER, D. C., WILLERT, K., HINTZ, L., NUSSE, R. & WEISSMAN, I. L. 2003. A role for Wnt signalling in self-renewal of haematopoietic stem cells. *Nature,* 423**,** 409.

REYES, J. M., FERMANIAN, S., YANG, F., ZHOU, S. Y., HERRETES, S., MURPHY, D. B., ELISSEEFF, J. H. & CHUCK, R. S. 2006. Metabolic changes in mesenchymal stem cells in osteogenic medium measured by autofluorescence spectroscopy. *Stem Cells,* 24**,** 1213-1217.

RICO, P., HERNÁNDEZ, J. C. R., MORATAL, D., ALTANKOV, G., PRADAS, M. M. & SALMERÓN-SÁNCHEZ, M. 2009. Substrate-induced assembly of fibronectin into networks: influence of surface chemistry and effect on osteoblast adhesion. *Tissue Engineering Part A,* 15**,** 3271-3281.

RICO, P., MNATSAKANYAN, H., DALBY, M. J. & SALMERÓN-SÁNCHEZ, M. 2016a. Material-Driven Fibronectin Assembly Promotes Maintenance of Mesenchymal Stem Cell Phenotypes. *Advanced Functional Materials,* 26**,** 6563-6573.

RICO, P., MNATSAKANYAN, H., DALBY, M. J. & SALMERÓN-SÁNCHEZ, M. 2016b. Material-Driven Fibronectin Assembly Promotes

Maintenance of Mesenchymal Stem Cell Phenotypes. *Advanced Functional Materials*.

RODRIGUEZ-FRATICELLI, A. E., WOLOCK, S. L., WEINREB, C. S., PANERO, R., PATEL, S. H., JANKOVIC, M., SUN, J., CALOGERO, R. A., KLEIN, A. M. & CAMARGO, F. D. 2018. Clonal analysis of lineage fate in native haematopoiesis. *Nature,* 553**,** 212.

RÖMISCH-MARGL, W., PREHN, C., BOGUMIL, R., RÖHRING, C., SUHRE, K. & ADAMSKI, J. 2012. Procedure for tissue sample preparation and metabolite extraction for high-throughput targeted metabolomics. *Metabolomics,* 8**,** 133-142.

ROSE-JOHN, S. & HEINRICH, P. C. 1994. Soluble receptors for cytokines and growth factors: generation and biological function. *Biochemical Journal,* 300**,** 281.

RUOSLAHTI, E. 1996. RGD and other recognition sequences for integrins. *Annual review of cell and developmental biology,* 12**,** 697-715.

RYOO, H.-M., LEE, M.-H. & KIM, Y.-J. 2006. Critical molecular switches involved in BMP-2-induced osteogenic differentiation of mesenchymal cells. *Gene,* 366**,** 51-57.

SALMERON-SANCHEZ, M., RICO, P., MORATAL, D., LEE, T. T., SCHWARZBAUER, J. E. & GARCIA, A. J. 2011. Role of material-driven fibronectin fibrillogenesis in cell differentiation. *Biomaterials,* 32**,** 2099-105.

SAMPATH, P., PRITCHARD, D. K., PABON, L., REINECKE, H., SCHWARTZ, S. M., MORRIS, D. R. & MURRY, C. E. 2008. A hierarchical network controls protein translation during murine embryonic stem cell self-renewal and differentiation. *Cell stem cell,* 2**,** 448-460.

SARMA, N. J., TAKEDA, A. & YASEEN, N. R. 2010. Colony forming cell (CFC) assay for human hematopoietic cells. *Journal of visualized experiments: JoVE*.

SAVILL, J., WYLLIE, A., HENSON, J., WALPORT, M., HENSON, P. & HASLETT, C. 1989. Macrophage phagocytosis of aging neutrophils in inflammation. Programmed cell death in the neutrophil leads to its recognition by macrophages. *The Journal of clinical investigation,* 83**,** 865-875.

SCHMITZ, N., PFISTNER, B., SEXTRO, M., SIEBER, M., CARELLA, A. M., HAENEL, M., BOISSEVAIN, F., ZSCHABER, R., MÜLLER, P. & KIRCHNER, H. 2002. Aggressive conventional chemotherapy compared with high-dose chemotherapy with autologous haemopoietic stem-cell transplantation for relapsed chemosensitive Hodgkin's disease: a randomised trial. *The Lancet,* 359**,** 2065-2071.

SCHNEIDER, R. K., PUELLEN, A., KRAMANN, R., RAUPACH, K., BORNEMANN, J., KNUECHEL, R., PÉREZ-BOUZA, A. & NEUSS, S. 2010. The osteogenic differentiation of adult bone marrow and perinatal umbilical mesenchymal stem cells and matrix remodelling in three-dimensional collagen scaffolds. *Biomaterials,* 31**,** 467-480.

SCHOFIELD, R. 1978. The relationship between the spleen colony-forming cell and the haemopoietic stem cell. *Blood cells,* 4**,** 7-25.

SCHUSTER, J. A., STUPNIKOV, M. R., MA, G., LIAO, W., LAI, R., MA, Y. & AGUILA, J. R. 2012. Expansion of hematopoietic stem cells for transplantation: current perspectives. *Experimental hematology & oncology,* 1**,** 12.

SCHWARTZ, M. A. & GINSBERG, M. H. 2002. Networks and crosstalk: integrin signalling spreads. *Nature cell biology,* 4**,** E65.

SEO, C. H., FURUKAWA, K., MONTAGNE, K., JEONG, H. & USHIDA, T. 2011. The effect of substrate microtopography on focal adhesion maturation and actin organization via the RhoA/ROCK pathway. *Biomaterials,* 32**,** 9568-9575.

SHEKARAN, A., GARCÍA, J. R., CLARK, A. Y., KAVANAUGH, T. E., LIN, A. S., GULDBERG, R. E. & GARCÍA, A. J. 2014. Bone regeneration using an alpha 2 beta 1 integrin-specific hydrogel as a BMP-2 delivery vehicle. *Biomaterials,* 35**,** 5453-5461.

SHI, S. & GRONTHOS, S. 2003. Perivascular niche of postnatal mesenchymal stem cells in human bone marrow and dental pulp. *Journal of bone and mineral research,* 18**,** 696-704.

SIEBURG, H. B., CHO, R. H., DYKSTRA, B., UCHIDA, N., EAVES, C. J. & MULLER-SIEBURG, C. E. 2006. The hematopoietic stem compartment consists of a limited number of discrete stem cell subsets. *Blood,* 107**,** 2311-2316.

SIEG, D. J., HAUCK, C. R., ILIC, D., KLINGBEIL, C. K., SCHAEFER, E., DAMSKY, C. H. & SCHLAEPFER, D. D. 2000. FAK integrates growth-factor and integrin signals to promote cell migration. *Nature cell biology,* 2**,** 249.

SIMSEK, T., KOCABAS, F., ZHENG, J., DEBERARDINIS, R. J., MAHMOUD, A. I., OLSON, E. N., SCHNEIDER, J. W., ZHANG, C. C. & SADEK, H. A. 2010. The distinct metabolic profile of hematopoietic stem cells reflects their

location in a hypoxic niche. *Cell stem cell,* 7**,** 380-390.

SLAVIN, S., NAGLER, A., NAPARSTEK, E., KAPELUSHNIK, Y., AKER, M., CIVIDALLI, G., VARADI, G., KIRSCHBAUM, M., ACKERSTEIN, A. & SAMUEL, S. 1998. Nonmyeloablative stem cell transplantation and cell therapy as an alternative to conventional bone marrow transplantation with lethal cytoreduction for the treatment of malignant and nonmalignant hematologic diseases. *Blood,* 91**,** 756-763.

SMITH, C. A., WILLIAMS, G. T., KINGSTON, R., JENKINSON, E. J. & OWEN, J. J. 1989. Antibodies to CD3/T-cell receptor complex induce death by apoptosis in immature T cells in thymic cultures. *Nature,* 337**,** 181.

SMITS, H. H., ENGERING, A., VAN DER KLEIJ, D., DE JONG, E. C., SCHIPPER, K., VAN CAPEL, T. M., ZAAT, B. A., YAZDANBAKHSH, M., WIERENGA, E. A. & VAN KOOYK, Y. 2005. Selective probiotic bacteria induce IL-10–producing regulatory T cells in vitro by modulating dendritic cell function through dendritic cell–specific intercellular adhesion molecule 3–grabbing nonintegrin. *Journal of Allergy and Clinical Immunology,* 115**,** 1260-1267.

SOBOTKOVÁ, E., HRUBÁ, A., KIEFMAN, J. & SOBOTKA, Z. 1988. Rheological behaviour of bone marrow. *Progress and Trends in Rheology II.* Springer.

STENDERUP, K., JUSTESEN, J., CLAUSEN, C. & KASSEM, M. 2003. Aging is associated with decreased maximal life span and accelerated senescence of bone marrow stromal cells. *Bone,* 33**,** 919-926.

STIER, S., KO, Y., FORKERT, R., LUTZ, C., NEUHAUS, T., GRÜNEWALD, E., CHENG, T., DOMBKOWSKI, D., CALVI, L. M. & RITTLING, S. R. 2005. Osteopontin is a hematopoietic stem cell niche component that negatively regulates stem cell pool size. *Journal of Experimental Medicine,* 201**,** 1781-1791.

SUGIYAMA, T., KOHARA, H., NODA, M. & NAGASAWA, T. 2006. Maintenance of the hematopoietic stem cell pool by CXCL12-CXCR4 chemokine signaling in bone marrow stromal cell niches. *Immunity, 2*5**,** 977-988.

TAICHMAN, R. S., REILLY, M. J. & EMERSON, S. G. 1996. Human osteoblasts support human hematopoietic progenitor cells in vitro bone marrow cultures. *Blood,* 87**,** 518-524.

TAKEICHI, M. 1991. Cadherin cell adhesion receptors as a morphogenetic regulator. *Science,* 251**,** 1451-1455.

TANIGUCHI, H., TOYOSHIMA, T., FUKAO, K. & NAKAUCHI, H. 1996. Presence of hematopoietic stem cells in the adult liver. *Nature medicine,* 2**,** 198.

TANNOURY, C. A. & AN, H. S. 2014. Complications with the use of bone morphogenetic protein 2 (BMP-2) in spine surgery. *The Spine Journal,* 14**,** 552-559.

TAUTENHAHN, R., CHO, K., URITBOONTHAI, W., ZHU, Z., PATTI, G. J. & SIUZDAK, G. 2012a. An accelerated workflow for untargeted metabolomics using the METLIN database. *Nature biotechnology,* 30**,** 826.

TAUTENHAHN, R., PATTI, G. J., RINEHART, D. & SIUZDAK, G. 2012b. XCMS Online: a web-based

platform to process untargeted metabolomic data. *Analytical chemistry,* 84**,** 5035-5039.

TERSTAPPEN, L., HUANG, S., SAFFORD, M., LANSDORP, P. M. & LOKEN, M. R. 1991. Sequential generations of hematopoietic colonies derived from single nonlineage-committed CD34+ CD38-progenitor cells. *Blood,* 77**,** 1218-1227.

THOMAS, E. D., LOCHTE, H. L., CANNON, J. H., SAHLER, O. D. & FERREBEE, J. W. 1959. Supralethal whole body irradiation and isologous marrow transplantation in man. *The Journal of clinical investigation,* 38**,** 1709-1716.

THOMAS, E. D., STORB, R., CLIFT, R. A., FEFER, A., JOHNSON, F. L., NEIMAN, P. E., LERNER, K. G., GLUCKSBERG, H. & BUCKNER, C. D. 1975. Bone-marrow transplantation. *New England Journal of Medicine,* 292**,** 895-902.

THOMSON, J. A., ITSKOVITZ-ELDOR, J., SHAPIRO, S. S., WAKNITZ, M. A., SWIERGIEL, J. J., MARSHALL, V. S. & JONES, J. M. 1998. Embryonic stem cell lines derived from human blastocysts. *science,* 282**,** 1145-1147.

TILL, J. E. & MCCULLOCH, E. A. 1961. A direct measurement of the radiation sensitivity of normal mouse bone marrow cells. *Radiation research,* 14**,** 213-222.

TJABRINGA, G., ZANDIEH- DOULABI, B., HELDER, M., KNIPPENBERG, M., WUISMAN, P. & KLEIN-NULEND, J. 2008. The polymine spermine regulates osteogenic differentiation in adipose stem cells. *Journal of cellular and molecular medicine,* 12**,** 1710-1717.

TORISAWA, Y.-S., SPINA, C. S., MAMMOTO, T., MAMMOTO, A., WEAVER, J. C., TAT, T., COLLINS, J. J. & INGBER, D. E. 2014. Bone

marrow–on–a–chip replicates hematopoietic niche physiology in vitro. *Nature methods,* 11**,** 663.

TREBEDEN- NEGRE, H., CHOQUET, S., TANGUY, M. L., ROZENZWAJG, M., AZAR, N., LEFRÈRE, F., HESHMATI, F., BELHOCINE, R., VIEILLARD, V. & NOROL, F. 2017. A clinical trial combining megakaryocytes and haematopoietic stem cells to promote engraftment after autologous transplantation. *British journal of haematology*.

TRINCHIERI, G. 1989. Biology of natural killer cells. *Advances in immunology.* Elsevier.

TSAI, M. S., LEE, J. L., CHANG, Y. J. & HWANG, S. M. 2004. Isolation of human multipotent mesenchymal stem cells from second- trimester amniotic fluid using a novel two- stage culture protocol. *Human reproduction,* 19**,** 1450-1456.

TSIMBOURI, P. M., MCMURRAY, R. J., BURGESS, K. V., ALAKPA, E. V., REYNOLDS, P. M., MURAWSKI, K., KINGHAM, E., OREFFO, R. O., GADEGAARD, N. & DALBY, M. J. 2012. Using nanotopography and metabolomics to identify biochemical effectors of multipotency. *ACS nano,* 6**,** 10239-10249.

TURNER, W. S., SEAGLE, C., GALANKO, J. A., FAVOROV, O., PRESTWICH, G. D., MACDONALD, J. M. & REID, L. M. 2008. Nuclear magnetic resonance metabolomic footprinting of human hepatic stem cells and hepatoblasts cultured in hyaluronan- matrix hydrogels. *Stem Cells,* 2*6***,** 1547-1555.

TYAGI, S., RAGHVENDRA, S. U., KALRA, T. & MUNJAL, K. 2010. Applications of metabolomics-a systematic study of the unique chemical fingerprints: an overview. *Int. J. Pharm. Sci. Rev. Res,* 3**,** 83-86.

URIST, M. R. 1965. Bone: formation by autoinduction. *Science,* 150**,** 893-899.

URIST, M. R. & STRATES, B. S. 1971. Bone morphogenetic protein. *Journal of dental research,* 50**,** 1392-1406.

VAN DEN BERG, R. A., HOEFSLOOT, H. C., WESTERHUIS, J. A., SMILDE, A. K. & VAN DER WERF, M. J. 2006. Centering, scaling, and transformations: improving the biological information content of metabolomics data. *BMC genomics,* 7**,** 142.

VARUM, S., RODRIGUES, A. S., MOURA, M. B., MOMCILOVIC, O., EASLEY IV, C. A., RAMALHO-SANTOS, J., VAN HOUTEN, B. & SCHATTEN, G. 2011. Energy metabolism in human pluripotent stem cells and their differentiated counterparts. *PloS one,* 6**,** e20914.

VISSER, J., BAUMAN, J., MULDER, A., ELIASON, J. & DE LEEUW, A. 1984. Isolation of murine pluripotent hemopoietic stem cells. *Journal of Experimental Medicine,* 159**,** 1576-1590.

VOSE, J. M., BIERMAN, P. J., LYNCH, J. C., ATKINSON, K., JUTTNER, C., HANANIA, E., BOCIEK, G. & ARMITAGE, J. O. 2001. Transplantation of highly purified CD34+ Thy-1+ hematopoietic stem cells in patients with recurrent indolent non-Hodgkin's lymphoma. *Biology of Blood and Marrow Transplantation,* 7**,** 680-687.

WAGERS, A. J. & WEISSMAN, I. L. 2004. Plasticity of adult stem cells. *Cell,* 116**,** 639-648.

WALASEK, M. A., VAN OS, R. & DE HAAN, G. 2012. Hematopoietic stem cell expansion: challenges and opportunities. *Annals of the New York Academy of Sciences,* 1266**,** 138-150.

WANG, E. A., ROSEN, V., D'ALESSANDRO, J. S., BAUDUY, M., CORDES, P., HARADA, T., ISRAEL, D. I., HEWICK, R. M., KERNS, K. M. & LAPAN, P. 1990. Recombinant human bone morphogenetic protein induces bone formation. *Proceedings of the National Academy of Sciences,* 87**,** 2220-2224.

WANG, F., ROWAN, R., CREER, M., HAY, A., DORFNER, M., PEESAPATI, S., CONNELL, B., NAKAMURA, Y., INAGAKI, A. & OTANI, I. 2004a. Detecting human CD34+ and CD34-hematopoietic stem and progenitor cells using a Sysmex automated hematology analyzer. *Laboratory hematology: official publication of the International Society for Laboratory Hematology,* 10**,** 200-205.

WANG, H. S., HUNG, S. C., PENG, S. T., HUANG, C. C., WEI, H. M., GUO, Y. J., FU, Y. S., LAI, M. C. & CHEN, C. C. 2004b. Mesenchymal stem cells in the Wharton's jelly of the human umbilical cord. *Stem cells,* 22**,** 1330-1337.

WANG, J., KIMURA, T., ASADA, R., HARADA, S., YOKOTA, S., KAWAMOTO, Y., FUJIMURA, Y., TSUJI, T., IKEHARA, S. & SONODA, Y. 2003. SCID-repopulating cell activity of human cord blood–derived CD34− cells assured by intra–bone marrow injection. *Blood,* 101**,** 2924-2931.

WANG, L. D. & WAGERS, A. J. 2011. Dynamic niches in the origination and differentiation of haematopoietic stem cells. *Nature reviews Molecular cell biology,* 12**,** 643.

WANG, X., BURGHARDT, R. C., ROMERO, J. J., HANSEN, T. R., WU, G. & BAZER, F. W. 2015. Functional roles of arginine during the peri-implantation period of pregnancy. III. Arginine stimulates proliferation and interferon tau

production by ovine trophectoderm cells via nitric oxide and polyamine-TSC2-MTOR signaling pathways. *Biology of reproduction,* 92**,** 75, 1-17.

WARD, A. C., TOUW, I. & YOSHIMURA, A. 2000. The Jak-Stat pathway in normal and perturbed hematopoiesis. *Blood,* 95**,** 19-29.

WATT, F. M. & HOGAN, B. L. 2000. Out of Eden: stem cells and their niches. *Science,* 287**,** 1427-1430.

WEBB, N. J., BOTTOMLEY, M. J., WATSON, C. J. & BRENCHLEY, P. E. 1998. Vascular endothelial growth factor (VEGF) is released from platelets during blood clotting: implications for measurement of circulating VEGF levels in clinical disease. *Clinical science,* 94**,** 395-404.

WEISEL, K. C., GAO, Y., SHIEH, J.-H. & MOORE, M. A. 2006. Stromal cell lines from the aorta-gonado-mesonephros region are potent supporters of murine and human hematopoiesis. *Experimental hematology,* 34**,** 1505-1516.

WEISSMAN, I. L. 2000. Stem cells. *cell,* 100**,** 157-168.

WILLIAMS, R. L., HILTON, D. J., PEASE, S., WILLSON, T. A., STEWART, C. L., GEARING, D. P., WAGNER, E. F., METCALF, D., NICOLA, N. A. & GOUGH, N. M. 1988. Myeloid leukaemia inhibitory factor maintains the developmental potential of embryonic stem cells. *Nature,* 336**,** 684.

WINER, J. P., JANMEY, P. A., MCCORMICK, M. E. & FUNAKI, M. 2008. Bone marrow-derived human mesenchymal stem cells become quiescent on soft substrates but remain responsive to chemical or mechanical stimuli. *Tissue Engineering Part A,* 15**,** 147-154.

WOO, B. H., FINK, B. F., PAGE, R., SCHRIER, J. A., JO, Y. W., JIANG, G., DELUCA, M., VASCONEZ,

H. C. & DELUCA, P. P. 2001. Enhancement of bone growth by sustained delivery of recombinant human bone morphogenetic protein-2 in a polymeric matrix. *Pharmaceutical research,* 18**,** 1747-1753.

WU, A., TILL, J., SIMINOVITCH, L. & MCCULLOCH, E. 1967. A cytological study of the capacity for differentiation of normal hemopoietic colony-forming cells. *Journal of cellular physiology,* 69**,** 177-184.

WUCHTER, P., SAFFRICH, R., GISELBRECHT, S., NIES, C., LORIG, H., KOLB, S., HO, A. D. & GOTTWALD, E. 2016. Microcavity arrays as an in vitro model system of the bone marrow niche for hematopoietic stem cells. *Cell and tissue research,* 364**,** 573-584.

XIA, J., MANDAL, R., SINELNIKOV, I. V., BROADHURST, D. & WISHART, D. S. 2012. MetaboAnalyst 2.0—a comprehensive server for metabolomic data analysis. *Nucleic acids research,* 40**,** W127-W133.

XIAN, L., WU, X., PANG, L., LOU, M., ROSEN, C. J., QIU, T., CRANE, J., FRASSICA, F., ZHANG, L. & RODRIGUEZ, J. P. 2012. Matrix IGF-1 maintains bone mass by activation of mTOR in mesenchymal stem cells. *Nature medicine,* 18**,** 1095.

XIAO, L., RAO, J. N., ZOU, T., LIU, L., MARASA, B. S., CHEN, J., TURNER, D. J., PASSANITI, A. & WANG, J.-Y. 2007. Induced JunD in intestinal epithelial cells represses CDK4 transcription through its proximal promoter region following polyamine depletion. *Biochemical Journal,* 403**,** 573-581.

XIE, T. & SPRADLING, A. C. 1998. decapentaplegic is essential for the maintenance and division of germline stem cells in the Drosophila ovary. *Cell,* 94**,** 251-260.

YANES, O., CLARK, J., WONG, D. M., PATTI, G. J., SÁNCHEZ-RUIZ, A., BENTON, H. P., TRAUGER, S. A., DESPONTS, C., DING, S. & SIUZDAK, G. 2010. Metabolic oxidation regulates embryonic stem cell differentiation. *Nature chemical biology,* 6**,** 411.

YODER, M. & WILLIAMS, D. 1995. Matrix molecule interactions with hematopoietic stem cells. *Experimental hematology,* 2*3***,** 961-967.

YOSHIDA, M., KASHIWAGI, K., SHIGEMASA, A., TANIGUCHI, S., YAMAMOTO, K., MAKINOSHIMA, H., ISHIHAMA, A. & IGARASHI, K. 2004. A unifying model for the role of polyamines in bacterial cell growth, the polyamine modulon. *Journal of Biological Chemistry,* 279**,** 46008-46013.

YOSHIHARA, H., ARAI, F., HOSOKAWA, K., HAGIWARA, T., TAKUBO, K., NAKAMURA, Y., GOMEI, Y., IWASAKI, H., MATSUOKA, S. & MIYAMOTO, K. 2007. Thrombopoietin/MPL signaling regulates hematopoietic stem cell quiescence and interaction with the osteoblastic niche. *Cell stem cell,* 1**,** 685-697.

ZANJANI, E. D., ALMEIDA-PORADA, G., LIVINGSTON, A., FLAKE, A. & OGAWA, M. 1998. Human bone marrow CD34-cells engraft in vivo and undergo multilineage expression that includes giving rise to CD34+ cells. *Experimental hematology,* 2*6***,** 353-360.

ZHANG, C. C. & LODISH, H. F. 2008. Cytokines regulating hematopoietic stem cell function. *Current opinion in hematology,* 15**,** 307.

ZHANG, J., NIU, C., YE, L., HUANG, H., HE, X., TONG, W.-G., ROSS, J., HAUG, J., JOHNSON, T., FENG, J. Q., HARRIS, S., WIEDEMANN, L. M., MISHINA, Y. & LI, L. 2003. Identification of the haematopoietic stem cell niche and control of the niche size. *Nature,* 425**,** 836-841.

ZHAO, T., GOH, K. J., NG, H. H. & VARDY, L. A. 2012. A role for polyamine regulators in ESC self-renewal. *Cell Cycle,* 11**,** 4517-4523.

ZHU, J. & CLARK, R. A. 2014a. Fibronectin at select sites binds multiple growth factors (GF) and enhances their activity: expansion of the collaborative ECM-GF paradigm. *The Journal of investigative dermatology,* 134**,** 895.

ZHU, J. & CLARK, R. A. 2014b. Fibronectin at select sites binds multiple growth factors and enhances their activity: expansion of the collaborative ECM-GF paradigm. *Journal of Investigative Dermatology,* 134**,** 895-901.